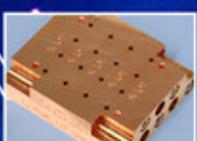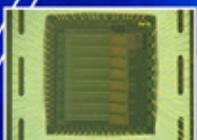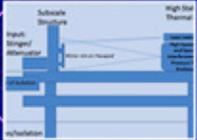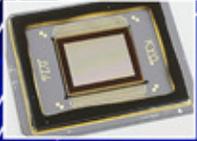National Aeronautics and Space Administration

Cosmic Origins
**Program Annual
Technology Report**

Cosmic Origins
Program Office
October 2016

The report cover links our age-old observation of the skies, seeking to understand the universe we live in and how it came to be, with modern astrophysics.

The Mayan El Caracol observatory in Chichen Itza demonstrates that the importance of astronomical observations extends back to ancient times.

Modern astronomy has expanded far beyond objects visible to the naked eye. For example, the Hubble Space Telescope has captured countless images of distant objects such as the Eagle Nebula, some 7000 light-years from Earth, seen in the Pillars of Creation image. The Cosmic Web, the large-scale filamentary structure of the universe seen at the top of the cover, is believed to contain about half of the "ordinary" matter in the universe. Overlaying these astronomical objects is a notional representation of a segmented mirror comprised of hexagonal segments, as developed for the James Webb Space Telescope.

The Strategic Astrophysics Technology project images at the left edge of the cover demonstrate our ongoing efforts to identify and develop the technologies needed to advance humankind's ability to observe and understand our universe.

Table of Contents

http://cor.gsfc.nasa.gov

COR 2016 PATR
Executive Summary

What is the Cosmic Origins (COR) Program?

From ancient times, humans have looked up at the night sky and wondered: Are we alone? How did the universe come to be? **How does the universe work?** COR focuses on the second question. Scientists investigating this broad theme seek to understand the origin and evolution of the universe from the Big Bang to the present day, determining how the expanding universe grew into a grand cosmic web of dark matter enmeshed with galaxies and pristine gas, forming, merging, and evolving over time. COR also seeks to understand how stars and planets form from clouds in these galaxies to create the heavy elements that are essential to life – starting with the first generation of stars to seed the universe, and continuing through the birth and eventual death of all subsequent generations of stars. The COR Program's purview includes the majority of the field known as astronomy, from antiquity to the present.

The Laser Interferometer Gravitational-Wave Observatory (LIGO) recently recorded the first direct measurement of long-theorized gravitational waves (GWs). Another surprising recent discovery is that the universe is expanding at an ever-accelerating rate, the first hint of so-called "dark energy," estimated to account for 75% of mass-energy in the universe. Dark matter, so called because we only observe its effects on regular matter, accounts for another 20%, leaving only 5% for regular matter and energy. Scientists now also search for special polarization in the cosmic microwave background to support the notion that in the split-second after the Big Bang, the universe inflated faster than the speed of light! The most exciting aspect of this grand enterprise today is that we can finally develop the tools needed for such discoveries.

Why is COR Technology Development Critical?

A 2008 Space Review paper noted that robust technology development and maturation is crucial to reducing flight project schedule and cost over-runs: "*…in the mid-1980s, NASA's budget office found that during the first 30 years of the civil space program, no project enjoyed less than a 40% cost overrun unless it was preceded by an investment in studies and technology of at least 5 to 10% of the actual project budget that eventually occurred*" [1]. Such technology maturation program is most efficiently addressed through focused R&D projects, rather than in flight projects, where "marching armies" make the cost of delays unacceptably high. The National Academies of Science 2010 Decadal Survey, "New Worlds, New Horizons in Astronomy and Astrophysics" (NWNH) stressed that "*Technology development is the engine powering advances in astronomy and astrophysics... Failure to develop adequately mature technology prior to a program start also leads to cost and schedule overruns*" [2].

NASA requires flight projects to demonstrate technology readiness level (TRL) 6[*] by Preliminary Design Review (PDR) for all technologies they need. However, this can only occur with a process in place to correctly identify and adequately fund development of relevant "blue sky" technologies to TRL 3[†], and then mature them to TRL 5[‡] or 6, across the so-called "mid-TRL gap," where sustained funding frequently falls short.

What's in this Report? What's New?

This sixth Program Annual Technology Report (PATR) summarizes the Program's technology development activities for fiscal year (FY) 2016. It lists technology gaps identified by the astrophysics community and two mission-concept studies with priorities assigned by the COR Technology Management Board

---

[*] TRLs are fully described in NPR 7123.1B, Appendix E, with TRL definitions reproduced in Appendix A below; TRL 6 is defined as: "*System/sub-system model or prototype demonstration in a relevant environment*."

[†] TRL 3 is defined as: "*Analytical and experimental critical function and/or characteristic proof-of-concept*."

[‡] TRL 5 is defined as: "*Component and/or breadboard validation in relevant environment*."

(TMB; see p. 20). Following this year's prioritization, the Program Office recommends NASA Astrophysics Division at HQ solicit and fund the maturation of the following technologies with the highest priority:

- Lightweight large-aperture high-performance telescope mirror systems;
- High-efficiency ultraviolet (UV) multi-object spectrometers;
- Large-format, high-sensitivity, high-dynamic-range UV/Far UV (FUV) detectors;
- Band-shaping and dichroic filters for UV/Visible light (Vis);
- Large Cryogenic Optics for the Far infrared (IR);
- Large-format, low-noise and ultralow noise far-IR (FIR) direct detectors;
- Compact, integrated spectrometers for 100 to 1000 μm;
- Heterodyne FIR detector arrays and related technologies; and
- High-performance, sub-Kelvin coolers.

These recommendations represent technologies most critical for substantive near-term progress on strategic priorities and take into account technology development needs identified by the Science and Technology Definition Teams (STDTs) studying the FIR Surveyor (FIRS) and the Large UV/Optical/IR (LUVOIR) Surveyor. These STDTs, along with those studying an X-Ray Surveyor (XRS) and a Habitable Exoplanet (HabEx) imaging mission, were charged by the Astrophysics Division Director to develop the science case, technology assessment, design reference mission with strawman payload, and a cost assessment. This is being done in preparation for the upcoming 2020 Decadal Survey. These Surveyors are three of five described in the Astrophysics Roadmap, "Enduring Quests, Daring Visions," released in December 2013, while HabEx was described in the NWNH.

Meanwhile, the Program is pleased to announce two newly awarded COR Strategic Astrophysics Technology (SAT) projects for FY 2017 start (alphabetically, by Principal Investigator, PI):

- "Predictive Thermal Control Technology for Potential HabEx Mission," H. Philip Stahl, MSFC; and
- "High-Efficiency Continuous Cooling for Cryogenic Instruments and sub-Kelvin Detectors," James Tuttle, GSFC.

Including these, the Astrophysics Division has awarded 18 COR SAT projects to date, funded by COR Supporting Research and Technology (SR&T), and intended to develop telescopes, optics, coatings, and detectors from the Far-IR to the Far-UV, applicable to strategic COR missions. Of the eight projects reporting in 2015, one, developing advanced UV-reflective coatings, was completed, and two transitioned into 2016-start projects. Five continuing from prior years and five 2016-start projects all report significant progress, except for the one project that was funded recently, and has just begun work. This PATR reports on the progress, current status, and activities planned for the coming year for the 10 projects funded in FY 2016. We thank the PIs of our ongoing projects for their informative progress reports (Appendix B – Quad Charts, p. 55; Appendix C – Development Status, p. 66), and welcome our new awardees, one of whom is a returning SAT PI (proposal abstracts are at the end of Appendix C).

The following are some examples where Program-funded technologies were infused, or are planned to be infused, into projects and missions:

- TES bolometer detector was selected to support the Stratospheric Observatory for Infrared Astronomy (SOFIA) High-resolution Airborne Wide-bandwidth Camera (HAWC) instrument (deployed 2015);
- COR technology funding made possible the selection of the High-Resolution Mid-infrarEd Spectrometer (HIRMES) for development as a third-generation facility for SOFIA;
- High-efficiency Solid-state Photon-counting Ultraviolet Detector (SPUD) will be flight-tested on the Faint Intergalactic medium Redshifted Emission Balloon (FIREBall) (2017 launch);
- High-reflectivity UV coatings were used to coat optics for Ionospheric Connection (ICON) and Global-scale Observations of the Limb and Disk (GOLD) Explorers (2017 planned launches); and
- The Wide-Field Infrared Survey Telescope (WFIRST) project adopted the H4RG near-IR detector to address some of the most enduring questions in astrophysics (mid-2020s launch).

1. Program Science Overview

The goal of the COR Program is to understand the origin and evolution of the universe from the Big Bang to the present day. On the largest scale, COR's broad-reaching science question is to determine how the expanding universe grew into a grand cosmic web of dark matter enmeshed with galaxies and pristine gas, forming, merging, and evolving over time. COR also seeks to understand how stars and planets form from clouds in these galaxies; how stars create the heavy elements essential to life – starting with the first generation of stars to seed the universe, and continuing through the birth and death of stars to today. The majority of the field known as astronomy, from antiquity to the present, falls within the purview of COR.

Background

The Program encompasses multiple scientific missions aimed at meeting Program objectives, each with unique scientific capabilities and goals. The Program was established to integrate those space, suborbital, and ground activities into a cohesive effort that enables each project to build on the technological and scientific legacy of its contemporaries and predecessors. Each project operates independently to achieve its unique set of mission objectives, which contribute to the overall Program objectives.

Current COR missions:

Hubble Space Telescope (HST)

HST's 1990 launch began one of NASA's most successful and long-lasting science missions. Over 26 years, HST relayed over a million observations back to Earth, shedding light on many of the great mysteries of astronomy. HST helped determine the age of the universe, peer into the hearts of quasars, study galaxies in all stages of evolution, find proto-planetary disks where gas and dust around young stars are birthing grounds for new planets, and provide key evidence for the existence of dark energy.

Spitzer Space Telescope

Spitzer, which recently celebrated the 13th anniversary of its launch, provides sensitive IR observations that allow scientists to peer into cosmic regions hidden from optical telescopes, such as dusty stellar nurseries, centers of galaxies, and still-forming planetary systems. Many of its investigations have focused on objects that emit very little visible light, including brown dwarf stars, extra-solar planets, and giant molecular clouds. Although the primary phase of Spitzer's mission ended in 2009 with the exhaustion of its onboard cryogen, the Spitzer "warm" mission continues valuable work on COR science goals.

Stratospheric Observatory for Infrared Astronomy

SOFIA, the world's largest airborne observatory is operated as a partnership between NASA and the German Aerospace Center (DLR), performing imaging and spectroscopy across the IR spectrum. SOFIA was declared fully operational in May 2014. The SOFIA Program Office and aircraft are based at NASA's Armstrong Flight Research Center (AFRC), with science mission operations based at NASA's Ames Research Center (ARC). SOFIA is managed outside the COR program, but because SOFIA science is well-aligned with COR science, and because SOFIA represents an important platform for maturing COR technologies that may be applicable to future space missions, certain SOFIA science objectives are considered strategic in relation to applicable prioritization criteria described in Section 3.

Herschel Space Observatory

The European Space Agency (ESA) Herschel Space Observatory has revealed new information about the earliest, most distant stars and galaxies, as well as those forming and evolving closer to home. NASA contributed significant portions of Herschel's instrumentation, data processing, and science analyses. Herschel was decommissioned in June 2013, but data refinement and analysis will continue until 2017.

COR Development Portfolio 2016

The COR Program Office manages the investment of SR&T funds in a variety of avenues to advance COR technology needs. Appendix C details recent progress of projects supported during FY 2016. In 2016, the COR Program development portfolio includes:

WFIRST – Mission in Formulation

WFIRST is a NASA observatory project within the astrophysics Exoplanet Exploration Program (ExEP) designed to perform wide-field imaging and slit-less spectroscopic surveys of the Near-IR sky. It was the top-ranked large space mission in NWNH, and is expected to launch in the mid-2020s. Because WFIRST survey data will address major COR science questions, such as galaxy evolution, the COR Program supported pre-formulation studies and technology development until late 2013, when they were moved into the WFIRST study. The program continues to follow WFIRST development with specific attention to COR science goals.

James Webb Space Telescope (JWST)

A partnership between NASA and ESA, JWST is the largest science mission under development, and will address important COR science objectives. JWST will collect Near-IR and mid-IR data, allowing investigations of the earliest observable objects in the universe, tracing the evolution of galaxies, and probing obscured star-formation regions in our own and other galaxies. Currently under development, JWST is managed outside the COR Program. However, JWST operations will be managed under the COR Program when the mission transitions to Phase E after launch and commissioning in 2018.

Technology Development

The COR Program is responsible for ensuring that NASA is technologically ready to continue mission developments into the future and to advance the broad scope of COR science goals. Accordingly, the Program Office is charged with overseeing the science of missions in formulation, implementation, and operations, as well as the maturation of technologies in development for these missions.

US astrophysics priorities were last refined in 2010 when the National Research Council (NRC) released the NWNH report. Following the NWNH recommendations, the COR Program has supported focused technology development and mission-concept studies. In NWNH, the NRC placed high value on COR missions relating to Cosmic Dawn (the science theme most closely identifiable with COR). With JWST still in development, the NRC-prioritized recommendations did not include a new specific NASA-led mission that fit solely within COR. However, several of the NWNH recommendations are directly relevant to the COR Program.

- The NWNH report's first priority space recommendation, WFIRST, will address many key COR science goals, such as the formation and evolution of structure and galaxy growth.
- The report gave high priority to technology development in support of a future 4-m UV/Visible-band space telescope.
- The recommendations include a NASA instrument contribution to the Japanese Aerospace Exploration Agency (JAXA) Space Infrared Telescope for Cosmology and Astrophysics (SPICA) mission, if affordable. The Astrophysics Division's "Astrophysics Implementation Plan" (AIP), released in December 2012 and updated in 2014, clarified that the desired contribution would exceed available NASA budgets.
- The report also strongly recommended an augmentation to the Explorers Program that supports astrophysics with rapid, targeted, competed investigations, that are selected largely based on scientific merit and technological readiness. Explorer missions provide an additional robust way to accomplish COR science: four of the six Medium-Class Explorers (MIDEX)/Small Explorers (SMEX) missions launched in the past 15 years primarily support COR objectives.

Since the COR Program was formulated in 2009 and the NWNH report was released in 2010, fiscal constraints have become significantly more restrictive than anticipated. The Program is committed to managing available funds strategically to foster COR science objectives.

The COR Program is committed to preparing for the next UV/Visible astrophysics mission. NWNH recommends developing technology for a large UV/Visible mission that will continue and extend HST's science accomplishments, through a 4-m-class mission covering wavelengths shorter than HST's primary range. However, the COR Program has chosen to consider a broader range of possible future endeavors.

A 2012 Request for Information (RFI) regarding science objectives and requirements for future UV/Visible astrophysics mission(s) led to a September 2012 community workshop based on 34 responses, which are posted on the COR website. A second community workshop in June 2015 continued working towards community consensus on science objectives and technology needs. Further, two independent (non-Program-sponsored) studies considering a future large UV/Visible observatory developed requirements that are likely to help guide the prioritization of COR SR&T technology development needs. Most technology development toward future strategic UV/Visible missions is also expected to benefit the Explorer Program.

In 2012, the Program also studied the feasibility of an instrument contribution to SPICA, then slated for launch around 2022. The Program concluded that based on the readiness level and development risk of possible NASA-provided SPICA instruments, all possible instrument contributions required funding beyond what was available, and could not meet JAXA's schedule constraints. Two Program-sponsored workshops on the future of Far-IR space astrophysics were held in May 2014 and June 2015, to identify the most pressing science questions that can be addressed with Far-IR techniques, to determine technologies needed, and to build community consensus regarding future possible Far-IR astrophysics missions. As in the UV/Visible range, technology development towards future strategic Far-IR missions will also benefit Explorers.

SOFIA, which provides a platform for observations across the IR spectrum, with the possibility of frequent instrument upgrades, started Science Cycle 4 in early 2016. The recent upgrade to SOFIA's HAWC instrument will offer observers polarimetric optics and new Far-IR detectors. The new HAWC+ detectors were matured with COR funding in prior years, an example of how COR technology development investment can be handed off to a flight project once the appropriate TRL is reached. A new, third-generation, instrument for SOFIA will be selected in fall 2016, and will infuse technology developed under the COR SR&T program. New technology is expected to continue to be infused into SOFIA though future instrument calls.

The activity given first priority in NWNH for a future large space mission, WFIRST, was formally approved for formulation work in early 2016. WFIRST is managed by the ExEP at the Jet Propulsion Laboratory (JPL), so it is not formally within the COR Program's suite of future missions. However, it still holds great interest for COR science. The mission will use a 2.4-m repurposed telescope, and is expected to launch in the mid-2020s. The COR Program supported this high-priority mission activity through SAT-funded detector development until the work was moved into the WFIRST study office in 2014. The COR Program continues to pay attention to planned capabilities that will serve COR science.

Planning for the Future

In early 2016, in preparation for the 2020 Decadal Study of Astronomy and Astrophysics, NASA's Astrophysics Division initiated four community-based concept studies for possible future strategic

missions (for information about the study teams' activities and progress, click on the mission links below). If selected, these would explore the nature of the universe from its earliest moments, in its most extreme conditions, and at the largest scales. Two of the possible missions address science topics within the COR program's purview: FIRS and a LUVOIR Surveyor. Either of these missions will require substantial technology advances, which will help guide the COR Program's technology development starting in late 2016. The other two possible mission studies, HabEx Imaging Mission, and XRS, are expected to have significant interest for COR science as well, but will not directly influence the COR Program technology planning. Most of the technology development needed for these large missions as well will benefit the Explorer Program.

2. Strategic Technology Development Process and Portfolio

The COR, PCOS, and ExEP Program Offices were set up by NASA HQ Science Mission Directorate (SMD) Astrophysics Division to manage all aspects of these focused astrophysics programs. The Program Offices shepherd critical technologies toward infusion into Program-relevant flight projects. The Offices follow Astrophysics Division guidance, and base their recommendations on science community input, ensuring the most relevant technologies are solicited and developed. The COR Program Office, located at NASA GSFC, serves as HQ's implementation arm on COR Program-related matters. The Astrophysics Division achieves efficiency by having the same staff and physical facilities serve both the COR and PCOS Program Offices. The Astrophysics Division funds technology development at all TRLs. Early-stage development (TRL ≤ 3) and technologies related to non-strategic missions are typically funded by APRA. Final maturation (TRL ≥ 6) is mission-specific and thus handled by flight missions. The SAT program, launched in 2009, funds maturation of technologies across the mid-TRL gap (3 ≤ TRL < 6).

The COR Technology Development Process

The COR Program Office is charged to develop and administer a technology development and maturation program, moving innovative technologies across the mid-TRL gap to enable strategic COR missions. The Program Office facilitates, manages, and implements the technology policies of the Program. Our goal is to facilitate technology infusion into COR missions, including the crucial phase of transitioning nascent technologies into targeted projects' technology programs during mission formulation. COR SAT projects are funded by the COR SR&T budget. Our work is guided by the priorities set forth in the AIP, the Astrophysics Roadmap, and other current strategic guidance. The AIP describes the Astrophysics Division's planned implementation of space-based priority missions and activities identified in NWNH, updated due to more recent budgetary developments. The Roadmap strives to inspire and challenge the community to pursue the missions and technologies needed over the next three decades to address NWNH-identified science goals.

Our technology development process (Fig. 2-1) places the science community's inputs at the center of our efforts through the Decadal Survey process and ongoing identification of technology gaps. The community is encouraged to submit gaps at any time via the COR Program Analysis Group (COPAG) or directly through the COR Program website. The COPAG Executive Committee (EC) is asked to review gaps submitted before the annual June 1 cutoff date, consolidating, enhancing, and adding to them as needed to create a complete, accurate, and compelling set of gaps for TMB evaluation. The Program Office charges its TMB annually to evaluate and determine which of the submitted technology developments would meet Program objectives, and to prioritize them for further development consideration. The TMB ranks gaps based on Program objectives, strategic ranking of relevant science/missions, benefits and impacts, and urgency. The TMB, a Program-level functional group, thus provides a formal mechanism for input to, and review of, COR technology development activities.
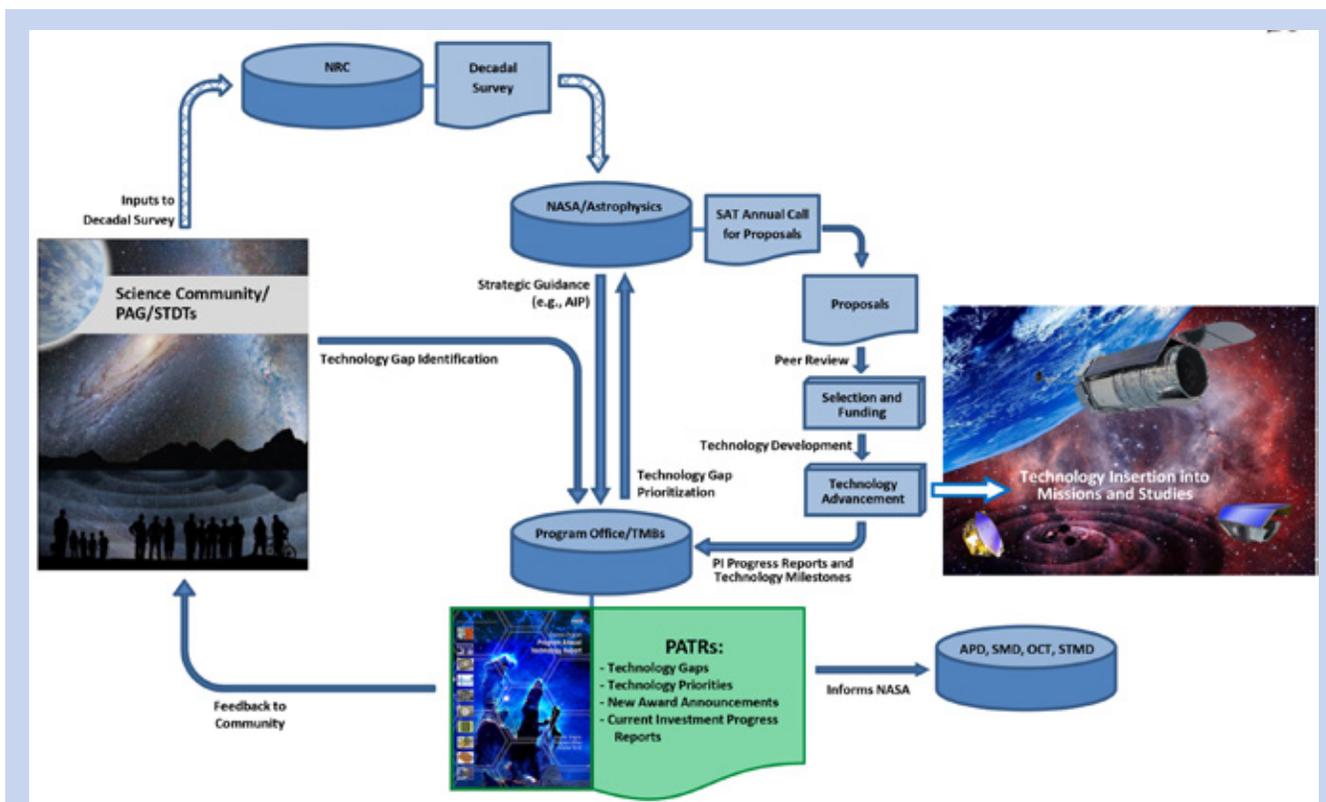
Fig. 2-1. *The COR technology development process receives community input on technology gaps, recommends priorities, manages SAT-funded activities, and informs NASA and the science community about progress.*

TMB priority recommendations inform Astrophysics Division decisions on what technologies to solicit in the upcoming annual SAT call for proposals, and help guide proposal selections. HQ's investment considerations are made within a broader context, with programmatic factors apparent at the time of selection affecting funding decisions. HQ evaluates submitted technology development proposals, considering overall scientific and technical merit, programmatic relevance, and cost reasonableness given the scope of work. Awardees work to mature their technologies from their initial TRL, normally 3 or 4[§], through TRL 5. PIs report progress and plans to the Program Office periodically, and submit their technologies for TRL advancement review as appropriate. Progress in these projects allows infusion of newly mature technologies into NASA missions and studies, enabling and enhancing their capabilities with acceptable programmatic costs and risks.

As seen in the process graphic, the PATR plays an important role in our technology development process. Through PI reports and quad charts, it describes the status of all current investments in strategic COR technologies. It reports technology gaps articulated by the scientific community, and starting this year also by the large-mission-concept study teams, with a prioritized list of technologies for future solicitation and funding. The PATR is an open source for the public, academia, industry, and the government to learn about the status of enabling technologies required to fulfill COR science objectives. The report informs NASA organizations, including but not limited to the Astrophysics Division, and updates the community regarding technology development progress, as input for future technology gap submissions. Technological progress and programmatic decisions change the landscape of requirements for COR needs; therefore, the process is repeated annually to ensure continued relevance of priority ranking. Indeed, in any given year, new SAT award decisions are informed by PATRs published over the prior two years, a new SAT solicitation is informed by the prior-year PATR and the current year's TMB priority ranking, and the current PATR provides recommendations for next year's SAT.

§   TRL 4 is defined as: "*Component and/or breadboard validation in laboratory environment.*"

This technology development and maturation process identifies existing and emerging needs in a transparent manner, improves the relevance of COR technology investments, provides the community a voice in the process, and promotes targeted external technology investments by defining needs and identifying NASA as a potential customer for innovative technologies. It also identifies providers of technologies and expertise, the Program PIs, to potential customers and collaborators within and beyond NASA. This encourages industry and other players to invest in enabling technologies for future missions, and promotes formation of productive collaborations. Beyond involvement in the Decadal Survey process and technology gap submission, the science community is a key stakeholder in Program technology development activities. The community provides feedback and inputs to the technology development process; and participates in COPAG and other committees and workshops, ad-hoc studies, and in technology development by responding to SAT solicitations.

TRL Vetting

SAT funding helps mature technologies expected to enable and/or significantly enhance future strategic astrophysics missions. These technologies typically enter the SAT program at TRLs 3 or 4, and are intended to progress toward higher TRLs. TRL assertions above a technology's approved entry level are not official until a TRL-vetting TMB concurs with the development team's assessment. When PIs believe their team has demonstrated the required progress, they may request a review to present their case for TRL update. The Program Office then convenes a TMB consisting of Program Office and HQ senior staff along with subject matter experts to assess the request and, when warranted, approve the new TRL. The typical forum for such a request is during the PI's end-of-year presentation to the Program Office, but it can be made at any time. One project in the COR portfolio has already gone through this process, and the PIs of several more are considering TRL vetting this coming year.

Why review TRLs?

TRLs are used throughout the agency to help assess the maturity of technologies. The Program Office's charge includes a requirement that it monitor the progress of the Astrophysics Division's investments in technology maturation through SAT projects relative to the TRL plan and milestones submitted by the PI in the SAT proposal. A key indicator of such progress is TRL advancement as vetted by the Program Office, providing a consistent method of assessing progress across our full portfolio of projects.

What does our vetting mean?

When the Program's TMB approves a higher TRL asserted by the PI, it provides an independent assessment and verification that the project has achieved that TRL. The TMB consists of scientists, technologists, and systems engineers from the Program; and subject matter experts from the community and Aerospace Corporation, who provide an objective and informed assessment. The primary purpose for issuing this assessment is to inform the Program Office of significant progress in preparing the technology for possible infusion into strategic missions. It also informs the science community of an improved state of readiness.

What is expected?

The TRL vetting process is initiated when a PI notifies the Program Office that the milestones necessary for TRL advancement have been met. The PI team prepares a brief but compelling presentation that makes the case for the higher TRL, and the PI presents it to the TRL-vetting TMB which considers the TRL assertion. The TMB is guided by TRL definitions in NASA Systems Engineering Processes and Requirements, also known as NASA Procedural Requirement (NPR) 7123.1B. Recognizing that PI teams are busy and must concentrate their efforts on the work of maturing their technology, the Program Office is satisfied to rely on a cogent exposition of the same reports, graphs, and test results the team captures for its own records.

The Program Office has tools to help PIs assess their progress and is available to provide information on the TRL process. Finally, if the project is still ongoing, we recommend the PI present a plan for further TRL advances, if any, allowing the TMB to offer feedback and make recommendations.

What are the benefits for the PI and the Program?
The Program Office's TRL vetting process serves as an opportunity to capture and collect the needed documentary evidence and present it to a group of independent experts. This can strengthen a potential future TRL case presentation, whether in person or in writing, to flight projects, proposal teams considering adding the technology to their mission, and/or proposal reviewers. Another leveraging opportunity might be in collaboration opportunities. As alluded to above, the TMB can help the PI team fine-tune its plan for future work to achieve the claimed TRL if the current claim was not vetted, or for the next TRL if it was.

Finally, TRLs are NASA's technology development assessment language, and TRL advancement is one of the key success criteria for SAT projects. Our TRL vetting is an objective process, rendering an independent verification of achievement, increasing the credibility of the technology's maturity and its potential for continued funding, infusion into flight missions, and consideration by community assessments such as STDT studies and Decadal Surveys.

The COR Technology Development Portfolio as of 2016

For FY 2016, the driving objective is to maintain progress in key enabling technologies for the FIRS and LUVOIR Surveyor, to enable compelling cases for both in the upcoming 2020 Decadal Survey.

Eighteen COR SAT grants have been awarded to date. Table 2-1 provides top-level information on the 10 projects that received funding in FY 2016, including where each is described in detail in the appendices. Appendix B provides one-page "quad chart" project summaries, while Appendix C provides in-depth reports detailing development status, progress over the past year, and planned near-term development activities. The appendices provide technology overviews and status, not flight implementation details. For additional information, please contact the COR Program Office or the PIs directly. Contact information for each PI appears at the end of his or her report.

The Astrophysics Division collaborated with NASA's Space Technology Mission Directorate (STMD) in certain solicitations, developments, proposal reviews, and technology co-funding. The Division is open to collaboration efforts when possible, as this leverages limited funding to advance technologies that meet the respective goals of the collaborating organizations. Such joint investments are "win-win-win" opportunities for the Astrophysics Division, STMD (or other organizations), and the PI. The Program looks forward to implementing additional jointly beneficial opportunities in the future.

Strategic Astrophysics Technology Selection for FY 2017 Start

The COR Program funds SAT investigations to advance the maturation of key technologies to make feasible their implementation in future flight missions. The Program focuses on advancing those technologies most critical for substantive near-term progress on strategic priorities. Three technology areas were called out in the 2015 COR SAT solicitation as being of particular interest for the Program: next-generation detectors from the extreme UV to Far-IR; optical coatings, gratings, and filters; and precision large optics.

Technology Development Title	PI	Institution	Start Year & Duration	Current TRL	Quad Chart & PI Report Page Locations
Ultraviolet Coatings, Materials, and Processes for Advanced Telescope Optics	K. 'Bala' Balasubramanian	JPL	FY13; 3 yrs	3	56, 67
Advanced FUVUV/Visible Photon-Counting and Ultralow-Noise Detectors	Shouleh Nikzad	JPL	FY16; 3 yrs	3	57, 82
Development of Digital Micro-mirror Device (DMD) Arrays for use in Future Space Missions	Zoran Ninkov	RIT	FY14; 3 yrs	4	58, 88
Ultra-Stable Structures: Development and Characterization Using Spatial Dynamic Metrology	Babak Saif	GSFC	FY16; 4 yrs	3	59, 95
Improving UV Coatings and Filters using Innovative Materials Deposited by ALD	Paul Scowen	ASU	FY16; 3 yrs	4	60, 97
Advanced UVOIR Mirror Technology Development for Very Large Space Telescopes	H. Philip Stahl	MSFC	FY14; 3 yrs	3	61, 105
Cross-Strip Micro-Channel-Plate Detector Systems for Spaceflight	John Vallerga	UC Berkeley	FY16; 2 yrs	4	62, 114
Raising the Technology Readiness Level of 4.7-THz Local Oscillators	Qing Hu	MIT	FY16; 3 yrs	3	63, 131
A Far-Infrared Heterodyne Array Receiver for CII and OI Mapping	Imran Mehdi	JPL	FY14; 3 yrs	4	64, 134
Kinetic Inductance Detector Arrays for Far-IR Astrophysics	Jonas Zmuidzinas	Caltech	FY13; 3 yrs	3	65, 145

Table 2-1. *COR Technology Development Portfolio as of FY 2016 (organized by science topic and PI name). Note that project durations include approved no-cost extensions.*

The COR SAT proposals selected for FY 2017 start, announced in August 2016, advance two technologies in two of these areas (Table 2-2). The first effort is in the area of large precision optics, specifically to develop and demonstrate predictive thermal control technology to effectively enable a thermally stable space telescope. The second is in the area of next-generation detectors. This investigation proposes to develop a compact Adiabatic Demagnetization Refrigerators (ADRs) continuous cooling system to simplify and optimize the thermal design for the requirements of future focal-plane assemblies. These technology areas address the requirements of most strategic astrophysics missions, including FIRS, the LUVOIR Surveyor, XRS, and the HabEx Imaging Mission.

Technology Development Title	PI	Institution	Duration	Initial TRL	Abstract Page Locations
Predictive Thermal Control Technology for Potential HabEx Mission	H. Philip Stahl	MSFC	3 years	3	153
High-Efficiency Continuous Cooling for Cryogenic Instruments and Sub-Kelvin Detectors	James Tuttle	GSFC	3 years	3	154

Table 2-2. *COR SAT Development Starts in FY 2017 (alphabetically by PI).*

These new SAT selections were based on the following factors:

- Overall scientific and technical merit;
- Programmatic relevance of the proposed work, including urgency; and
- Cost reasonableness of the proposed work.

Since these projects have only recently been selected for funding, their status is not presented yet. First-year progress for each will appear in the 2017 COR PATR, with only abstracts appearing in this year's Appendix C.

Large-Mission-Concept Studies toward the 2020 Decadal Survey

As mentioned in Section 1, this year the Astrophysics Division set up STDTs to study four large-mission concepts – FIRS, HabEx Imaging Mission, LUVOIR Surveyor, and XRS. The STDTs are each charged to develop the science case and design reference mission, assess technology development needs, and estimate the cost of their mission concept. These studies will guide our efforts to mature technology components and architectures required to offer four equally compelling cases for the 2020 Decadal Survey's consideration. Similarly, the L3ST was chartered to help us understand how NASA might participate in ESA's L3 GW mission, inform our engagement through L3's earliest stages, and prepare for the 2020 Decadal Survey.

Each of these ambitious mission concepts promises breakthrough science results, but implementing them will require us to overcome daunting technology development challenges. The SAT program is certain to play a major role in funding these technology development efforts. We encourage all members of the community to support our efforts to identify the highest-priority technology gaps we need to close to make these missions feasible, and continue to submit proposals in response to SAT solicitations. As of this writing, notices of intent to submit for the next SAT round are due January 20, 2017, with proposals due March 17, 2017. As described in Section 3, starting this year, the FIRS and LUVOIR Surveyor STDTs provide their own technology gap lists to the COR Program Office. The Program Office combined these lists with the one reviewed by the COPAG EC, and submitted the resulting list to the TMB for prioritization.

Historical Record of TCOR Proposals and Awards

The TCOR section of the SAT program (Table 2-3) received 14 proposals in response to the 2010 solicitation, its first year; 24 for 2011; 13 for 2012; none for 2013 as the Program did not solicit SATs that year; 14 for 2014; and 12 for 2015. Of the first set, three proposals were selected, with five more the following year, three in the third year, four last year, and as reported here, two selected in the latest round. This makes the historical selection rate for COR SAT proposals 22%, with the latest round selecting 17% of submissions.

Solicitation Year	TCOR Proposals		Proposal Success Ratio
	Submitted	Awarded	
2010	14	3	21%
2011	24	5	21%
2012	13	3	23%
2013	Not solicited	N/A	N/A
2014	14	5	36%
2015	12	2	17%
Total to Date	**77**	**18**	**23%**

Table 2-3. *Number of TCOR SAT Proposals and Awards.*

3. Technology Gaps, Priorities, and Recommendations

Enabling strategic astrophysics missions that are decades away requires identifying and closing gaps between state-of-the-art (SOTA) performance and that required for those missions. As current technologies develop and mature and as our understanding of the missions' concept designs mature, those gaps evolve.

As shown in Fig. 2-1, we solicit technology gaps from the community on an ongoing basis. Anyone may submit a technology gap directly to the Program Office, downloading a form from the COR website, or through the COPAG. Gaps may be submitted throughout the year, however, since gaps are assessed and prioritized annually in late July, the Program Office set a June 1 cutoff date for consideration in the same year. This allows the COPAG EC to review the list of gaps for completeness, merge overlapping gaps, and complete and improve entries where the submission did not adequately address the requested information. Then, the EC returns the list to the Program Office for final preparation for the TMB's assessment.

To maximize the likelihood of high priority ranking, the Program Office encourages submitters to include as much of the information requested as possible. Importantly, we ask submitters to describe a capability gap, not a specific implementation process or methodology. The goals and objectives should be clear and quantified. Additionally, a complete description of the needed capability with specific performance goals based on mission needs is very valuable. Such information serves several important purposes:

1. The TMB is best able to understand and thus correctly assess the identified technology gap.
2. NASA HQ is best able to develop precise technology development proposal calls.
3. The community is clearly informed and best able to match candidate technologies to mission needs.

Aside from submitter information, the technology gap form requests the following information:

- **Technology gap name:** Identifies the gap, and optimally the type of mission filling it would enable;
- **Brief description:** Summarizes the technology gap and associated key performance criteria; in general, well-defined technology gaps receive higher priority than vague ones;
- **Assessment of TRL:** Describes the SOTA, allowing the TMB to appreciate the gap between what's available and what's needed – **SOTA TRL** Specifies the current TRL per NPR 7123.1B Appendix E of relevant SOTA technology; and **Full-Solution TRL** Specifies the current TRL of candidate technologies that could provide a full solution; the SAT program funds projects to advance technologies from TRL 3 up through TRL 5, so those with full solutions already at TRL 6 rank lower unless the existing technology is significantly deficient in some significant way (e.g., cost, complexity, yield, etc.); note that full-solution TRL can never exceed the SOTA TRL, else this full-solution technology would *be* the SOTA;
- **Target goals and objectives:** Details the quantifiable goals and/or objectives for a candidate technology to fill the described gap. For example, "*The goal is to produce a detector with a sensitivity of X over a wavelength of Y to Z nm;*" Technology gaps with clearly quantified objectives may receive higher priority than those without quantified objectives;
- **Scientific, engineering, and/or programmatic benefits:** Describes the benefits of closing the technology gap; for enabling technology, describes how and why it is such; if enhancing, describes, and if possible quantifies, the impact; benefits could be better science, lower resource requirements (e.g., mass, power, etc.), and/or programmatic (e.g., reduced risk, cost, or schedule); for example, "*Material X is 50% stronger than the current state of the art and will enable the optical subsystem for a 2-m telescope to be Y kg lighter;*" technology gaps with greater potential mission benefits receive higher scores;

- **Application and potential relevant missions:** Technologies enabling or enhancing missions ranked highly by the AIP, Astrophysics Roadmap, or NWNH, will score higher; technologies applicable to a wide range of COR missions, as well as PCOS and/or ExEP missions will rank better; and
- **Time to Anticipated Need:** Specifies when the strategic mission enabled or enhanced by the technology is planned to launch. In cases where there is a more immediate driving need (e.g., demonstrating credibility in time for consideration by the 2020 Decadal Survey), this driving requirement is also considered; technology gaps with shorter time windows relative to required development times receive higher priority.

Technology Gaps Submitted to the 2016 TMB

As in 2015, the COPAG EC agreed to review the list of technology gaps compiled by the Program Office. The Program Office forwarded to the EC 20 gaps from the 2015 TMB list plus 12 new community entries, where four were minor edits to 2015 gaps, that were included in the relevant gaps. We thank the community for their engagement in this process and for their thoughtful gap submissions. The EC thus received a list of 28 gaps in all, and after removing one entry considered as not being a technology gap, returned the remaining 27 gaps, commenting that there was quite a bit of duplication and questionable statements as to state-of-the-art for some technologies. The EC is considering setting up a Technology Interest Group (TIG) to provide rigorous fact-checking of statements made in technology gap entries. In parallel, the two STDTs submitted to the Program Office a combined 15 gaps. The LUVOIR Surveyor STDT submitted seven gaps, identifying three as "highest priority," and four as "important;" while the FIRS STDT submitted eight. Of the seven LUVOIR gaps, two were deemed outside the scope of COR science, and removed from the COR TMB list as more appropriate for prioritization by the ExEP Program Office. To facilitate and streamline the TMB prioritization process, a subset of the full TMB consolidated the remaining 40 entries into 26 unique gaps, of which six were new relative to the 2015 list. At the start of the its meeting, the full TMB decided to further merge gaps, resulting in a final list of 18 distinct gaps that were prioritized. Almost all technologies developed to close these gaps would enable and/or enhance high-priority strategic missions per the AIP, the Astrophysics Roadmap, and/or NWNH. We deeply appreciate the efforts of the EC, LUVOIR Surveyor STDT, and FIRS STDT, and look forward to continued collaboration in the future. Having the EC and study teams review gap entries and propose new ones where appropriate, prior to TMB prioritization, serves several important purposes:

- Providing a set of expert-vetted, unique, and compelling technology gaps, such that the resulting entries potentially merit higher priority ranking;
- Ensuring the gaps accurately reflect the current situation per the community and study teams; and
- Making the process of generating unique technology gaps more transparent to the community.

Prioritizing Technology Gaps

In its prioritization meeting, the TMB followed an agreed-upon set of evaluation criteria, resulting in the priorities shown below. TMB membership included senior staff from NASA HQ Astrophysics Division, the Program Office, STMD, and the Aerospace Corporation. For 2016, the TMB used a prioritization approach similar to that used in prior years, with a streamlined set of four criteria. These included strategic alignment, benefits and impacts, scope of applicability, and urgency.

- **Strategic alignment:** How well does the technology align with COR science and programmatic priorities of current programmatic guidance (i.e., AIP, Roadmap, and NWNH)?
- **Benefits and impacts:** How much impact does the technology have on COR-relevant science in applicable mission(s)? To what degree does the technology enable and/or enhance achievable science objectives, reduce cost, and/or reduce mission risks?
- **Scope of applicability:** How cross-cutting is the technology? How many Astrophysics programs and/or mission concepts could it benefit?
- **Urgency:** When are launches and/or other schedule drivers of missions enhanced or enabled by this technology anticipated?

The TMB assigned weighting factors, reflecting the relative importance placed on each criterion. Each technology gap received a score of 0 to 4 for each criterion. The scores were multiplied by their respective weights, and the products were summed. Some technologies could be scored based on several missions or mission classes. In such cases, the TMB scored each scenario independently, assigning the highest overall score (e.g., a gap might receive an overall score of 91 for a highly aligned mission, but only 75 for a less-aligned class of missions, in which case it would be assigned the higher score). Table 3-1 details the criteria descriptions, weighting factors, and TMB scoring guidelines.

Criterion	Weight	Max Score	Max Weighted Score	General Description/ Question	4	3	2	1	0
Strategic Alignment	10	4	40	How well does the technology align with COR science and programmatic priorities of current programmatic guidance (i.e., AIP, Roadmap, NWNH)?	Technology enables COR-relevant science within mission concept receiving highest programmatic consideration or recommended by an STDT	Technology enables COR-relevant science within mission concept receiving mid to high programmatic consideration in AIP or in Roadmap as "Surveyor" but not being studied	Technology enables COR-relevant science within mission concept receiving low current programmatic consideration in AIP or Roadmap	Technology enables COR-relevant science within mission concept not considered in AIP or Roadmap, but positively addressed in NWNH	Technology does not enable COR-relevant science within any mission concept considered by current programmatic guidance
Benefits and Impacts	8	4	32	How much impact does the technology have on COR-relevant science in applicable mission(s)? To what degree does the technology enable and/or enhance achievable science objectives, reduce cost, and/or reduce mission risks?	Critical and key enabling technology; required to meet COR-science-relevant mission concept objectives; without this technology, mission would not launch or COR science return would be significantly impaired	Highly desirable; not mission-critical to COR-science-relevant objectives, but significantly enhances COR science capability, reduces critical resources needed, and/or reduces mission risks; without it, missions may launch, but COR science return would be compromised	Desirable; not required for COR-science-relevant mission success, but offers significant COR-relevant science or implementation benefits; if technology is available, would almost certainly be implemented in missions for COR purposes	Minor COR-relevant science impact or implementation improvements; if technology is available would be considered for implementation in missions for COR purposes	No COR-relevant science impact or implementation improvement; even if available, technology would not be implemented in missions for COR purposes
Scope of Applicability	3	4	12	How cross-cutting is the technology? How many Astrophysics programs and/or mission concepts could it benefit?	Applies widely to COR mission concepts and both PCOS and exoplanet mission concepts	Applies widely to COR mission concepts and either PCOS or exoplanet mission concepts	Applies widely to COR mission concepts	Applies to a single COR mission concept	No known applicable COR mission concept
Urgency	4	4	16	When are launches and/or other schedule drivers of missions enhanced or enabled by this technology anticipated?	Launch anticipated in next 5-9 years (2021-2025) or other schedule driver requires progress in 3-4 years (2019-2020)	Launch anticipated in next 10-14 years (2026-2030) or other schedule driver requires progress in 5-9 years (2021-2025)	Launch anticipated in next 15-19 years (2031-2035)	Launch anticipated in next 20-24 years (2036-2040)	Launch anticipated in 25 or more years (2041 or later)

Table 3-1. *Clear, strategic criteria provide a rigorous, transparent process for prioritizing technology gaps.*

This process provides a rigorous and transparent ranking of technology gaps based on the Program's goals, community scientific rankings of relevant missions, Astrophysics Division priorities as outlined in the AIP and Astrophysics Roadmap, and the external programmatic environment. Since the SAT program is intended to promote development and maturation of technologies relevant to missions and concepts identified as strategic, the strategic alignment criterion is driven by strategic documents such as the AIP, the Astrophysics Roadmap, and the NWNH. The AIP details highly ranked science missions and technology development, which for COR include instruments to be flown on SOFIA and technologies for future UV/Vis/Far-IR missions; and prioritizes those based on current budget realities. This year, the TMB considered technologies identified by the FIRS and LUVOIR STDTs as having the highest strategic alignment, and SOFIA instrument technologies considered highly aligned.

Prioritization Results

As mentioned above, in 2016, the COR TMB received 26 technology gap entries, and after some merging, prioritized 18 entries. Reviewing the scores, the TMB binned the technology gaps into three groups based on a number of factors, including primarily a natural grouping of overall scores.

Priority 1: Technologies the TMB determined to be of the highest interest to the COR Program. Advancing these key enabling technologies is judged to be most critical to making substantive near-term COR-science-relevant progress on the highest-priority strategic astrophysics missions, including FIRS and the LUVOIR Surveyor. The TMB recommends SAT calls and award decisions address these technology gaps first.

Priority 2: Typically, technologies the TMB believes would be highly desirable or desirable for a variety of strategic missions. The TMB recommends that should sufficient funding be available, SAT calls and award decisions address closing these technology gaps as well.

Priority 3: Technologies the TMB deemed supportive of COR objectives, but scoring lower than Priority 1 and 2 technology gaps.

Table 3-2 lists the gaps prioritized by the TMB, including gap names, science topics addressed, gap submission sources, 2016 assigned priorities, and where in Appendix A you can find detailed gap entries.

From 2011 through 2016, nearly all gaps achieving Priority 1 maintained that rank or changed by one level due to minor shifts in how priority scores break up naturally into groups. Also, funded projects have addressed high-priority gaps, mostly Priority 1, and occasionally Priority 2. For example, six of the nine 2016 Priority 1 gaps have already been addressed by SAT projects or will be addressed by 2017-start SATs, as have three of the seven Priority 2 gaps.

2016 Priority	Technology Gap Name	Science Addressed	Submitted By	Gap Detail Page Location
Priority 1	Large-format, low-noise and ultralow noise Far-IR direct detectors	FIR	FIRS STDT and General Community	44
	Heterodyne Far-IR detector arrays and related technologies	FIR	FIRS STDT and General Community	45
	Large cryogenic optics for the Far-IR	FIR	FIRS STDT and General Community	49
	High-performance, sub-Kelvin coolers	FIR	FIRS STDT and General Community	51
	Compact, Integrated Spectrometers for 100 to 1000 μm	FIR	FIRS STDT	53
	Large-format, high-sensitivity, high-dynamic-range UV/FUV detectors	UV/FUV	LUVOIR STDT	30
	High-efficiency UV multi-object spectrometers	UV	General Community	32
	Band-shaping and dichroic filters for the UV/Vis	UV/Vis	General Community	40
	Lightweight large-aperture high-performance telescope mirror systems	UV/Vis/IR	General Community	33
Priority 2	Advanced Cryocoolers	FIR	FIRS STDT and General Community	52
	Mid-IR spectral coronagraph	Mid-IR	FIRS STDT	54
	High-performance spectral dispersion component/device	UV/Vis/IR, FIR	General Community	39
	High-reflectivity mirror coatings for UV/Vis/NIR	UV/Vis/IR	LUVOIR STDT and General Community	42
	High-contrast segmented aperture coronagraphy	UV/Vis/IR	LUVOIR STDT	35
	Ultra-stable opto-mechanical systems	UV/Vis/IR	LUVOIR STDT	36
	Very-large-format, high-QE, low-noise, radiation-tolerant detectors for UV/Vis/NIR	UV/Vis/IR	LUVOIR STDT and General Community	28
Priority 3	Wide-bandwidth, high-spectral-dynamic-range receiving system	FIR	General Community	47
	FIR interferometry	FIR	FIRS STDT and General Community	50

Table 3-2. *Summary of 2016 COR technology gaps and their TMB-assigned priorities. Gaps shown by priority tier and science theme. All gaps within a specific tier have equal priority.*

The Program Office continues to solicit and compile technology gap submissions from the community, and as was done this year, will maintain its collaboration with the EC and study teams to ensure the gaps ranked by the TMB continue to be complete, distinct, and compelling.

4. Benefits and Successes Enabled by the COR SAT Program

The main benefit of the SAT program is in maturing technologies across the mid-TRL gap, so they can be infused into strategic COR missions and/or international collaborative missions relevant to Program goals, as part of a US contribution. All SAT projects have made significant progress in maturing their technologies, with several claiming TRL advances in at least some aspects of their technologies. These have yet to be vetted by a TMB.

Where appropriate, newly matured technologies may also be implemented in ground-based projects, suborbital experiments, Explorers, and Probe-class missions. These often extend beyond the COR Program to PCOS, ExEP, and even beyond missions managed by Astrophysics Division.

The following are examples of TCOR SAT project developments contributing to missions and projects:

- H4RG Near-IR detectors matured with SAT support were adopted by WFIRST (PI, Bernard Rauscher);
- TES bolometer detector was selected to support the SOFIA HAWC instrument (PI, S. Harvey Moseley);
- HIRMES was selected as a third-generation facility for SOFIA (PI, S. Harvey Moseley);
- Advanced UV-reflective coatings, matured with SAT support, were implemented on Explorer missions ICON and GOLD (PI, Manuel Quijada);
- Heterodyne detector technology matured with SAT support was incorporated into the Stratospheric TeraHertz Observatory (STO) balloon experiment, and is baselined for a proposed third-generation SOFIA instrument, Stratospheric Heterodyne Array for Spectroscopic Terahertz Astronomy (SHASTA), intended to study large-scale, high-angular resolution FIR spectral line images of the Milky Way and nearby galaxies (PI, Imran Mehdi); and
- Advanced high-efficiency, photon-counting CCD detectors, matured with SAT support, were implemented into the FIREBall long-duration balloon mission, the Guide and Focus CCDs for Wafer-Scale Imager for Prime (WaSP) instrument at Palomar, and for Caltech Optical Observatory's Zwiki Transient Facility (PI, Shouleh Nikzad).

As in prior years, the Program Office surveyed current PIs about additional benefits resulting from their SAT funding. Of the 10 PIs represented in this PATR, five provided information about collateral benefits. Of these, three reported they were able to leverage SAT funding to generate other support, (e.g., co-funding from a DARPA project and a Caltech Summer Undergraduate Research Fellowship), set up collaborations with researchers at other institutions on proposals and new programs, and generate industry interest in their technologies. All five PIs report having hired students and/or post-doctoral fellows to assist their technology development work (slightly more on average than one undergraduate student, two graduate students, and one post-doctoral fellow per project), helping train the next generation of researchers and technologists needed to support future missions (Fig. 4-1). The PIs reported that former students and post-docs have proceeded to PhD programs, and positions at other institutions and high-tech industry; proving that the SAT Program is helping train and shape the future astrophysics work force as well as the wider technological work force. Several PIs went on to successfully propose additional technology development projects through the SAT and APRA programs, including one of the two new COR SATs selected for FY 2017 start, as well as non-astrophysics programs.

Involving Students and Postdocs in SAT Projects

The COR SAT projects have involved dozens of students and postdocs, helping train the future astrophysics workforce (see Appendix C for details). As can be seen in the following quotes, the Program is making a deep impact on these future technologists, and through them promotes astrophysics missions over many decades to come.

The work... was interesting and exciting and even as... a graduate student, I was able to make significant contributions to the project... taught me to never accept current technology as good enough – detectors... coatings... telescopes can be made better.
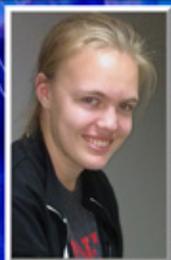
After completing my degree requirements, I converted to a full-time civil servant as an optical engineer in the thinfilms coatings laboratory at NASA/GSFC...

It is very rewarding, as a scientist, to know that my effort on this project will produce results which will be useful for instrument designers (including myself) in the future.

In June 2016, the Program presented a poster of COR and PCOS technology development at the SPIE meeting in Edinburgh, Scotland (Fig. 4-2), displaying the breadth of scope of our SAT investment, explaining the Programs' technology development process and current priorities, and explaining how the four large-mission-concept STDTs will be involved in technology development. A similar poster was presented at the January 2016 American Astronomical Society (AAS) meeting in Kissimmee, Florida.

Fig. 4-2. *Poster presented at the June 2016 SPIE meeting in Edinburgh, Scotland. The Program promotes exposure of current technology developments and investment priorities at national and international meetings, and informs the community of upcoming SAT funding opportunities.*

The Broad Impacts of the SAT Program

Figure 4-3 depicts the geographic breadth of SAT program (both COR and PCOS) impacts, showing the locations of our PI institutions, their collaborators and partners, and the universities and colleges where the students and post-doctoral fellows involved in SAT projects attend school and work.
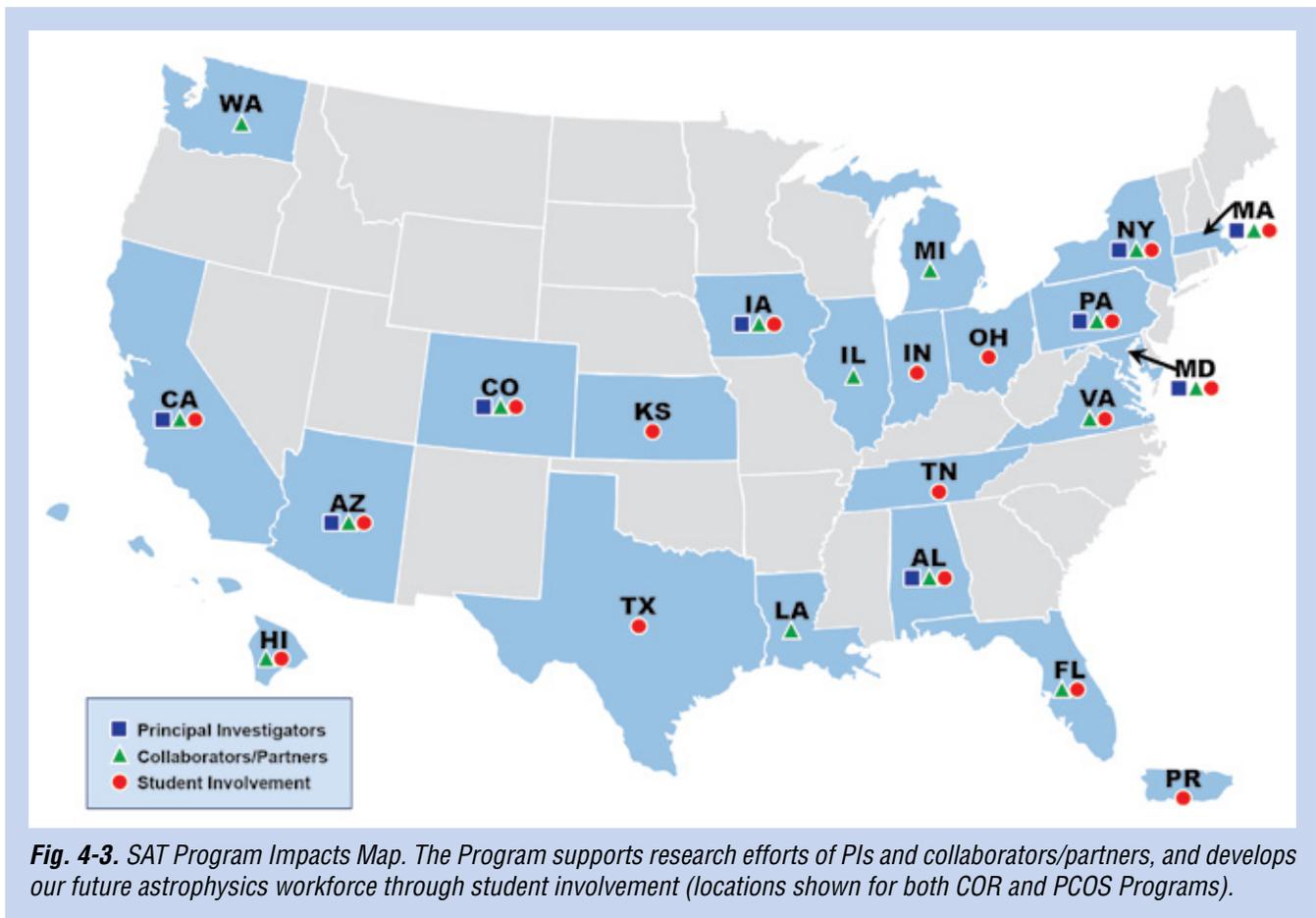
Fig. 4-3. *SAT Program Impacts Map. The Program supports research efforts of PIs and collaborators/partners, and develops our future astrophysics workforce through student involvement (locations shown for both COR and PCOS Programs).*

5.   Closing Remarks

This 2016 COR PATR serves as a snapshot of the dynamic state of technology development managed by the Program Office and provides future directions for technology planning and maturation. As we complete another year of COR technology development activities, we see many positive developments.

Our technology development portfolio is growing, and continues to deliver significant advancements. All funded technologies are maturing toward higher TRLs, with several providing direct benefit to ground-based experiments and flight missions. New SAT awards slated to start in FY 2017 will fund thermal control and cooling technology work applicable to future COR, PCOS, and ExEP missions. COR SAT investments are also generating benefits beyond direct advancement of strategic technologies. This includes leveraging internal and external (including non-NASA) funding; using contributed materials, parts, and facility/equipment; hiring students and post-docs, thereby training our future astrophysics workforce; and generating research collaborations and industry partnerships, in support of COR science goals.

Our technology gap prioritization process continues to adhere to strategic guidance based on the AIP; Astrophysics Roadmap "Surveyor" concepts, especially those being studied by STDTs; and NWNH; with the TMB assigning the most significant weight in technology gap prioritization to strategic alignment. As a result, the Astrophysics Division is likely to continue to fund SAT proposals addressing technology gaps identified by the TMB as having the highest priority. The latest set of highest-priority TMB recommendations, submitted to the Astrophysics Division and reported here, include technology developments related to the FIRS and LUVOIR Surveyor.

To support the ever-evolving technology needs of the COR community, we continue to interact with the broad scientific and technical communities through the COPAG, through various workshops, via public outreach activities, and at public scientific conferences. These activities identify and incorporate the astrophysics community's ideas about new science, current technology progress, and new needs for technology in an open and proven process. Each year, we incorporate new lessons learned and make appropriate improvements to our process. In parallel, we incorporate the technology needs identified by the large-mission-concept study teams into our technology gaps identification and prioritization process.

We would like to thank the COR scientific and technical communities, the PIs and their teams, the COPAG EC, and the large-mission-concept STDTs for their efforts and inputs that make this annual report current and meaningful. We welcome continued feedback and inputs from the community in developing next year's PATR, which should be sent to Program Office Technology Development Manager. For more information about the Program and its activities, or to provide your feedback and inputs, please visit the COR website.

References

[1]   J. Mankins, "*The critical role of advanced technology investments in preventing spaceflight program cost overrun*", The Space Review, December 1, 2008. Available at http://www.thespacereview.com/article/1262/1. Accessed May 2014

[2]   National Research Council, "*New Worlds, New Horizons in Astronomy and Astrophysics,*" Washington, DC: The National Academies Press, 2010. Available at www.nap.edu/catalog.php?record_id=12951. Accessed May 2014

Appendix A
Technology Gaps Evaluated by TMB in 2016

This appendix details the technology gaps prioritized by the COR Program Technology Management Board (TMB) in 2016. These are gaps between the current state of the art (SOTA) technology readiness levels (TRLs, defined in Table A-1) and capabilities needed for future missions.

The order of the gaps is similar to that of prior-year Program Annual Technology Reports (PATRs). Specifically, we've grouped the gaps by science topic, and within that, by technology type. Where submitted gaps had significant overlap, they were merged into a single gap by the COR Program Analysis Group (COPAG) Executive Committee (EC) or by the TMB. Gap priority ranking is shown on p. 20 above. Submitted entries not ranked may have been merged into others; deemed outside the purview of the COR program (e.g., better addressed by SAT programs other than COR or associated with launch vehicles, rovers, avionics, spacecraft systems, etc.); deemed as not being technology gaps (i.e., specific implementations or not technologies at all); or deemed too mature for the SAT program.

Each entry lists the source of the gap next to the gap name. Sources include the general community, a large-mission-concept study team, or both. This last case is the case where similar gaps were submitted both by a member of the general community and a study team, and the TMB merged the gaps. We thank the EC, the Far-IR Surveyor (FIRS) Science and Technology Study Team (STDT), the Large UV/Optical/IR (LUVOIR) STDT, and the general community for their engagement in and support of our technology gap identification process.

The Program Office considers gaps submitted by a study team, or by both the community and a study team, as "owned" by the study team until the team submits its final report. In practical terms, this means that the Program Office will forward to the study team any edits to such a gap that are submitted by the general community by the June 1 deadline. The study team will then consider these edits for possible inclusion into the following-year version of the gap. The study teams' unmatched expertise in the technology needs of their respective mission concepts gives great credibility to their opinions on such technologies; increasing the likelihood of higher priority ranking for gaps owned by the teams.

TRL	Definition
1	Basic principles observed and reported.
2	Technology concept and/or application formulated.
3	Analytical and experimental critical function and/or characteristic proof-of-concept.
4	Component and/or breadboard validation in laboratory environment.
5	Component and/or breadboard validation in relevant environment.
6	System/subsystem model or prototype demonstration in a relevant environment.
7	System prototype demonstration in an operational environment.
8	Actual system completed and "flight qualified" through test and demonstration.
9	Actual system flight proven through successful mission operations.

Table A-1. *TRL definitions from* NASA Procedural Requirements (NPR) 7123.1B Appendix E*, which provides a full description of the TRLs.*

Gap Name	Very-large-format, high-QE, low-noise, radiation-tolerant detector arrays for UV/Vis/NIR *Submitted by LUVOIR STDT and General Community*
Description	Observations in astronomy typically require a combination of large format, high quantum efficiency (QE), and low noise to achieve photon- or sky-background-limited sensitivity over the full field of view (FOV) of a telescope or spectrograph. Large-format, high-QE detectors with very low intrinsic read-noise and dark current are essential in the UV, where sky background is low; and in some Vis/NIR applications where high cadence (time-domain studies and high-contrast imaging applications) or high spectral resolution are needed. For NIR high-contrast imaging applications, non-cryo technologies are of particular interest to help mitigate vibration concerns associated with cryocoolers. Detector arrays need to provide fast measurements with high dynamic range in high-radiation environments. They also need to be mosaicable into Gpix formats. The LUVOIR STDT identified as a medium urgency gap "Vis/NIR detectors for exoplanet science" which is more than addressed by this entry
Current State-of-the-Art (SOTA)	Current SOTA achieves only part of the required capability. Flight systems (e.g., Kepler and Gaia) include moderate-sized (0.1 Gpix) mosaicked CCD focal-plane arrays (FPAs) with modest noise performance (1~5 e-/pix/read, and dark current of 0.01 e-/s/pix). Some MCPs (0.016 Gpix) have low-to-moderate QE (10-40%), zero-read-noise (photon-counting) capability and very low dark current (< 0.000001 e-/pix/s). Visible-photon-counting Mpix EMCCDs achieved QE > 60%, but reducing clock-induced charge would be beneficial. Arrays of transition-edge sensors (TESs) and microwave kinetic inductance detectors (MKIDs) have been used at telescopes for UVOIR astronomy, with spectral resolution R ~ 10, and R ~ 100 feasible. Relevant technologies include TES KIDs, and superconducting tunnel junctions. CCDs and HgCdTe arrays in few-megapixel formats are at TRL > 6. However, CCDs are not radiation-hard. Radiation-hard HgCdTe arrays theoretically have sensitivity through the NUV when the substrate is removed. Scientific use in this wavelength regime hasn't been explored extensively and there is the potential of severe QE degradation or even device damage. In general, hybrid CMOS detectors (including HgCdTe) have higher readout noise than the best CCDs. NIR photon-counting HgCdTe arrays have much higher dark-count rates. State of the art for NIR photon counting is arguably HgCdTe APD arrays, pioneered by the defense community for laser communications and laser range-gated imaging. They have also benefitted from substantial NASA investment for LIDAR, but are lower TRL (~3). Groups such as U. Hawaii and the European Southern Observatory started working with APD arrays for astronomy, with an initial application of wavefront sensing. Although promising, the < 0.001 e-/s/pixel dark-current rates required for spectroscopic biomarker detection with coronagraphs has yet to be demonstrated. Moreover, there are practical reasons why good impact-ionization gains may be inconsistent with the required ultra-low dark current using existing HgCdTe fabrication technology. Estimated current cost is > ~0.1 $/pixel

TRL	SOTA	4
	Solution	

Performance Goals and Objectives	Target goals for detector arrays are: • Wavelength range 400 – 2500 nm, possibly using more than one array; • Pixel-count 1-4 (0.25-1) Gpix UV/Vis (NIR) possibly through mosaicability; • Pixel size 5-10 (10-20) microns UV/Vis (NIR) to achieve diffraction-limited imaging given typical telescope designs; • QE > 0.5 (> 0.9) UV (Vis/NIR); • Read-noise: < 0.1 (< 1) e-/pix/read UV (Vis/NIR); • Dark current: <0.000003 (<0.00003) e-/s/pix UV (Vis/NIR) at typical operating temperatures (superconducting solutions at cryo temperatures are a possible avenue, though non-cryo solutions may be preferred for coronagraph applications to reduce the impact of vibrations from cryocoolers on wavefront error stability); • Well-depth: > 2×10^5 e-; • Ionizing-radiation tolerance sufficient for many years at L2; and • Cost < 0.01-0.001 \$/pixel.
Scientific, Engineering, and/ or Programmatic Benefits	Detector QE and FOV determine instrument etendue, which sets instrument survey power. Higher etendue allows deeper or wider astronomical surveys with space-based telescopes on much shorter timescales. It also enables instrument designs that exploit the telescope aperture size and full working FOV. UV, Vis, and/or NIR detectors that simultaneously achieve all these technical goals are essential for maximizing future space observatory science return, increasing mission science impact ×10-1000, depending on areal coverage and QE. Deep full wells with low persistence and radiation tolerance enable transit imaging and spectroscopy at all wavelengths. Photon-counting visible and NIR arrays will enable coronagraphic spectroscopy for bio-signature characterization and starlight-suppression wavefront sensing. Superconducting detectors may be especially interesting. Because of the very small superconducting gap (compared to semiconductor band gaps), it is possible to detect and count individual photons with minimal read noise and dark current, though they would need to be optimized for the required spectral resolution. Moreover, by exploiting the energy resolution these technologies offer, it should be possible to achieve spectroscopic resolution R ≥ 70 in the pixel. These essentially quantum-limited detectors could potentially mitigate cost and associated complexity.
COR Applications and Potential Relevant Missions	This is a key technology for a LUVOIR mission. The ATLAST mission concept identified a (400 - 1800 nm) exoplanet imager and spectrograph as key instruments for the mission and these need visible-photon-counting detectors for starlight-suppression wavefront sensing and control, and spectroscopy. Other relevant missions include Probe-class and Explorer missions that can conduct wide-field surveys, enabling them to obtain science currently only available with much larger apertures. They would also greatly increase the science return of small-sat or suborbital experiments that can advance technology while addressing one or more COR science objectives. These detectors are crosscutting technologies, applicable for astrophysics, planetary, and space sciences. Biological, medical, and security/surveillance applications will also benefit from pushing the limits of sensor technology, particularly for low-light imaging.
Time to Anticipated Need	Need to demonstrate credibility before the 2020 Decadal Survey, and would require TRL 6 by mission PDR anticipated in the mid-2020s. Rapid development and availability of these arrays will enable numerous classes of missions from suborbital, through Explorers and Probes, to strategic missions even sooner.

Gap Name	Large-Format, High-Sensitivity, High-Dynamic-Range UV/FUV Detectors *Submitted by LUVOIR STDT*
Description	Future large aperture sizes and unprecedented stability will naturally provide gains in sensitivity and image quality at all wavelengths. However, in order to enable new science in the UV, additional improvements are required in UV detector sensitivity (QE, radiation hardness, and noise performance), dynamic range, and pixel count.
Current State-of-the-Art (SOTA)	There are three basic technologies considered for UV detectors. Micro-channel plates (MCPs) with "solar-blind" photocathodes, low dark current, and zero read noise that are fairly mature and have rich flight heritage. However, MCPs have limited dynamic range and issues with long-term "gain-sag" (burn-in of regions exposed to prolonged high illumination levels). Delta-doped electron-multiplying charge-coupled devices (EMCCDs) offer new options in terms of format and dynamic range, but are less mature, less solar-blind, and less robust with respect to the radiation environment. Commercially available, low-noise scientific complementary metal-oxide-semiconductor (sCMOS), if optimized for the UV, offer another interesting direction for technology development. A principal goal for all technologies is the development of a large-format detector with high pixel count to allow for wide-field imaging and multi-object spectroscopy (MOS) in the UV. All technologies need additional development to achieve these high fill-factor focal planes with a large pixel count, while maintaining other capability requirements. Curved detectors that have the potential to simplify relay optics and reduce the number of reflections for wide-field of view performance should also be considered.

TRL	SOTA	3-9
	Solution	2-3

Performance Goals and Objectives	General performance goals are: • Operational bandpass: 90-300 nm; • Read noise: required to be < 5e-rms/read with a highly desired goal of 0 e-; • Dark current: 0 e- / resol* / s; • Spurious count rate: < 0.05 counts/cm^2/s; • QE: 75% peak; • Resol size ≤ 10 μm; • Dynamic range (max count rate): ≥ 10^4 Hz / resol; • Time resolution: ≤ 100 ms; • Format: ≥ 8-16k pixels per side with high fill factors; • Radiation hardness: unaffected performance over 5-year mission lifetime at SEL2; and • Solar-blind or red-leak suppressing by 3-4 orders of magnitude. * Note, due to the fundamentally different architecture between MCPs and EMCCD/sCMOS devices, we use the term "resol" to refer to a spatial resolution element for MCPs, and a two-pixel width for EMCCDs and sCMOS.
Scientific, Engineering, and/ or Programmatic Benefits	This technology will directly benefit any mission with a science objective in the UV regime. It will specifically enable wide-FOV UV imaging and spectroscopy. High dynamic range performance will enable time-resolved observations of bright objects. It could enable new science regimes and increase science impact by factors of 100 – 1000.
COR Applications and Potential Relevant Missions	This technology has been identified as a high-priority mission-enabling technology for the Large UV/Optical/Infrared (LUVOIR) mission by the LUVOIR Science & Technology Definition Team (STDT) and Study Office. This technology could also be enabling or enhancing for many UV-centric missions such as Astrophysics Probes or Explorers.

Time to Anticipated Need	For LUVOIR, this technology needs to demonstrate credibility before the 2020 Astrophysics Decadal Survey, and would require a TRL-6 demonstration by mission PDR, anticipated to be the mid- to late-2020s. Significant improvements can be applied quickly in suborbital missions or Explorers, to improve technology readiness.

Gap Name	High-efficiency UV multi-object spectrometers
	Submitted by General Community

Description	Future NASA UV missions devoted to spectroscopy require high-throughput (> 50%), multi-object spectrometer (> 100 sources; R~3000 or greater) architectures and components for operation at 100-400 nm or broader band (e.g., digital micro-mirror device, DMD; advanced diffraction gratings; micro-shutter arrays; fiber-fed spectrographs; and integral-field spectrometers).
Current State-of-the-Art (SOTA)	DMD is at TRL 5, based on European studies for Euclid, and particle-radiation tests at LBL. Micro-shutters for longer wavelengths (> 0.6 microns) are at TRL 6. Low-scatter Echelle gratings are currently at TRL 2.

TRL	**SOTA**	$2 - 6$
	Solution	

Performance Goals and Objectives	Routinely produce large-format, high-QE, moderate-resolution systems that can be used in a variety of Explorer, medium, and strategic missions. Key performance criteria for customization, maturation, and characterization of object-selection components (such as DMDs, micro-shutters, or reconfigurable fibers) for UV/Vis/NIR space astronomy include: ● Sensitivity over the spectral interval 0.20-1.7 μm, (90-180 nm for DMDs); ● Effective sky background blockage (e.g., zodiacal light); and ● Low instrumental background (optical scattering, thermal background). Low-scatter Echelle gratings are required for high-resolution far-UV (λ = 90-180 nm) spectroscopy. Performance goals for gratings include scattered-light control comparable to the best first-order diffraction grating currently flying (HST-COS), ~10^{-5} of peak intensity at $\Delta\lambda = 10\,\text{Å}$ from fiducial wavelength λ_o. In the short term, scattering < 10^{-3} would enable deeper, high-resolution UV spectroscopy than currently available with HST, in an Explorer-class mission.
Scientific, Engineering, and/ or Programmatic Benefits	High-performance spectrometers can increase the science impact of missions by orders of magnitude. Space telescopes today can obtain slit spectra of a single object or slit-less spectra of a field, but not slit spectra of multiple objects in a field. A UV/visible slit selector (DMD, micro-shutter array, or multi-fiber) would eliminate confusion and block unwanted background (e.g., zodiacal light). Better gratings improve contrast and thereby sensitivity. Enabling technology for small, wide-field telescopes appropriate for an Explorer mission.
COR Applications and Potential Relevant Missions	UV/Vis/IR slit selectors are needed for astrophysics, heliospheric, and Earth-science missions.
Time to Anticipated Need	Should come as early as possible since mission definition and capabilities are built around instrument performance. Development for space astronomy is needed in time to respond to an expected announcement of opportunity for an Explorer-class mission in 2015 – 2016.

Gap Name	Lightweight, large-aperture, high-performance telescope mirror systems *Submitted by General Community*
Description	Future UV/Vis/NIR space telescopes will require larger apertures to answer questions raised by HST, JWST, Planck, and Herschel; and to complement ≥ 30-m ground-based telescopes. They will require: 1. 8-m-or-greater aperture. 2. Diffraction-limited optical quality. 3. UV to NIR wavelength coverage. (4. For exoplanet science: pm-level wavefront error stability to enable starlight suppression.) Extraordinary wavefront stability will require a systems-level approach to technology development for the optical telescope assembly (OTA), including mirror fabrication, disturbance isolation/damping, metrology, actuators, thermal control, and detailed integrated modeling. Investments are needed in mirror systems to prove system performance, thermal and dynamic stability, UV compatibility, and low mass. Investments could include detailed model-based analysis of mirror system performance, especially addressing dynamic and thermal stability to the levels required for coronagraphy; as well as mirror system testing at the pm level to validate the models. Segmented architectures provide a low-cost, low-risk approach that leverages the significant investment made by NASA for JWST. Telescope mirror assemblies require improvements in surface figure error, areal density, areal production rate, and areal cost.
Current State-of-the-Art (SOTA)	Primary mirror segment technologies have been developed at the needed size (1.2-1.4 m) by NASA and other agencies (for example – beryllium mirrors for JWST). ULE® glass and SiC-based designs offer alternatives to the Be mirrors used by JWST at lower cost and faster production rates: - Be mirrors are TRL 6; - SiC mirrors are at TRL 6; and - Borosilicate glass mirrors are TRL 5. Thermal control has been demonstrated for figure stability and figure control with actuators in some mirror types: Lightweight ULE® segments with alignable edges offer < 10 nm rms surface figure error (projected), < 5 Å micro-roughness (projected) and < 25 kg/m^2 total at a size of 1.4 m. SiC mirrors using actuated hybrid mirrors have been demonstrated at 0.5-m to 1.35-m size, < 14 nm rms surface figure error, < 10 Å micro-roughness (projected), and < 25 kg/m^2 total. Other mirror types are at lower TRLs: - Extreme-lightweighted Zerodur® demonstrated at 1.2 m (TRL 4); - Diffractive membrane optics demonstrated at laboratory brass-board level (TRL 3); and - Frozen-membrane-mirror technology in early stages of development (TRL 3).

TRL	SOTA	3
	Solution	

| **Performance Goals and Objectives** | Decrease OTA areal density, including primary mirror, its support structure, and mass of additional hardware required to produce an image (e.g., wavefront-control system or chromatic corrector), from current trends of 74 kg/m^2 (JWST) to OTA areal densities on the order of 10-36 kg/m^2 or less, surface figure error of 5 to 10 nm rms, and mechanical and thermal wavefront error stability ~10 pm rms per wavefront control step.

Telescope fabrication time should be short enough to not be a significant schedule driver, with areal production rates on the order of 30 – 50 m^2/year. |

Scientific, Engineering, and/ or Programmatic Benefits	Closing this technology gap may enable rigid monolithic primary mirrors, or affordable but reliable deployment techniques for segmented apertures; either would provide increased capabilities. Scientific: greater collecting area increases sensitivity; larger diameter enables greater angular resolution. Both enable important new science for COR and Exoplanets. Engineering: lower-mass primary allows lighter structure, larger margins; simplified deployment concepts and mechanisms allow larger apertures in smaller launch vehicles. Programmatic: A lighter and cheaper telescope allows greater allocation of mass and money for the science instrument, and could enable smaller missions.
COR Applications and Potential Relevant Missions	This is an enabling technology for a LUVOIR mission, a HabEx mission, and perhaps a FIR Surveyor mission. This technology development will enable (current) MidEx-class science with a SMEX, Astrophysics Probe-class science with a MidEx, and more ambitions larger-mission science with an Astrophysics Probe-class implementation. Development of inexpensive 1-3-m monolithic lightweight stiff mirrors will benefit suborbital, Explorer, and Astrophysics Probe missions.
Time to Anticipated Need	Need to demonstrate credibility before the 2020 Decadal Survey, and would require TRL 6 by mission PDR anticipated in the mid-2020s. Significant improvements can be applied quickly in suborbital missions to increase technology readiness. Rapid development will benefit suborbital, Explorer and Astrophysics Probe-class missions.

Gap Name	**High-Contrast Segmented Aperture Coronagraphy** *Submitted by LUVOIR STDT*
Description	One of the primary science goals of future large-aperture space telescopes is to detect and characterize habitable exoplanets around nearby stars. To achieve exoplanet yields large enough to enable a statistical study of habitability requires a large aperture telescope, likely greater than 8 meters in diameter. Such an aperture must be segmented in order to fit into current and planned launch vehicle fairings. Therefore, any coronagraphic instrument that is used to perform the exoplanet survey and characterization must be compatible with a segmented aperture telescope. A small but important subset of COR science also requires high contrast observations that would be enabled by space-based coronagraphs.
Current State-of-the-Art (SOTA)	Recent achievements in the development of the WFIRST coronagraphic instrument have dispelled the widely-held belief that high-contrast imaging with a coronagraph could only be performed with a monolithic, unobscured, off-axis telescope. WFIRST coronagraphs have achieved ~10^{-8} contrast at an inner working angle (IWA) of 3 λ/D over a 10% bandpass with an obscured monolithic aperture, in part by using the coronagraph's internal deformable mirrors (DMs) to compensate for the additional diffraction caused by the aperture obscurations. Modeling indicates that current WFIRST coronagraph designs will achieve Airy throughputs of less than 5%, however, defined as the fraction of photons in the full-width-half-maximum (FWHM) of the planet point-spread function (PSF) divided by the number of planet photons entering the telescope aperture. These results are specific to WFIRST. Improvement is needed to meet future performance requirements using large segmented aperture systems.

TRL	SOTA	4-5
	Solution	2-4

Performance Goals and Objectives	The goal is to demonstrate a coronagraphic instrument with contrast of 10^{-10} at an inner working angle of 2 λ/D with a bandpass $\geq$ 10% and Airy throughputs of >10% with a segmented aperture pupil. The demonstration should include a wavefront sensing and control system necessary to correct for relevant instabilities (pointing, low-order wavefront, segment phasing errors, etc.). For certain missions, it is also desired to demonstrate this level of performance with UV-compatible mirror coatings to enable missions with community-wide appeal.
Scientific, Engineering, and/ or Programmatic Benefits	A small but important subset of COR science that requires high contrast observations will be enabled by space-based coronagraphs. These include very-high-resolution scattered-light imaging and spectroscopy of circumstellar disks, nebulosity, and outflows very near both young and evolved stars, as well as studies of quasar host galaxies, jets, and accretion disks. Contrast ratio > 10^{-9} is required to cover the full range of circumstellar phenomena detected by unresolved IR photometry.
COR Applications and Potential Relevant Missions	LUVOIR, HabEx, and coronagraphic Probe missions. This technology was identified as a critical mission-enabling technology for the LUVOIR mission by the LUVOIR STDT and Study Office. This technology is also potentially enabling for the Habitable Exoplanet (HabEx) Imager, should a segmented aperture architecture be chosen for that mission. More generally, this technology would improve performance of coronagraphs for smaller obscured, or segmented-aperture telescopes.
Time to Anticipated Need	Need to demonstrate credibility before the 2020 Decadal Survey, and would require TRL 6 by mission PDR anticipated in the mid-2020s.

Gap Name	**Ultra-Stable Opto-Mechanical Systems** *Submitted by LUVOIR STDT*
Description	A small but important subset of COR science that requires high contrast observations will be enabled by space-based coronagraphs. These include very high resolution scattered-light imaging and spectroscopy of circumstellar disks, nebulosity, and outflows very near both young and evolved stars, as well as studies of quasar host galaxies, jets, and accretion disks. Coronagraph performance is critically dependent on unprecedented stability and exceptional telescope optics quality. The most critical and challenging requirement on the opto-mechanical system is that of wavefront error stability of order 10 pm per wavefront control step. Several key technologies are required to enable thermal and dynamic stability: •< 10 mK level thermal control; •Very stable materials, stiff structures, and systems for rigidizing the backplane; •Active and passive vibration isolation (e.g., noncontact active isolation schemes that physically separate the payload from the spacecraft); •Wavefront sensing and control: actuators with ~1 nm step sizes; and •High-speed, pm-scale metrology (required for ground testing and to validate linearity assumptions used in integrated modeling), to detect relative distances over pm length scale (e.g., capacitive sensing, laser-based trusses, generalized interferometric sensing, or nested combinations of these techniques). All the above must have a path to spaceflight qualification.

Current State-of-the-Art (SOTA)	**1. Stable Structures and Mirrors** High-stability composites, such as those used on JWST, Chandra, and HST. **2. Disturbance Isolation** Passive disturbance isolation on JWST achieves 80 dB attenuation at frequencies > 40 Hz. Non-contact isolation systems have been modeled at 70 dB attenuation with 6 dof low-order active pointing. **3. Thermal Control** For mirrors, ULE®, Zerodur®, and silicon carbide (SiC) are all possible, and modeling has shown what type of thermal controls are needed for each. For room-temperature operation, mirror thermal control needs to be 1 mK for ULE® and Zerodur®, and ~0.1 mK for SiC. At temperatures up to 140 K, the coefficient of thermal expansion of SiC drops to levels below that of ULE®, and the thermal control requirements rise. **4. Sensing Technologies** Two general classes of sensor technologies exist: a. Systems using light from objects being observed to sense the wavefront, such as image-based techniques or the Zernike wavefront sensor used by the WFIRST coronagraph's Low-Order Wavefront Sensing & Control system. Image-based wavefront sensing techniques are baselined as the primary means to commission and maintain alignment of JWST, predicted to take 14 days to 'passively' achieve 31 nm rms WFE response to a worst-case thermal slew of 0.22 K. HST's WFE changes by 10 to 25 nm every 90 min (1–3 nm per 10 min) as it moves in and out of the Earth's shadow. b. External metrology systems: Laser trusses, ideal for maintaining primary-to-secondary mirror alignment (heritage in developing flight systems for the Space Interferometry Mission); shorter-range sensors used in commercial microlithography have achieved 10-pm-rms sensitivity. New techniques use dual-laser-frequency methods, laser trusses, and broadband laser interferometry. Sub-10-pm level sensitivities have been demonstrated in the laboratory with laser systems, with path to space qualification. High-speed interferometry has achieved nm-level measurements at 2.5 KHz in the lab. Capacitive edge sensors baselined for the Thirty Meter Telescope as part of the mirror co-phasing system. Capacitive sensing is used in control of air-gapped etalons to the 10 pm level. Control Technologies: Once wavefront drift is sensed, there are several options to control it: Rigid-body hexapods for 6-dof mirror control, Warping harnesses for low-order surface-figure modes, Embedded surface figure actuators to control higher-order surface-figure error, and macro-scale or MEMS Deformable mirrors, allowing wavefront correction at several stages: in the optical system, including within the coronagraph instrument; and also actuation of the primary mirror itself, especially if segmented.

TRL	SOTA	3-9
	Solution	2-4

Performance Goals and Objectives	Significant technology development is needed to produce 'stable' isothermal or thermally 'insensitive' telescopes. Ultimate performance goals are mirror surface figure errors < 5 nm rms, and end-to-end wavefront error stability of 10 pm rms per wavefront control step.
	A Systems Perspective The systems-level nature of the wavefront stability problem requires a <u>systems-level approach</u>. Mirrors, structures, sensors, actuators, materials, modeling, and the overall architecture must be developed together, as a system. Design and development activities to demonstrate closed-loop pm-class wavefront performance for segmented apertures, and the ability to verify that stability on the ground is required. Furthermore, it would be advantageous to pursue concurrent, competitive development of pm component sensing and control technologies along with architecture feasibility demonstrations and assessments.
	Disturbance Isolation 140-dB attenuation > 20 Hz between spacecraft reaction wheels and telescope. Demonstration of required isolation including power and data transmission across bus/payload i/f. Several isolation techniques may be combined to meet dynamic stability requirements to reduce system risk.
	Thermal • Thermal design techniques validated by traceable characterization testing of components; • Passive thermal isolation; • Active thermal sense at the < 0.1 mK level and control at the < 10 mK level; and • Validated thermal performance models (for either monolithic or segmented mirror systems).
	Sensing and Control Measurement sensitivity and stability of 10 pm per wavefront control step, where the step-time is driven by integration time needed to collect sufficient photons to close control loops on active wavefront control.
	Autonomous, closed-loop, onboard wavefront sensing and control with over 100 Gigaflop operations/s/W and control bandwidth of 1 per 5 min. High-speed pm-level metrology for ground-based testing in air to anchor integrated modeling assumptions.
Scientific, Engineering, and/ or Programmatic Benefits	A small but important subset of COR science requires high contrast observations only enabled by space-based coronagraphs. The large-diameter telescopes with active optics, high-stability deformable mirrors, and ultrastable opto-mechanical systems (providing pm-level wavefront stability required for exoplanet imaging at the 10^{-10} contrast level using coronagraphic instruments) will also provide unprecedented performance for astronomical observations in the far-UV. Observations include very-high-resolution scattered-light imaging and spectroscopy of circumstellar disks, nebulosity, and outflows very near both young and evolved stars, as well as studies of quasar host galaxies, jets, and accretion disks. A contrast ratio > 10^{-9} is required to cover the full range of circumstellar phenomena detected by unresolved IR photometry).
COR Applications and Potential Relevant Missions	LUVOIR, Habitable Exoplanet (HabEx), and coronagraphic Probe missions.
	This technology has been identified as a critical mission-enabling technology for the LUVOIR mission by the LUVOIR STDT and the Decadal Study Office.
	This is technology is also potentially enabling for the HabEx Imaging Mission, should it require a coronagraphic instrument to perform its key exoplanet science goals.
Time to Anticipated Need	Need to demonstrate credibility before the 2020 Decadal Survey, and would require TRL 6 by mission PDR anticipated in the mid-2020s.

Gap Name	High-performance spectral dispersion component/device *Submitted by General Community*
Description	1. A highly spectral-dispersive compact component/device can be inserted into a converging beam before the telescope focus as a slitless spectrograph or grism. <u>Note:</u> a presently promising solution to this gap is Freeform Diffractive Optical Surfaces. 2. High-efficiency gratings with a relatively flat diffraction efficiency over the grating free spectral range (minimum > 85% over the free spectral range; 90% is preferred; the higher, the better). <u>Note:</u> a presently promising solution is to modify the groove profile from blazed grating.
Current State-of-the-Art (SOTA)	For Item 1 above: Current SOTA slitless spectrometer in Euclid mission is being designed and built as a standalone instrument, including corrector, imager, and grism assembly, to cover the requirement indicated in Item 1 [Proc. of SPIE **9143,** 91430K-1 (2014)]. For Item 2 above: Current SOTA diffraction efficiency reaches high 90%. It is achieved with blazed transmission grating. However, the diffraction efficiency quickly drops to 70% at the edges.

TRL	SOTA	3
	Solution	3

Performance Goals and Objectives	The technical goal is as follows: ● Compact enough to be installed in the spectral-filter wheel as one filter element; ● Accommodate large FOV (> 0.25 square degrees in sky); ● Diffraction limited (or nearly so) in the wavelength range; ● Relatively high spectral resolution (> 600 λ); ● Dispersion wavelength range reaches, or is close to, the grating free spectral range. It can be used between 600 to 2400 nm; ● High diffraction efficiency (>95% at peak wavelength); ● Par-focal with other filter elements; and ● Spread the unwanted orders on the detector so much as to be buried in detector noise. The objective is to develop a compact spectral dispersive device/component that can be simply inserted into a converging beam as a slitless spectrograph. The technical goal is also to develop a transmission grating with a high and relatively uniform diffraction efficiency. The objective is to ease spectral-intensity calibration and shorten exposure time.
Scientific, Engineering, and/ or Programmatic Benefits	<u>Science benefit:</u> dramatically reduce ghost-spectra intensity, increase element throughput, and shorten exposure time for larger survey area. <u>Engineering benefit:</u> Make a standalone instrument into a component greatly simplifying the entire engineering process and saving precious spacecraft volume for other applications. <u>Programmatic benefit:</u> Reduce risk and lower cost, as well as shorten delivery time.
COR Applications and Potential Relevant Missions	Any mission that needs a spectrograph, e.g., LUVOIR and its Probe, as well as Far-IR Surveyor. Can also be used for heliophysics, planetary, and Earth science. Beyond that, the technique will be very useful to many commercial applications.
Time to Anticipated Need	As soon as possible.

Gap Name	Band-shaping and dichroic filters for the UV/Vis
	Submitted by General Community

Description	Bandpass filters are employed throughout astronomy, and efficient transmissive designs are standard in the Vis/NIR. There is a pressing need for high-efficiency UV-transmitting filters. Because some classes of UV detectors have significant visible-light sensitivity, UV-transmitting "red-blocking" filters are also of high value. This includes narrowband (bandpass) or band-selectable (dichroic, longpass) imaging applications, or spectroscopic applications where multiple UV channels or order-sorting is required.
	Detector-integrated filters of various types (bandpass, visible blocking, and graded thickness) can offer improved performance over stand-alone optical components by improving overall system throughput and reducing the total number of optical surfaces in an instrument.
	Finally, UV/Vis/NIR dichroic filters are useful in creating multiple channels in an instrument, allowing simultaneous observation using band-optimized instrumentation and detectors over the widest possible FOV.
Current State-of-the-Art (SOTA)	Commercial optical filters are mature and widely available for visible and NUV wavelengths (> 250 nm). Current state of the art UV-transmission filters have efficiencies of < 10-20% below 180 nm and < 50% for 180-280 nm. Robust commercial high-efficiency UV-transmitting filter solutions are not frequently available.
	Red-blocking "Woods filters" with low efficiency (< 10-15%) and lifetime issues have been employed for solar-blind imaging.
	All dielectric designs are less commonly available at shorter FUV wavelengths due in part to the lack of transparent high-refractive-index materials in this wavelength.
	Dichroic filters have been designed for the UV, for example the FUV/NUV split in the GALEX instrument, but efficiency in each channel (50/80%) and effective bandwidth in each channel (< 50 nm) is limited at current SOTA.
	In the FUV, metal-dielectric structures have been successfully implemented as bandpass filters for broadband detector systems (e.g., HST, SWIFT) but with low throughput (< 20% below 200 nm). Similar designs have been implemented in laboratory settings directly on silicon FPAs to provide integrated red rejection capabilities with increased throughput (>50% below 200 nm).

TRL	SOTA	4
	Solution	

Performance Goals and Objectives	• Filter transmittance in UV for R~5 bandpass filter: > 50% (80%) FUV (NUV); • Red-blocking transmittance: > 50-75% (UV), < 0.0001%-0.01% Vis-NIR; • Dichroic: Mid-UV Split: R (FUV) > 0.8, T (NUV) > 0.9; • Bandwidth: FUV (100 nm), NUV (100-200 nm); • Minimum wavelength: 100-105 nm; • Improved dielectric designs (dichroics, edge filters); dichroic: UV/Vis Split: R (UV) > 0.9, T (Vis) > 0.9; and • Detector-integrated filters (red rejection, narrowband, or broadband AR) on large scale.

Scientific, Engineering, and/ or Programmatic Benefits	High efficiency and low noise resulting from out-of-band rejection, and multi-channel instruments using dichroics allow deep astronomical surveys to be conducted with space-based telescopes on much shorter, feasible timescales, and enable instrument designs that exploit the aperture size (geometrical area) and full working FOV of the telescope.
	The integration of UV-filtering elements directly on a sensor system has the potential to improve in-band sensitivity while providing out-of-band rejection. Eliminating discrete optical component can reduce instrument complexity.
	Relevant experience with UV, Vis, and/or NIR filters and dichroics that achieve the technical goals set forth above is essential for maximizing the return of future space observatories. This technology is crosscutting, with applications across astrophysics, planetary, and space sciences. Commercial applications similarly benefit from high throughput and band-rejection.
COR Applications and Potential Relevant Missions	COR science requires deep multi-wavelength measurements of galaxies and AGN to study their evolution from the formation of the first stars and black holes to structures observed on all scales in the present-day universe.
	High priority for observations of unseen phenomena such as the cosmic web of intergalactic and circumgalactic gas and resolved light from stellar populations in a representative sample of the universe.
	Potentially relevant missions include a LUVOIR space telescope, Explorer and Probe-class missions that can conduct wide-field surveys, and small-sat experiments that can advance technology while addressing one or more COR science objectives.
Time to Anticipated Need	Need to demonstrate credibility before the 2020 Decadal Survey, and would require TRL 6 by mission PDR anticipated in the mid-2020s.

Gap Name	High-reflectivity mirror coatings for UV/Vis/NIR
	Submitted by LUVOIR STDT and General Community

Description	High-reflectivity, highly uniform mirror coatings with low polarization are required to deliver high-throughput UV observations and support high-contrast imaging via starlight suppression. High-reflectivity coatings would allow multiple reflections with minimal throughput penalty in the UV, while still providing broadband performance out to NIR wavelengths. For a UVOIR flagship telescope, a single reflective coating that has excellent reflectivity and precise wavefront control over the UV/Vis/NIR (potentially down to 90 nm) would increase mission science return. Exoplanet observations drive the requirements for reflectance uniformity and control of polarization effects that might compromise the performance of a coronagraph. This capability includes: 1. High-reflectance broadband mirrors for the UV/Vis/NIR. 2. Access to the FUV (90-120 nm) spectrum, with minimal impact to sensitivity and wavefront in Vis and NIR. 3. Ultra-high reflectance for multi-mirror instruments with high degrees of multiplexing (Integral Field Units, IFUs; or MOS), particularly in the UV and FUV. 4. Safe, effective, reliable, last-minute or in-flight mirror cleaning technologies.
Current State-of-the-Art (SOTA)	The best current coatings provide > 90% reflectivity for wavelengths 300-2500 nm and longer, ~90% reflectivity for 120-300 nm (HST), and < 50% for 90-120 nm (FUSE). Current physical vapor deposition coatings can provide 2% uniformity at wavelengths greater than 120 nm and require coating thicknesses greater than 15 nm in order to maintain performance. Conventional technologies such as chemical vapor deposition with precision controls have been developed for producing high-performance mirror coatings on large-diameter substrates. New coating technologies such as atomic layer deposition (ALD) have potential to improve reflectivity and polarization properties by reducing the thickness of the protective coating. However, these have only been applied to small optical component prototypes (< 0.5 m). As to mirror cleaning, existing approaches (e.g., CO_2 snow, or electrostatic wands with AC excitation), do not remove molecular contamination. Promising methods (e.g., electron or ion beams) could clean off molecular layers as well as dust on substrates.

TRL	SOTA	3
	Solution	

Performance Goals and Objectives	1. Coatings with excellent UV and FUV efficiency, particularly in the 90 to 2500 nm range (> 90% for as much as possible of this spectral range). 1a. Also coatings with excellent UV and acceptable IR efficiency. 2. High-uniformity coatings (< 1%), over a large spectral range (90-2500 nm), with low polarization (< 1%) for wavelengths 200-1800 nm, for high-contrast imaging. 3. Coating application to large optics (0.5-4+ m) as well as to smaller instrument optical elements. 4. Pre-launch stability of ultra-thin coatings. 5. On-orbit lifetimes of > 10 years for these high-performance coatings. 6. Techniques for last-minute ground or in-flight cleaning technology to remove molecular coatings as well as dust.

Scientific, Engineering, and/ or Programmatic Benefits	High coating reflectivity in UV makes possible high-performance optical systems that can be highly multi-passed, significantly increasing potential impact of future missions.
	Wideband coatings could enable a combined UV to IR mission with very broad scientific potential from general astrophysics to exoplanet imaging and spectroscopy.
	Having a prototype telescope as a test-bed for demonstrating coating performance on shaped optics would reduce programmatic risk and costs.
	The availability of effective, safe, last-minute ground-based cleaning technologies, or in-flight cleaning technologies, could reduce the high cost of keeping equipment clean for a decade in clean rooms. Mirror-cleaning technology could simplify mirror processing before launch and reduce schedule (cost) and mitigate the risks of re-coating. Post-launch cleaning would improve on-orbit performance and could extend mission life.
COR Applications and Potential Relevant Missions	NWNH noted the importance of technology development for a future ≥ 4-m class UV/Vis mission for spectroscopy and imaging. This technology would also support the next generation of UV missions, including Explorers, Probes, and large (> 4-m apertures) future UV/Optical/IR telescopes, and is key for a LUVOIR Surveyor.
	All future missions with optics, particularly missions with an important FUV or UV component, will benefit from improved coatings.
	Benefits will also accrue to planetary, heliospheric, and Earth missions utilizing the UV band.
Time to Anticipated Need	Need to demonstrate credibility before the 2020 Decadal Survey, and would require TRL 6 by mission PDR anticipated in the mid-2020s.
	Mirror cleaning would be immediately useful for missions already in development

Gap Name	Large-format, low-noise and ultralow noise far-infrared (FIR) direct detectors *Submitted by FIRS STDT and General Community*
Description	The most important technology for the FIR/submillimeter is large-format detectors that operate with high efficiency (≥ 80%), low noise, and relatively fast time constant.
	Arrays containing thousands of pixels are needed to take full advantage of spectral information content. Arrays containing tens of thousands of pixels are needed to take full advantage of the focal plane available on a large, cryogenic telescope.
	Detector sensitivity is required to achieve background-limited performance, using direct (incoherent) detectors to avoid quantum-limited sensitivity.
Current State-of-the-Art (SOTA)	Single detectors are at TRL ~5, but demonstrated array architectures are lagging at TRL ~3.
	Sensitive, fast detectors (TES bolometers, and MKIDs in small arrays) are at TRL 3.

TRL	SOTA	3
	Solution	3

Performance Goals and Objectives	Detector format of at least 16×16 with high fill-factor and sensitivities (noise-equivalent power, NEP) of 10^{-19} W/√Hz are needed for wide-band photometry.
	Detector sensitivities with NEP of ≈ 3×10^{-21} W/√Hz are needed for spectroscopy, available in a close-packed configuration in at least one direction.
	The detector system should be scalable to enable ~million-pixel total format in a large mission.
	Fast detector time constant (~200 μs) is needed for Fourier-transform spectroscopy. For a filled aperture [interferometer] these values are:
	NEP at or below 3×10^{-20} [1×10^{-19}] W/√Hz.
	Number of pixels scales with aperture size > 256×256 [128×128] scalable to 1K×1K.
	Pixel time constant < 1 ms [~ 0.1 ms]
	For a detector system that can scale to ~1 million pixels, additional needs are:
	● very low focal-plane dissipation (~1 pW per pixel); ● High multiplexing factor (~1000 detectors per circuit) to minimize wiring parasitics; and ● (ambient-temperature) readout electronics with dissipation on order 1 mW per pixel.
Scientific, Engineering, and/ or Programmatic Benefits	Sensitivity reduces observing times from many hours to a few minutes (≈ 100× faster), while array format increases areal coverage by ×10-100. Overall mapping speed can increase by factors of thousands.
	Sensitivity enables measurement of low-surface-brightness debris disks and protogalaxies with an interferometer. This is enabling technology.
	Suborbital and ground-based platforms can be used to validate technologies and advance TRL of new detectors.
COR Applications and Potential Relevant Missions	FIR detector technology is an enabling aspect of all future FIR mission concepts, and is essential for future progress.
	This technology can improve science capability at a fixed cost much more rapidly than larger telescope sizes.
	This development serves Astrophysics almost exclusively (with some impact on planetary and Earth studies).
Time to Anticipated Need	Need to demonstrate credibility before the 2020 Decadal Survey, and would require TRL 6 by mission PDR anticipated in the mid-2020s.

Gap Name	Heterodyne FIR detector arrays and related technologies *Submitted by FIRS STDT and General Community*
Description	Suborbital and space missions, as well as NASA's SOFIA observatory, could achieve a significant observational-capability increase by upgrading from single-pixel coherent (heterodyne) spectrometers to arrays. Heterodyne FPAs are needed for high-sensitivity, spectrally resolved mapping of interstellar clouds, star-forming regions, and solar system objects including comets. These arrays require mixers with low noise-temperature and wide intermediate frequency (IF) bandwidth, local oscillators (LOs) that are tunable but which can be phase-locked, and accompanying system technology including optics and low-cost, low-power digital spectrometers. Specifically, LO sources at frequencies above 2 THz that can generate $\geq$ 10 mW of power will be essential for large-format heterodyne receiver arrays to observe many spectral lines important for COR (e.g., HD at 2.7 THz and OI at 4.7 THz). Largely because of the lack of such sources, the only large arrays developed thus far are direct detectors or heterodyne receivers below 1 THz.
Current State-of-the-Art (SOTA)	For SOFIA, 10-pixel receivers have been developed for flight; arrays of 64 pixels are approaching TRL ~4. LOs above 2 THz are at TRL 2.

TRL		
	SOTA	4
	Solution	2

Performance Goals and Objectives	Develop broad-tunable-bandwidth array receivers for operation at frequencies of 1-5 THz. Arrays of 10 to 100 pixels are required to build on the discoveries of Herschel and exploit the sub-millimeter/FIR region for astronomy. Should include optics and accompanying system components. For mixers, IF bandwidths of 8 GHz at shorter wavelengths (< 100 microns) are essential to analyze entire galactic spectrum in one observation. Sensitive mixers not requiring cooling to 4 K (e.g., based on high critical temperature superconductors) will be essential for application on space platforms, especially with the benefit of increased IF bandwidth. For LOs, sources with output power levels $\geq$ 10 mW at frequencies above 2 THz. For digital spectrometers, 8 GHz bandwidth with > 8000 spectral channels, and < 1W power per pixel will be necessary for large arrays used in space missions.
Scientific, Engineering, and/ or Programmatic Benefits	Ability to observe and map spectral lines (such as OI at 4.774 THz) to study star formation and galactic chemical evolution. Observations of transitions of water are necessary to probe the early phases of planet formation, and to determine the origin of the Earth's oceans. Development of such systems and associated technology will make imaging observations over 10× faster. They will also significantly benefit laboratory spectroscopy and biomedical imaging.
COR Applications and Potential Relevant Missions	Potential use in FIR Surveyor Mission. Needed for future sub-millimeter/FIR suborbital missions (instruments for SOFIA and balloon missions such as Stratospheric Terahertz Observatory, STO and Galactic/Xtragalactic ULDB Spectroscopic Stratospheric Terahertz Observatory, GUSSTO) and for potential small-sat and Explorer missions beyond Herschel. Solar system studies of planetary atmospheres will directly benefit. For Earth observing, FPAs will improve coverage speed and provide small spot sizes with reasonably sized antennas

Time to Anticipated Need	Need to demonstrate credibility before the 2020 Decadal Survey, and would require TRL 6 by mission PDR anticipated in the mid-2020s.
	The next round of SOFIA instruments will need to reach TRL 6 by the end of the decade (i.e., 3-5 years).

Gap Name	Wide-bandwidth, high-spectral-dynamic-range receiving system
	Submitted by General Community

Description	Receiving systems consisting of an antenna and associated electronics to amplify, filter, and sample the highly redshifted neutral hydrogen signals from Cosmic Dawn, i.e., at redshifts z > 10. The desired signals of interest have amplitudes of milli-Kelvins to potentially a few hundred milli-Kelvin (measured as brightness temperatures), relative to galactic and other foreground emissions at the level of 1000 to 10,000 K, implying spectral dynamic ranges of order 1 million or more (60 dB). Further, signals of interest are generated over a wavelength range comparable to their central wavelength.
	Finally, given signal weakness, the antenna and associated electronics either must not introduce spectral features at levels comparable to those expected from the signals of interest or the spectral behavior of the antenna and associated electronics must be stable and allow sufficient characterization to enable calibration to remove any such spectral features.
Current State-of-the-Art (SOTA)	Notional designs exist for full systems; proof-of-concept subsystems have been demonstrated in laboratory environments, and the individual components likely to be used in a full system have been demonstrated in relevant environments. A demonstration of subsystems and a full system in a relevant environment has not yet been accomplished.

TRL	SOTA	4
	Solution	

Performance Goals and Objectives	The goals of a program to address this gap are two-fold: demonstrate capability to make measurements of sky-averaged highly redshifted neutral-hydrogen signals; and demonstrate capability to collect highly redshifted neutral-hydrogen signals in a manner allowing later imaging. If the first goal can be met, the technology capability required for the second goal will also be met.
	A system capable of fulfilling the first goal can be divided into three key sub-systems:
	I. Antenna: Proof-of-concept antennas able to receive signals over at least a 3:1 wavelength range have been constructed; the objective is to construct an antenna with a sufficiently stable frequency response that it changes by only a small amount over range of temperatures expected for a space-based antenna;
	II. Analog receiver: The receiver amplifies and, if needed, filters and conditions for further processing signals collected by the antenna; the receiver must allow characterization at a level sufficient to allow extraction of the cosmological hydrogen signal at a level of 1 ppm of signals received by antenna; designs for such receivers exist; the objective is to construct one in a lab environment, demonstrate its performance, and then construct one for the thermally controlled environment expected for a spacecraft; and
	III. Digital spectrometer: The spectrometer converts analog signals to digital, and forms them into spectra with sufficient spectral resolution to detect the cosmological hydrogen signal; digital spectrometers with the required performance have been developed in a lab environment; the objective is to implement a spectrometer with flight-qualified hardware in the thermally controlled environment of a spacecraft.
Scientific, Engineering, and/ or Programmatic Benefits	This technology capability would benefit studies of "Cosmic Dawn," one of the three science objectives for this decade as identified by the NWNH report. Studies of the highly redshifted neutral-hydrogen signals will probe the Epoch of Reionization (EoR) NWNH science frontier discovery area, and address the science frontier question "*What were the first objects to light up the universe and when did they do it?*" from the Origins theme. Studies of highly redshifted neutral-hydrogen signals may also be able to probe into the true Dark Ages, before any stars had formed. Such studies would complement COR objectives, and address goals of the PCOS Program.

COR Applications and Potential Relevant Missions	The application is for space- and lunar-based missions designed to find highly redshifted ($z > 10$) signals from neutral hydrogen. Potentially relevant missions described in the Astrophysics Roadmap include a precursor lunar orbiter mission (Introduction to Chapter 6 of the Astrophysics Roadmap) and an eventual Cosmic Dawn Mapper.
Time to Anticipated Need	Two to three years for a precursor lunar orbiter mission.

Gap Name	Large cryogenic optics for the Far IR
	Submitted by FIRS STDT and General Community
Description	Large telescopes (of order 10 m in diameter) provide both light-gathering power to see the faintest targets, and spatial resolution to see the most detail and reduce source confusion. To achieve the ultimate sensitivity, their emission must be minimized, which requires these telescopes to be operated at temperatures (depending on the application) as low as 4 K. These telescopes will probably need in-orbit adjustability and should be designed for low-cost optical-performance verification before launch. Some material properties, such as damping for telescope structures, are also needed.
Current State-of-the-Art (SOTA)	JWST Be mirror segments may meet requirements now, so TRL 5 with an extremely expensive technology; TRL 3 exists for other materials like SiC. Cryogenic low-dissipation actuators exist at TRL 3-5.

TRL	SOTA	5
	Solution	3

Performance Goals and Objectives	Develop a feasible and affordable approach to producing a 10-m-class telescope with sufficiently high specific stiffness, strength, and low areal density to be launched; while maintaining compatibility with cryogenic cooling and FIR surface quality/figure of ~1µm rms. Material property measurements at cryogenic temperatures for structures and optics such as damping, emissivity, thermal conductivity, etc.
Scientific, Engineering, and/ or Programmatic Benefits	Low-cost, lightweight cryogenic optics at reasonable cost are required to enable development of large-aperture FIR telescopes in the 2020s. Large apertures are required to provide the spatial resolution and sensitivity needed to follow up on discoveries from the current generation of space telescopes.
COR Applications and Potential Relevant Missions	This is a key enabling technology for any future single-aperture FIR telescope, and an enhancing technology for a FIR interferometer.
Time to Anticipated Need	Need to demonstrate credibility before the 2020 Decadal Survey, and would require TRL 6 by mission PDR anticipated in the mid-2020s.

Gap Name	FIR interferometry
	Submitted by FIRS STDT and General Community

Description	Interferometry in the FIR provides sensitive integral field spectroscopy with sub-arcsec angular resolution and R ~ 3000 spectral resolution. It could resolve proto-planetary and debris disks; and measure the spectra of individual high-z galaxies, at resolutions beyond what is currently envisioned for single-dish FIR telescopes. A structurally connected interferometer would have these capabilities. Telescopes need to operate at temperatures as low as 4 K.
Current State-of-the-Art (SOTA)	Wide-FOV spatio-spectral interferometry has been demonstrated in the lab at visible wavelengths with a test-bed that is functionally and operationally equivalent to a space-based FIR interferometer, the error terms are well understood, and experiments have been conducted with an astronomically realistic test scene. Further, single-pixel spatio-spectral interferometry has been demonstrated in the lab at THz frequencies, demonstrating the desired broadband far-IR wavelength response of the beam combiner

TRL	SOTA	4
	Solution	4

Performance Goals and Objectives	Interferometric baselines in the tens of meters, up to ~100 m, are required to provide the spatial resolution needed to follow up on discoveries made with the Spitzer and Herschel space telescopes, and to provide information complementary to that attainable with ALMA and JWST.
	Develop a single science instrument providing both dense coverage of the u-v plane for high-quality, sub-arcsec imaging and Fourier Transform Spectroscopy over the entire spectral range, 25-400 microns, in an instantaneous FOV > 1 arc minute.
Scientific, Engineering, and/ or Programmatic Benefits	Experimentation with and simulation of data acquisition with a rotating interferometer, "single dish" (standard FTS) mode, and further development of spatio-spectral reconstruction software will close the gap. This is enabling technology for a space-based far-IR interferometer.
COR Applications and Potential Relevant Missions	Wide-field spatio-spectral interferometry is a key technology for a FIR astrophysics mission, consistently given high priority by the FIR astrophysics community since the 2000 Decadal Survey.
	Applicable to the FIR Surveyor, described in the NASA Astrophysics Roadmap, "Enduring Quests, Daring Visions," currently under study.
	Will be used in balloon experiments such as BETTII, and potentially in a Probe-class FIR mission.
	Potential applications also exist in NASA's planetary and Earth science programs.
Time to Anticipated Need	Need to demonstrate credibility before the 2020 Decadal Survey, and would require TRL 6 by mission PDR anticipated in the mid-2020s.

Gap Name	High-performance, sub-Kelvin coolers *Submitted by FIRS STDT and General Community*	
Description	Optics and detectors for FIR, sub-millimeter, and certain X-ray missions require very low temperatures of operation, typically in the tens of milli-Kelvins. Compact, low-power, lightweight coolers suitable for space-flight are needed to provide this cooling. Both evolutionary improvements in conventional cooling technologies (adiabatic demagnetization and dilution refrigerators) with higher cooling power, and novel cooling architectures are desirable. Novel cooling approaches include optical, microwave, and solid-state techniques.	
Current State-of-the-Art (SOTA)	Existing adiabatic demagnetization refrigerators with low cooling power at 50 mK are at TRL 7-9 (Hitomi/SXS) but high-cooling-power versions are at TRL 4. Dilution refrigerators and solid-state cooling approach based on quantum tunneling through normal-insulator-superconductor (NIS) junctions are both at TRL 3.	
TRL	**SOTA**	3-4
	Solution	3-4
Performance Goals and Objectives	A sub-Kelvin cooler operating from a base temperature of ~4 K and cooling to 30 mK with a continuous heat lift of 5 µW at 50 mK and 1 µW at 30 mK is required for several mission concepts. Features such as compactness, low input power, low vibration, intermediate cooling, and other impact-reducing design aspects are desired.	
Scientific, Engineering, and/ or Programmatic Benefits	Sub-Kelvin cryocoolers are required to achieve astrophysical photon-background-limited sensitivity in the FIR and high-resolution sensitive X-ray microcalorimetry. Techniques to lower cooling costs and improve reliability will aid the emergence of powerful scientific missions in the FIR and X-ray.	
COR Applications and Potential Relevant Missions	This technology is a key enabling technology for any future FIR mission, including the FIR Surveyor. Sensors operating near 100 mK are envisioned for future missions for X-ray astrophysics, measurements of the CMB, and FIR imaging and spectroscopy. Applicable to missions of all classes (balloons, Explorers, Probes, and flagship observatories).	
Time to Anticipated Need	Need to demonstrate credibility before the 2020 Decadal Survey, and would require TRL 6 by mission PDR anticipated in the mid-2020s.	

Gap Name	Advanced cryocoolers
	Submitted by FIRS STDT and General Community

Description	Passive cooling becomes impractical for cooling below 25 K. Cryocoolers are required for achieving very low temperatures (e.g., ~4 K) for optics and as precoolers for sub-Kelvin detector coolers for COR missions.
	Eliminating the need for expendable materials (cryogens) will increase achievable lifetime and reduce system mass and volume. Improvements are needed in terms of performance, especially low power consumption and low vibration levels.
Current State-of-the-Art (SOTA)	For several-Kelvin temperature designs, the current SOTA includes pulse-tube, Stirling, and Joule-Thomson coolers which are at high TRL but are expensive, and do not yet have good enough performance. An example is the development of the 6-K cooler system for MIRI, which was extremely problematic, slow, and costly.
	In the past, cryocoolers were largely custom developments (e.g. and Planck, Herschel), and while successful, this is a major deterrent to small and medium missions as well as to more ambitious missions using cooled telescopes.

TRL	SOTA	3-6
	Solution	4

Performance Goals and Objectives	Several mission concepts require sustaining temperatures of a few Kelvin, with continuous heat-lift levels of a few dozen to ~200 mW at temperatures ranging from 4 to 18 K.
	Other concepts could benefit from greater heat lifts at somewhat higher temperatures. All this needs to be accomplished with < 200 W input power. Such coolers need to be compact, and impose only low levels of vibration on the spacecraft.
	Large FIR telescopes are likely to pose more stringent requirements, if a cryocooler is used to cool the primary mirror.
	A sub-Kelvin cooler will be implemented in some applications, and an advanced few-Kelvin cryocooler able to maintain the sub-Kelvin cooler's hot zone at a steady (e.g.) 4 K will be very beneficial.
Scientific, Engineering, and/ or Programmatic Benefits	Cryocoolers able to operate near 4 K, cooling detectors and optics directly, as well as serving as a backing stage for ultra-low-temperature (sub-Kelvin) coolers will enable large FIR telescopes, as well as ultra-low-noise operation of cryogenic detectors for other bands.
	Increased heat lift, lower mass, lower volume, increased operational lifetime, and reduced cost will enable such missions to fly extended durations without wasting critical resources on cooling.
	Large-capacity cryocoolers are required to achieve astrophysical photon-background-limited sensitivity in the FIR and meet sensitivity requirements to achieve the science goals for future FIR telescopes or interferometers.
COR Applications and Potential Relevant Missions	This technology is a key enabling technology for any future FIR mission, including the FIR Surveyor.
	It is also applicable to balloons, airborne platforms, Explorers, and Probes. For example, it would improve performance of STO2 long/ultra-long duration balloon and SOFIA instruments. Explorer missions would also be very positively impacted
Time to Anticipated Need	Need to demonstrate credibility before the 2020 Decadal Survey, and would require TRL 6 by mission PDR anticipated in the mid-2020s.

Gap Name	Compact, integrated spectrometers for 100 to 1000 μm _Submitted by FIRS STDT_
Description	A key technology for the far-IR is a compact, integrated spectrometer operating in the 100 micron to 1 mm band which can provide a wide (e.g. 1:1.6) instantaneous bandwidth at resolving power ($R = \lambda / \Delta\lambda = \nu / \Delta\nu$) ~500 with high efficiency in a compact (~10-cm) package that could be arrayed in a focal plane to provide integral-field mapping or multi-object spectroscopy capability.
Current State-of-the-Art (SOTA)	Multiple compact spectrometers are under development: including compact silicon gratings and grating analogs, as well as superconducting filter banks. These systems are promising, and in some cases are approaching photon-noise-limited performance suitable for ground-based observations, but have not yet been demonstrated in a scientific application.

TRL		
	SOTA	3
	Solution	3

Performance Goals and Objectives	To completely fill the gap, an integrated spectrometer + detector array system would demonstrate 1:1.7 bandwidth (or greater), high efficiency (> 50%, including detector absorption), resolving power > 400, and a coupling scheme compatible with a telescope beam (e.g., an f/4 Gaussian beam). To enable observatories with hundreds of spectrometers, a single spectrometer + detector array would be packaged on a silicon wafer on the order of tens of square cm in size (i.e., less than one 4" wafer).
Scientific, Engineering, and/ or Programmatic Benefits	Large-format spectrometers in the far-IR through millimeter enable 3-D spatial-spectral surveys over large areas. The combination of large spatial coverage (many to tens of square degrees) and spectral bandwidth (giving redshift, or line –of-sight distance) will simultaneously find galaxies and measure their redshifts in large numbers (e.g., on order millions with the Far-IR Surveyor). This measurement addresses key questions in galaxy evolution and the reionization epoch. This is enabling technology.
COR Applications and Potential Relevant Missions	Compact spectrometers are key for a future far-IR flagship such as the far-IR Surveyor (whether single-dish or interferometer), but they also enable interim opportunities such as involvement with SPICA, and balloon-borne far-IR experiments which are being proposed.
Time to Anticipated Need	Need to demonstrate credibility before the 2020 Decadal Survey, and would require TRL 6 by mission PDR anticipated in the mid-2020s.

Gap Name	Mid-IR spectral coronagraph
	Submitted by FIRS STDT
Description	Characterization of the atmospheres of cool exoplanets in wide orbits (> 5 AU, ice giants, and more massive planets) requires spectrally dispersed coronagraphy in the 7-30 micron range with contrasts of 10^{-6} and IWA of 0.1" at the shortest wavelength. The spectral resolving power should be moderate (R~100-500).
Current State-of-the-Art (SOTA)	The current SOTA for mid-IR coronagraphs are the three four-quadrant phase masks of JWST-MIRI. These provide narrow-band imaging with contrasts up to 10^{-4} in three narrow bands from 10.65-15.5 micron with inner working angles of 0.33-0.49". The MIRI coronagraphs do not offer spectral dispersion.

TRL	**SOTA**	
	Solution	

Performance Goals and Objectives	The goal is to construct a spectro-imaging instrument with and inner working angle of 0.1" at 10 micron. This is likely less than 2 λ/D for the available aperture. The best IWA is needed to detect a 300-K Neptune-sized planet at 10 parsec at a 1-2 AU separation, and the contrast should be 10^{-6} to detect Saturn at 10 parsec (~1 microJy @ 24 micron, 3 λ/D for 16-m aperture) with R~10. The maximum spectral dispersion should be sufficient to resolve the 15-micron CO_2 band (R~500).
Scientific, Engineering, and/ or Programmatic Benefits	Mid-IR coronagraphic spectroscopy would support a variety of COR science cases, including resolved studies of solid-state features indicative of amorphous or crystalline grain mineralogy in protostellar, protoplanetary, and debris disks, as well as studies of dust and gas around evolved stars and AGN. The low mid-IR contrast ratio between hot central stars and warm surrounding dust make circumstellar dust investigations especially interesting in this wavelength range.
COR Applications and Potential Relevant Missions	Far-IR Surveyor (single aperture architecture).
Time to Anticipated Need	Need to demonstrate credibility before the 2020 Decadal Survey, and would require TRL 6 by mission PDR anticipated in the mid-2020s.

Appendix B
Program Technology Development Quad Charts

UV/Vis/IR

Far-IR

Ultraviolet Coatings, Materials, and Processes for Advanced Telescope Optics

PI: K. 'Bala' Balasubramanian / JPL

Objectives and Key Challenges:

- Development of UV coatings with high reflectivity (>90-95%), high uniformity (<1-0.1%), and wide bandpasses (~100 nm to 300-1000 nm) is a major technical challenge; this project aims to address this key challenge and develop feasible technical solutions
- Materials and process technology are the main challenges; improvements in existing technology base and significant innovations in coating technology such as Atomic Layer Deposition (ALD) will be developed

Significance of Work:

- This is a key requirement for future Cosmic Origins and exoplanet missions

ALD chamber at JPL   1.2-m coating chamber at Zecoat Corp.

Approach:

- Develop a set of experimental data with MgF_2-, AlF_3-, and LiF-protected Al mirrors in the wavelength range 100-1000 nm for a comprehensive base of measurements, enabling full-scale developments with chosen materials and processes
- Investigate and develop enhanced coating processes including ALD
- Improve characterization and measurement techniques

Key Collaborators:

- Stuart Shaklan, Nasrat Raouf, John Hennessey, and Shouleh Nikzad (JPL)
- Paul Scowen (ASU)
- Manuel Quijada (GSFC)

Current Funded Period of Performance:

Jan 2013 – Dec 2015 with no-cost extension in 2016

Recent Accomplishments:

- ✓ Upgraded coating chamber with sources, temperature controllers, and other monitors to produce various coatings
- ✓ Upgraded measurement tools at JPL and GSFC
- ✓ Produced and tested several coatings with MgF_2, AlF_3, and LiF
- ✓ Fabricated several iterations of protective coatings on Al mirrors
- ✓ Developed ALD coating processes for MgF_2, AlF_3, and LiF at JPL
- ✓ Produced and characterized first set of test coupons representing 1-m-class mirror

Next Milestones:

- Enhancements to conventional coating techniques (Dec 2016)
- Further improvements in ALD and other enhanced coating processes for protected and enhanced aluminum mirrors (Dec 2016)

Application:

- Future astrophysics and exoplanet missions intended to capture key spectral features from far-UV to near-IR

TRL $_{In}$ = 3   TRL $_{Current}$ = 3   TRL $_{Target}$ = 5

Advanced FUVUV/Visible Photon-Counting and Ultralow-Noise Detectors

Shouleh Nikzad / JPL

Objectives and Key Challenges:

- Develop and advance TRL of solar-blind (SB), high-efficiency, photon-counting, and ultralow-noise solid-state detectors, especially in FUV (λ < 200 nm)
- SB silicon, large-format arrays, reliable and stable high response in the FUV

Significance of Work:

- Key innovation are high and stable UV response through atomic-level control of surface and interfaces; the breakthrough in rendering Si detectors with optimized in-band response and out-of-band rejection; versatility with CMOS and CCD

Edge of conduction band for SL doped silicon
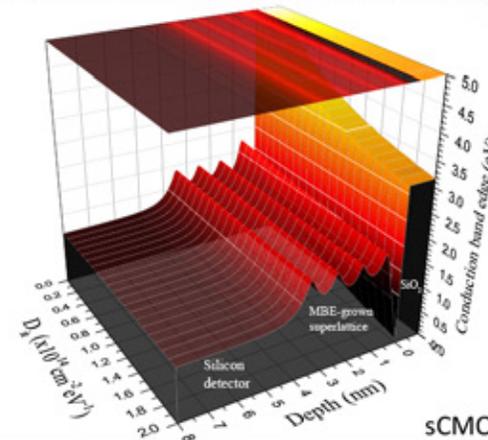
Superlattice doped EMCCD
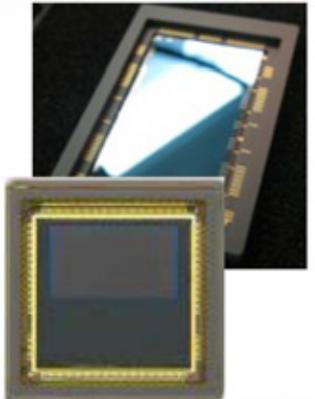
sCMOS example of ultralow-noise CMOS

Approach:

- Fabricate and process UV detectors by super-lattice (SL) doping Electron Multiplying CCDs (EMCCDs) and ultralow-noise CMOS wafers
- Develop multi-stack, integrated, SB filters using atomic-layer deposition (ALD)
- Combine integrated SB filters and SL with sCMOS and EMCCDs
- Characterize and validate

Key Collaborators:

- Chris Martin (Caltech)
- David Schiminovich (Columbia University)
- Michael Hoenk (JPL)
- e2v

Current Funded Period of Performance:

Dec 2015 – Dec 2018

Recent Accomplishments:

New task

Next Milestones:

- Procure two-megapixel EMCCD wafers (Feb 2016)
- Procure sCMOS wafers (Mar 2016)
- Process wafers by thinning and bonding (Jun 2016)
- Begin design of FUV integrated filters (Jul 2016)

Applications:

- Large UV/Optical/NIR Telescope
- Probes, Explorers

$TRL_{In} = 3$ $TRL_{Current} = 3$ $TRL_{Target} = 4\text{-}5$

Development of DMD Arrays for Use in Future Space Missions

PI: Zoran Ninkov / RIT

Objectives and Key Challenges :

- A technology is needed that allows target selection in a field of view that can be input to an imaging spectrometer for remote sensing and astronomy
- We are looking to modify and develop Digital Micro-mirror Devices (DMDs) for this application

Significance of Work:

- Existing DMDs need to have the commercial windows replaced with appropriate windows for the scientific application desired
- The devices need to be evaluated for survivability in a space environment

Palette of eight re-windowed DMDs ready for vibration testing at NASA/GSFC

Approach:

- Use available 0.7 XGA DMDs to develop window removal procedures, and then replace delivered window with a hermetically sealed UV-transmissive window of Magnesium Fluoride, HEM sapphire, and fused silica
- Test and evaluate such devices and as well as Cinema DMDs

Key Collaborators:

- Sally Heap, Manuel Quijada, Jonny Pellish, and Tim Schwartz (NASA/GSFC)
- Massimo Robberto (STScI)
- Alan Raisanen (RIT)

Current Funded Period of Performance:

May 2014 – May 2017

Recent Accomplishments:

- ✓ 0.7 XGA DMD and 1.2 DC2K DMDs delivered
- ✓ XGA devices re-windowed with MgF_2, Sapphire, and fused silica
- ✓ Proton and heavy-ion testing show good results (only SEUs)
- ✓ Contrast measurements indicate high contrast (>5000:1)

Next Milestones:

- Analysis and publication of heavy-ion testing (Dec 2016)
- Measurement, analysis, and publication of scattering measurements (Dec 2016)
- Cinema DMD testing (Feb 2017)

Application:

- Can be used in any hyper-spectral imaging mission
- Galaxy Evolution Spectroscopic Probe

$TRL_{In} = 4$ $TRL_{Current} = 4$ $TRL_{Target} = 5$

Ultra-Stable Structures: Development and Characterization Using Spatial Dynamic Metrology

PI: Babak N. Saif / GSFC

PCOS Physics of the Cosmos

NASA

COR Cosmic Origins

High speed Optical Stability Testbed (HOST)

Vacuum Chamber — Subscale Structure — High Stability Thermal Shroud: — Input: Stinger/ Attenuator — Mirror sim on Hexapod — Laser metrology — High Speed CoC and Speckle Interferometer in Pressure Tight Enclosure — 2nd layer of isolation — Bellows/Isolation (Exists)

Objectives and Key Challenges:

- Developing surface picometer metrology of mirrors and structures
- Developing stimuli system for picometer excitations
- Developing structures and mirrors with controlled dynamics at picometer levels

Significance of Work:

- Stability and dynamics of large structures and mirrors are requirements for large space missions such as ATLAST and exoplanet missions

Approach:

- GSFC will work with a vendor to develop a Dynamical Digital Speckle Pattern Interferometer with picometer precision
- Develop an isolated table-top setup to measure dynamics and drift of material and small structures
- Redesign and model dynamics of the measured material/structures

Key Collaborators:

- Babak Saif and Lee Feinberg (GSFC)
- Dave Chaney (Ball Aerospace)
- Marcel Bluth (SGT)
- Perry Greenfield (STScI)

Current Funded Period of Performance:

2016-2018

Recent Accomplishment:

✓ Finalizing contract with the vendor for developing the interferometer

Next Milestone:

- Work with vendor to develop interferometer as well as verification and testing plans for each stage of development

Applications:

- Future large Astronomy/Astrophysics missions
- Exoplanet missions

$TRL_{In} = 3$ $TRL_{Current} = 3$ $TRL_{Target} = 4$

Improving Ultraviolet Coatings and Filters using Innovative Materials Deposited by ALD

PI: Paul Scowen / ASU

Objectives and Key Challenges:

- Use a range of oxide and fluoride materials to build stable optical layers using PEALD to reduce adsorption, scattering, and impurities
- Layers will be suitable for protective overcoats with high UV reflectivity and unprecedented uniformity (compared to thermal ALD)
- Development of single-chamber system to deposit metal oxide and dielectric layers without breaking vacuum

Significance of Work:

- The improved ALD capability can help leverage innovative UV/optical filter construction

Photograph and schematic of UHV system; the chamber highlighted in blue and the chambers currently being built, which will support oxygen-free deposition and processing.

Approach:

- Development of existing PEALD system to a single-chamber model
- Demonstration of Al film deposition
- Demonstration of fluoride deposition on top of Al films
- Demonstration of VUV reflectivity, uniformity, and stability

Key Collaborators:

- Paul Scowen, Robert Nemanich, Brianna Eller, Franz Koeck, Hongbin Yu (ASU)
- Tom Mooney (Materion)
- Matt Beasley (Planetary Resources, Inc.)

Current Funded Period of Performance:

Dec 2015 – Nov 2018

Recent Accomplishments:

- ✓ Program just getting started, but designs for chambers and milestones and metrics have been defined
- ✓ Design for additional equipment has been completed and parts have been ordered

Next Milestones:

- Install in-situ VUV spectrometer to measure performance <120 nm; calibrate performance using NIST-calibrated UV detector (Aug 2016)
- Demonstrate deposition of Al films using PEALD and measure UV reflectivity to accuracy better than 3% (Dec 2016)
- Demonstrate the deposition of low-loss oxides on evaporated Al surfaces; provide surface for reflection <190 nm (Sep 2016)

Application:

- LUVOIR / HDST / ATLAST

$TRL_{In} = 4$ $TRL_{Current} = 4$ $TRL_{Target} = 5$

Advanced UVOIR Mirror Technology Development for Very Large Space Telescopes

PI: H. Philip Stahl / MSFC
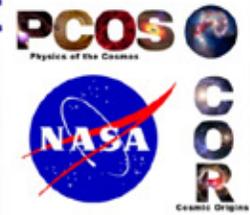
Objectives and Key Challenges:

- Advance TRL of key technology challenges for the primary mirror of future large-aperture Cosmic Origins UVOIR space telescopes
- Include monolithic and segmented optics design paths
- Conduct prototype development, testing, and modeling
- Trace metrics to science mission error budget

Significance of Work:

- Deep-core manufacturing method enables 4-m-class mirrors with 20-30% lower cost and risk
- Design tools increase speed and reduce cost of trade studies
- Integrated modeling tools enable better definition of system and component engineering specifications

1.5-m fused mirror at Harris

Approach:

- Science-driven systems engineering
- Mature technologies required to enable highest-priority science and result in high-performance, low-cost, low-risk system
- Provide options to science community by developing technology enabling both monolithic- and segmented-aperture telescopes
- Mature technology in support of 2020 Decadal process

Key Collaborators:

- AMTD team at MSFC
- Stuart Shaklan (JPL)
- Al Ferland, Rob Egerman, and Katie Hannon (Harris)
- Steve Sokach (Schott)
- Tony Hull (UNM)
- Martin Valente (AOS)
- Gary Mosier (GSFC)

Current Funded Period of Performance:

Sep 2011 – Dec 2016

Recent Accomplishments:

- ✓ Fabricated faceplate, 18 core elements, and backplate
- ✓ Fused 1.5-meter ULE© mirror substrate
- ✓ Generated support structure designs for Harris and Schott mirrors
- ✓ Increased Arnold Mirror Modeler capability
- ✓ Analyzed interaction between optical telescope wavefront stability and coronagraph contrast leakage
- ✓ Mentored four undergraduate students

Next Milestones:

- Demonstrate Slumping of 1/3rd-scale mirror (Sep 2016)
- Validate thermal & mechanical model predictions by test (Jun 2017)

Applications:

- Flagship optical missions; Explorer-type optical missions
- Department of Defense and commercial observations

TRL $_{In}$ = **3 - 5**   TRL $_{Current}$ = **3 - 5**   TRL $_{Target}$ = **4 - 5**
(values depend on specific technology)

Cross-Strip MCP Detector Systems for Spaceflight

PI: John Vallerga / U.C. Berkeley
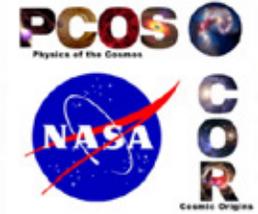
Objectives and Key Challenges:

- Cross strip (XS) MCP photon-counting UV detectors have achieved high spatial resolution (12 μm) at low gain (500k) and high input flux (MHz) using laboratory electronics. We plan to develop new ASICs that improve this performance, which includes amps and ADCs in a small, low-mass, and low-power package crucial for spaceflight; and demonstrate its performance to TRL 6
- A new ASIC with amplifiers 5× faster yet with similar noise characteristics as existing amplifier ASIC
- GHz analog sampling and a low-power ADC per channel
- FPGA control of ASIC chip(s)

Significance of Work:

- Allow high-speed, photon-counting UV detection in package small enough and low enough power and mass to be usable in space

Existing 50-mm detector (without MCPs)
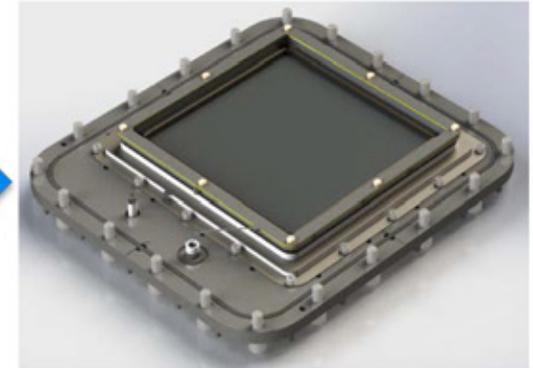
100-mm MCP detector with ASIC electronics qualified for flight

Approach:

- Develop the ASIC in stages, by designing the four major subsystems (amplifier, GHz analog sampler, ADC, and output multiplexor) using sophisticated simulation tools for CMOS processes
- Plan two runs of full-up GRAPH design (CSA preamp and "HalfGRAPH")
- In parallel, design and construct an FPGA readout circuit for the ASIC as well as a 50-mm XS MCP detector that can be qualified for space; our following SAT program will scale this up to 100 x 100 mm and include radiation testing of the ASICs

Key Collaborators:

- Prof. Gary Varner (U. Hawaii)
- Dr. Oswald Siegmund (U.C. Berkeley)

Current Funded Period of Performance:

May 2012 – Apr 2018

Recent Accomplishments:

- ✓ 50-mm detector design and fabrication
- ✓ Confirmed detector performance with PXS electronics
- ✓ Successful thermal test of 50-mm detector (-30°C to +47°C)
- ✓ Successful vibration test of 50-mm detector (14.1 Grms)
- ✓ Fabrication and performance testing of CSAv3

Next Milestones:

- ASIC integration with control FPGA boards (Jun 2016)
- Initiate 100-mm detector design, send for fab quotes (Jun 2016)
- Full ASIC electronics test with detector (Summer 2016)
- Environmental tests of 50-mm Detector + ASICs (Fall 2016)

Applications:

- High performance UV(1-300nm) detector for astrophysics, planetary, solar, heliospheric, or aeronomy missions
- Particle or time-of-flight detector for space physics missions
- Neutron radiography/tomography for material science

$TRL_{In} = 4$ $TRL_{Current} = 4$ $TRL_{Target} = 6$

Raising the Technology Readiness Level of 4.7-THz Local Oscillators

PI: Qing Hu / MIT

Objectives and Key Challenges:

- This project seeks to raise the TRL of 4.7-THz local oscillators (LOs) based on THz quantum-cascade lasers
- The key challenges are to increase the output power level from the current level of <1 mW to 5 mW, and to increase the operating temperature from a lab-demonstrated ~10 K to ~40 K that can be provided in a space-based or suborbital observatory

Significance of Work:

- The 4.744 THz [OI] fine-structure line is the dominant cooling line of warm, dense, neutral atomic gas. Observation of this line will provide valuable information for studies of cosmic origins.
- This project will be important to the proposed GUSTO project.

Array of DFB lasers at ~4.7 THz. The harmonic mixer is used to phase-lock the QCL LO.

Approach:

- Develop perfectly phase-matched 3rd-order DFB structures at 4.7 THz with robust single-mode operations with good beam patterns.
- Develop phase-matched 3rd-order DFB coupled with integrated antennae to increase the output power level to ~5 mW, and to increase the wall-plug power efficiency to 0.5%.

Key Collaborators:

- J.L. Reno (Sandia Nat'l Lab)
- J.R. Gao (SRON/Delft)

Current Funded Period of Performance:

Mar 2016 – Feb 2019

Recent Accomplishments:

- Project started March 1, 2016

Next Milestones:

- Complete the design of perfectly phase-matched 3rd-order DFB lasers aimed for ~4.7 THz (Feb 2017)
- Develop a high-yield dry-etching process using ICP (inductive-coupled plasma) to achieve clean and smooth side walls with high aspect ratios (Feb 2017)
- Grow ~3 MBE wafers based on improved QCL designs (Feb 2017)
- Fabricate devices using combination of dry and wet etching (Feb 2017)
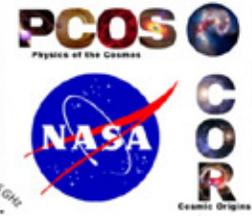
Application:

- GUSTO (The Gal/xgal U/LDB Spectroscopic/Stratospheric THz Observatory)

$TRL_{In} = 3$ $TRL_{Current} = 3$ $TRL_{Target} = 5$

A Far-Infrared Heterodyne Array Receiver for CII and OI Mapping

PI: Imran Mehdi / JPL

16-pixel 1.9-THz all-solid-state LO source

Objectives & Key Challenges:

- The project will advance the TRL of Far-IR heterodyne array receivers so they can be deployed on airborne platforms such as SOFIA or future suborbital and space missions
- Developing a 16-pixel heterodyne receiver system to cover both the C+ and the O+ lines.

Significance of Work:

- Heterodyne technology is necessary to answer fundamental questions such as: How do stars form? How do circumstellar disks evolve and form planetary systems? What controls the mass-energy-chemical cycles within galaxies?

Approach:

- Use JPL-developed membrane diode process to construct tunable sources in the 1.9 - 2.06-THz range
- Use novel, waveguide-based, active-device, power-combining schemes to enhance power at these frequencies
- Design and build compact, micro-machined, silicon housing for HEB mixer chips
- Use CMOS technology for back-ends/synthesizer
- Characterize and test multi-pixel receivers to validate stability and field performance

Key Collaborators:

- Paul Goldsmith (Science Lead), Jon Kawamura, Jose Siles, Choonsup Lee, and Goutam Chattopadhyay (JPL)
- Frank Chang (UCLA)

Current Funded Period of Performance:

Oct 2013 – Sep 2016
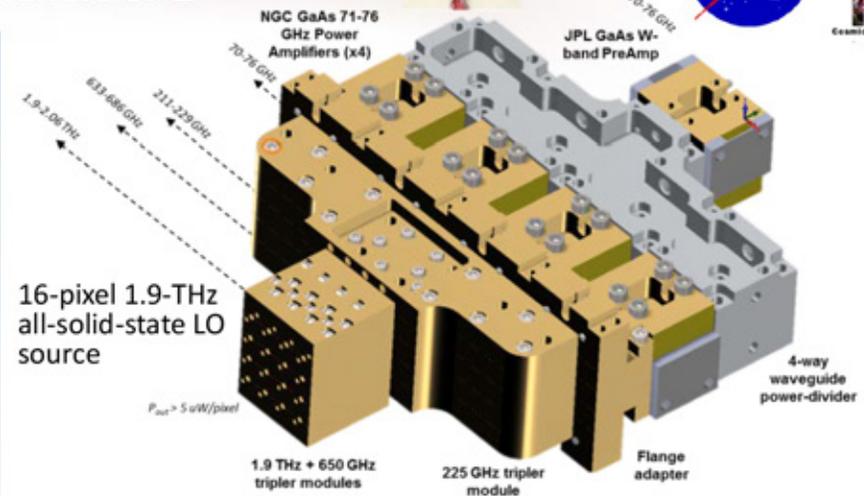
Recent Accomplishments:

- ✓ Fabricated multiplier devices for updated LO scheme
- ✓ Demonstrated 4-pixel LO source at 1.9 THz (at room temperature)
- ✓ Demonstrated 4-pixel receiver at 1.9 THz with Trx = 600 K DSB
- ✓ Completed design and fabrication of 16-pixel LO sub-unit
- ✓ Procured, packaged, and tested GaN-based power amplifiers
- ✓ Designed 16-pixel mixer block

Next Milestones:

- Assemble 16-pixel LO sub-unit, test at room temperature (Aug 2016)
- Assemble and test 16-mixer mixer waveguide sub-unit (Aug 2016)
- Design optical elements to accommodate 16-pixel receiver (Sep 2016)
- Assemble and test 16-pixel receiver from 1.9 to 2.06 THz (Oct 2016)
- Measure receiver performance and stability (Aug 2016)

$TRL_{In} = 4 \quad TRL_{Current} = 4 \quad TRL_{Target} = 5$

Kinetic Inductance Detector Arrays for Far-IR Astrophysics

PI: Jonas Zmuidzinas / Caltech
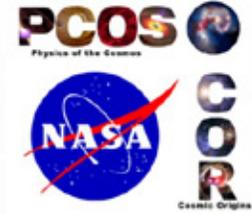
Objectives and Key Challenges:

- Half of the electromagnetic energy emitted since the Big Bang lies in the far-IR. Large-format far-IR imaging arrays are needed to study galaxy formation and evolution, and star formation in our galaxy and nearby galaxies. Polarization-sensitive arrays can provide critical information on the role of magnetic fields.
- We will develop and demonstrate far-IR arrays for these applications

Significance of Work:

- Far-IR arrays are in high demand but are difficult to fabricate, and therefore expensive and in short supply. Our solution is to use titanium nitride (TiN) and aluminum absorber-coupled, frequency-multiplexed kinetic inductance detectors (KIDs).

Demo at CSO: 350 µm image of Sgr B2

Approach:

- Raise the TRL of these detectors so investigators may confidently propose them for a variety of instruments:
  - Ground telescope demo, 350 µm, 3×10^{-16} W Hz$^{-1/2}$
  - Lab demo for space, 90 µm, 5×10^{-19} W Hz$^{-1/2}$

Key Collaborators:

- Goutam Chattopadhyay, Peter Day, Darren Dowell, Rick Leduc (JPL)
- Chris McKenney (JPL/NIST)
- Pradeep Bhupathi, Matt Holllister, Attila Kovacs (Caltech)

Current Funded Period of Performance:

Mar 2013 – Feb 2017

(4th year of 2-year project; completing no-cost extension period)
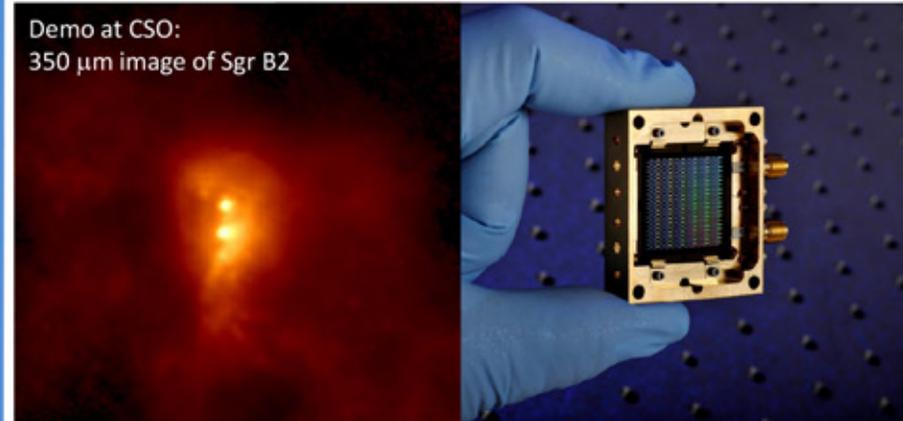
Recent Accomplishments:

- ✓ Successful 350 and 850 µm demo on telescope (image above)
- ✓ Photon-noise-limited 350 µm lens-coupled arrays
- ✓ Low-cost, high-yield multiplexing of 500-pixel arrays
- ✓ Process improvement (high yield) in aluminum KID for space-background operation
- ✓ Demonstration of new chirped readout technique at telescope

Next Milestones:

- Optical tests of space-sensitivity arrays (through end of project)

Applications:

- Future space missions, e.g., Far-IR Surveyor
- Suborbital projects: SOFIA instruments and balloon payloads
- Cameras and spectrometers for ground-based telescopes
- CMB arrays – now under development at Columbia University

$TRL_{In} = 3$ $TRL_{PI-Asserted} = 3-6$ $TRL_{Target} = 4-6$

Appendix C
Program Technology Development Status

UV/Vis/IR

Far-IR

Abstracts for SAT Projects Starting in 2017

Ultraviolet Coatings, Materials, and Processes for Advanced Telescope Optics

Prepared by: K. 'Bala' Balasubramanian (PI; JPL/Caltech); John Hennessy, Nasrat Raouf, Shouleh Nikzad, and Stuart Shaklan (JPL/Caltech); Paul Scowen (ASU); and Manuel Quijada (NASA/GSFC)

Summary

NASA's Cosmic Origins (COR) program and the astrophysics community seek to develop and advance coating technologies for telescope optics needed for large missions such as the Large Ultraviolet (UV)/Optical/Infrared (IR) (LUVOIR) Surveyor and the Habitable Exoplanet (HabEx) Imaging Mission in the upcoming decades. Development of high-reflectivity coatings, particularly for the UV, is a technology challenge requiring significant materials research and process development.

A successful pathway to achieve the objectives, namely to develop durable mirror coatings that will provide high reflectance over the extended spectral band in the Far-UV (FUV) to near-infrared (NIR), requires the best choice of materials and processes. Void-free thin films of absorption-free materials are required to protect and maintain high reflectivity and durability of aluminum mirrors in laboratory and pre-launch environments. A precisely controllable and scalable deposition process is also required to produce such coatings on large telescope mirrors.

During the first year of our three-year project commencing in 2013, we investigated the applicability of common materials and known processes, and identified promising candidates [1-3]. MgF_2, LiF, and AlF_3 stand out as the most promising materials for protective coatings while GdF_3, LaF_3, and LuF_2 are other potential materials to be considered. Coatings of some of these materials using a conventional vacuum deposition process were produced and characterized. Our initial results were reported in a poster paper presented at the American Astronomical Society (AAS) meeting in Baltimore, MD [4]. Preliminary results with coating experiments on Al mirrors protected with MgF_2 and AlF_3 were also reported in our report in the 2014 and 2015 COR Program Annual Technology Reports (PATRs).

Our recent experiments focused on Atomic Layer Deposition (ALD) to produce thin MgF_2, AlF_3, and LiF protective coatings in addition to conventional techniques. With the 1.2-m coating chamber at our sub-contract vendor, Zecoat Corp. of Torrance, CA, we produced a number of samples with chosen recipes using conventional evaporation techniques as detailed below. Similarly, several samples of newly developed ALD protective coatings on Al were produced at JPL. A Perkin Elmer UV/Vis spectrophotometer at JPL and an Acton FUV spectrophotometer at the NASA Goddard Space Flight Center (GSFC) were used to measure the reflectance properties of these samples. A spectroscopic ellipsometer was also used at JPL to characterize the films. Theoretical-model fits of measured characteristics were analyzed. Key advances were made this year on the ALD front with successful process development for AlF_3 and LiF coatings at faster rates and lower temperatures. Further process development for protected Al coatings with these chosen materials is in progress. Papers [5, 6] on the most recent ALD results were presented at the ALD conference in Portland, OR on June 29, 2015 and at the 2015 SPIE Annual Conference in San Diego in July 2015. Comprehensive refereed papers [7, 8] have been accepted for publication in the Journal of Vacuum Science and Technology (JVST) and in the Journal of Astronomical Telescopes, Instruments, and Systems (JATIS).

Background

It has been recognized that in the Far-UV to Mid-UV wavelengths ($90 < \lambda < 300$ nm), it is possible to detect and measure important astrophysical processes, which can shed light on the physical conditions of many environments of interest in the universe. For example, in the local interstellar medium (LISM), all but two of the key diagnostic resonance lines (Ca II H and K lines) are in the UV [9]. In addition to the fruitful science areas that UV spectroscopy has contributed since the early 1970s, France et al. [10] have emphasized the role of UV photons in the photo-dissociation and photochemistry of H_2O and CO_2 in terrestrial-planet atmospheres, which can influence their atmospheric chemistry, and subsequently the habitability of Earth-like planets. However, only limited spectroscopic data are available for exoplanets and their host stars, especially in the case of M-type stars. Similarly, new areas of scientific interest are in the detection and characterization of the hot gas between galaxies and the role of the intergalactic medium (IGM) in galaxy evolution [11].

The 2011 COR PATR (Technology Needs, Table 7, Item 8.1.3., page 43, Oct 2011) [12] defined the primary goal that we have adopted for this project: "Development of UV coatings with high reflectivity (> 90-95%), high uniformity (< 1-0.1%), and wide bandpasses (~100 nm to 300-1000 nm)." More recently, the Advanced-Technology Large-Aperture Space Telescope (ATLAST) technology team assessed and stressed the importance of technology development for maturing mirror coatings for the FUV spectral range [13]. A comprehensive summary of the FUV science requirements (a Science Traceability Matrix, STM) was compiled by Paul Scowen [14], a Co-I on our project. Table 1 lists some of the important spectral lines in the FUV region for general astrophysics. High reflectivity coatings covering the 100-300-nm spectral range are considered important for studying intergalactic matter. The COR Program Analysis Group (COPAG) assessed this, stating, "*The COPAG is considering a future large UVOIR (UV/Optical/Infrared) mission for general astrophysics that would also perform exoplanet imaging and characterization. Some technologies may be specifically required to make these two missions compatible, for example telescope coatings,*" and concluded the degree of difficulty is very high [15, see p. 5]. Bolcar et al. also assessed these technology requirements [16].

Objectives and Milestones

The main objectives of our three-year project were: a) to explore materials and processes to produce protective coatings for Al mirrors providing high reflectivity over a wide spectral range from FUV to NIR, and b) to demonstrate fabrication of durable mirror coatings with chosen processes on distributed coupons representing a meter-class mirror. Conventional coating processes and advanced ALD processes are pursued and investigated to achieve these goals. During the reporting period, from June 2015 to May 2016, the primary objectives were:

1. Fabricate and test coatings of Al protected by MgF_2, AlF_3, and LiF deposited by conventional coating processes.
2. Optimize ALD process for absorption-free thin AlF_3 and LiF coatings and characterize them.
3. Conduct coating experiments with AlF_3-protected and LiF-protected Al mirrors.
4. Measure time-dependent changes in the reflectance characteristics of these mirror samples.
5. Develop and perform environmental tests of mirror samples. Measure reflectance before and after environmental tests, and characterize the surface microscopically; this task is moved to the latter half of 2016 for prioritizing ALD process optimization.

The major objectives listed above are adopted from our original proposal and reprioritized to start on the promising ALD process development early on.

Wavelength (nm)	Species	Significance	Bodies of Interest
68.1, 69.4	Na IX	Coronal-gas (> 10^6 K) diagnostic (density, ionization state, etc.)	IGM, quasi-stellar object (QSO) sight lines
77.0	Ne VIII	Warm-hot-gas (5×10^5 - 10^6 K) diagnostic (density, ionization state, etc.)	IGM, QSO sight lines
99.1, 175.0	N III	Gas-temperature diagnostic	Stellar-atmosphere abundances
102.6	H, Ly-α	Lyman Series H recombination line	Plasma diagnostics for ionized gas in astrophysical contexts
103.2, 103.8	O VI	Recombination-line doublet	Diagnostic for presence of coronal gas and the boundaries between such gas and cooler gas envelopes or media
108.5, 164.0	He II	Balmer line for He	Stellar-atmosphere diagnostic used to trace flares and coronal-mass ejections (CMEs)
117.5	C III	Gas-electron-density diagnostic	Stellar atmospheres and stellar winds
120.6	Si III	Optically thin emission line of silicon	Used as a diagnostic line sensitive to time-variability in emitted or ionizing flux
121.6	H, Ly-α	Lyman Series H recombination line	Plasma diagnostics for ionized gas in astrophysical contexts – especially used for cosmological targets such as reionization-era galaxies and stars
123.8, 124.3	N V	Gas-emission diagnostic	Used to study extended stellar coronae
133.5	C II	Absorption line for ionized carbon	Used as a diagnostic and tracer for stellar chromospheres and planetary atmospheres
139.4, 140.3	Si IV	Emission line of silicon	Used to perform diagnostics of stellar coronae including density, temperature, and abundance
140.7	O IV	Gas-density-sensitive doublet	Used to study upper chromospheres in stars
148.8	N IV	Gas diagnostic line – sensitive in particular to electron collision strengths	Used to study stellar coronae and changes in their emission and bulk motion
154.8, 155.1	C IV	Gas-density-sensitive doublet	Used to diagnose most ionized-gas phases including stellar atmospheres and nebulae
166.3	O III	Gas-temperature and density-sensitive diagnostic	Used to diagnose nebula-gas emission
175.0	N III	Gas-temperature-sensitive diagnostic	Used for stellar-plasma observations and diagnosis
189.5	Si III	Gas-density-sensitive diagnostic	Used to study astrophysical plasmas
190.9	O III	Gas-temperature and density-sensitive diagnostic	Used to diagnose nebula-gas emission
232.6	C II	Absorption line for ionized carbon	Used as a diagnostic and tracer for stellar chromospheres and planetary atmospheres
233.6	Si II	Gas-density-sensitive diagnostic	Magnetic-field diagnostic in stellar atmospheres; density diagnostic in stellar chromospheres

Table 1. *Significant diagnostic spectral lines in the UV (50-250 nm) (Courtesy: Paul Scowen).*

Progress and Accomplishments

Single-layer coatings of applicable transparent protective materials by conventional deposition process.
Single-layer coatings of MgF_2, LiF, AlF_3, LaF_3, Na_3AlF_6, and GdF_3 were produced initially with conventional coating processes in a ZeCoat Corp 1.2-m chamber (Fig. 1) fitted with resistive sources, electron gun, ion gun, heater lamps, liquid-nitrogen (LN) traps, cryo-pumps, residual-gas analyzers, and computer controls; at pressures between 2×10^{-7} and 1×10^{-6} Torr and temperatures between 20° and 200°C. A sample transport with masking mechanism was installed in the chamber, enabling multiple coatings on different samples without breaking vacuum. A FUV optical monitoring system was also installed to measure reflected signal from the growing film during deposition and post-deposition, while monitoring varying total pressure, water vapor and oxygen content, etc., for diagnostic purposes.
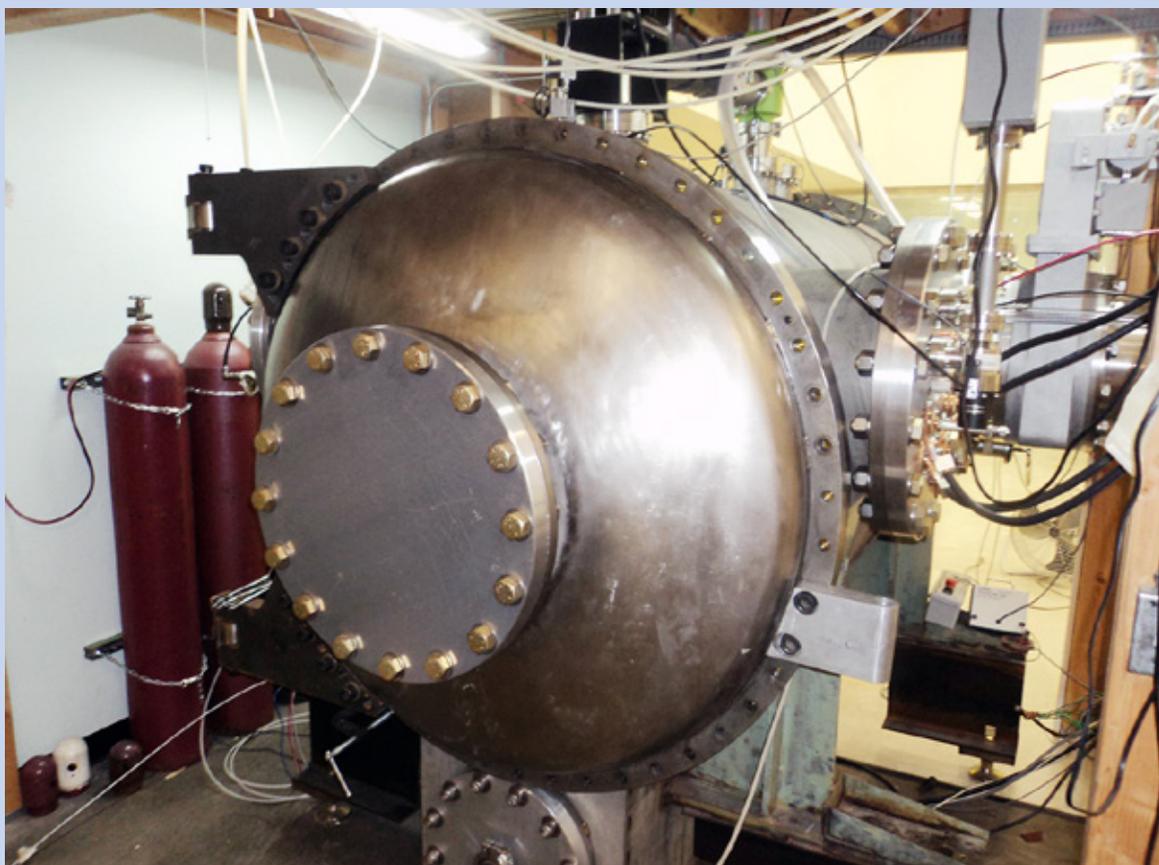
Fig. 1. *A 1.2-m coating chamber fitted with process controllers, thickness monitor, and gas analyzer (courtesy: Zecoat Corp).*

MgF_2, LiF, and AlF_3 are considered the most promising coatings based on their UV transparency, as evidenced by results from these initial experiments. Other materials, particularly high-index fluorides, could be employed in other multilayer devices such as filters and beam splitters. Several coatings were prepared on fused silica and silicon substrates. Spectral performance characteristics of these coatings were measured with a state-of-the-art UV/Vis spectrophotometer (PerkinElmer Lambda 1050) as well as with an Acton FUV spectrometer at GSFC.

Protected Al mirror coatings

MgF_2, AlF_3, and LiF single-layer- and bi-layer-protected Al mirror samples were produced in 2014 and 2015 with a conventional deposition process in the chamber described above. Figure 2 shows the reflectance of bi-layer-protected Al mirror samples from initial experimental runs in the same chamber. These samples remained in the lab in a dry-nitrogen flow-box except during measurements, involving a few days of exposure to normal lab environment with ~30 to 50% humidity. Figure 3 shows the spectral reflectance performance of a bi-layer-protected ($LiF+AlF_3$) Al mirror sample for FUV to NIR, measured over a period of ~14 months after fabrication. The data show excellent stability. Figure 4 shows the details of the spectral reflectance performance in the FUV range, extended to 23 months. While UV-to-NIR (200- to 1000-nm) reflectance measurements were done at JPL, FUV (50- to 200-nm) measurements with an Acton FUV spectrophotometer were done at GSFC under the guidance of Dr. Manuel Quijada. These samples were produced using conventional deposition techniques. Optimization and enhancement of reflectance in the 100- to 200-nm range is a subject of further experimental investigation of process conditions and layer structures. In this context, research done at GSFC has been reported [17, 18] at an SPIE conference and at the AAS meeting in Baltimore, MD. ALD deposition of such coatings is now in progress at JPL.
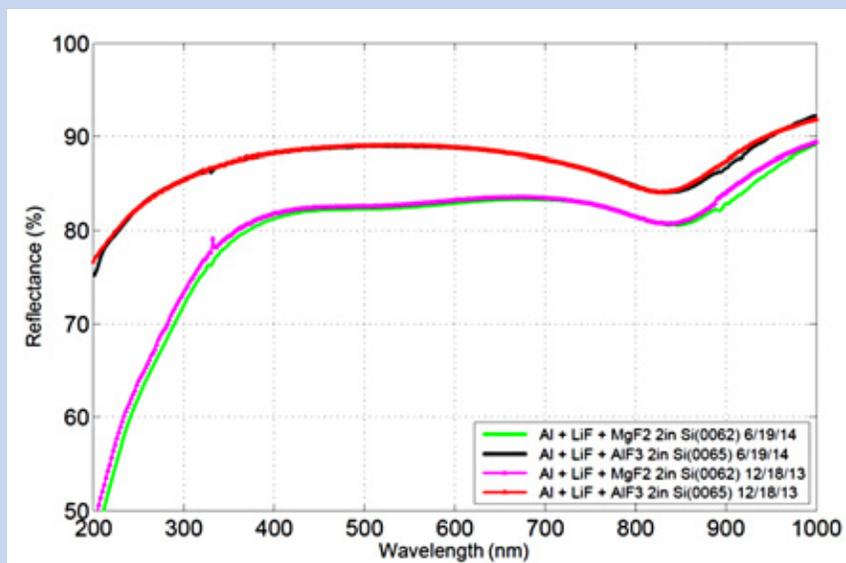
Fig. 2. *Reflectivity of Al+LiF mirror samples with MgF$_2$ and AlF$_3$ protective layers. Measured six months after fabrication, these samples show little degradation.*
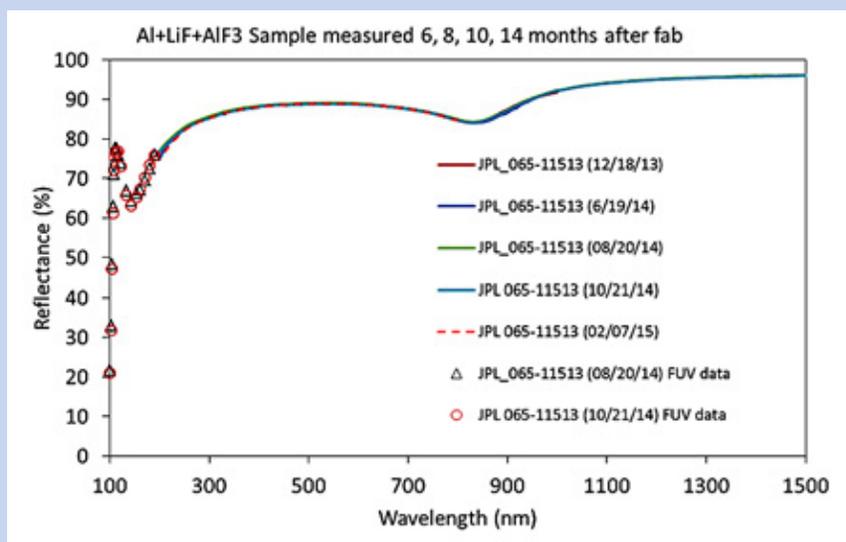

Fig. 3. *Measured reflectance of a bi-layer-protected Al mirror sample (AlF$_3$+LiF on Al) measured 6, 8, 10, and 14 months after fabrication showing excellent stability. Results over the FUV to NIR spectral range.*
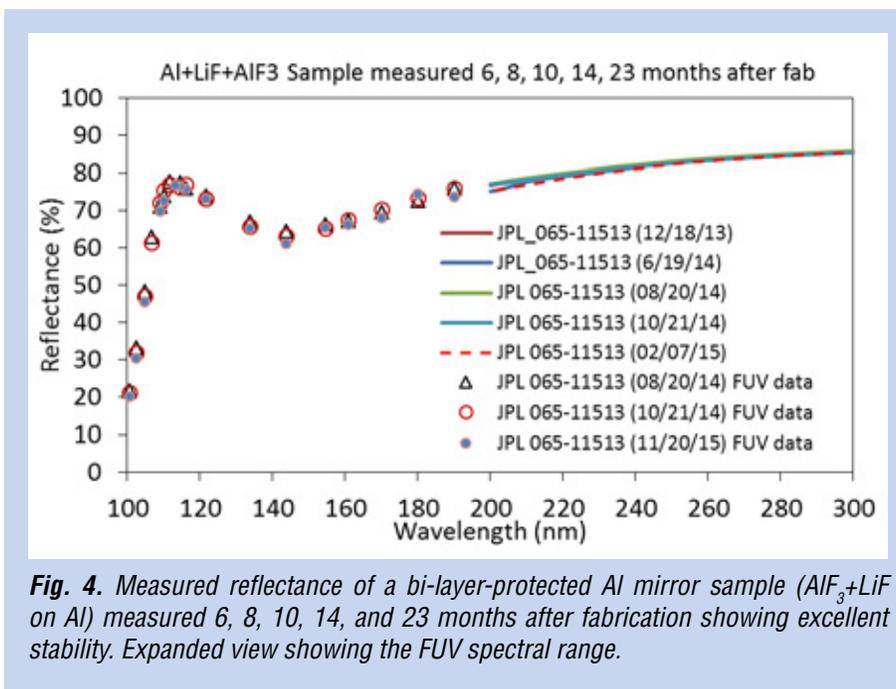
Fig. 4. *Measured reflectance of a bi-layer-protected Al mirror sample (AlF_3+LiF on Al) measured 6, 8, 10, 14, and 23 months after fabrication showing excellent stability. Expanded view showing the FUV spectral range.*

With further refinement of process controls in the conventional coating chamber, we prepared new samples of MgF_2- and AlF_3-protected mirrors with Al and LiF layers. FUV measurements of such tri-layer samples indicate a reflectance greater than 75% achievable at 110 nm and greater than 50% at 100 nm (Fig. 5). Further optimization of coating thicknesses and process parameters is expected to enhance the FUV reflectance.
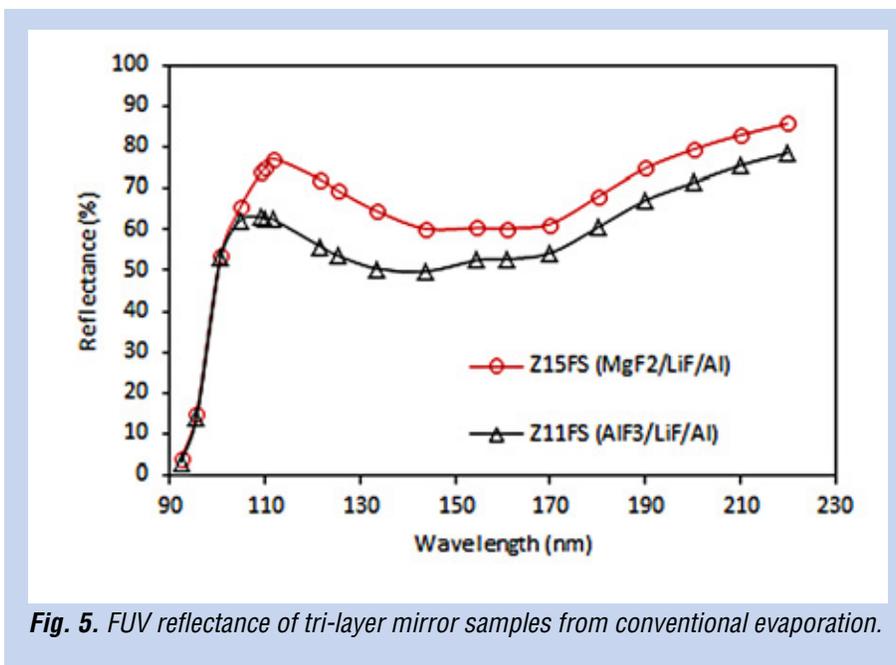

Fig. 5. *FUV reflectance of tri-layer mirror samples from conventional evaporation.*

Atomic Layer Deposition
ALD processes are under development at JPL to produce MgF_2 and AlF_3 protective coatings for high-reflectivity mirrors using an Oxford OpAl showerhead-style ALD reactor and a Beneq ALD system (Fig. 6).

Fig. 6. *ALD systems at JPL.* Left: *Oxford OpAl showerhead-style ALD reactor with gas feedthroughs and process controls enabling AlF$_3$ and MgF$_2$ coatings development.* Right: *Beneq ALD deposition system.*

ALD films were deposited using bis(ethylcyclopentadienyl) magnesium (Mg(EtCp)$_2$) and trimethylaluminum (TMA) as the metal-containing precursors and anhydrous hydrogen fluoride (HF) as the fluorine-containing precursor in our Oxford reactor. Although metal fluorides are not common ALD materials, there have been several previous reports of their deposition using metal fluorides such as TaF$_5$ or TiF$_4$ as the fluorine-containing source [19, 20]. This tends to create residual metal contamination which degrades the absorption properties in the FUV and results in a process which can only be performed at substrate temperatures greater than 250°C. This high deposition temperature causes the fluoride films deposited with this method to crystallize readily, resulting in significant surface morphology, which is undesirable for many optical applications. In contrast, the JPL-developed ALD process using HF results in fluorides with lower residual contamination that can also be deposited at low temperature, generating smoother, denser films.

As part of this effort, MgF$_2$ and AlF$_3$ were deposited at substrate temperatures ranging from 100°C to 250°C. Film thickness and refractive index were measured by spectroscopic ellipsometry and monitored as a function of process conditions such as process purge times and substrate temperature. Recent reports on the same JPL ALD materials have also shown good optical performance at wavelengths down to 90 nm [5, 21].

Typical ALD conditions involve heating the Mg(EtCP)$_2$ precursor, which is then bubbled with Ar into the process chamber with exposure times of approximately 1 s. TMA and HF are delivered by vapor draw at room temperature with shorter exposure times of 15-30 ms. The chamber is purged with Ar between each half-cycle exposure in the ALD process, to ensure saturated, self-limiting deposition. We have demonstrated both MgF$_2$ and AlF$_3$ with thickness uniformities better than 1% over six inches in diameter. Initial X-ray-Photoelectron-Spectroscopy (XPS) measurements suggest the films are approximately stoichiometric, and future studies will investigate how material composition changes as a function of process conditions. A key goal in developing an ALD process is to optimize the process at acceptably low temperature, i.e., below 100°C, to enable large mirror coatings in high vacuum. Our recent experiments indicate that this is feasible for the relevant fluorides.

Reflectance degradation of Al with oxide formation: Evaporation Rate, Surface Roughness, and Reflectance Stability

To assess the nature and progression of oxide formation on fresh Al coating, we conducted a series of control experiments with Al coatings of different thicknesses deposited at different rates at a high vacuum of ~2×10⁻⁹ Torr in an ultra-high vacuum (UHV) chamber at JPL. Figure 7 shows the measured (symbols) and modeled (lines) performance of an unprotected Al mirror in the wavelength range from 190 to 290 nm over a period of about 1500 minutes after deposition. A very thin layer of oxide formation (only about 10-Å thick) is estimated to be sufficient to degrade the reflectance as shown. Figure 8 shows the measured FUV reflectance of an unprotected Al mirror and its model fit with oxide formation at different thicknesses. These measurements and simulations show that an oxide layer of less than 2-nm thickness affects the FUV reflectance dramatically.
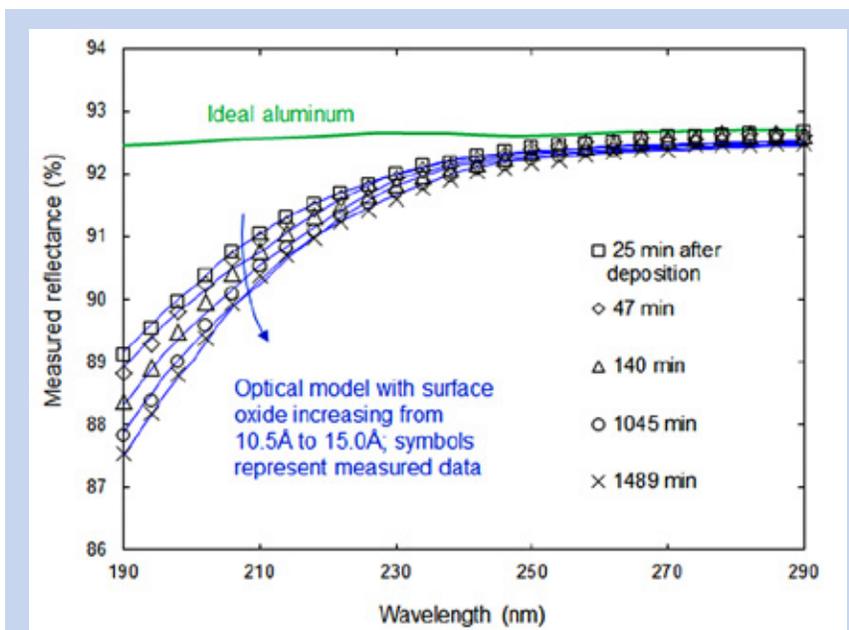

Fig. 7. *Oxidation-induced near-UV reflectance reduction of Al mirror samples; model fits match a progressive increase of oxide formation.*
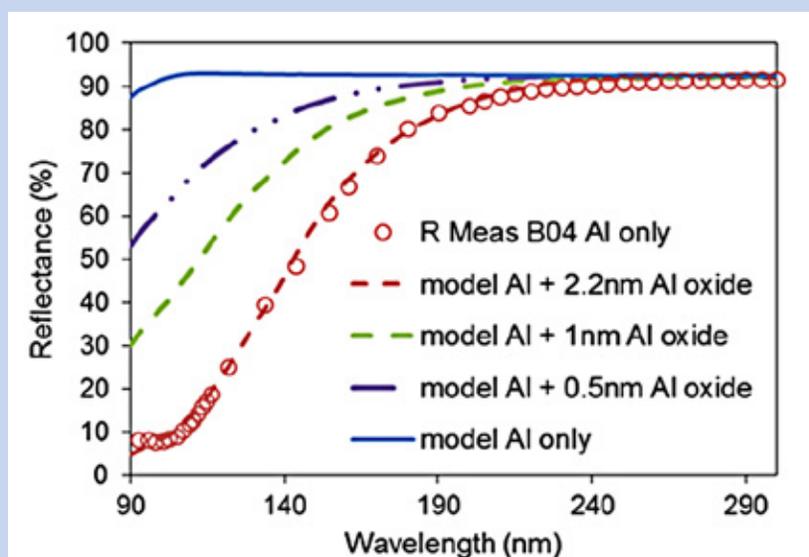

Fig. 8. *Unprotected Al reflectance per models with a thin oxide layer in comparison with measured characteristics (sample B04) in the FUV spectral range.*

Unprotected and protected samples with ALD coatings were also fabricated and measured within about 20 minutes and thereafter for several days to assess the nature of degradation and the effectiveness of a thin protective layer. Figure 9 shows the drop in reflectance over time at wavelengths from 190 to 240 nm as measured by a UV/Vis spectrophotometer. Careful study indicates that the drop is significant in the first two hours and especially within the first few minutes. Encouragingly, as Fig. 10 shows, a very thin protective layer of AlF_3 preserves the reflectance adequately in laboratory conditions. This ensures a pathway to enhance and preserve the FUV reflectance of Al below 120 nm with an appropriate thin protective layer. Rate of deposition of the Al layer is a critical parameter that affects the reflectance as well as its stability over time. Samples were fabricated at different rates at high vacuum. While further experiments are in progress, initial measurements indicate (Fig. 11, Table 2) that a rate of about 20 Å/s or higher is favorable for obtaining better reflectance in the FUV due to denser microstructure and lower oxidation in the bulk of the layer compared to lower-rate samples.
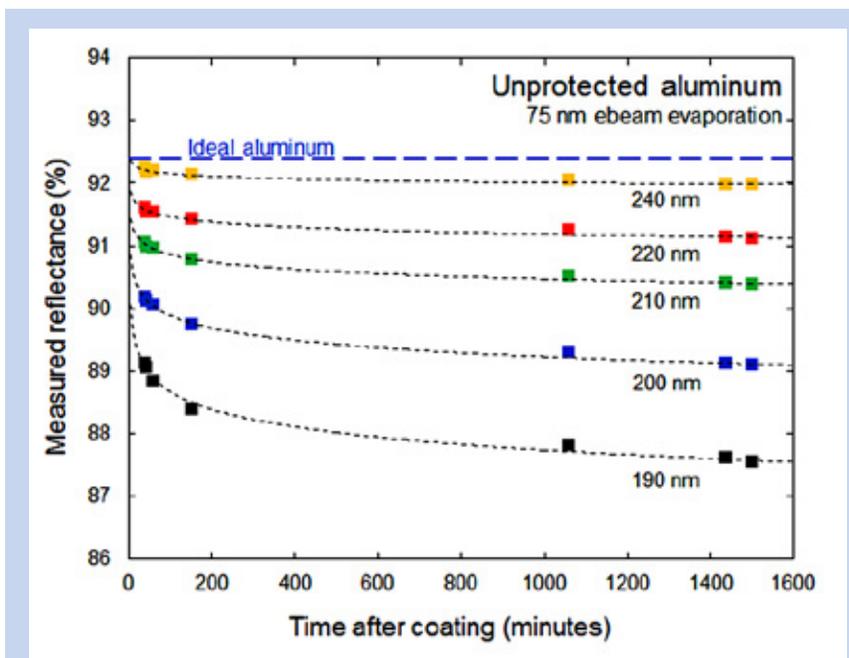

Fig. 9. Unprotected aluminum degradation over time (sample L1). Shorter wavelengths (below 190 nm) would suffer greater degradation, not captured in the above measurements.
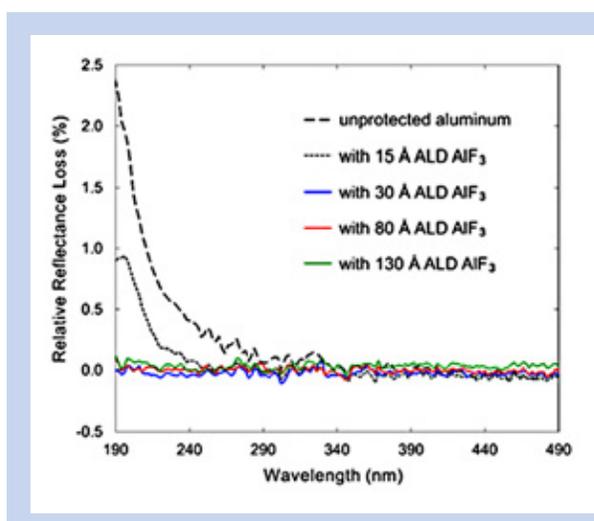

Fig. 10. Stability of Al mirror (sample K series) coated with thin AlF_3 layer using ALD in comparison with unprotected Al mirror; Reflectance loss after 10 days from fabrication. The loss rate will be greater in the FUV. Even 3 nm of AlF_3 provides adequate protection against reflectance loss.
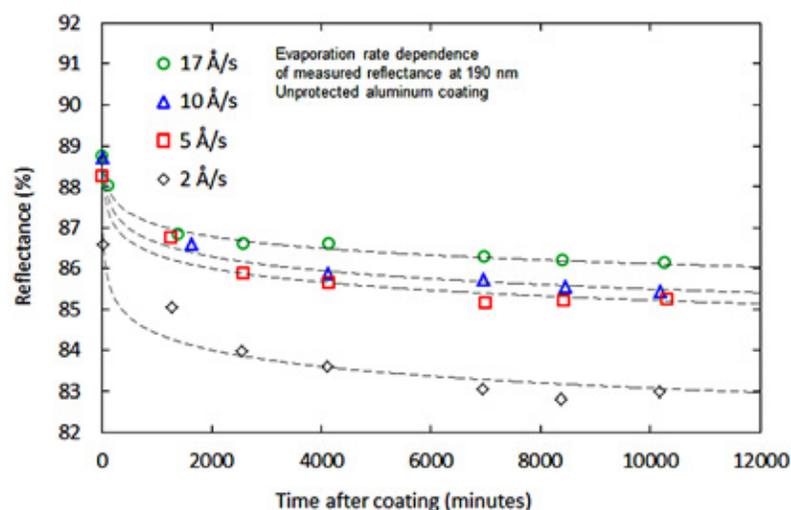
Fig. 11. Measured reflectance at 190 nm vs. elapsed time of unprotected Al mirror samples produced at different evaporation rates at a base pressure of 2×10^{-9} Torr. Initial reflectance as well as rate of degradation are better with higher deposition rate. Dashed lines indicate an approximate power law dependence.

Evaporation Rate (Å/s)	Micro-roughness 1 μm × 1 μm (nm rms)	XPS [O 1s] / [Al 2p] ratio	Reflectance after 1 week at 190 nm (%)
2	2.05 (±0.14)	1.3 (±0.2)	83.0
5	1.45 (±0.09)	1.3 (±0.2)	85.2
10	1.30 (±0.08)	1.3 (±0.2)	85.5
17	1.18 (±0.03)	1.1 (±0.2)	86.1

Table 2. The influence of evaporation rate on the UV reflectance at 190 nm for Al thin films deposited by electron beam evaporation at a base pressure of 2×10^{-9} Torr. The mean rms roughness and standard deviation averaged over five scans for each of the four samples analyzed in Fig. 11.

Protected Al mirrors

A series of AlF$_3$-coated Al mirror samples were prepared with different thicknesses of the protective fluoride coated using the ALD process. The UV reflectance of four of these samples was measured over several days. Figure 11 shows the stability or change in reflectance from immediately after fabrication to more than six days after fabrication.

In this context, we examined the surface roughness of the Al samples deposited in UHV at different rates. Figure 12 compares atomic-force microscope (AFM) images of samples deposited at 2 Å/s and 17 Å/s, clearly indicating that greater smoothness is achieved with higher deposition rates.
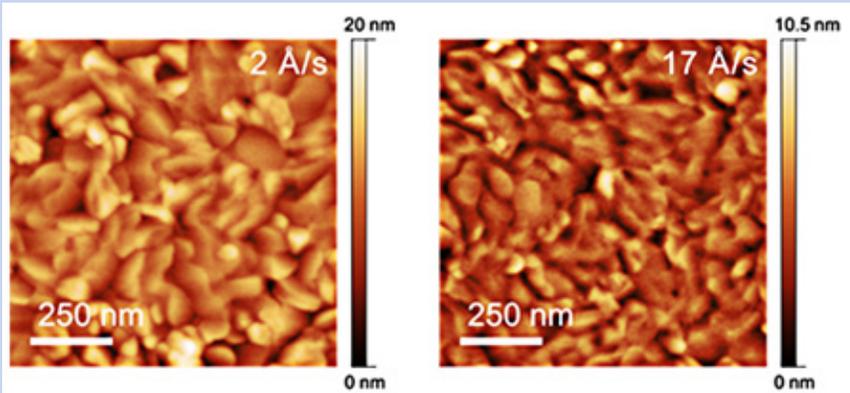

Fig. 12. AFM images of UHV electron beam evaporated Al films (60-nm thickness) at deposition rates of 2 Å/s (left) and 17 Å/s (right) at a length scale of 1 μm.

FUV performance of ALD AlF₃-protected Al samples

Figure 13 shows the FUV reflectance of the AlF₃-protected Al mirror samples measured several days after fabrication. Model fits indicate a smaller level of oxide formation in the Al layer when a thicker protective coating is applied. However, due to the delay in transferring the Al-coated sample from the UHV chamber to the ALD reactor for applying the protective fluoride layer, some oxidation still occurs. FUV-performance comparison of a subsequent set of samples with different thicknesses of protective fluoride is shown in Fig. 14. A phenomenological refractive index model was developed to estimate the optical properties of the surface oxide and assess the performance impact of a brief air exposure prior to deposition of a protective layer. Details of this model and analysis can be found in [8]. The n and k derived from such a model are plotted in Fig. 15 (adapted from [8]).
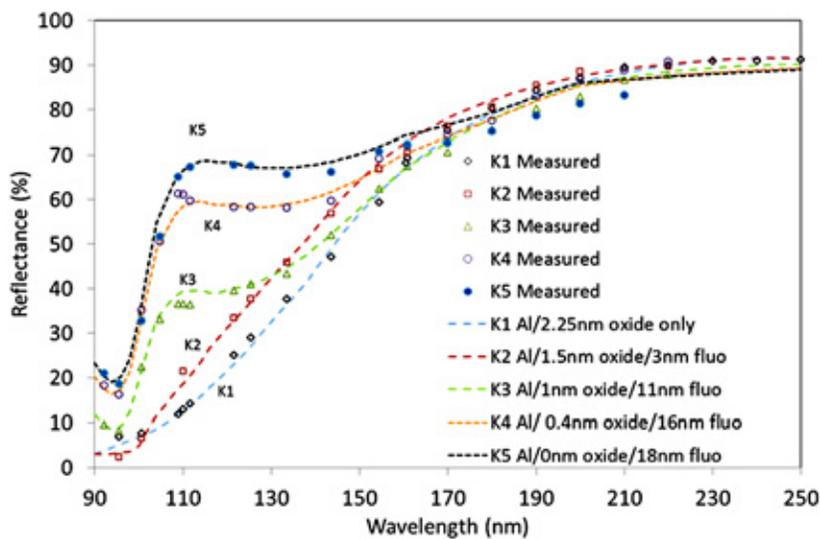
Fig. 13. Model fits (dashed lines) and measurements (symbols) of FUV reflectance of unprotected (sample K1) and AlF₃-protected samples (K2 to K5). Formation of an oxide layer before the application of a protective AlF₃ layer is matched by models showing that the oxide formation is arrested by the fluoride layer, though not yet adequately. This is primarily due to the few-minute delay in transferring the sample from the UHV chamber to the next ALD reactor for fluoride coating.

Fig. 14. Measured FUV reflectance (symbols) and the corresponding calculated optical model (dashed lines) of ALD AlF₃ protective coatings of various thicknesses deposited on e-beam-evaporated Al thin films, compared to an unprotected Al coating and a typical high-performance Phyical Vapor Deposition (PVD) MgF₂-protected mirror.

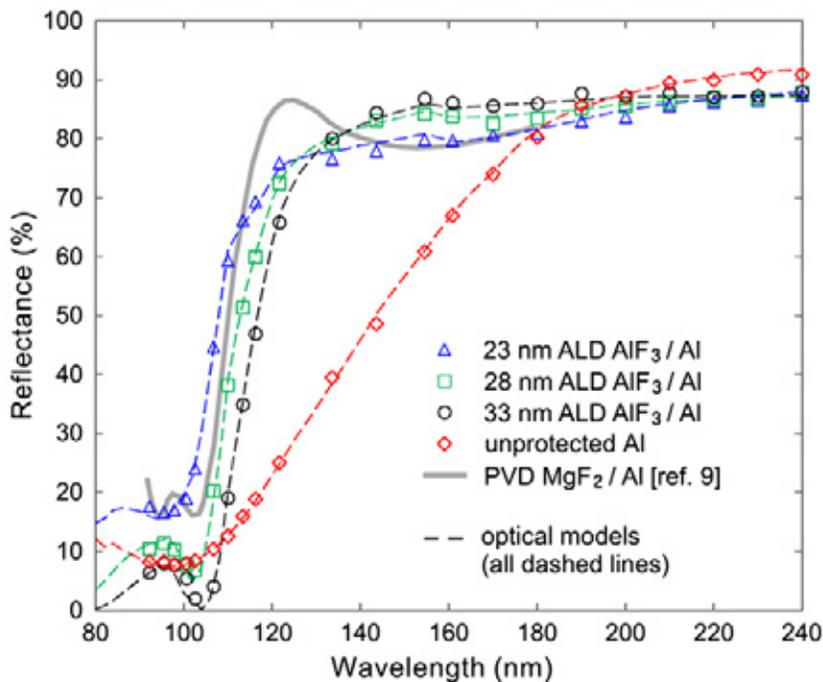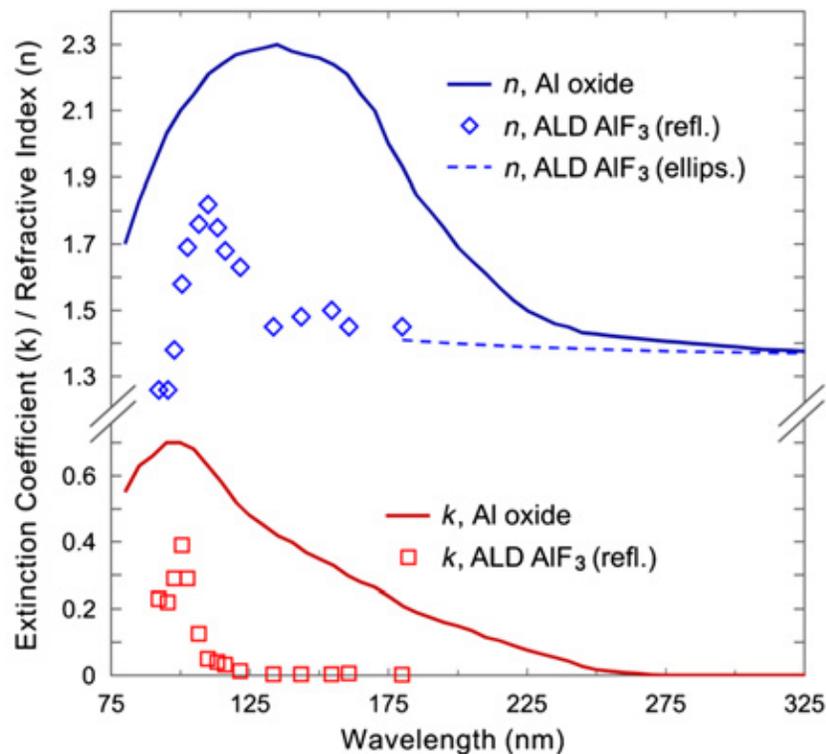Fig. 15. Phenomenological refractive index model for the interfacial native oxide on evaporated Al thin films, and the refractive-index model for ALD AlF$_3$ derived from iso-reflectance analysis in the FUV.

Figure 16 compares the performance of protected Al samples produced by conventional evaporation techniques and by e-beam followed by ALD. Moving the absorption further to the FUV end toward 90 nm is the subject of further optimization of layer structures and thicknesses. While a LiF layer allows moving the edge to the shorter wavelengths, it reduces the reflectance in the midrange of FUV when these typical structures are employed. Hence thinner layers are considered necessary if adequate protection can be ensured.

Fig. 16. FUV reflectance of tri-layer mirror samples produced by conventional thermal evaporation (samples Z11 and Z15) and of bi-layer mirror samples produced by e-beam of Al and ALD of AlF$_3$ (samples K5 and Q11).

Uniformity tests with conventional evaporation

A preliminary study was conducted (Fig. 17) to test the uniformity of the Al coating deposited with conventional e-beam evaporation techniques on a meter-class opti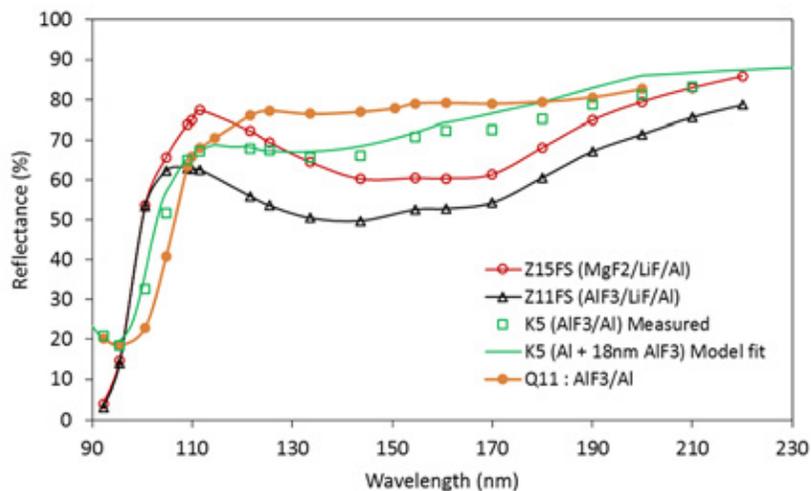c, with a number of small coupons placed along the diameter of Zecoat Corp's coating chamber, which is fitted with a moving e-gun source. The process was not optimized for the UV and hence the results show a larger variation of reflectance in UV than in the visible range. However this is a subject of further process optimization to achieve better than 1% uniformity across a 1-m-diameter optic. In contrast, the ALD process is inherently uniform as it is not based on line of sight deposition. Thermal conditions and gas flow over the area of the optic will determine the uniformity achievable with ALD.
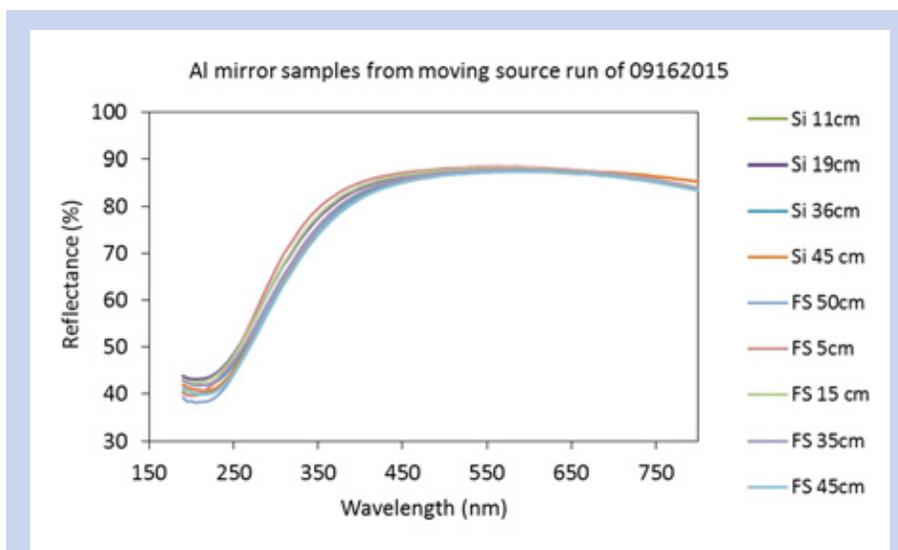
Fig. 17. *Uniformity tests. Coating experiment done with a moving source in a 1.2-m chamber at Zecoat Corp. Legends indicate location of the samples from the center of the substrate holder geometry. Further optimization of process conditions and geometry is feasible to achieve better results, particularly in the UV.*

Path Forward

In the remainder of the year, we will focus on further optimizing deposition parameters of the ALD process and preparing samples of protected-aluminum mirrors for reflectivity measurements. Lower-temperature processes with faster cycle times are being developed in the new Beneq ALD system now. Our models predict that very thin protective layers deposited by ALD can accomplish higher reflectance in the FUV as shown in Fig. 18. Details of these models can be found in Hennessy et al. [8].

Fig. 18. *The calculated reflectance at 121.6 nm and 102.6 nm as a function of coating thickness for films of MgF$_2$, AlF$_3$, and LiF on ideal Al.*
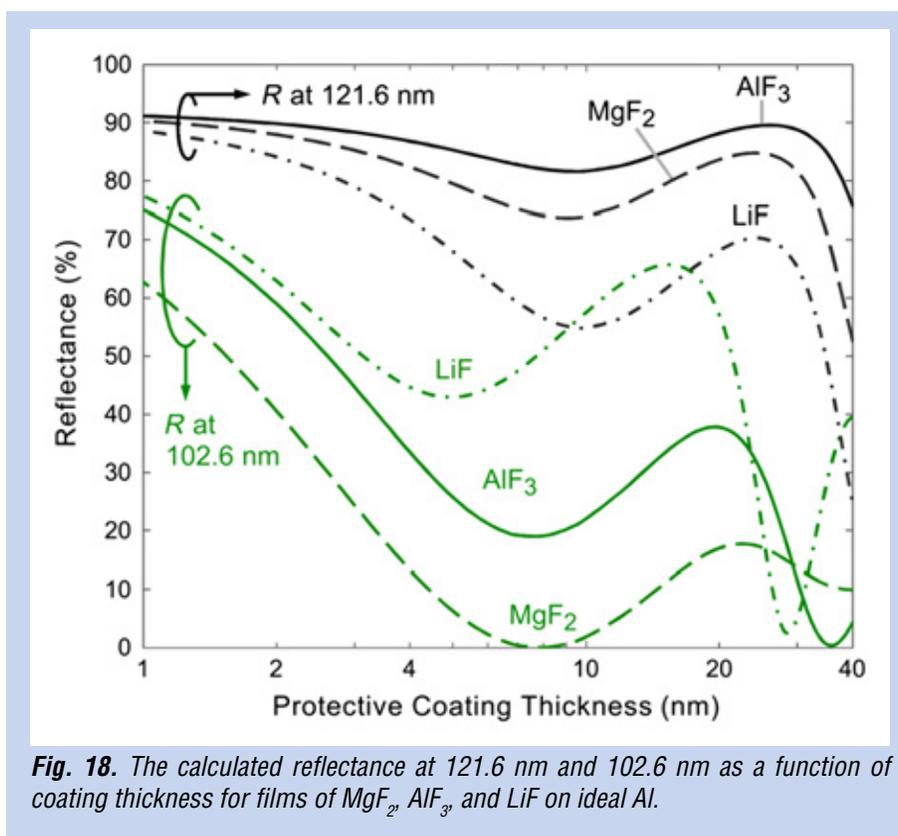
Samples will be subjected to environmental tests with particular attention to FUV performance. An old FUV spectrometer is currently being refurbished at JPL to enable measurements in addition to detailed characterization of samples at GSFC.

Acknowledgements

References

[1] F. Bridou et al., "*Experimental determination of optical constants of MgF$_2$ and AlF$_3$ thin films in the vacuum ultraviolet wavelength region (60–124 nm), and its application to optical designs,*" Opt. Communications, **283**, 1351-1358 (2010)

[2] R.A.M. Keski-Kuha et al., "*Optical coatings and applications for ultraviolet space applications,*" (NASA GSFC) ASP Conference Series, **164**, J.A. Morse, et al.; eds. (1999)

[3] M. Yang, A. Gatto, and N. Kaiser, "*Aluminum-enhanced optical coatings for the VUV spectral range,*" Proc. SPIE, **5963** (2005)

[4] K. Balasubramanian et al., "*Protective coatings for FUV to NIR advanced telescope mirrors,*" AAS 223 Poster paper on the progress presented at the AAS meeting in Baltimore, MD (Jan 2014)

[5] J. Hennessy et al., "*Thin ALD fluoride films to protect and enhance Al mirrors in Far UV,*" 15th International Conference on Atomic Layer Deposition, Portland, OR (June 28th – July 1st 2015)

[6] K. Balasubramanian, et al., "*Coatings for UVOIR telescope mirrors,*" presented at the SPIE Optics + Photonics conference, San Diego, CA, Aug 9-13, 2015; Proc SPIE **9602** (2015)

[7] J. Hennessy, A.D. Jewell, K. Balasubramanian, and S. Nikzad, "*Ultraviolet optical properties of aluminum fluoride thin films deposited by atomic layer deposition,*" JVST A **34**, 01A120 (2016)

[8]   J. Hennessy, K. Balasubramanian, C.S. Moore, A.D. Jewell, S. Nikzad, K. France, and M. Quijada, "*Performance and prospects of far ultraviolet aluminum mirrors protected by atomic layer deposition*," J. Astron. Telesc. Instrum. Syst. **2** (4), 041206, doi: 10.1117/1. JATIS.2.4.041206 (2016)

[9]   S. Redfield, "*The Local Interstellar Medium*," in ASP Conference Series 352, New Horizons in Astronomy, **79**, arXiv:astro-ph/0601117v1 (2006)

[10]   K. France et al., "*From Protoplanetary Disks to Extrasolar Planets: Understanding the Life Cycle of Circumstellar Gas with Ultraviolet Spectroscopy*," arXiv:1208.2270 [astro-ph.SR] (2012)

[11]   J.M. Shull et al., "*The baryon census in a multiphase intergalactic medium: 30% of the baryons may still be missing*," The Astrophysical Journal, **759**:23 (2012)

[12]   Cosmic Origins Program Annual Technology Report and Space Telescope Science Institute Cosmic Origins Program Analysis Group (COPAG) Workshop (2011)

[13]   Stahle et al., "*The Advanced Technology Large-Aperture Space Telescope (ATLAST)*," 224th AAS Meeting, Boston (June 4, 2014)

[14]   P. Scowen, in http://cor.gsfc.nasa.gov/RFI2012/rfi2012-responses.php

[15]   J. Dalcanton, L. Hillenbrand, K. Sembach, J. Gardner, C. Lillie, P. Goldsmith, D. Leisawitz, and C. Martin (Chair), "*COPAG Technology Assessment*," **v.1.3** (Nov 10, 2011)

[16]   M. Bolcar et al., "*A Technology Gap Assessment for a Future Large-Aperture Ultraviolet-Optical-Infrared Space Telescope*," submitted to the Journal of Astronomical Telescopes, Instruments, and Systems (JATIS) 2016, and Proc. SPIE **9602** (2015)

[17]   M. Quijada et al., "*Enhanced MgF_2 and LiF Over-coated Al Mirrors for FUV Space Astronomy*," Proc. SPIE **8450** (2012)

[18]   M. Quijada et al., "*Enhanced Fluoride Over-coated Al Mirrors for FUV Space Astronomy*," Poster paper presented at the AAS meeting in Baltimore, MD (Jan 2014)

[19]   T. Pilvi et al., "*Study of a novel ALD process for depositing MgF_2 thin films*," J. Mater. Chem., **17**, 5077 (2007)

[20]   M. Mantymaki et al., "*Atomic Layer Deposition of LiF Thin Films from Lithd, $Mg(thd)_2$, and TiF_4 Precursors*," Chem. Mater. **25**, 1656 (2013)

[21]   C. Moore et al., "*Recent developments and results of new ultraviolet reflective mirror coatings*," presented at SPIE Astronomical Telescopes + Instrumentation, Montreal (2014)

For additional information, contact K. Balasubramanian: kbala@jpl.nasa.gov

Advanced FUVUV/Visible Photon-Counting and Ultralow-Noise Detectors

Prepared by: Shouleh Nikzad (PI; JPL), Chris Martin (Caltech), David Schiminovich (Columbia University), and Michael Hoenk (JPL)

Summary

In this three-year Strategic Astrophysics Technology (SAT) effort that began in January 2016, we develop and advance the Technology Readiness Level (TRL) of solar-blind (SB), high-efficiency, photon-counting, and ultralow-noise solid-state detectors especially in far ultraviolet (FUV) with $\lambda < 200$ nm. We will combine superlattice (SL) doping (Fig. 1) integrated SB filters (Fig. 2), and antireflection (AR) coatings with ultralow-noise scientific CMOS (e.g., sCMOS) and large-format electron multiplying CCDs (EMCCDs). We will fabricate, characterize, and validate these detectors in a relevant space environment.
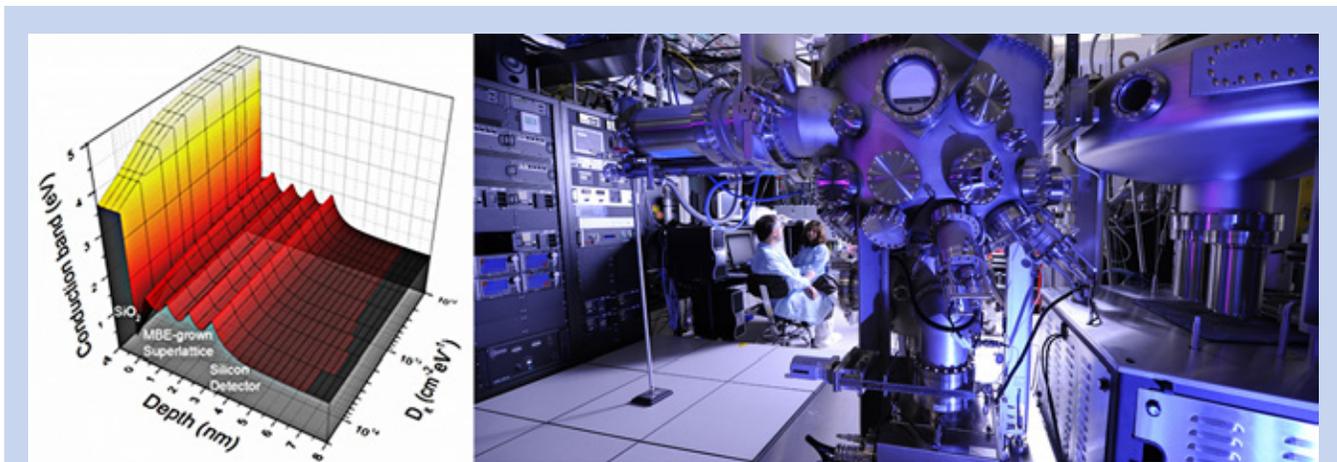
Fig. 1. Left: *Bandiagram of a SL-doped silicon surface.* Right: *JPL's 8"-wafer-capacity silicon molecular beam epitaxy (MBE) facility, where SL doping is performed.*
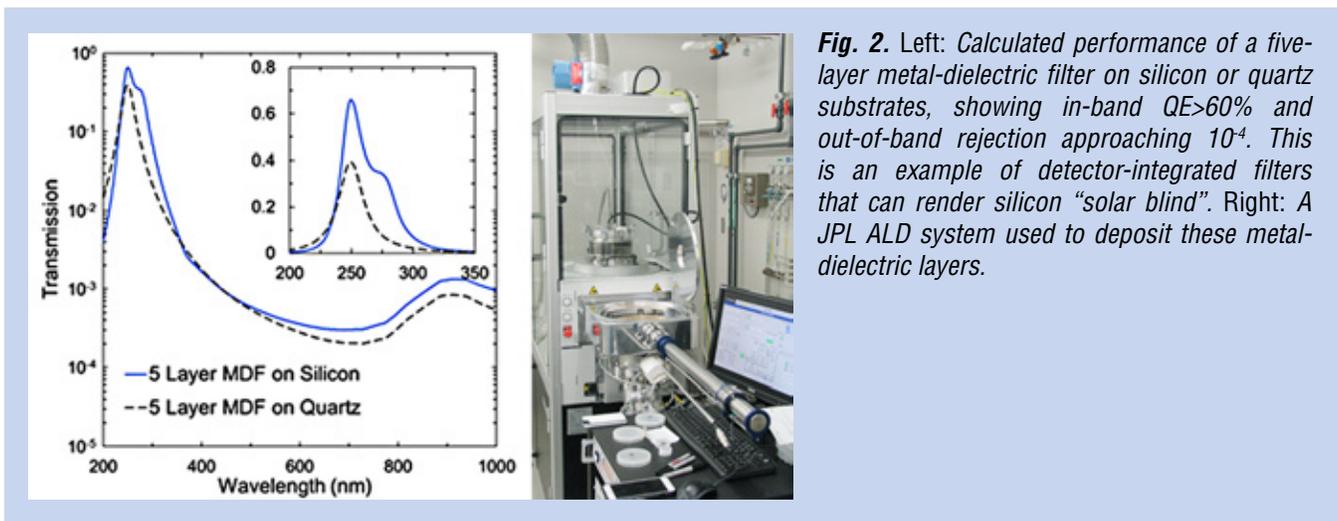
Fig. 2. Left: *Calculated performance of a five-layer metal-dielectric filter on silicon or quartz substrates, showing in-band QE>60% and out-of-band rejection approaching 10^{-4}. This is an example of detector-integrated filters that can render silicon "solar blind".* Right: *A JPL ALD system used to deposit these metal-dielectric layers.*

The detectors under development in this effort offer potentially game-changing performance and capabilities, directly addressing the Technology development for Cosmic Origins (TCOR) requirements outlined in the SAT call for detectors with high quantum efficiency (QE) for $\lambda < 200$ nm, large format, photon-counting capability, and ultralow noise. High-performance ultraviolet (UV) detector and coating technologies will be an essential part of the Large UV/Optical/Infrared (LUVOIR) Surveyor, a leading contender to be one of the next flagship missions. Additionally, the photon counting and ultralow noise in either UV or visible bands will have a high impact on a Habitable Exoplanet (HabEx) imaging mission. Because of the dramatic efficiency increase in the detector, flagship-class science will be possible with smaller-size apertures, offering great impact on future Probe- and Explorer-class missions. Our coating processes, with films prepared by atomic layer deposition (ALD), also advance UV coatings for optics.

SL doping (or multilayer delta doping; Fig. 1) was invented at JPL [1], and has been proven to achieve high internal QE on electron EMCCDs and CMOS arrays [2-5]. SL-doped EMCCDs and SL-doped CMOS are at TRL 4. Integrated visible-rejection filters have been demonstrated and proven on avalanche photodiodes (APDs) and extensively tested [6]; they are at TRL 3. The resulting combination of these SL-doped, AR-coated (SLAR) and SB EMCCD [7, 8] and sCMOS arrays are at TRL 3. Furthermore, we will extend the capability to $\lambda < 200$ nm. Devices will be produced to meet our QE, noise, and visible-rejection requirements; and will be thermally cycled, and characterized and validated in a relevant radiation environment, advancing them to TRL 4-5 by the end of this three-year effort.

Our team includes members with complementary expertise in materials, detectors, instrument building, and observational science. The team is uniquely qualified to carry out this project. By forming alliances between technology developers, instrument builders, and mission PIs (Profs. D. Schiminovich and C. Martin, PI of Galaxy Evolution Explorer, GALEX; as well as suborbital missions such as Faint Intergalactic medium-Redshifted Emission Balloon, FIREBall), our team has a natural path for TRL advancement and flight insertion.

Background

The 2010 Decadal Survey, New Worlds, New Horizons in Astronomy and Astrophysics (NWNH) [9] set a priority for path-finding work towards a 4m+ UV/Optical flagship mission as a successor to the Hubble Space Telescope (HST). Great emphasis on Explorer missions is also anticipated in this decade.

Recently, mid-decadal studies have been ongoing that build on the work of the NWNH. These studies have consistently set forth technology development goals aimed at enabling a future LUVOIR flagship mission, and increasing the scientific reach of smaller missions in this decade. The Cosmic Origins Program Analysis Group (COPAG) is now evaluating and recommending technology investments toward these goals through Science Interest Groups (SIGs), and the Exoplanet Program Analysis Group (ExoPAG) has also embraced this recommendation. In both of these scientific focus areas, single-photon-counting or ultralow-noise detectors are a priority. Furthermore, these recommendations set as a goal very-large-format (100 Megapixel to Gigapixel), high-QE, UV-sensitive detectors. These new recommendations from Association of Universities for Research in Astronomy (AURA), COPAG SIGs, and NWNH reflect the new understanding of the scientific opportunities enabled by technological breakthroughs in large-scale detector fabrication. Our objectives are tied to the needs of and recommendations for future NASA missions in the NWNH, guided by the mid-decadal studies being carried out by COPAG and AURA.

Frontier astrophysical investigations are necessarily conducted at the limits of resolution, etendue, and sensitivity. A future 10-m UV/Optical telescope mission will require significant detector advances beyond HST, GALEX, and Far Ultraviolet Spectroscopic Explorer (FUSE) detector technologies, particularly in QE, spectral responsivity in the UV, resolution, and pixel count. Our primary performance metric, detector QE in the UV, represents a dramatic increase (5- to 10-fold) over previous missions. Most telescope performance/sensitivity metrics scale as $(\varepsilon A)^n$, where ε is efficiency and A is effective area. The primary driver of mission cost is telescope diameter, D [10], with a conservative scaling of cost $\sim\$0.4B \times (D/1\ m)^{1.2}$. A factor-of-five gain in efficiency means that a \$2B 4-m-class mission with our proposed detector would have the same sensitivity as a ~\$6B 9-m space telescope using an existing detector technology, providing huge implied cost savings. Conversely, dramatically increasing the efficiency of the detectors could allow Explorer-class or Probe-class missions to perform flagship-mission science.

A solid-state detector with high efficiency and photon counting offers scalability and reliability that are necessary and attractive features for reliable, high-performance, and cost-effective instruments. LUVOIR's requirements are directly applicable to the objectives of this effort. Additionally, detectors developed under this SAT, optimized for visible light, would have a high impact on the HabEx mission as well.

Objectives and Milestones

Table 1 shows the project's milestones and schedule.

Milestone	Year 1				Year 2	Year 3
	Q1	Q2	Q3	Q4		
Demonstrate SB SLAR EMCCD						
Procure wafers of standard larger-format EMCCDs	Δ					
Thin, bond, SL-dope wafers		▬	Δ	Δ	Δ	Δ
Incorporate advanced ALD filters (200-240 nm)				▬	Δ	
Demonstrate SB SLAR Low-noise CMOS						
Select low-noise CMOS design		▬			Δ	
Procure wafers of low-noise CMOS (e.g., sCMOS)					Δ	
Thin, bond, SL-dope sCMOS					▬	Δ
Incorporate advanced ALD filters (200-240 nm)					▬	Δ
Extend visible-blind filter to FUV						
Extend multilayer design to center at 140 or 150 nm					▬	Δ
Integrate with SLAR EMCCD				▬	Δ	
Integrate with SLAR sCMOS					▬	Δ
Validation and Environmental testing						
Test noise and QE in temperature, illumination; test lifetime					▬	Δ

Table 1. Project milestones and schedule.

Progress and Accomplishments

We have made excellent progress in all task objectives and the task is on track:

- EMCCD wafers were procured and received; wafer bonding is in progress;
- An EMCCD wafer left from a previous task was processed by bonding, thinning, and superlattice doping (Figs. 3 and 4). Several devices were sent to e2v for characterization. Two devices were further tested at Caltech. One device was taken to Palomar to collect on-sky data. Due to cloudy skies, no observation was made. The device was tested with the Cosmic Web Imager (CWI) imaging spectrograph at Palomar, and results will be reported in the next period;

- Contacted top groups in ultralow-noise CMOS development, such as Fairchild for sCMOS; Celeaste, e2V, Sarnoff, and Rutherford Appleton Laboratory (RAL) regarding wafer procurement and collaboration; non-disclosure agreement is in process with Sarnoff as a potential CMOS supplier;
- Metal dielectric filters for enhancement in the 140-150-nm wavelength range have been designed; and
- Fabricated five-layer Al/AlF$_3$ filters on silicon for 200-250-nm range as proof of concept and to constrain optical models.
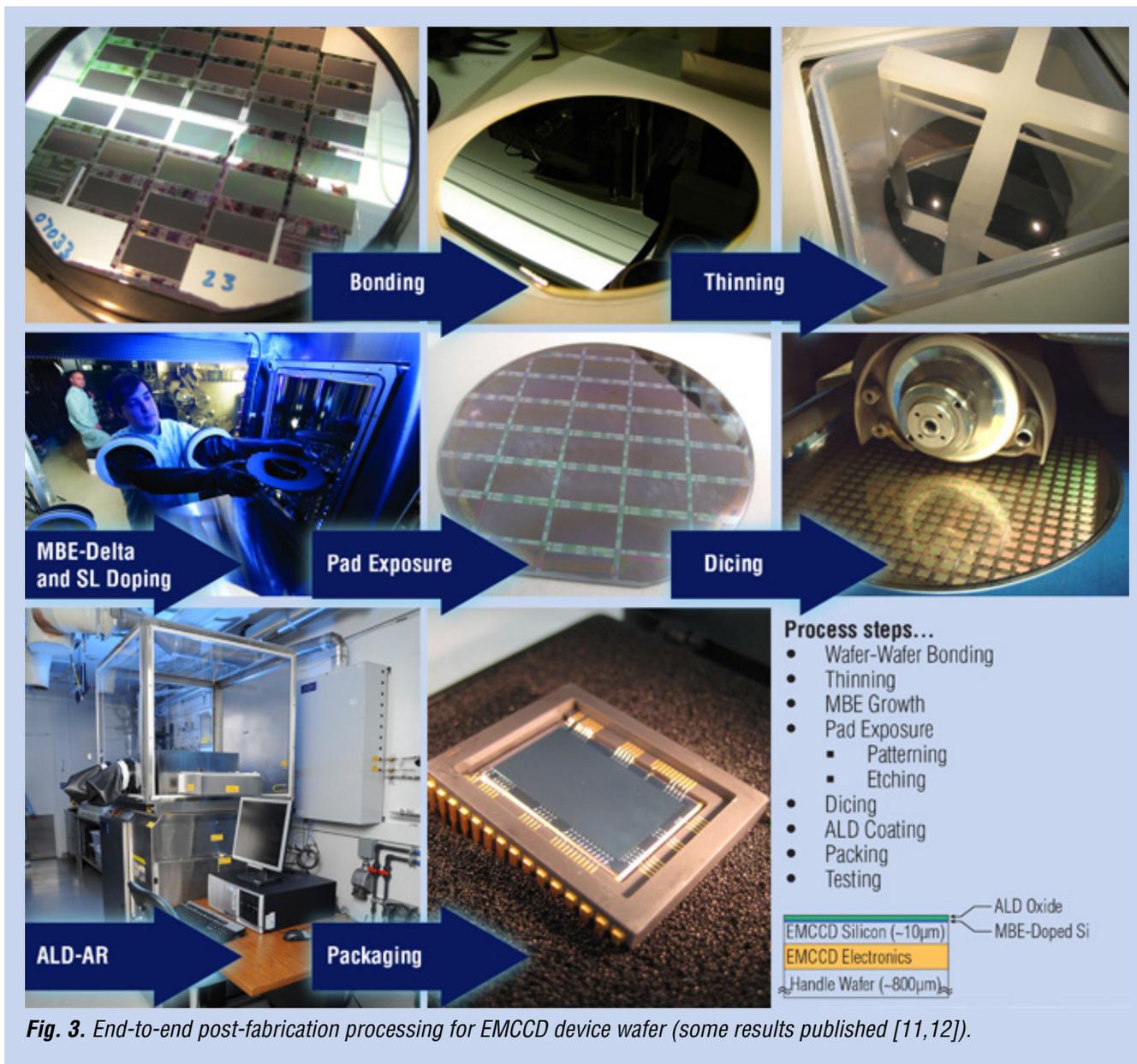

Fig. 3. *End-to-end post-fabrication processing for EMCCD device wafer (some results published [11,12]).*
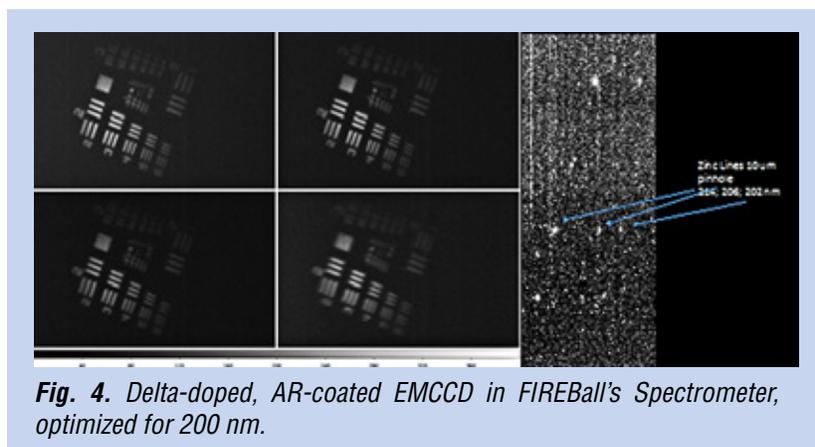
Fig. 4. *Delta-doped, AR-coated EMCCD in FIREBall's Spectrometer, optimized for 200 nm.*

Path Forward

We will process one more wafer in order to produce several devices for fabrication of 2-megapixel arrays. We will evaluate and characterize the QE, dark noise, and uniformity of devices from the second and third wafer serially. In parallel, we will work on metal dielectric films and characterization and will optimize their design on blank wafers. Further optimization will be necessary once the filters are integrated into the detector. In order to get closer to the absolute value of QE, we are verifying the measured QE in other systems. The Caltech group also characterizes the read noise and works through optimizing the parameters to reduce other sources of noise. We will visit the low-noise CMOS vendors and work on procuring wafers from our selected vendors.

References

[1]   M.E. Hoenk, P.J. Grunthaner, F.J. Grunthaner, M. Fattahi, H-F. Tseng, and R.W. Terhune, "*Growth of a Delta-Doped Silicon Layer by Molecular-Beam Epitaxy on a Charge-Coupled Device for Reflection-Limited Ultraviolet Quantum Efficiency*," Appl. Phys. Lett., **61**, 1084 (1992)

[2]   S. Nikzad, M.E. Hoenk, P.J. Grunthaner, R.W. Terhune, F.J. Grunthaner, R. Winzenread, M. Fattahi, and H-F. Tseng, "*Delta-doped CCDs: High QE with Long-term Stability at UV and Visible Wavelengths*," Proc. SPIE, **2198**, 907 (1994)

[3]   J. Blacksberg, S. Nikzad, M.E. Hoenk, S.E. Holland, and W. Kolbe, "*Near-100% Quantum Efficiency of Delta Doped Large-Format UV-NIR Silicon Imagers*," IEEE Trans. On Electron Devices, **55**, 3402, (2008)

[4]   M.E. Hoenk, T.J. Jones, M.R. Dickie, F. Greer, T.J. Cunningham, E.R. Blazejewski, and S. Nikzad, "*Delta-doped back-illuminated CMOS imaging arrays: Progress and prospects*," Proc. SPIE, **74190**, 74190-74115 (2009)

[5]   S. Nikzad, M.E. Hoenk, P.J. Grunthaner, R.W. Terhune, R. Winzenread, M. Fattahi, H-F. Tseng, and F.J. Grunthaner, "*Delta-doped CCDs As Stable, High Sensitivity, High Resolution UV Imaging Arrays*," Proc. SPIE, **2217**, 355 (1994)

[6]   E. Hamden, F. Greer, M.E. Hoenk, J. Blacksberg, T.J. Jones, M. Dickie, B. Jacquot, S. Monacos, C. Martin, P. Morrissey, D. Schiminovich, and S. Nikzad, "*Antireflection Coatings Designs for use in UV Imagers*," Applied Optics, **50**, 4180-4188 (2011)

[7]   P. Jarram, P. Pool, R. Bell, D. Burt, S. Bowring, and S. Spencer, "*LLLCCD—Low Light Level Imaging without the need for an intensifier*," Proc. SPIE, **4306**, 178 (2001)

[8]   J. Hynecek, "*Impactron – A New Solid State Image Intensifier*," IEEE Transaction on Electron Devices, **48** No. 10, 2238-2241 (2001)

[9]   Blandford et al., "*New Worlds, New Horizons in Astronomy and Astrophysics*," National Academy of Sciences (2010)

[10] H.P. Stahl, T. Henrichs, and C. Dollinger, "*Parametric Cost Models for Space Telescopes*," International Conference on Space Optics, Rhodes, Greece (October 2010)

[11] E. Hamden, D. Schiminovich, S. Nikzad, and C. Martin "*UV photon-counting CCD detectors that enable the next generation of UV spectroscopy missions: AR coatings that can achieve 80-90% QE*," Proc. SPIE, **8453**, High Energy, Optical, and Infrared Detectors for Astronomy V, 845309 (2012)

[12] S. Nikzad, M.E. Hoenk, F. Greer, B. Jacquot, S. Monacos, T. Jones, J. Blacksberg, E. Hamden, D. Schiminovich, C. Martin, and P. Morrissey, "*Delta doped Electron Multiplied CCD with Absolute Quantum Efficiency over 50% in the near to far Ultraviolet Range for Single Photon Counting Applications*," Applied Optics, **51**, 365 (2012)

For additional information, contact Shouleh Nikzad: Shouleh.Nikzad@jpl.nasa.gov

Development of DMD Arrays for Use in Future Space Missions

Prepared by: Zoran Ninkov (PI; Rochester Institute of Technology, RIT); Sally Heap and Manuel Quijada (NASA/GSFC); Massimo Robberto (STScI); and Alan Raisanen, Dmitry Vorobiev, and Anton Travinsky (RIT)

Summary

This two-year NASA Strategic Astrophysics Technology (SAT) project began in May 2014. The project seeks to investigate the feasibility of using a digital micro-mirror device (DMD) as the slit mask for a multi-object spectrograph (MOS) system for a variety of future NASA space missions. In particular, we are investigating a number of key operating parameters for Texas Instruments (TI) commercial-off-the-shelf DMDs including: replacing the borosilicate window with windows transmissive at ultraviolet (UV) and infrared (IR) wavelengths, tolerance to particle-radiation effects, and non-specular scattering properties of the DMDs. The team includes Sally Heap at NASA/GSFC, who provides us with insight into the connection between astronomical measurement requirements and our laboratory testing; Massimo Robberto at the Space Telescope Science Institute (STScI), who provides test design guidance and has previous experience with proposed DMD use by the European Space Agency (ESA); Manuel Quijada at GSFC, who provides considerable optics experience and the use of the Carey 5000 Spectrometer at GSFC; and Alan Raisanen at RIT, who provides the necessary microsystems experience to allow for replacement of DMD windows in the RIT cleanroom. Additionally, we have begun collaborating with Jonny Pellish (GSFC Code 561) to proceed with heavy-ion testing of DMDs at Texas A&M and Tim Schwartz (GSFC Code 549) for vibration and shock testing. The project has made significant progress this year including window replacement with UV and IR windows on TI-delivered DMD arrays, complete measurement of light scattering from the TI DMD, measurement of heavy-ion effects on the DMDs at the Texas A&M University Cyclotron, and delivery and initial testing of a large-format Cinema-class DMD and electronics.

Background

Our ultimate objective is to address two key questions of NASA's Cosmic Origins (COR) Program:

1. How did galaxies evolve from the very first systems to the elliptical and spiral types we observe today?
2. How did super-massive black holes affect the lives of galaxies in which they reside and vice versa?

Ground-based telescopes and the Hubble Space Telescope (HST) have shown us that the Hubble sequence of elliptical and spiral galaxies was in place by redshift z = 1. However, what physical processes drove z > 1 galaxies to join the Hubble sequence? To understand galaxy evolution, we need to carry out a large spectroscopic survey of the sky with a particular focus on galaxies at redshifts of z = 1~2. Experience with the Sloan Digital Sky Survey [1] indicates that several hundred thousand galaxies need be observed in order to distinguish among the many possible drivers of galaxy evolution (e.g., accretion, mergers, star formation, stellar evolution and feedback, growth of black holes, etc.).

A large spectroscopic survey requires an MOS able to record the spectra of hundreds of galaxies in a single exposure. The MOS must have adjustable slits to eliminate confusion with nearby sources and to block out unwanted zodiacal background, which would otherwise swamp the light from these faint galaxies. The MOS should have access to the far UV (1200-2000 Å) radiation emitted by a z~1 galaxy because this spectral region has a rich set of diagnostics of stars, gas, and dust in the galaxy. Access to

the blue-red spectral regions (2000-8000 Å) is also essential for determining the precise redshift of a galaxy, its stellar mass, and its elemental abundances; and for characterizing dust extinction. Because the light from a z~1 galaxy is redshifted before reaching us, a large spectroscopic survey should be sensitive over the spectral interval 2000-16000 Å.

The Problem: No existing MOS has such a wide spectral range, let alone access to the UV. TI's DMD would make an excellent slit selector for a spectrograph if it were sensitive in the UV. However, commercial DMD windows block UV light.

Scientific Impact: A UV-transmitting DMD window enables a breakthrough in observational power sufficient to address two key COR science issues. No other telescope, ground- or space-based, present or planned, can accomplish this investigation, because it can't observe all the spectral diagnostics from Ly α (~1200 Å) to Hα + [N II] (~6600 Å) in the same high-redshift galaxy.

Our project intends to investigate the applicability of DMDs to this and other space-based applications by testing the radiation hardness and light-scattering properties of these devices. In addition, our project will look at approaches to replacing the commercially provided windows on DMDs.

The Solution: We therefore propose to optimize the performance of DMDs for the UV region. This requires replacing the DMD window with a UV-transmitting window (> 2000 Å) with an anti-reflection coating on each side, optimized for the UV, optical, and IR. Because the target galaxies are at a redshift of z~1, the observed spectrum of a galaxy over 0.2 – 1.6 µm records the light emitted by the galaxy in the spectral range 0.1 – 0.8 µm. This wavelength region contains virtually all the important spectral diagnostics of stars, gas, and dust in the galaxy.

Objectives and Milestones

Table 1 provides the major milestones of this project. Our project started more slowly than expected, principally because it took longer than expected to identify vendors for the needed components (e.g., windows, DMDs) and services (L-1 Standards & Technology). There was also a long delay in getting purchase orders through the GSFC system. Finally, although we received a quote from a US-based distributor to acquire TI Cinema DMDs when we submitted the proposal, it turned out they could not resell those in the USA. The only way to get these DMDs was through TI's European distributor, at a higher-than-budgeted cost. STScI provided the additional funds, but there was a delay in placing the sub-contract and thus the order.

Progress and Accomplishments

For DMD arrays to be suitable for future NASA missions, a number of performance issues must be addressed. This project attempts to investigate these questions, and to improve DMDs to make them more suitable for such instrumentation requirements. The two commercially available DMDs we will be evaluating are the 0.7 XGA 1024 × 768 13.6-µm pixel pitch and the Cinema 2048 × 1080 13.6-µm DMD.

Milestone	Vendor/Work Location	Dates	Comments
Receipt of MgF$_2$ windows	Photonics Solutions Group Blue Ridge Optics	Received Apr 2015 Received Sep 2015	First batch of MgF$_2$ windows were warped; a second batch had to be made, resulting in substantial delay
Receipt of Heat Exchanger Method (HEM) Sapphire windows	GT Crystal Systems Blue Ridge Optics	Received Sep 2015	GT Crystal Systems went into bankruptcy protection in Nov. 2014, then emerged; first batch of HEM Sapphire did not meet specifications; second batch was excellent
Receipt of Cinema DMDs + drive electronics	VISITECH, Germany	Received Jan 2016	Final quote for these items was higher than budgeted; supplemental funding from STScI allowed order to proceed
Replacement of TI DMDs windows with custom windows by RIT	Semiconductor & Microsystem Fabrication Laboratory, RIT	Apr 2015 (1st device with quartz window); further devices Aug 2015 & Jan 2016	DMDs with sapphire and MgF$_2$ windows have been fabricated as have devices with Kapton and Mica windows for heavy-ion testing
Replacement of TI DMDs window by commercial vendor	L-1 Standards & Technology	Received Dec 2015	Devices all accepted
Measurement of light scattering from eXtended Graphics Array (XGA) DMD	Carey 5000 at GSFC Code 551	First measurements in Apr – May 2015 & Mar 2016; final measurement expected Aug 2016	We have assembled stages and fixture to allow mounting within Carey 5000 Universal Measurement Accessory
Proton-testing of DMD and data analysis	LBNL 88" Cyclotron	Completed 2014	Results published
Heavy-ion testing of DMD and data analysis	Texas A&M Radiation Effects Facility	Tests Aug 2015 & Apr 2016; data analysis expected to complete Aug 2016	Custom test fixtures and software needed to conduct this testing
Testing of Cinema DMDs for scattering properties	Carey 5000 at GSFC Code 551	Initial test done in Feb 2016; more complete testing over the summer 2016	The fixturing for these tests will need to be modified and compared to current tests on the XGA DMD
Vibration and shock testing	GSFC Code 549	Testing completed in May 2016	Custom fixturing to allow eight DMDs to be tested simultaneously
Low-temperature testing and analysis	RIT Infrared Laboratory Dewar	Tests to 120 K completed in 2014; tests to 77 K to be done summer 2016	Initial results published

Table 1. *Milestones of this SAT project.*

Radiation Testing: Proton testing of XGA DMDs was conducted at the Lawrence Berkeley National Laboratory 88" Cyclotron using three different beam energies, specifically 21.0, 34.5, and 40.9 MeV [2]. The heavy-ion radiation testing was performed at the Cyclotron Institute of the Texas A&M University. The facility is equipped with three beam types: 15, 25, and 40 MeV/amu. For this testing we used the 25 MeV/amu beam with three different ions – Argon (Ar), Krypton (Kr), and Xenon (Xe). DMDs were re-windowed with 2-µm-thick pellicle and tested under accelerated heavy-ion radiation (control electronics shielded from radiation), with a focus on detection of single-event effects (SEEs) including latch-up events. Testing showed that while DMDs are sensitive to non-destructive ion-induced state changes, all SEEs were cleared with a soft reset (that is, sending a new pattern to the device). The DMDs did not experience single-event-induced permanent damage or functional changes that required a hard reset (power cycle), even at high ion fluence. The proton and heavy-ion testing suggests that the SSE rate burden (Fig. 1) will be manageable for a DMD-based instrument when exposed to solar-particle fluxes and cosmic rays in orbit.
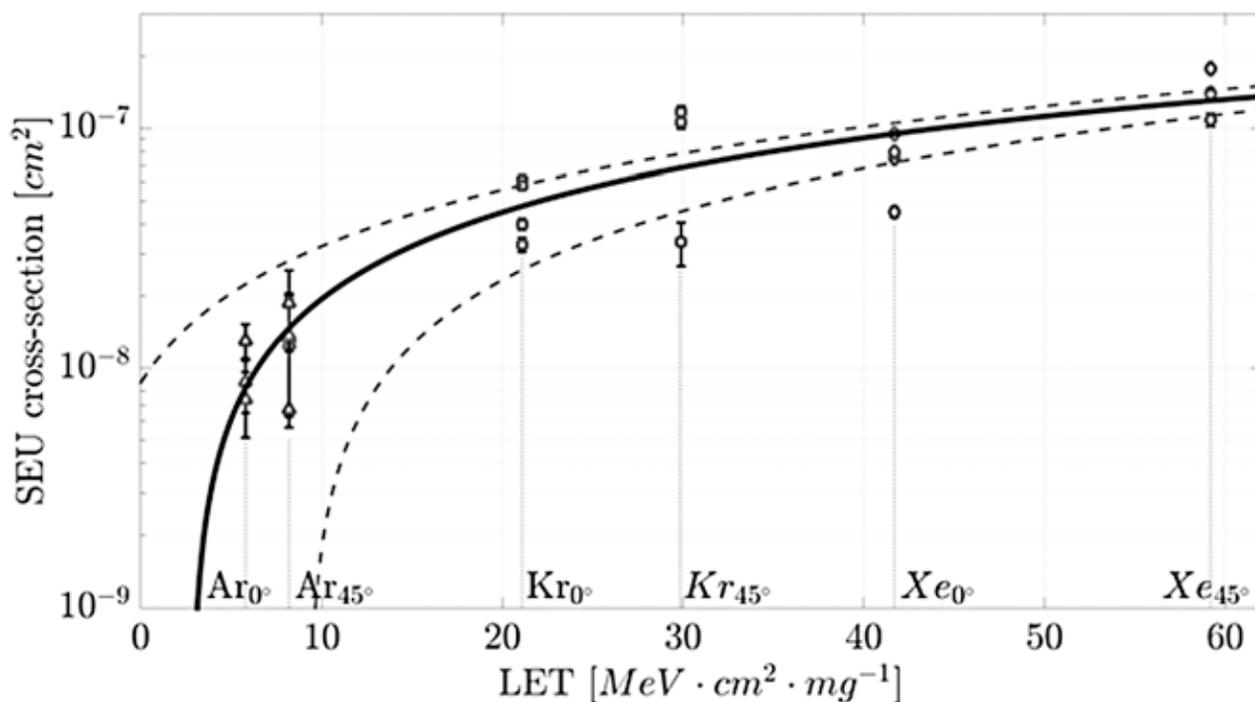
Fig. 1. *Experimental results reduced to single-event upset (SEU) cross-section vs. linear energy transfer (LET) graph and a fitted Weibull curve with 95% confidence level bounds. LET levels are marked with corresponding ions and incident angles.*

Low-Temperature Testing: A modified Infrared Laboratories liquid nitrogen dewar was assembled to house the DMD electronics board for low-temperature testing [3]. The DMD requires many electrical interconnects (~200), and routing this many high-speed electrical interconnects through the dewar for the low-temperature experiment was not practical. By mounting the control board in the dewar, only electrical feedthroughs for power, heater, and temperature monitoring needed to be wired through the dewar. A hermetic USB feedthrough was used to control the DMD with an external control computer.

The DMD was cooled from room temperature to ~130 K, with a new set-point established by the Lakeshore controller every 10 K. At each temperature, a series of test patterns were latched in the DMD to test its operation. It was found that DMDs can be latched for at least 30 minutes at low temperature without any hinge memory problems. Repeatedly re-landing the DMDs during cool-down was not required to avoid stiction effects during low-temperature operation. Testing to 77 K is being planned at the Johns Hopkins Applied Physics Laboratory (APL) over the summer of 2016.

Scattering Measurements: An experimental spot-scanning apparatus was assembled to measure the scattered light for a 0.7 XGA DMD at the focal plane [4-6]. The illumination conditions at several different wavelengths were similar to that expected in a typical space experiment. Automated data collection was implemented for scattered-light measurement as a function of sub-pixel spot position. The initial devices tested were VGA DMD 640 × 480, which showed contrast ratios close to those expected from modeling.

Scattering measurements were obtained using the new Carey 5000 Spectrometer available at GSFC Code 551. A fully adjustable fixture was built at RIT that integrates with the Carey 5000 and enables complete angular-scattering measurements. We are analyzing the scattering measurements made during several visits to GSFC. For un-windowed XGA DMDs the measurements imply an average contrast ratio of 5000:1 over the wavelength range 350 to 1000 nm. Further measurements are being made to cover a wider wavelength range, to investigate the windowed devices and the newer Cinema DMDs.

Shake, Shock, and Vibration Testing: We performed initial shock and vibrational tests to evaluate the mechanical robustness of the re-windowed devices, to investigate the ability of these devices to survive launch conditions. The devices were tested while in a powered-off state, powered-on state, and where the mirrors were continuously flipped between states. We performed residual gas analysis to study the outgassing properties of the new DMDs and evaluate the ability of the new seals to protect the device. The tested devices show near-hermetic seals before and after the mechanical testing. Analysis is ongoing, but initial observations indicate no mirror failures using a custom optical inspection system between images taken of the DMDs immediately before and after the testing.

Re-windowing: DMDs involve the use of a Micro-Electro-Mechanical-Systems (MEMS) device that needs to be maintained in a clean environment. TI provides such containment by fusing a borosilicate glass to the Kovar frame, sealing the unit when manufacturing is complete. The borosilicate window limits the usability of this device for our purposes, so this project seeks to replace the window. The alternate windows we have used are the following. A new, purer form of traditional sapphire called HEM sapphire with transmission into the IR (Fig. 2). This material, produced by GT Crystal Systems, has excellent transmission properties to wavelengths less than 200 nm, and a co-efficient of thermal expansion matching that of the Kovar metal frame to which it will be attached. For UV, we used both magnesium fluoride and UV-grade fused silica. Integration of the windows with the package will be done both by a commercial vendor, L-1 Standards & Technology, and at the RIT Semiconductor and Microsystems Fabrication Laboratory (SMFL). To this end, we developed at RIT techniques to remove the existing window, as well as a fusion method for attaching replacement windows using a space-qualified epoxy.
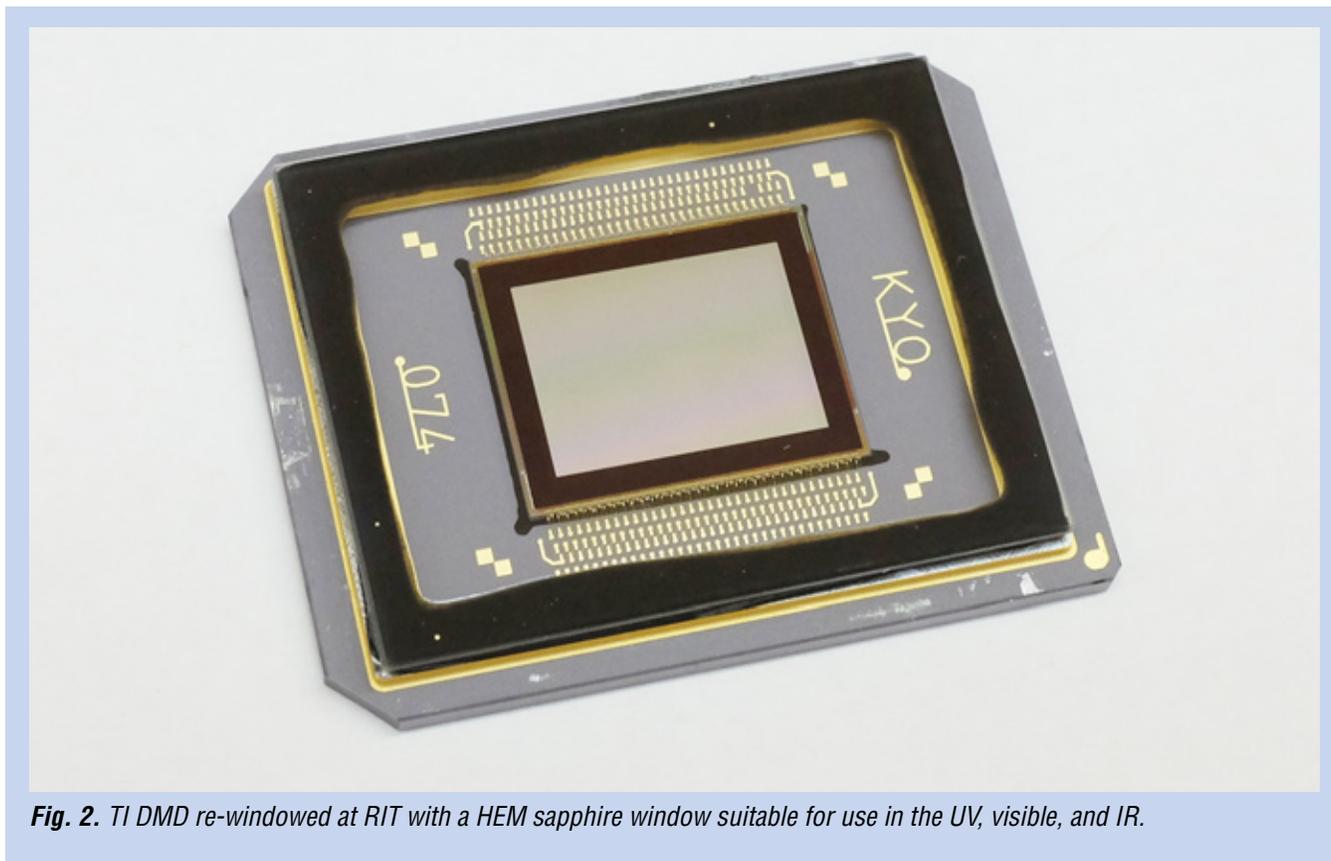

Fig. 2. *TI DMD re-windowed at RIT with a HEM sapphire window suitable for use in the UV, visible, and IR.*

Path Forward

Much remains to be done in this project, specifically:

1. Complete analysis of radiation testing data from Texas A&M and then use the numbers derived to determine in-orbit upset rates.
2. Complete the optical examination and leak checking of the 14 DMDs that were shake/shock/vibration-tested at GSFC.
3. Complete scattering measurements on the re-windowed XGA and DC2K devices. We want to extend those measurements to 200 nm in the UV and 2.5 µm in the IR. In addition, complete optical DMD modeling and compare model results to scattering measurements, verifying our understanding of the scattering mechanisms.
4. Examine a new process for re-windowing the DMDs without epoxy, producing devices that are as hermetic as the original devices from TI.
5. Disseminate the results of this work at the 2016 Society of Photo-optical Insturmentation Engineers (SPIE) Astronomical Telescopes and Instruments meeting in Edinburgh in a series of papers and submit to journals later this year.
6. Complete low-temperature testing, radiation testing, and shock/shake/vibration testing in preparation for a TRL advancement review later this year.

References

[1] Gunn et al., "*The 2.5-m Telescope of the Sloan Digital Sky Survey*," The Astronomical Journal, **131**, Issue 4, 2332-2359 (2006)

[2] K. Fourspring, Z. Ninkov, B. Fodness, M. Robberto, S. Heap, and A. Kim, "*Proton radiation testing of digital micromirror devices for space applications*," Optical Engineering **52** (9):11 091807 doi: 10.1117/1.OE.52.9.091807 (2013)

[3] K. Fourspring, Z. Ninkov, S. Heap, M. Robberto, and A. Kim, "*Testing of digital micromirror devices for space-based applications*," Proc. SPIE, **8618**, Emerging Digital Micromirror Device Based Systems and Applications V, id. 86180B (2013)

[4] K. Fourspring and Z. Ninkov, "*Optical characterization of a micro-grid polarimeter*," Proc. SPIE **8364**, p 83640M (2012)

[5] K.D. Fourspring, Z. Ninkov, and J.P. Kerekes, "*Subpixel scatter in digital micromirror devices*," Proc. SPIE **7596**, Emerging Digital Micromirror Device Based Systems and Applications II (2010)

[6] K.D. Fourspring, Z. Ninkov, and J.P. Kerekes, "*Scattered light in a DMD based multi-object spectrometer*," Proc. SPIE **7739**, Modern Technologies in Space- and Ground-Based Telescopes and Instrumentation (2010)

Publications

1. D. Vorobiev, A. Travinsky, A.D. Raisanen, Z. Ninkov, T.A. Schwartz, M. Robberto, and S.R. Heap, "*Shock and vibration testing of digital micromirror devices (DMDs) for space-based applications*," Proc. SPIE **9912**, Advances in Optical and Mechanical Technologies for Telescopes and Instrumentation II, 99125M (2016)

2. D. Vorobiev, A. Travinsky, M.A. Quijada, Z. Ninkov, A.D. Raisanen, M. Robberto, and S.R. Heap, "*Measurements of the reflectance, contrast ratio, and scattering properties of digital micromirror devices (DMDs)*," Proc. SPIE **9912**, Advances in Optical and Mechanical Technologies for Telescopes and Instrumentation II, 99125U (2016)

3. M.A. Quijada, A. Travinsky, D. Vorobiev, Z. Ninkov, A. Raisanen, M. Robberto, and S.R. Heap, "*Optical evaluation of digital micromirror devices (DMDs) with UV-grade fused silica, sapphire, and magnesium fluoride windows and long-term reflectance of bare devices*," Proc. SPIE **9912**, Advances in Optical and Mechanical Technologies for Telescopes and Instrumentation II, 99125V (2016)

4. A. Travinsky, D. Vorobiev, Z. Ninkov, A.D. Raisanen, J.A. Pellish, M. Robberto, and S.R. Heap, "*Heavy-ion radiation testing of digital micromirror devices (DMDs)*," Proc. SPIE **9912**, Advances in Optical and Mechanical Technologies for Telescopes and Instrumentation II, 99125W (2016)

5. S.R. Heap, Z. Ninkov, M. Robberto, T. Hull, and L. Purves, "*Galaxy evolution spectroscopic explorer: scientific rationale*," Proc. SPIE **9905**, Space Telescopes and Instrumentation 2016: Ultraviolet to Gamma Ray, 990505 (2016)

6. A. Travinsky, D. Vorobiev, A.D. Raisanen, J.A. Pellish, Z. Ninkov, M. Robberto, and S.R. Heap, "*The effects of heavy ion radiation on digital micromirror device performance*," Proc. SPIE **9761**, Emerging Digital Micromirror Device Based Systems and Applications VIII, 976108 (2016)

7. R.H. Barkhouser, M. Robberto, S.A. Smee, Z. Ninkov, M. Gennaro, and T. Heckman, "*The optical design of GMOX: a next-generation instrument concept for Gemini*," Proc. SPIE **9908**, Ground-based and Airborne Instrumentation for Astronomy VI, 990852 (2016)

8. S.A. Smee, R.H. Barkhouser, M. Robberto, Z. Ninkov, M. Gennaro, and T.M. Heckman, "*The opto-mechanical design for GMOX: a next-generation instrument concept for Gemini*," Proc. SPIE **9908**, Ground-based and Airborne Instrumentation for Astronomy VI, 99084Z (2016)

9. M. Robberto, M. Donahue, Z. Ninkov, S.A. Smee, R.H. Barkhouser, M. Gennaro, and A. Tokovinin, "*SAMOS: a versatile multi-object-spectrograph for the GLAO system SAM at SOAR*," Proc. SPIE **9908**, Ground-based and Airborne Instrumentation for Astronomy VI, 99088V (2016)

For additional information, contact Zoran Ninkov: ninkov@cis.rit.edu

Ultra-Stable Structures: Development and Characterization Using Spatial Dynamic Metrology

Prepared by: Babak Saif (PI; NASA/GSFC) and Lee Feinberg (NASA/GSFC)

This SAT project was funded very recently, thus this PI report only outlines project objectives and plans. A full report will be included in next year's PATR.

Summary

We plan to demonstrate breakthrough ultra-stable-structure technologies with associated picometer-class, dynamic spatial metrology that are key technological needs to enable large segmented space telescopes that can support both general-class astrophysics and high-contrast imaging. The technology proposed is directly traceable to the science requirements for 10- to 12-m-class segmented Large Ultraviolet/Optical/Infrared (LUVOIR) observatory concepts such as the Advanced Technology Large Aperture Space Telescope (ATLAST) [1], and the newly proposed High Definition Space Telescope (HDST) called out by the Beyond JWST (James Webb Space Telescope) AURA (Association of Universities for Research in Astronomy) committee [2]. This effort is also traceable to the 2010 Decadal recommendation for developing technologies for UVOIR telescopes. The ATLAST 10-m-class reference mission builds on JWST heritage, but with a non-contact, isolated primary-mirror system that minimizes the dynamic disturbances at the primary mirror. While slower instabilities can be actively controlled, high-speed motions are too fast to easily correct and are, therefore, highly isolated in this architecture. This project will demonstrate and characterize the enabling telescope technologies needed to show that this picometer-class, high-speed stability can be achieved.

Background

The stability of large segmented telescopes is the key technological challenge required for ATLAST and related missions to both support the general-class UVOIR science and achieve the contrast levels needed for observing exoearths (i.e., 10^{-10}). While the contrast requirement is more driving, the impact of this effort will be to enable the required ultra-stable structure technologies in a cost-effective, scalable design that serves all needs together. This effort builds on the composite-structure and mirror-mount heritage of JWST, Chandra, and HST in a scalable way. In addition, the proposed component testing, metrology, testbed, and modeling work may have applications to other high-stability systems like Laser Interferometer Space Antenna (LISA) and evolved LISA (eLISA), as well as X-ray and ultraviolet systems, where it can offer alternative methods for achieving comparable stability.

Groundbreaking breakthroughs in these technologies would provide a critical and enabling capability required for ATLAST/HDST in the key, uncontrollable dynamic range (1 – 100 Hz). This dynamic range is not easily correctable using metrology or target-star-based sense-and-control strategies due to signal-to-noise (SN) limitations and the number of degrees of freedom involved. It is critical because it is the operational bandwidth of reaction wheels, the standard method to point a large observatory. Feinberg [3] showed by scaling the dynamic performance of JWST to ATLAST, that a picometer structural-stability solution is possible, if structures can be linearly scaled into the picometer regime. This work will develop the component and subscale technologies, together with demonstrations that prove or bound the linearity of their dynamic performance, which is key to enabling the required system stability.

Objectives and Milestones

The following are the key objectives for this project, with the key milestones shown in Table 1.

1. Demonstrate an ultra-stable nano-composite structure and the associated actuator and hexapod mount needed for a segmented telescope with picometer-class dynamic stability.
2. Build a breakthrough high-speed speckle interferometer capable of < 50-picometer-class spatial dynamic measurements of an ultra-stable composite structure and mirror system [4, 5].
3. Develop an ultra-stable spatial dynamics testbed for model validation to the picometer level that will bound and characterize the picometer-scale nonlinearities.

Project Year	Key Milestones
1	Procure/build interferometer
2	Component test/calibrations
3	Subscale testing

Table 1. *Key project milestones.*

Progress and Accomplishments

With funding now in place, we've moved forward with placing a contract with a vendor to develop the interferometer.

Path Forward

The following work is planned for the near future.

- Work closely with the vendor to develop the metrology device;
- Develop software for the device;
- Secure a chamber on a floated optical table to start testing calibration pieces to verify the repeatability and precision of the interferometer; and
- Start designing opto-mechanical parts and plan for testing them under different stimuli.

References

[1] W. Oegerle et al., "*ATLAST-9.2m: a large-aperture deployable space telescope*," Proc. SPIE **7731**, Space Telescopes and Instrumentation 2010: Optical, Infrared, and Millimeter Wave, DOI: 10.1117/12.857622, 10 (2010)

[2] D. Redding et al., "*Beyond JWST: A Technology Path to the Next Great UVOIR Space Telescope*," 225th AAS Meeting Seattle (January 4, 2015)

[3] L.D. Feinberg, A. Jones, G. Mosier; N. Rioux, D. Redding, and M. Kienlen, "*A cost-effective and serviceable ATLAST 9.2-m telescope architecture*," Proc. SPIE **9143**, Space Telescopes and Instrumentation 2014: Optical, Infrared, and Millimeter Wave, 914316, DOI: 10.1117/12.2054915 (2 August 2014)

[4] B. Saif et al., "*Nanometer level characterization of the James Webb Space Telescope optomechanical systems using high-speed interferometry*," Appl. Optics, **54** (13), 4285-4298 (2015)

[5] B. Saif et al., "*Measurements of large cryogenic structures using a spatially phase-shifted digital speckle pattern interferometer*," Applied Optics IP, **47** (6), 737-745, DOI: 10.1364/AO.47.000737 (2008)

For additional information, contact Babak Saif: Babak.n.saif@nasa.gov

Improving Ultraviolet Coatings and Filters using Innovative Materials Deposited by ALD

Prepared by: Paul Scowen (PI; Arizona State University, ASU); Brianna Eller, Robert J. Nemanich, and Hongbin Yu (ASU); Tom Mooney (Materion); and Matt Beasley (Planetary Resources)

Summary

The goal of this work is to use plasma-enhanced atomic layer deposition (PEALD) to synthesize mirrors and filters compatible with near-ultraviolet (UV) and far-UV optics. The development of this technology will ultimately provide diagnostic tools to access a range of topics for study, including protostellar and protoplanetary systems, intergalactic-medium (IGM) gas from galactic star formation, and the most distant of objects in the early universe. Since the beginning of the year, our team, from the School of Earth and Science Exploration and the Physics Department at ASU, Materion, and Planetary Resources, has been working to initiate this research. Our most significant progress to date has been to design, develop, and build the equipment necessary to complete this research.

Background

Atomic layer deposition (ALD) is a layer-by-layer deposition technique that synthesizes ultra-thin, uniform, and conformal films as shown in Fig. 1. The high quality of these films has consequently resulted in augmented coatings and optical elements. At the same time, major advances have been made in optical designs and detector technologies. As a result, measurement of far-UV and near-UV bands has improved dramatically. The development of this technology ultimately allows access to emission and absorption lines in the UV, which are emitted from a range of targets, including protostellar and protoplanetary systems, IGM gas from galactic star formation, and the most distant of objects in the early universe. These diagnostic tools require the implementation of stable optical layers, including high-UV-reflectivity coatings and UV-transparent films [1].
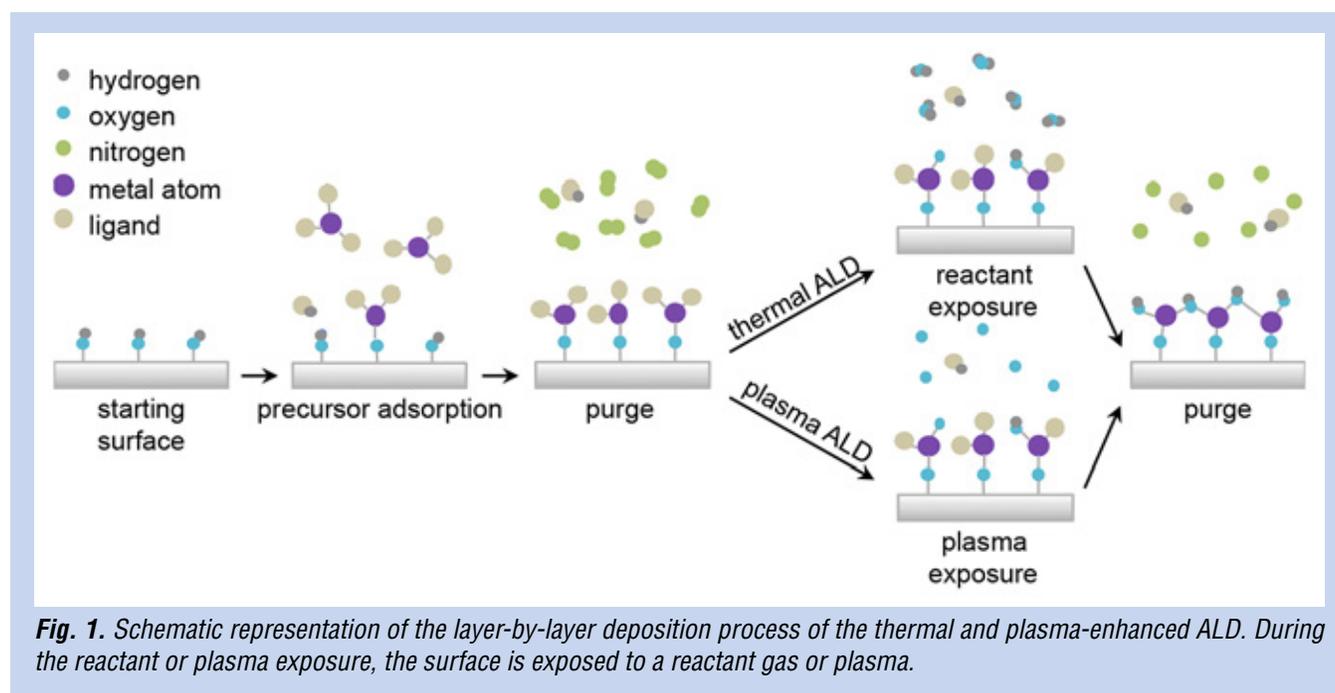

Fig. 1. *Schematic representation of the layer-by-layer deposition process of the thermal and plasma-enhanced ALD. During the reactant or plasma exposure, the surface is exposed to a reactant gas or plasma.*

In this work, we will use a range of materials to implement stable protective overcoats with high UV reflectivity and unprecedented uniformity, and use that capability to leverage innovative UV/optical filter construction to enable the science mentioned above. The materials we will use include aluminum oxide and silicon oxide (as an intermediary step for development only) and a range of fluoride-based compounds (for production). These materials will be deposited in a multilayer format over a metal base to produce a stable construct. Specifically, we will use PEALD for deposition and construction of reflective layers that protect bare aluminum for mirror use in the UV. Our designs indicate that by using PEALD we can reduce adsorption and scattering in the optical films as a result of the lower concentration of impurities and increased control over the stoichiometry, yielding vastly superior quality and performance over comparable traditional thermal ALD techniques [2-17] currently being developed by other NASA-funded groups [18]. These capabilities will allow us to push the blue edge in usable UV reflectivity for magnesium-fluoride-protected aluminum below the current 115-nm limit.

This work will demonstrate for the first time whether loss-free oxides of materials such as Al, Hf, and Si can be deposited using ALD to lower cutoff reflectivities in the UV to as low as 92 nm. We will also demonstrate the use of PEALD to deposit low-loss thin films of fluoride-based materials, and aluminum metal. Using these techniques, we will then demonstrate our proof-of-concept of using these techniques together to construct thin-film, multilayer metal-dielectric cavities with a reflective surface as the foundation, that can be tuned to isolate specific emission lines of astronomical importance. The resulting optical technologies will advance the coating stability, thickness, and performance of thin films in the far-UV sought by NASA, to match recent UV detector advances. Such improvement will enable next-generation space-based far-UV missions, opening access to the wealth of diagnostic information the far-UV offers for exoplanet, star formation, and cosmological/IGM science.

Objectives and Milestones

Our research seeks to demonstrate several objectives:

- Films of material can be deposited to demonstrate the approach using PEALD techniques to produce loss-free films of e.g. silicon and aluminum oxide; the resulting coatings will be of a thickness and a purity far higher than can be delivered by current techniques that involve sputtering deposition;
- Using the same deposition techniques, PEALD can deposit thin (tens of nm) low-loss films of fluorides of aluminum and magnesium as well as e.g. lithium, lanthanum-calcium, and beryllium, that can serve as protective overcoats for materials which would otherwise be easily oxidized by exposure to air;
- Aluminum deposition, protective-layer deposition, and characterization can be completed in-situ in a controlled environment that minimizes contamination, improving the reflectivity of the resulting films and their interfaces by reducing scattering and adsorption;
- Deposition of such protective overcoats over aluminum metal can be achieved with PEALD to provide a sufficiently crystalline, uniform, and stable structure, pushing blueward the currently observed 115-nm cutoff in efficient reflectivity from atomic sputtering deposition of magnesium fluoride, thereby extending the range of diagnostic emission and absorption lines available for science;
- Extend the metal-dielectric overcoat process to concave mirrors to demonstrate the performance of the reflective surfaces in an optical test bed environment;
- Use our PEALD approach to apply alternating layers of metals and dielectrics, producing multi-cavity structures exhibiting very high performance; this goal is currently limited by the inability to deposit very thin layers with great accuracy, while demonstrating film toughness and 'bulk' thin-film material losses;
- Apply the multilayer approach to the construction of multi-layer dielectric mirrors to act as reflection filters or high reflectors in narrow band systems; and
- Similarly construct multi-layer broadband mirrors, thought to exhibit higher performance than metal-based mirrors (using a short-wave extension to prototype dichroics our group is already developing for space applications).

Table 1 summarizes the timeline to achieve these objectives, which to date is mostly unchanged.

Activity Name	Duration (Days)	Start Date	Finish Date
Upgrade in-situ reflectivity to 120 nm	130	1/1/16	6/30/16
Upgrade PEALD for aluminum deposition	196	1/1/16	9/30/16
PEALD of oxides on evaporated aluminum	261	1/1/16	12/30/16
PEALD of aluminum	131	7/1/16	12/30/16
PEALD of Al_2O_3 and SiO_2 on aluminum	131	7/1/16	12/30/16
Install precursors for PEALD of fluorides	131	10/3/16	4/3/17
Oxides on PEALD aluminum	195	10/3/16	6/30/17
Upgrade in-situ reflectivity to 90 nm	130	1/2/17	6/30/17
PEALD of magnesium fluoride on aluminum	195	1/2/17	9/29/17
PEALD of aluminum and magnesium fluoride	260	1/2/17	12/29/17
PEALD of aluminum fluoride on aluminum	195	4/3/17	12/29/17
Magnesium fluoride/aluminum filters	260	10/2/17	9/28/18
Oxide-fluoride multilayers and protective layers	261	1/1/18	12/31/18
Multi-layer broad band mirrors	261	1/1/18	12/31/18

Table 1. *Summary of timeline for objectives and milestones.*

Progress and Accomplishments

The initial state of this research has largely focused on developing the equipment necessary to synthesize and characterize the oxygen-free structures required to achieve the aforementioned objectives. Modifications to the system are well under way, where the chambers to be added to the ultra-high vacuum system are summarized in Fig. 2. Specifically, three new systems are being added to the setup:

- An oxide PEALD, developed in conjunction with the Advanced Research Projects Agency-Energy (ARPA-E) Ultimate Switches project;
- A fluoride PEALD system for both the aluminum metal and metal fluorides needed for this work; and
- A visible and UV (VUV) optical system, which will be used to characterize the films deposited without atmospheric contamination.
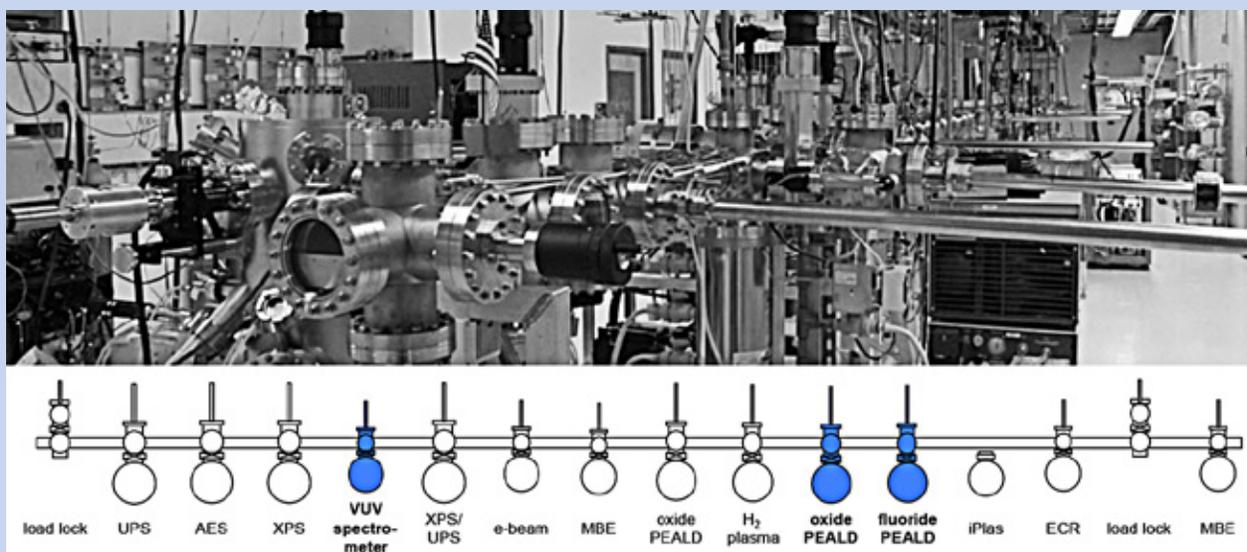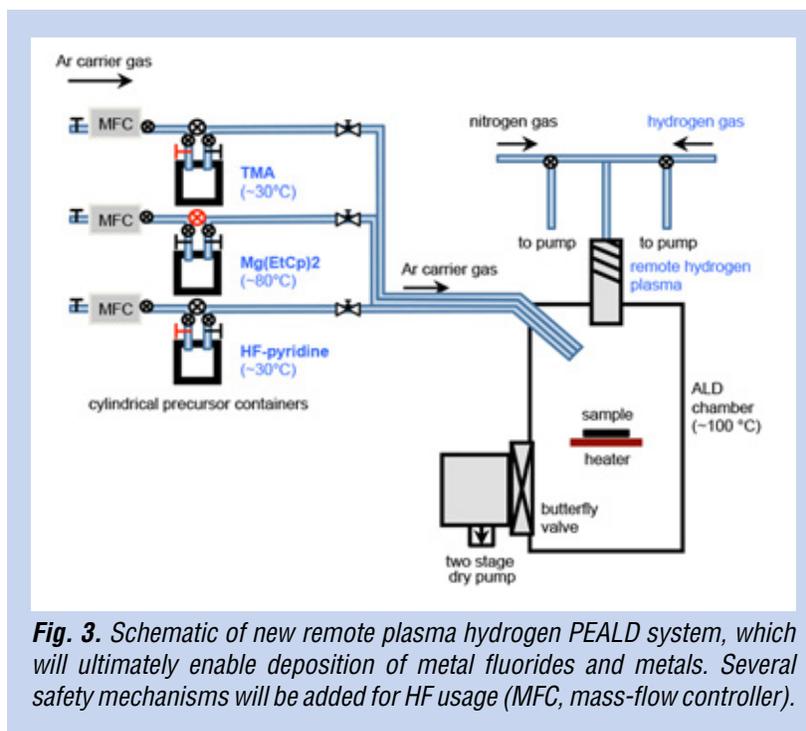

Fig. 2. *Photo (top) and schematic (bottom) of ASU in-situ ultra-high vacuum system; blue shows new systems in progress (UPS, UV Photoelectron Spectroscopy; AES, Auger Photoelectron Spectroscopy; XPS, X-ray Photoelectron Spectroscopy; MBE, Molecular Beam Epitaxy; iPlas, Innovative Plasma Chemical Vapor Deposition; ECR, Electron Cyclotron Resonance).*

A key component of this work is related to the in-situ nature of the deposition and characterization soon to be enabled. Since oxidation of aluminum has presented a significant challenge in previous research [18], this work will allow for the deposition of aluminum and metal fluorides without exposure to atmosphere.

1. Plasma-Enhanced Atomic Layer Deposition

The new PEALD system is in the initial stages of assembly and based on the previous oxide system available in the lab, with only a few alterations as shown in Fig. 3.

Fig. 3. *Schematic of new remote plasma hydrogen PEALD system, which will ultimately enable deposition of metal fluorides and metals. Several safety mechanisms will be added for HF usage (MFC, mass-flow controller).*

Specifically, the plasma was designed with a remote configuration, helping reduce ion bombardment of the sample, mitigating potential ion damage. Plasma will be ignited with 13.56-MHz RF-excitation applied at ~200 W to a helical copper coil wrapped around a 32-mm-diameter quartz tube, and maintained at a pressure of ~100 mTorr with a flow rate of ~35 sccm (standard cubic centimeters per minute). This system must achieve a background pressure of $< 5\times10^{-8}$ Torr and processing pressures of ~10 mTorr. The pumping requirements, therefore, vary during transfer and deposition. To assist with transfer, the system is equipped with a Pfeiffer turbo with pumping speed of 300 liters/sec and a dry backing pump, enabling lower pressures; however, the chemicals used during deposition are often too harsh, reducing the lifetime of the turbo pumps. Therefore, when operating, the turbo is isolated with a gate valve, and a two-state dry pump with a pumping speed of ~7000 liters/sec is used. The pumping stage is vented with nitrogen gas during operation to further ensure system longevity. In addition, the gas-flow mechanisms are designed to deliver the precursors to the chamber with the correct timing sequence using MFCs, nitrogen valves, and a custom Labview program. Metering valves were also added to the gas lines to further control the amount of precursor released into the chamber. Lastly, a butterfly valve before the two-stage dry pump is used to maintain the required pressures during processing.

Since PEALD is driven by precursor chemical reactions, these precursors can have a significant impact on the film quality achieved. The precursors chosen for the two PEALD processes are described below.

Metal PEALD. Fortunately, there has been some work done on PEALD of aluminum, using trimethylaluminum and hydrogen plasma [19]; therefore, this process will be adopted for this work.

Fluoride PEALD. Fluoride processes, on the other hand, have not been developed extensively. In fact, to date, there are no published processes for fluoride PEALD. However, there has been some work on thermal ALD processes, which use HF [20, 21], TiF_4 [22-25], and TaF_4 [26] as the fluorine source. While TiF_4 and TaF_4 come with significantly less safety hazards, the films deposited with these materials are typically characterized by some metal contamination, which will likely cause absorption in the desired wavelengths. A fluoride-based plasma was also considered for this work but dismissed due to concerns that it might lead to etching rather than deposition. Therefore, HF seems to be the best option at this point. To take advantage of the desirable properties of PEALD, the HF step will be coupled with a hydrogen plasma step to ensure film purity.

Unfortunately, the corrosiveness and toxicity of HF raise safety concerns that must be carefully considered for this process. To address these concerns, the following precautions are being considered:

- Storing the HF in a bubbler as an HF-pyridine mixture, which is less volatile than HF;
- Electroplating the bubbler with gold, to prevent corrosion;
- Replacing the quartz tube with sapphire, to prevent etching;
- Introducing a dry-air abatement system following the two-stage dry pump, to remove waste by-products; and
- Coating the chamber with a thick aluminum layer prior to using HF, to prevent etching of the chamber.

For aluminum and magnesium fluoride, trimethylaluminum and bis-ethylcyclopentadienylmagnesium have been chosen as the respective metal precursors.

2. Visible and Ultraviolet Optical System

We must establish in-situ reflectivity to 120 nm in order to characterize PEALD oxides and aluminum. In addition, the VUV optical system will need to be upgraded for lower wavelengths (> 90 nm) in the future. This system has also been designed (see design schematics in Fig. 4). The optical components of this system were purchased from McPherson, including a deuterium lamp to be used as the light source, a 1200 G/mm concave magnesium fluoride-coated aluminum grating, a magnesium-fluoride-coated aluminum toroidal mirror, and a VUV silicon-diode detector calibrated by NIST. A custom attachment was designed to mount the silicon-diode detector, enabling 360° rotation.
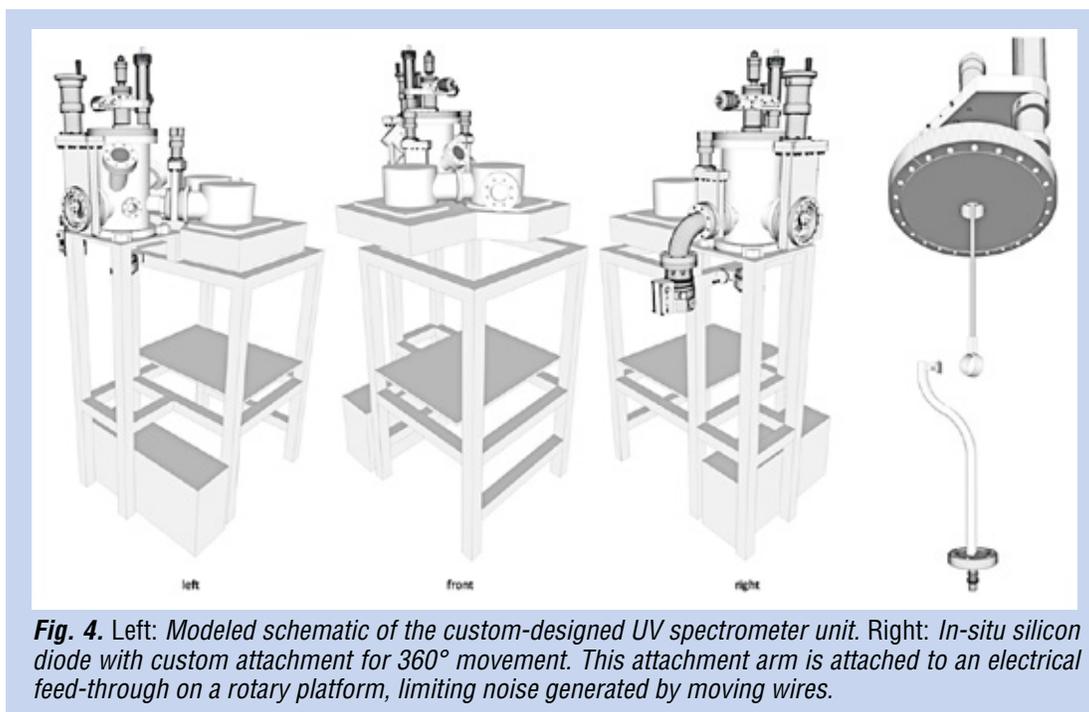

left   front   right

Fig. 4. Left: *Modeled schematic of the custom-designed UV spectrometer unit.* Right: *In-situ silicon diode with custom attachment for 360° movement. This attachment arm is attached to an electrical feed-through on a rotary platform, limiting noise generated by moving wires.*

Lastly, similar to the PEALD systems, a Pfeiffer turbo and dry backing pump were chosen to achieve the necessary pressures for transfer. When the system is modified for lower wavelengths (> 92 nm), the deuterium lamp must be replaced with a hollow-cathode lamp. In addition, this system must be windowless. Therefore, additional pumping will be added to each of the chambers of the monochromator as well as the light source itself.

Path Forward

The plan of work is structured around the goals and milestones stated above. In general, the plan is to initially demonstrate the use of ALD as a UV material deposition tool. Once the UV spectroscopy tool is operational, work will focus on developing the process to synthesize aluminum mirrors as well as metal fluoride overcoats. More specifically, the following will be necessary:

1. Demonstrate the use of PEALD to deposit loss-free oxides of silicon and aluminum on evaporated and e-beam-deposited aluminum surfaces. These oxides were selected based on their promise for stable, high-performance oxides. This is motivated because current methods produce lossy films, which are not usable below 190 nm.
2. Establish the capability for PEALD aluminum films and characterize the UV reflectivity of the films and the surface contamination using in-situ characterization tools. These aluminum surfaces will be the basis of the structures pursued in this program.
3. Demonstrate the feasibility of using PEALD to deposit low-loss films of fluoride compounds on ALD aluminum. The fluorides of interest include most significantly aluminum and magnesium fluoride, but others will be considered as well. We will need to demonstrate stability, uniformity, and performance before advancing.
4. Extend the reflectivity characterization to 90 nm and characterize the fluoride-aluminum structures. This is a critical step, as the aluminum-oxide/fluoride layer will serve as the foundation not only for simple reflective surfaces. For filters, we intend to show proof-of-concept in the next segment. The quality of aluminum and interface will define the required performance, which will be verified before advancing to the next stages.

In this first phase, of work will be conducted by Dr. Nemanich and his team, focusing on developing processes that result in optimized films. This first round of work and demonstrations are expected to be completed within the first 18 months of the project, i.e. by June 2017.

Before moving on to the next sequence, Dr. Scowen, Dr. Mooney, and Dr. Beasley will revisit the demonstrated performance of the three classes of product (above) and compare them to the models that initiated the work. Stability will be measured using vacuum exposure and spectral retest, and similarly humidity exposure followed by spectral retest. If there are differences in stability and reflectivity, we need to understand their origins before we can build prototype filters, since these parameters are critical for tuning an individual filter for a particular bandpass. Once this has been done, we will implement the techniques used above for the deposition of multilayer construction.

The next phase will then address the following goals:

5. Optimize far-UV reflectivity of fluorides on aluminum, to deliver a wide bandpass, far-UV-optimized mirror. The optimization will focus on minimizing interface contamination and optimizing material-growth parameters and film thickness for far-UV reflectivity. We will demonstrate performance as far as possible into the far-UV with our new VUV system.
6. Construct metal-dielectric Fabry-Perot band-pass filters using aluminum and magnesium fluoride, leading to multi-cavity structures that will exhibit very high performance—based on our models. This design approach is currently limited by the ability to deposit very thin layers with great accuracy, film toughness, and 'bulk' thin-film material losses. We believe only two to five layers will be needed to demonstrate proof-of-concept, with each layer ~10 nm thick.

7. Fine-tune approach and models to produce designs for multi-layer dielectric (narrowband) mirrors to act as reflection filters or high reflectors in narrow-band systems. We will demonstrate construction and performance.

8. Demonstrate the construction of multi-layer broadband mirrors, which we believe—based on models—will exhibit higher performance than metal-based mirrors.

We expect this second round of work to occupy most of 2017 and 2018. To achieve all this work, we will demonstrate our approach, designs, and methodologies deliver the necessary improvements in thickness control, lower 'bulk' losses, absence of color centers, smoother films (lower scatter), ability to deposit very thin films (with bulk-like optical properties), durability, and lower stress. The above plan, executed in this manner, will demonstrate all these goals.

References

[1] J.M. Shull and C.W. Danforth, "*Identifying the Baryons in a Multiphase Intergalactic Medium,*" arXiv1208.3249S (2012)

[2] O.K. Kwon, S.H. Kwon, H.S. Park, and S.W. Kang, "*PEALD of a ruthenium adhesion layer for copper interconnects,*" J. Electrochem. Soc. **151**, C753 (2004)

[3] O.K. Kwon, S.H. Kwon, H.S. Park, and S.W. Kang, "*Plasma-enhanced atomic layer deposition of ruthenium thin films,*" Electrochem. Solid-State Lett. **7**, C46 (2004)

[4] J.W. Lim, S.J. Yun, and J.H. Lee, "*Low temperature growth of SiO_2 films by plasma-enhanced atomic layer deposition,*" ETRI J. **27**, 118 (2005)

[5] W.J. Maeng, S.J. Park, and H. Kim, "*Atomic layer deposition of Ta-based thin films: Reactions of alkylamide precursor with various reactants,*" J. Vac. Sci. Technol. B **24**, 2276 (2006)

[6] M.K. Song and S.W. Rhee, "*Phase formation in the tantalum carbo-nitride film deposited with atomic layer deposition using ammonia,*" J. Electrochem. Soc. **155**, H823 (2008)

[7] J.S. Park, M.J. Lee, C.S. Lee, and S.W. Kang, "*Plasma-enhanced atomic layer deposition of tantalum nitrides using hydrogen radicals as a reducing agent,*" Electrochem. Solid-State Lett. **4**, C17 (2001)

[8] J.S. Park, H.S. Park, and S.W. Kang, "*Plasma-enhanced atomic layer deposition of Ta-N thin films,*" J. Electrochem. Soc. **149**, C28 (2002)

[9] J.Y. Kim, K.W. Lee, H.O. Park, Y.D. Kim, H. Jeon, and Y. Kim, "*Barrier Characteristics of TaN Films Deposited by Using the Remote Plasma Enhanced Atomic Layer Deposition Method,*" J. Korean Phys. Soc. **45**, 1069 (2004)

[10] J.Y. Kim, Y. Kim, and H. Jeon, "*Characteristics of TiN Films Deposited by Remote Plasma-Enhanced Atomic Layer Deposition Method,*" Jpn. J. Appl. Phys., **42** Part 2, No. 4B, L414 (2003)

[11] Y. Kim, J. Koo, J. W. Han, S. Choi, H. Jeon, and C.G. Park, "*Characteristics of ZrO_2 gate dielectric deposited using Zr t–butoxide and $Zr(NEt_2)_4$ precursors by plasma enhanced atomic layer deposition method,*" J. Appl. Phys. **92**, 5443 (2002)

[12] J. Koo, Y. Kim, and H. Jeon, "*ZrO_2 Gate Dielectric Deposited by Plasma-Enhanced Atomic Layer Deposition Method,*" Jpn. J. Appl. Phys., **41** Part 1, No. 5A, 3043 (2002)

[13] B. Hoex, J. Schmidt, P. Pohl, M.C.M. van de Sanden, and W.M.M. Kessels, "*Silicon surface passivation by atomic layer deposited Al_2O_3,*" J. Appl. Phys. **104**, 044903 (2008)

[14] J. Koo, S. Kim, S. Jeon, H. Jeon, Y. Kim, and Y. Won, "*Characteristics of Al_2O_3 Thin Films Deposited Using Dimethylaluminum Isopropoxide and Trimethylaluminum Precursors by the Plasma-Enhanced Atomic-Layer Deposition Method,*" J. Korean Phys. Soc. **48**, 131 (2006)

[15] P.K. Park and S.W. Kang, "*Enhancement of dielectric constant in HfO_2 thin films by the addition of Al_2O_3,*" Appl. Phys. Lett. **89**, 192905 (2006)

[16] P.K. Park, E.S. Cha, and S.W. Kang, "*Interface effect on dielectric constant of HfO_2/Al_2O_3 nanolaminate films deposited by plasma-enhanced atomic layer deposition,*" Appl. Phys. Lett. **90**, 232906 (2007)

[17]   P.K. Park, J.S. Roh, B.H. Choi, and S.W. Kang, "*Interfacial Layer Properties of HfO$_2$ Films Formed by Plasma-Enhanced Atomic Layer Deposition on Silicon,*" Electrochem. Solid-State Lett. **9**, F34 (2006)

[18]   J. Hennessy, A.D. Jewell, F. Greer, M.C. Lee, and S. Nikzad, "*Atomic layer deposition of magnesium fluoride via bis(ethylcyclopentadienyl)magnesium and anhydrous hydrogen fluoride,*" J. Vac. Sci. Technol. A **33**, 01A125 (2015)

[19]   J.-H. Park, D.-S. Han, Y.-J. Kang, S.-R. Shin, and J.-W. Park, "*Self-forming Al oxide barrier for nanoscale Cu interconnects created by hybrid atomic layer deposition of Cu–Al alloy,*" J. Vac. Sci. Technol. A **32**, 01A131 (2014)

[20]   Y. Lee and S.M. George, "*Atomic Layer Deposition of Metal Fluorides using Various Precursors and Hydrogen Fluorides,*" ALD conference (2015)

[21]   J. Hennesey, B.K. Balasubramania, A. Jewell, S. Nikzad, C.S. Morre, and K. France, "*Thin ALD films to Protect and Enhance Al Mirrors in Far UV,*" ALD conference (2015)

[22]   T. Pilvi, T. Hatanpää, E. Puukilainen, K. Arstila, M. Bischoff, U. Kaiser, N. Kaiser, M. Leskelä, and M. Ritala, "*Study of novel ALD process for depositing MgF$_2$ thin films,*" J. Mater. Chem. **17**, 5077 (2007)

[23]   M. Mäntymäki, J. Hämäläinen, E. Puukilainen, F. Munnik, M. Ritala, and M. Leskelä, "*Atomic Layer Deposition of LiF Thin Films from Lithd and TiF$_4$ Precursors,*" Chem. Vap. Dep. **19**, 111 (2013)

[24]   M. Mäntymäki, M. J. Heikkilä, E. Puukilainen, K. Mizohata, B. Marchand, J. Räisänen, M. Ritala, and M. Leskelä, "*Atomic Layer Deposition of AlF$_3$ Thin Films Using Halide Precursors,*" Chem. Mater. **27**, 604 (2015)

[25]   T. Pilvi, K. Arstila, M. Leskelä, and M. Ritala, "*Novel ALD process for depositing CaF$_2$ thin films,*" Chem. Mater. **19**, 3387 (2007)

[26]   T. Pilvi, E. Puukilainen, U. Kreissig, M. Leskelä, and M. Ritala, "*Atomic Layer Deposition of MgF$_2$ Thin Films Using TaF$_5$ as a Novel Fluorine Source,*" Chem. Mater. **20**, 5023 (2008)

For additional information, contact Paul Scowen: paul.scowen@asu.edu

Advanced UVOIR Mirror Technology Development for Very Large Space Telescopes

Prepared by: H. Philip Stahl, PhD (NASA/MSFC)

Summary

The Advanced Mirror Technology Development (AMTD) project is in Phase 2 of a multiyear effort initiated in Fiscal Year (FY) 2012, to mature toward the next Technology Readiness Level (TRL) critical technologies required to enable 4-m-or-larger monolithic or segmented ultraviolet, optical, and infrared (UVOIR) space telescope primary-mirror assemblies for general astrophysics and ultra-high-contrast observations of exoplanets.

Key hardware accomplishments of 2015/16 are the successful low-temperature fusion of a 1.5-m-diameter ultra-low-expansion (ULE®) mirror that is a 1/3 scale model of a 4-m mirror and the initiation of polishing of a 1.2-m extreme-lightweight Zerodur® mirror. Critical to AMTD's success is an integrated team of scientists, systems engineers, and technologists; and a science-driven systems engineering approach. Additionally, AMTD continued mentoring of next generation's scientists and engineers with four undergraduate student interns: Jacob Vehonsky of Arizona State University, Nathaniel Stepp of University of Alabama at Huntsville, Marshall Prince of Texas A&M, and Ahmed Abdelqader of City University of New York. AMTD results were presented at Mirror Tech Days 2015 and published in proceedings of the 2015 SPIE Optics and Photonics Conference (see list at report end).

Background

UVOIR measurements provide robust, often unique, diagnostics for investigating astronomical environments and objects. UVOIR observations are responsible for much of our current astrophysics knowledge and will produce as-yet-unimagined, paradigm-shifting discoveries. A new, larger UVOIR telescope is needed to help answer fundamental scientific questions such as:

- Does life exist on nearby Earth-like exoplanets?
- How do galaxies assemble their stellar populations?
- How do galaxies and the intergalactic medium interact?
- How did planets and smaller bodies in our own solar system form and evolve?

According to the 2010 Decadal Survey, New Worlds, New Horizons in Astronomy and Astrophysics (NWNH), an advanced, large-aperture UVOIR telescope is required to enable the next generation of compelling astrophysics and exoplanet science. NWNH also noted present technology is not mature enough to affordably build and launch UVOIR telescopes that are diffraction-limited at visible (or shorter) wavelengths, with apertures larger than 4 m. According to the 2012 NASA Space Technology Roadmaps and Priorities report, the highest priority technology in which NASA should invest to enable "*Objective C: Expand our understanding of Earth and the universe in which we live,*" is a new generation of low-cost, stable astronomical telescopes for high-contrast imaging and faint-object spectroscopy to "*Enable discovery of habitable planets, facilitate advances in solar physics, and enable the study of faint structures around bright objects.*" Finally, according to the NASA Office of Chief Technologist Science Instruments, Observatory, and Sensor Systems (SIOSS) Technology Assessment Roadmap, technology to enable a future UVOIR or high-contrast exoplanet mission needs to be at TRL 6 by 2018, so a viable flight mission can be considered by the 2020 Decadal Survey.

Objectives and Milestones

AMTD's objective is to mature technologies to enable large UVOIR space telescopes toward TRL 6. Because we cannot predict whether monolithic or segmented architectures will be needed, AMTD is pursuing technologies that can enable both.

AMTD's Phase 1 advanced technology readiness of six key technologies required to make an integrated primary mirror assembly (PMA) for a large aperture UVOIR space telescope:

1. Large-Aperture, Low-Areal-Density, High-Stiffness Mirror Substrates.
2. Support System.
3. Mid/High-Spatial-Frequency Figure Error.
4. Segment Edges.
5. Segment-to-Segment Gap Phasing.
6. Integrated Model Validation.

Phase 2 is continuing these efforts with three clearly defined milestones:

- Fabricate a 1/3-scale model of 4-m-class 400-mm thick deep-core ULE® mirror to demonstrate lateral scaling of the deep-core process;
- Characterize two candidate primary mirrors (PMs), the 1/3-scale mirror and a 1.2-m Extreme Lightweight Zerodur® Mirror owned by Schott, by measuring their modal performance and optical performance from 250 K to ambient; and
- Add capabilities and validate integrated design and modeling tools to predict the mechanical and thermal behavior of the candidate mirrors, validate models, generate Pre-Phase-A point designs, and predict on-orbit optical performance.

Progress and Accomplishments

Large-Aperture, Low-Areal-Density, High-Stiffness Mirror Substrates
Need: To achieve the ultra-stable mechanical and thermal performance required for high-contrast imaging, both (4-m to 8-m) monolithic and (8-m to 16-m) segmented primary mirrors require larger, thicker, and stiffer mirror substrates.

Accomplishments: During FY 2015/16, AMTD Phase 2 progressed in this technical area by successfully fusing the 1.5-m ULE® substrate, continuing to develop the Arnold Mirror Modeler (AMM), and using the AMM to develop candidate point designs for a potential Habitable Exoplanet (HabEx) mission.

Deep-Core Mirror-Substrate Technology: As previously reported, in Phase 1, AMTD partner Harris Corporation demonstrated a new five-layer 'stack & fuse' process for fabricating deep-core mirror substrates. Phase 1 made a 43-cm-diameter 'cut-out' of a 4-m-diameter, 40-cm thick, < 45 kg/m² mirror substrate. In FY 2014/15, as part of Phase 2, Harris designed a 1.5-m × 165-mm, 400-Hz-first-mode mirror. To demonstrate scalability, a 4-m monolithic mirror was designed and scaled down to 1.5 m. The design incorporated multiple proprietary lessons-learned from the 40-cm deep-core mirror to enhance manufacturability and ensure launch survival. While one would not use the stack & fuse technology for a 1.5-m-class mirror, it is sufficient to demonstrate scalability. Note that a single-core-layer version of this 400-Hz mirror would meet the performance needs for a 12- to 16-m segmented-aperture telescope.

In FY 2015/16, Harris fabricated the mirror's components (faceplate, 18 core elements, and backplate), then fused them together to form a planar substrate (Fig. 1, left). Before fusing, Harris used proprietary modeling tools to predict the viscoelastic performance of the mirror (Fig. 1, bottom right). Proprietary post-fusing data was acquired to validate by test the viscoelastic model predictions. In FY 2016/17, the substrate will be replicated to a sphere, polished, and its mechanical and thermal performance characterized. Finally, its internal structure will be measured via 3D X-ray tomography.
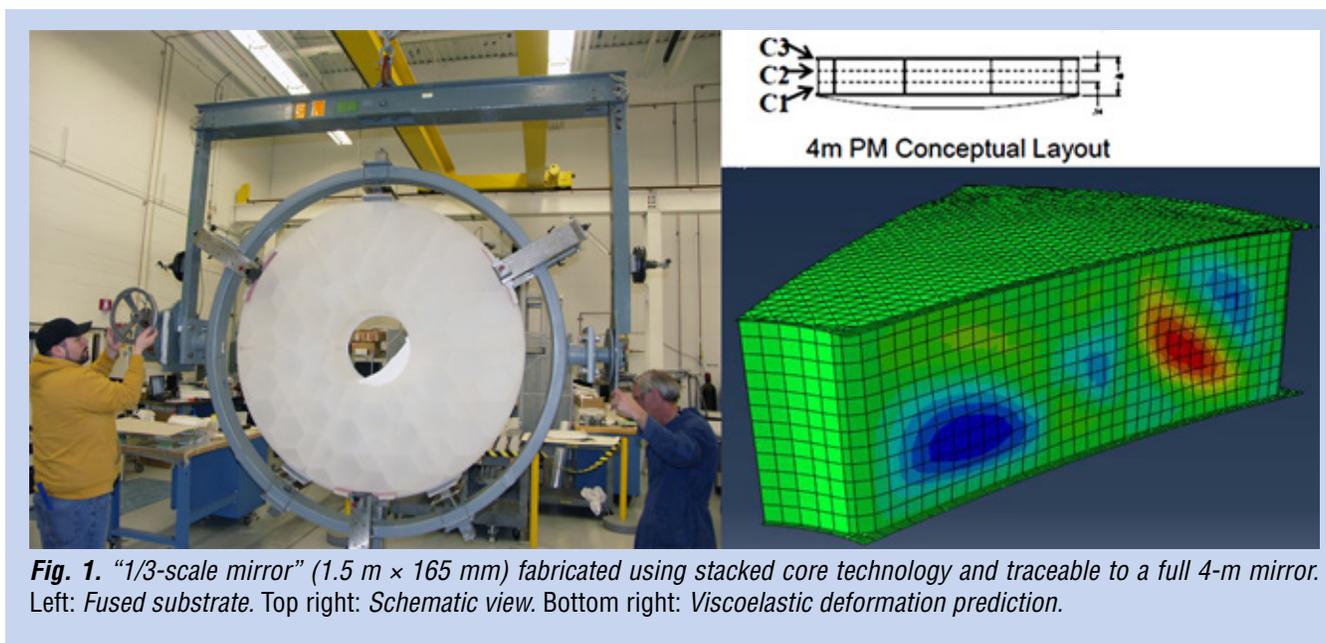
Fig. 1. *"1/3-scale mirror" (1.5 m × 165 mm) fabricated using stacked core technology and traceable to a full 4-m mirror.* Left: *Fused substrate.* Top right: *Schematic view.* Bottom right: *Viscoelastic deformation prediction.*

<u>Arnold Mirror Modeler:</u> Development of the AMM tool for rapid creation and analysis of detailed mirror designs continues. The AMM creates a complete analysis stream, including model, loads (static and dynamic), plots, and a summary file of input variables and results suitable for optimization or trade studies. Values of all settings can be archived and recalled to continue or redo any configuration. In FY 2015/16, capabilities were added, including (Fig. 2):

1. Stratospheric Observatory for Infrared Astronomy (SOFIA) '-style' shaped substrates, T-ribs for stiffer open back mirrors, elliptical apertures, and asymmetric substrates for off-axis monolithic mirrors.
2. Hex and petal segmented mirrors.
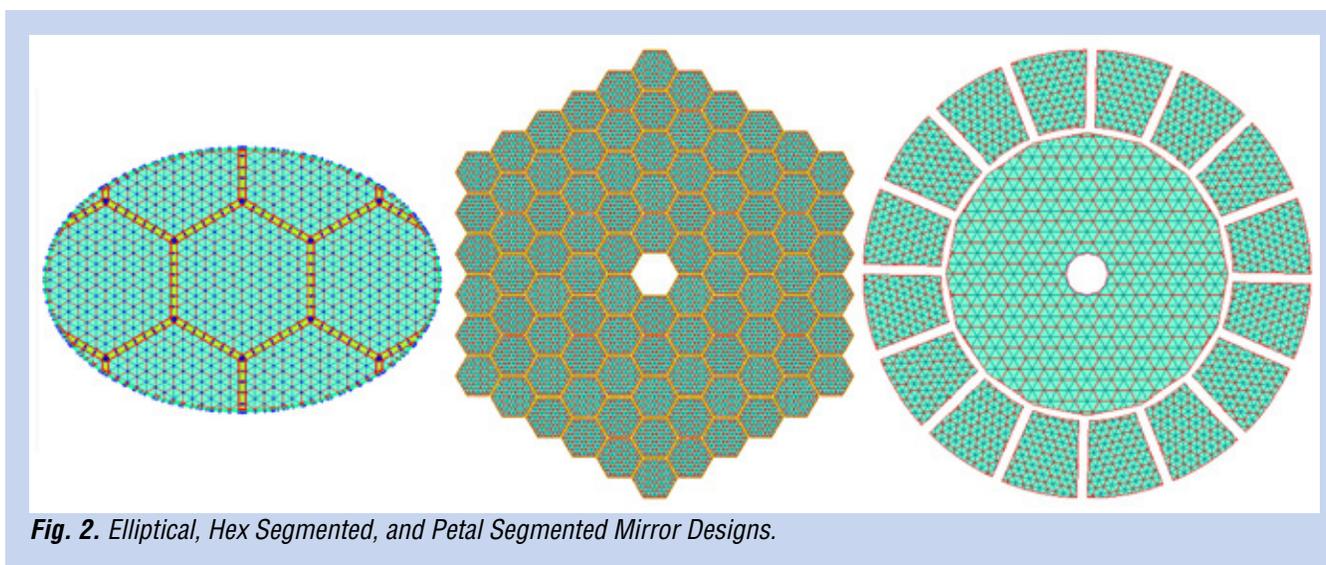3. Standard check cases for ANSYS, ABAQUS, and NASTRAN.

Fig. 2. *Elliptical, Hex Segmented, and Petal Segmented Mirror Designs.*

Progress related to mount systems and support structures is discussed below. Finally, approval from NASA was obtained to make the tool available to US Government contractors.

<u>4-m Point Designs:</u> In support of a potential HabEx mission, multiple point designs were developed for candidate 4-m mirrors. For a mass-constrained mission (i.e., launched via Delta-IVH), design concepts were developed for a 900-kg 4-m mirror with 100-Hz first mode. For a mission to be launched via a Space Launch System (SLS), we studied how relaxing the mass constraint allows for stiffer mirrors designs (Table 1). It is interesting to compare these results to the James Webb Space Telescope (JWST) 1.5-m segment's 200- to 220-Hz first-mode frequency and Hubble Space Telescope (HST) 2.4-m mirror's 260- to 280-Hz first mode.

Thickness [m]	Mass [kg]	First Mode [Hz]
0.40	900	100
0.45	2200	180
0.60	2560	215
0.75	2860	245

Table 1. *4-m Mirror point design results.*

Support System

Need: Large-aperture mirrors require large support systems to ensure they survive launch and deploy on-orbit stress-free and undistorted. Additionally, segmented mirrors require large structure systems that establish and maintain the mirror's shape.

Accomplishment: During FY 2015/16, AMTD Phase 2 progressed in this technical area by continuing to develop mount capabilities in the AMM.

<u>Arnold Mirror Modeler:</u> In FY 2015/16 capabilities were added, including:

1. Hexapod systems for curved-back segmented apertures.
2. Automatic mount-pad locator.
3. Support systems for elliptical mirrors.

As the segmented-mirror diameter increases, it becomes desirable to define the attachment plane for the segment-support systems as a curve (Fig. 3). This provides a more uniform strut stiffness for dynamic behavior. For ease of design, an algorithm was added that locates the mount pads aligned exactly with the center of a cell or the intersection of cell webs (Fig. 4).
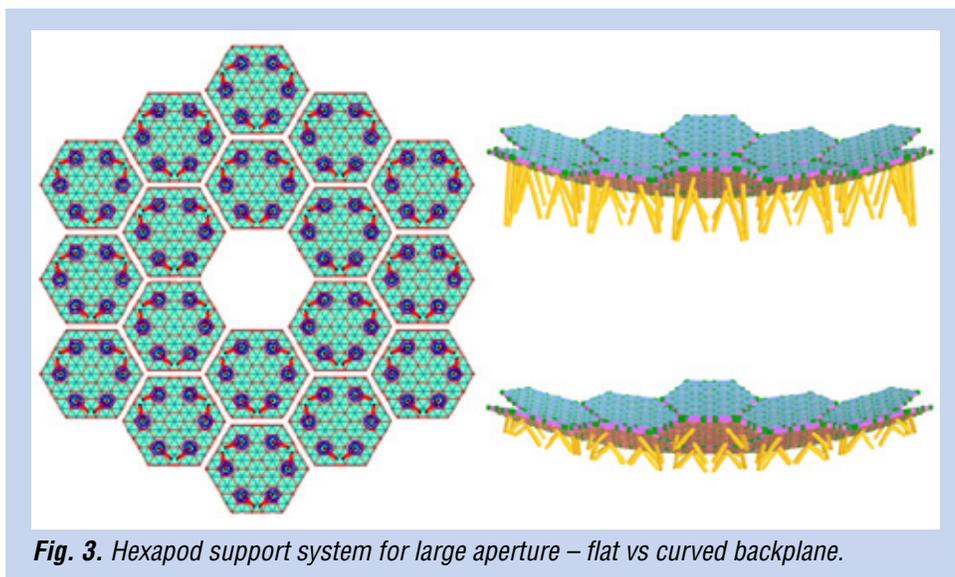

Fig. 3. *Hexapod support system for large aperture – flat vs curved backplane.*
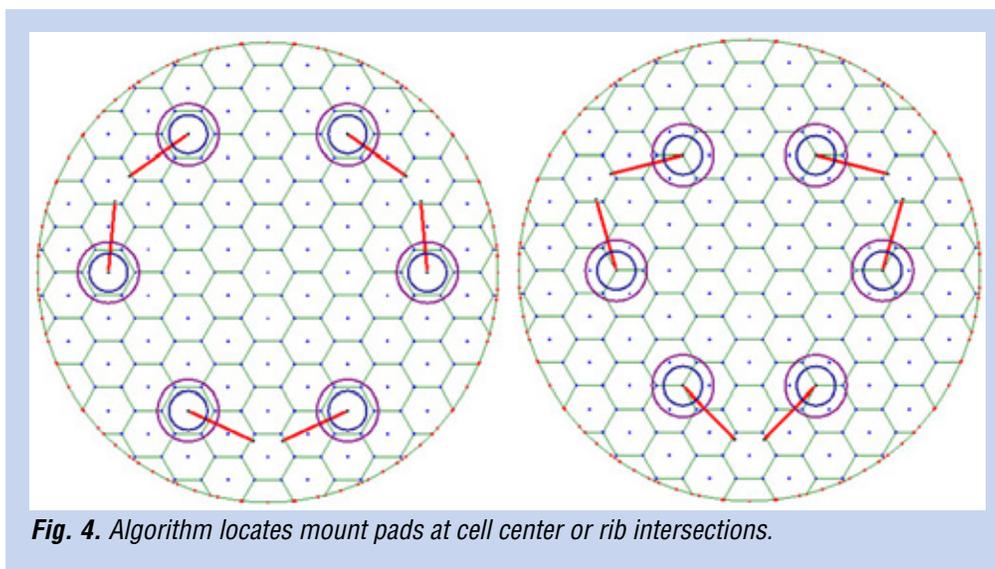
Fig. 4. *Algorithm locates mount pads at cell center or rib intersections.*

Hexapod interfaces work well with circularly symmetric mirrors. However, HabEx is considering an elliptical off-axis mirror, such a mirror requires a different system to provide the required launch and on-orbit performance (Fig. 5), which AMM models.
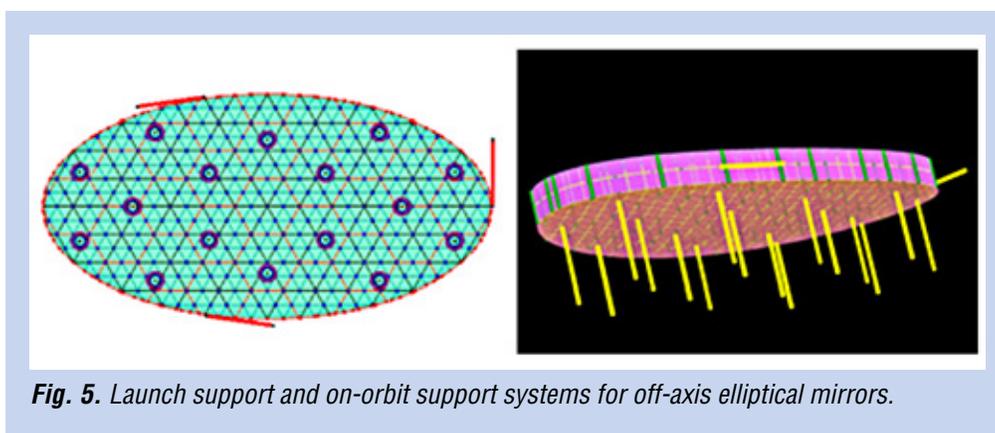
Fig. 5. *Launch support and on-orbit support systems for off-axis elliptical mirrors.*

Segment-to-Segment Gap Phasing
Need: To avoid speckle noise which can interfere with exoplanet observation, internal coronagraphs require an ultra-stable wavefront.

Accomplishment: During FY 2015/16, AMTD Phase 2 progressed in this technical area by continuing the systems engineering effort to understand the interaction between optical telescope wavefront stability and coronagraph contrast leakage.

Contrast Leakage vs. Segmentation: In support of a potential LUVOIR mission, analysis was conducted in FY 2014/15 on how segment-to-segment piston and tip/tilt motion affected contrast leakage for a 4th-order Lyot coronagraph as a function of number of segment rings. Leakage was reported as 10× more sensitive to piston than tip/tilt. In FY 2015/16, the analysis was refined to correct a normalization error, and leakage is now reported to be 2.5× more sensitive to piston than tip/tilt (Fig. 6). An intuitively obvious observation is that tip/tilt leakage as a function of λ/D distance has a clear dependence on the number of segment rings – D/N segment spatial frequency scatters energy into N λ/D.
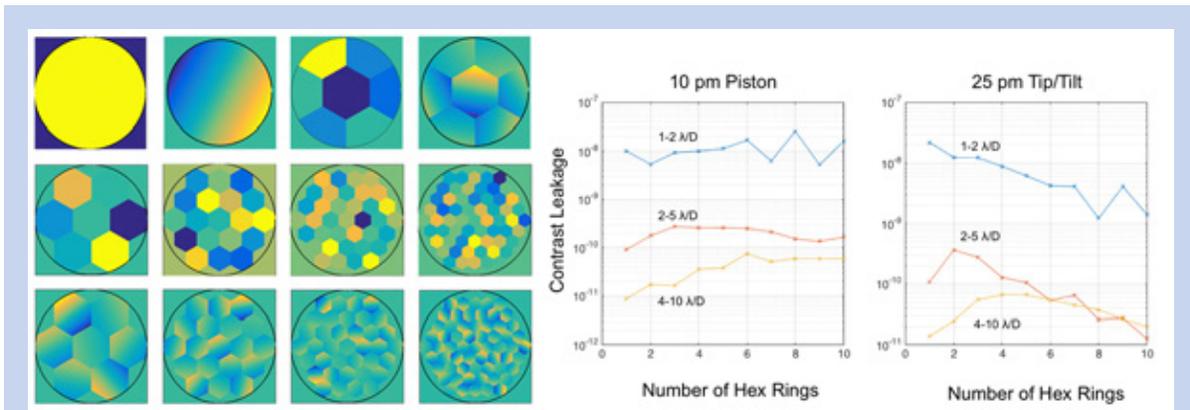
Fig. 6. *4th-order coronagraph contrast leakage for piston and tip/tilt as function of segmentation.*

Contrast Leakage for an Apodized Coronagraph: In support of a potential LUVOIR mission, in FY 2015/16, sensitivity to primary and secondary mirror motion was analyzed for an apodized shaped-pupil mask coronagraph, specifically designed for a JWST-style segmented aperture [1]. Coronagraph leakage was calculated for nine misalignment states (left to right in Fig. 7): PM segment piston, PM segment tip/tilt, PM segment power, secondary-mirror (SM) decenter, PM segment trefoil, PM segment astigmatism, PM or SM radius error, PM backplane bending, and PM or SM spherical error.
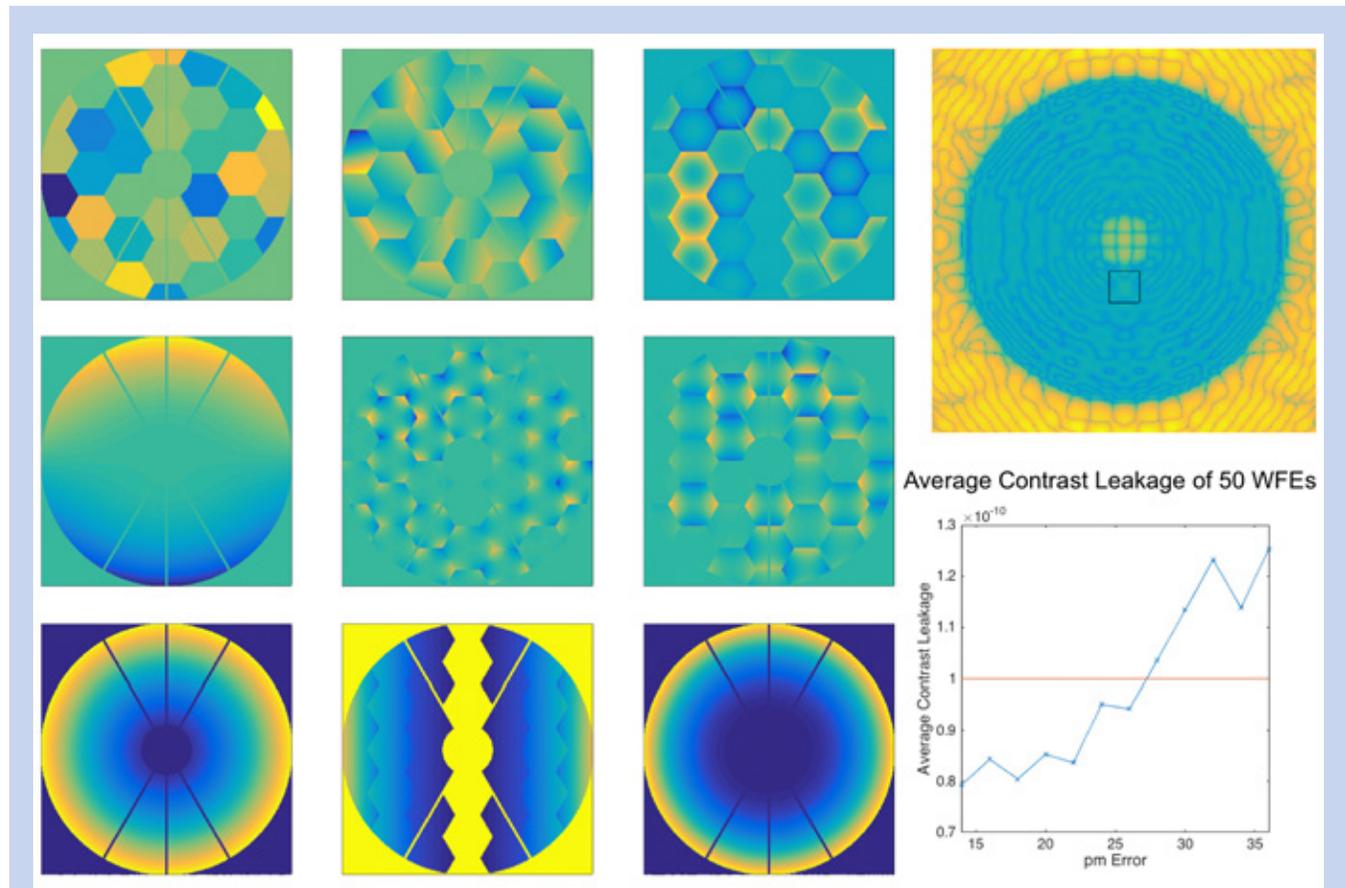
Fig. 7. *Maximum amplitudes for each misalignment error are defined to be when the average contrast leakage over 4 to 6 λ/D regions of interest is 10^{-10}.*

Leakage sensitivity for each error was determined by averaging over 50 random error realizations. AMTD defined the limit for each error to be when the average contrast leakage in the 4 to 6 λ/D region of interest is 10^{-10}. Table 2 summarizes the findings.

Segment Errors					Secondary Mirror			Backplane	
Piston	Tip/Tilt	Power	Astig	Trefoil	Power	Coma	Sphere	X-Bend	Y-Bend
10 pm	20 pm	30 pm	35 pm	65 pm	3000 pm	5800 pm	500 pm	500 pm	120 pm

Table 2. *Misalignment error amplitude for 10^{-10} average contrast leakage of apodized coronagraph.*

Integrated Model Validation

Need: On-orbit performance is driven by mechanical stability (both thermal and dynamic). As future systems become larger, compliance cannot be fully tested; performance verification will rely on results from a combination of sub-scale tests and high-fidelity models. It is necessary to generate and validate as-built models of representative prototype components to predict on-orbit performance for transmitted wavefront, point spread function (PSF), pointing stability, jitter, thermal stability, and vibro-acoustic and launch loads.

Accomplishment: During FY 2015/16, AMTD Phase 2 progressed in this technical area by continuing a systems engineering effort to understand the interaction between optical-telescope thermal environment and wavefront stability, and by continuing preparation for thermal vacuum testing of the 1.5-m-ULE® and 1.2-m-Zerodur® mirrors.

Thermal Stability: In FY 2014/15, a new methodology was developed for understanding how a PM responds to a dynamic thermal environment. This tool showed that a 4-m point-design PM wavefront error (WFE) remains below 10 pm for a 50-mK thermal oscillation of period shorter than 70 seconds. In FY 2015/16, this relationship was further explored as a function of a telescope's thermal sensitivity. Modeling indicates that WFE can meet the desired stability when the PM is inside a thermally controlled environment whose period and controllability meet the specifications shown in Fig. 8. Controllability is the maximum deviation of the shroud's temperature from the average temperature. Period of the control system is the time it takes for an entire heater cycle to occur.
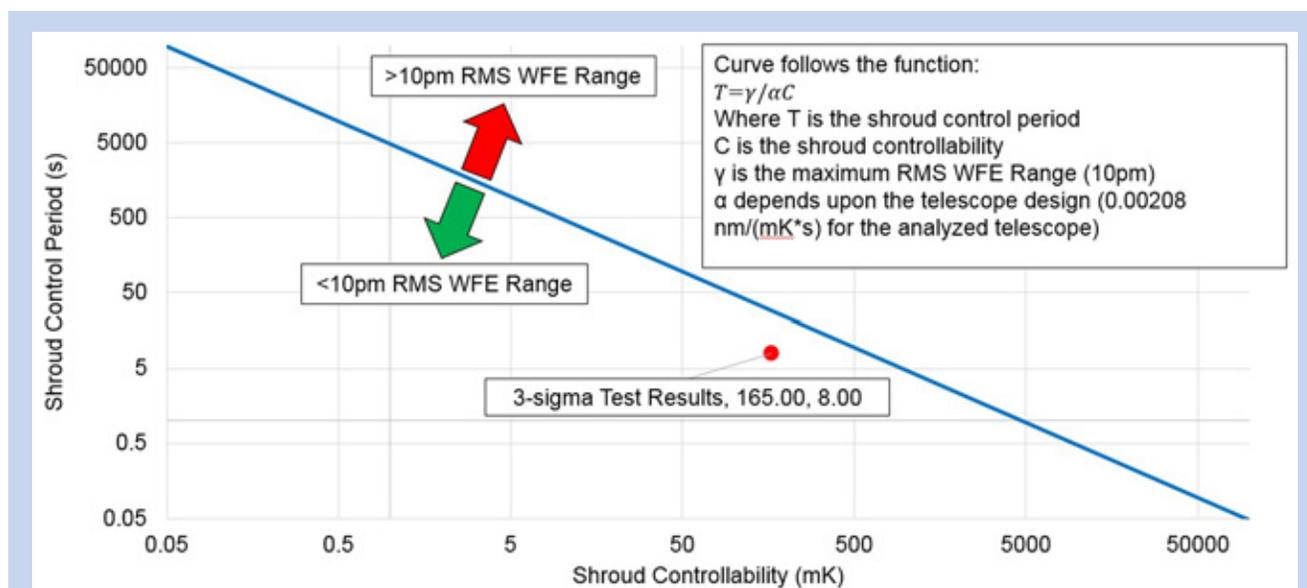

Fig. 8. *For a given telescope, wavefront stability can be kept below a specified value by varying shroud controllability and cycle period.*

Integrated modeling shows that the rms WFE range is inversely proportional to the mirror's mass and specific heat (c_p), and linearly proportional to the mirror's coefficient of thermal expansion (CTE). A closed-form derivation found similar relationships between thermal parameters and the thermal strain rate caused by heat imbalance:

$$\frac{dL}{dt} = \frac{(CTE)L}{V\rho c_p}\frac{dQ}{dt}$$

with L being length; Q, heat energy; ρ, density; and V, volume.

Based on these two findings, two figures of merit for thermally stable mirror materials are defined:

$$\text{Massive Active Opto-Thermal Stability, } MAOS = \frac{c_p\rho}{CTE}$$

$$\text{Active Opto-Thermal Stability, } AOS = \frac{c_p}{CTE}$$

Selecting a mirror substrate with a higher MAOS and AOS will result in a lower thermal strain rate in the mirror, i.e. a slower WFE change rate.

Thermal Vacuum Test Preparation: A key objective of AMTD is to validate-by-test integrated-model thermal-performance predictions. To enable testing of short-radius-of-curvature mirrors in the MSFC X-ray and Cryogenic Facility (XRCF), a pressure-tight enclosure (PTE) was built to place at the mirror's center of curvature: an interferometer to measure surface figure, an absolute-distance meter (ADM) to measure radius of curvature and a thermal camera to measure front-surface temperature distribution (Fig. 9). The PTE has two windows: one for the interferometer and ADM and a second for the infrared camera. In FY 2016/17, chamber qualification will be conducted to test and then characterize the static thermal performance of the 1.5-m-ULE® and 1.2-m-Zerodur® mirrors from 250 K to 300 K.

Fig. 9. *Pressure-tight enclosure enables center-of-curvature testing of mirror's radius of curvature, surface figure and front-surface thermal gradient.*
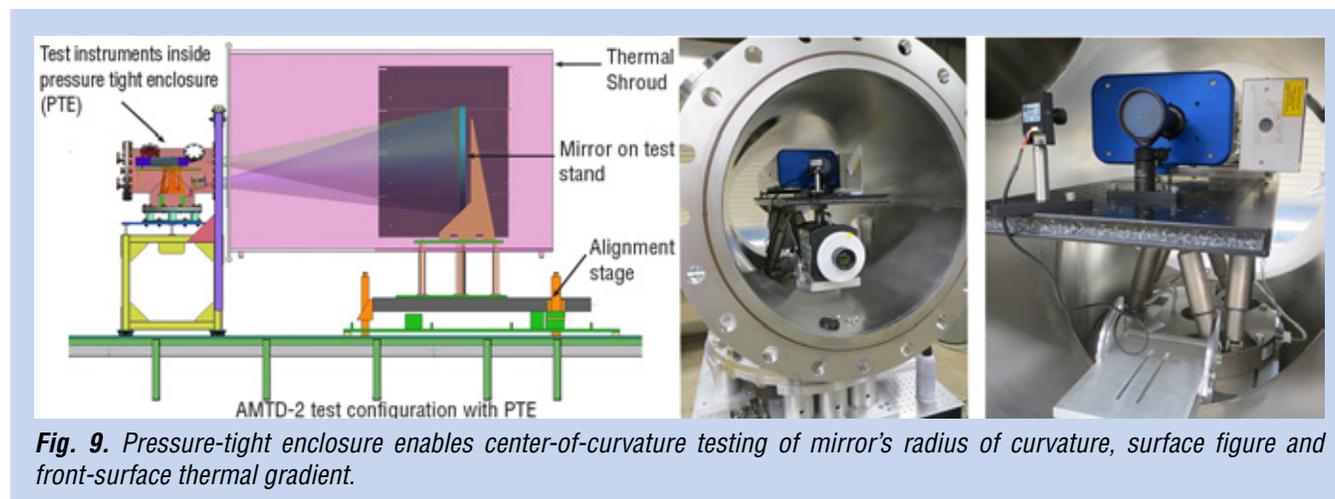
Path Forward
Milestone Schedule and Future Plans
AMTD has quantifiable milestones for each key technology. Figure 10 shows the Phase 2 schedule. The primary tasks for FY 2016/17 are to complete fabrication of the 1.5-m-ULE® and 1.2-m-Zerodur® mirrors; predict their thermal performance; and validate these predictions by test. Unfortunately, in FY 2015/16, AMTD-2 experienced a three-month schedule delay in obtaining critical-path components from suppliers and subcontractors.

Fig. 10. AMTD Phase 2 schedule.

Reference

[1] M. N'Diaye, R. Soummer, L. Pueyo, A. Carlotti, C.C. Stark, and M.D. Perrin, "*Apodized pupil Lyot coronagraphs for arbitrary apertures. V. hybrid shaped pupil designs for imaging earth-like planets with future space observatories*," ApJ, **818** (2), 163 (2016)

AMTD Publications

1. H.P. Stahl, "*Overview and accomplishments of advanced mirror technology development phase 2 (AMTD-2) project*," Proc. SPIE, **9602**, UV/Optical/IR Space Telescopes and Instruments: Innovative Technologies and Concepts VII, 960208, DOI: 10.1117/12.2186195 (September 22, 2015)

2. M.T. Stahl, H.P. Stahl, and S.B. Shaklan, "*Preliminary analysis of effect of random segment errors on coronagraph performance*," Proc. SPIE, **9605**, Techniques and Instrumentation for Detection of Exoplanets VII, 96050P, DOI: 10.1117/12.2190160 (September 24, 2015)

3. W.R. Arnold, "*Recent updates to the Arnold Mirror Modeler and integration into the evolving NASA overall design system for large space-based optical systems*," Proc. SPIE, **9573**, Optomechanical Engineering 2015, 95730H, DOI: 10.1117/12.2188750 (September 02, 2015)

4. W.R. Arnold, "*Evolving design criteria for very large aperture space-based telescopes and their influence on the need for integrated tools in the optimization process*," Proc. SPIE, **9573**, Optomechanical Engineering 2015, 95730G, DOI: 10.1117/12.2188570 (September 02, 2015)

5. T. Brooks, H.P. Stahl, and W.R. Arnold, "*Advanced Mirror Technology Development (AMTD) thermal trade studies*," Proc. SPIE, **9577**, Optical Modeling and Performance Predictions VII, 957703, DOI: 10.1117/12.2188371 (September 23, 2015)

6. R. Egerman, et al., "*Status of the Advanced Mirror Technology Development (AMTD) phase 2 1.5m ULE mirror*," Proc. SPIE, **9575**, Optical Manufacturing and Testing XI, 95750L, DOI: 10.1117/12.2188566 (August 27, 2015)

7. J.B. Knight, "*AMTD: Advanced Mirror Technology Development in mechanical stability*," Proc. SPIE, **9577**, Optical Modeling and Performance Predictions VII, 957704, DOI: 10.1117/12.2189312 (September 23, 2015)

For additional information, contact Philip Stahl: h.philip.stahl@nasa.gov

Cross-Strip MCP Detector Systems for Spaceflight

Prepared by: John Vallerga (Space Sciences Laboratory, UC Berkeley)

Summary

Micro-Channel Plate (MCP) detectors have been an essential imaging technology in space-based NASA ultraviolet (UV) missions for decades, and have been used in numerous orbital and interplanetary instruments. The Experimental Astrophysics group at the University of California (UC) Berkeley's Space Sciences Laboratory (SSL) was awarded an Astrophysics Research and Analysis (APRA) grant in 2008 to develop massively parallel cross-strip (XS) readout electronics. These laboratory XS electronics have demonstrated spatial resolutions of 12 μm full-width at half-maximum (FWHM), global output count rates of 2 MHz, and local count rates of 100 kHz; all at gains a factor of ~20 lower than existing delay-line readouts [1]. They have even been deployed in biomedical and neutron-imaging labs but are presently too bulky and high-power for space applications, though a current version has been successfully flown on a rocket flight in 2014 [2].

The goal of this Strategic Astrophysics Technology (SAT) program is to raise the Technology Readiness Level (TRL) of this XS technology by:

1. Developing new Application Specific Integrated Circuits (ASICs) that combine optimized faster amplifiers and associated Analog-to-Digital Converters (ADCs) in the same chip(s).
2. Developing a Field-Programmable-Gate-Array (FPGA) circuit that will control and read out groups of these ASICs so that XS anodes of many different formats can be supported.
3. Developing a spaceflight-compatible 50-mm XS detector that can be integrated with these electronics and tested as a system in flight-like environments. This detector design can be used directly in many rocket, satellite, and interplanetary UV instruments, and could be easily adapted to different sizes and shapes to match various mission requirements. Having this detector flight design available will also reduce cost and development risk for future Explorer-class missions. New technological developments in photocathodes (e.g., GaN) or MCPs (e.g., low-background, surface-engineered borosilicate-glass MCPs) could be accommodated into this design as their TRLs advance.

Since the start of our project in April of 2012, we have designed and constructed a 50-mm XS detector with a new low-noise anode, and have demonstrated its excellent performance using our best laboratory electronics. The second versions of our ASICs have been designed, fabricated, and tested, and are now being integrated into a full 160-channel (for 80 × 80 strips) electronic system that supports our 50-mm detector in full flight-like environmental tests. We recently started a follow-on SAT project which scales up the detector to 100 mm × 100 mm (320 channels) including a new version of our ASIC, fabricated in 130-nm CMOS process that combines the functions of the previous two versions to reduce board complexity while improving radiation hardness.

Background

The 2010 Decadal Survey, New Worlds, New Horizons in Astronomy and Astrophysics (NWNH), commenting on UV astronomy, noted, "*Key advances could be made with a telescope with a 4-meter-diameter aperture with large field of view and fitted with high-efficiency UV and optical cameras/spectrographs.*" Further, it recommends to "*invest in essential technologies such as detectors, coatings, and optics, to prepare for a mission to be considered by the 2020 decadal survey.*" Many of the White Paper submissions to the Decadal Survey on UV astrophysics missions require large fields of view (detector formats > 10 cm), and high spatial and/or spectral resolution recorded with high efficiency over a large wavelength range [3, 4]. Our SAT program plans to take our successful XS technology that achieves the performance goals above in the laboratory, and raise its TRL by lowering its mass and power and qualifying it for space use.

XS readouts collect the charge exiting from a stack of MCPs with two sets of coarsely spaced and electrically isolated orthogonal conducting strips (Fig. 1). When the charge collected on each strip is measured, a centroid calculation determines the incident location of the incoming event (photon or particle). This requires many (e.g., 80, 160) identical amplifiers whose individual outputs must all be digitized and analyzed. The advantage of this technique over existing and previous MCP readout techniques (wedge and strip, delay-line, intensifiers) is that the anode capacitance per amplifier is lower, resulting in lower noise. This allows (factor of ~20) lower MCP gain operation while still achieving better spatial resolution compared to the delay-line MCP readouts of current space missions [5], thereby increasing the dynamic range of MCP detectors by up to two orders of magnitude. This can also be scaled readily to large (> 100 mm × 100 mm) or unique formats (e.g., circular for optical tubes, rectangular for spectrographs, and even curved anodes to match curved MCP focal planes). The XS readout technology is mature enough to be presently used in the field in many laboratory environments producing quality scientific results [6, 7] and is ready for the next step of development – preparing for an orbital or deep-space mission implementation.
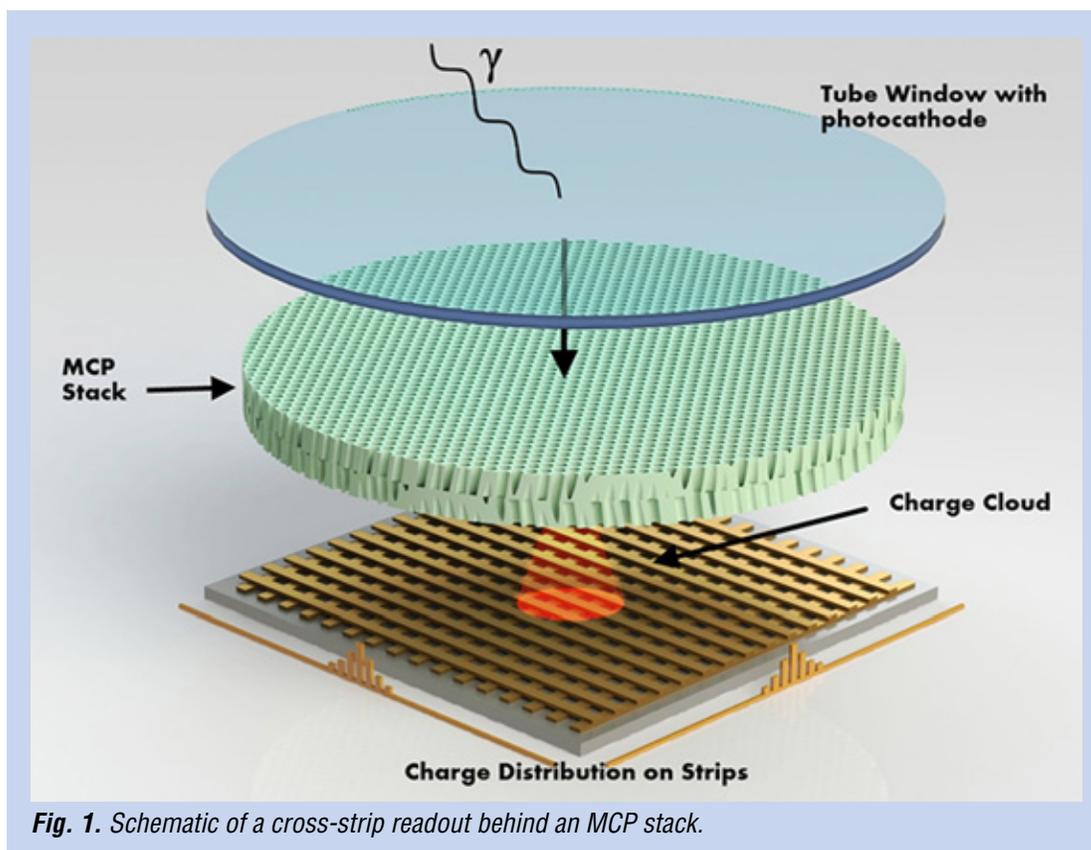
Fig. 1. *Schematic of a cross-strip readout behind an MCP stack.*

Our current laboratory XS readout electronics, called the Parallel XS (PXS) electronics, consist of a preamplifier board placed near the MCP anode and a boxed set of electronics containing ADCs and FPGAs. The PXS electronics performance presently meets or exceeds ALL of the specifications of the previous flight systems mentioned above. However, the PXS laboratory electronics are too bulky and massive, and use relatively high power and therefore are not currently suitable for a long-term space mission. One important goal of the present effort is to replace the PXS electronics with ASICs that combine the functionality of the preamp board and the downstream ADCs into one or two low-power, low-mass chip(s). When a set of these chips are combined with an FPGA and XS anode, we expect the performance to exceed the higher-power PXS electronics due to the noise improvement expected for the smaller-scale components.

In addition to space-flight-appropriate ASIC development, our first SAT program planned to construct a flight prototype 50-mm XS MCP detector with a XS readout using our new ASICs. The new ASICs and FPGA control electronics are being integrated into a compact package so the performance of the whole detector system can be qualified in space-like environments (e.g., thermal and vibration tests). This standard detector design will become the baseline XS detector and could be used in many proposed rocket and satellite missions. We note that many UV sounding rocket programs (e.g., at Johns Hopkins University and the University of Colorado) currently use MCP detectors. In fact, we expect this detector to be the baseline of many Explorer-class mission proposals in the future. This XS design can also be scaled easily to other useful formats required by specialized instruments. For example, doubling the length of one detector dimension entails adding more strips to the anode and more ASIC chips to read them out, but not a redesign of the ASIC.

Objectives and Milestones

As the 50-mm detector development winds down over the next few months and the 100-mm detector follow-on SAT program begins, we will reiterate the milestones of the first project and include additional milestones of the second, which scales up the first by a factor of four in area.

1. Design and fabricate ASICs to amplify and digitize cross-strip signal charges

A major thrust of our 50-mm program was developing new ASICs that can overcome the limitations on the front end of our laboratory electronics. We designed and fabricated input ASICs that had the following features:

a. An optimized front-end charge-sensitive amplifier (CSA) matched to the anode-strip load capacitance with fast signal rise and fall times to minimize event "collision."
b. Fast (~GHz) analog sampling to fully characterize both amplitude and arrival time of the intrinsically fast input charge pulse.
c. Digital conversion of the analog samples in the ASIC, avoiding complex, bulky, and high-power discrete ADCs downstream.
d. ASIC self-triggering capabilities to select and transfer only event data across long cables to the FPGA, where the centroiding and timing calculations take place.

The original 50-mm detector proposal called for an ASIC that included a multichannel preamp and an analog sampling and digitization circuit controlled externally by an FPGA. We soon realized that optimization of the analog amplifiers and digital circuits was best done using different fabrication technologies (IBM 130-nm 1.2-V CMOS process, 250 nm for the digital) and noise performance would also improve by not mixing the digital and front-end analog signals on the same piece of silicon. The original name for the combined ASIC (never built) was Gigasample Recorder of Analog Waveforms from a Photodetector ("GRAPH") but after separation of the amplifiers, the sampling digitizer was named the "HalfGRAPH."

After demonstrating two working ASICs (the CSAv3 and the HalfGRAPH2 ASIC described below), we now plan in our 100-mm effort to migrate our HalfGRAPH2 design to the 130-nm CMOS process, which should increase its robustness to radiation ("HalfGRAPH3"). We will characterize all three ASICs in realistic radiation environments (total ionizing dose, single event upsets, non-ionizing energy loss, etc.) consistent with MIL STD 833 TM1019 for low Earth orbit (~10 krad), interplanetary missions (~30 krad) as well as the higher doses associated with Jupiter missions (100 krad after shielding), since we have placed MCP detectors in all such environments. Early testing of the HalfGRAPH2 will inform the design of the HalfGRAPH3, and we have an opportunity to improve its robustness to radiation dose by using standard industry design techniques for radiation hardness.

As the new HalfGRAPH3 digitizer/sampler will now be in the same CMOS process as the CSAv3, we could realize the original "GRAPH" ASIC concept, combining both on a single die. However, to reduce risk, we do not propose to integrate both designs at this point. Indeed, doing so will require significant studies of power supply and substrate isolation, which we choose to defer until the HalfGRAPH3 is fully characterized and the benefit of a combined amplifier and sampler is more fully demonstrated.

2. FPGA system to read out HalfGRAPH ASICs

Our proposed parallel XS readout system was not simply comprised of the new ASICs. New board assemblies had to be designed, laid out, and constructed to couple these ASICs to our existing XS anodes, minimizing stray load capacitances. These boards also included control FPGAs that not only have a new input interface, but a new output interface to couple to the high-bandwidth computer interface required for our ultimate event rates.

3. Design of a 50-mm and 100-mm XS MCP detector incorporating new electronics

Key issues for large area XS MCP detector implementations include low-mass and robust construction schemes that can accommodate the capability for a high-vacuum sealed-tube configuration. Without incurring excessive costs, a reasonable format to accomplish this first was the 50-mm detector. This detector achieved spatial resolutions of ~20-μm FWHM, background rates < 0.1 events cm^{-2} sec^{-1}, low fixed-pattern noise, long lifetime, multi-MHz rate capability with low dead-time, and detector mass of a few hundred grams. The design and construction of brazed-body assemblies provides for the best packaging and diversity of applications, so this was one of the core tasks. The overall configuration represents a device compatible with many current sounding-rocket experiments, and was qualified in vibration and thermal-cycling tests, in a straightforward manner. This was a good stepping-stone for implementation of much-larger-format devices for large optics/missions.

In the 100 mm × 100 mm effort, we plan to scale up the brazed-body assembly, detector backplate, XS anode, and number of channels by a factor of 2 in each dimension (320 electronic channels total) while maintaining performance parameters; and test them in appropriate flight-like environments (thermal and vibrational), along with radiation testing of the ASICs.

Progress and Accomplishments

Three parallel efforts are coming together in the final year of the 50-mm program and will continue in the 100-mm effort – ASIC design fabrication and test at the University of Hawaii; FPGA control electronics at UC Berkeley; and 50-mm and 100-mm XS detector design, also at UC Berkeley. Two versions each of the ASICs have been fabricated and tested, as has the 50-mm detector (albeit using the PXS readout electronics). The 160-channel FPGA-controlled amplifier and digitizer boards have been fabricated along with their electronics boxes. The 100-mm brazed body and backplate design has started and is out for fabrication quotes. Initial radiation testing of the ASICs is being planned.

ASIC Design

We have successfully fabricated and tested two working ASIC designs: the 16-channel CSA called "CSAv3" (Fig. 2) and the 16-channel HalfGRAPH2. The sections below discuss these designs and their testing to date.

Fig. 2. *CSAv3 die layout showing 16 channels along with the regions of control circuitry including Digital-to-Analog Converters (DACs) and registers.*
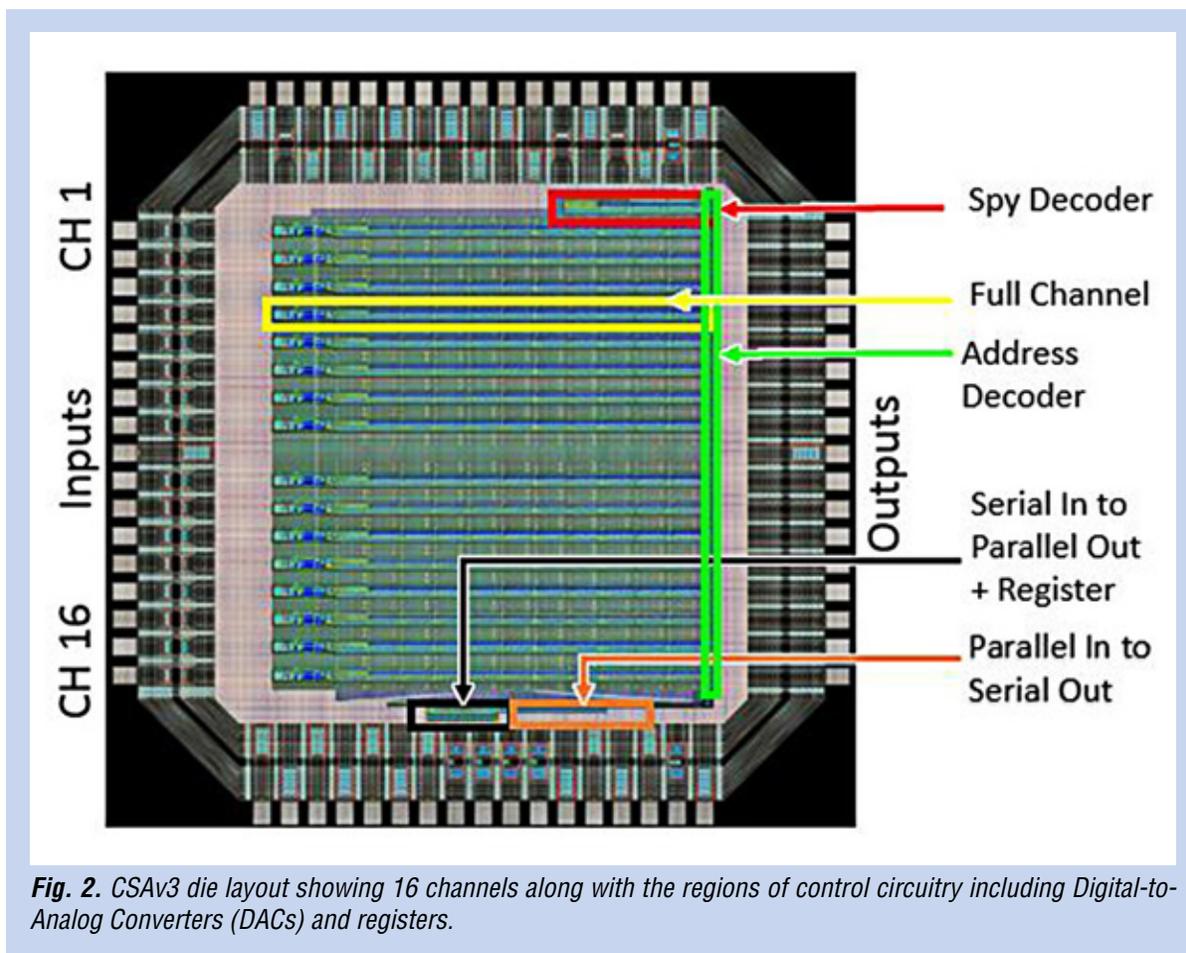
CSAv3

Our goal for the new preamp CSAv3 was to maintain the noise figure of the existing laboratory "PreShape32" amplifiers of around 1000 e$^-$ rms, but also to narrow the waveform, halving the rise-time to 20 ns and decreasing the return to baseline to below 100 ns. This significantly reduces the pileup at high event rates. In addition, the chip does not require additional external components for biasing, reducing its overall footprint on the printed circuit board.

At an MCP gain of 10^6 (160 fC), the largest signal expected on a single strip is ~50 fC. We chose the number of channels per die to be 16 to help with the fan-in from the 80 inputs from the 50-mm anode. The CSAv3 amplifier was designed to drive the input of the HalfGRAPH2 including the short trace between them. We designed the amplifier to have linear output swings of ±600 mV.

The components of a single amplifier stage (Fig. 3) consist of a charge-sensitive preamp followed by a pole-zero cancelation (PZC) network, a shaper, an optional polarity inverter, and a buffer amp to drive the downstream HalfGRAPH2. The preamp is an inverting folded-cascade integrator, with the feedback circuit time constant controlled by a PMOS (P-type metal-oxide-semiconductor) transistor operating as a voltage-controlled resistor. The PZC circuit cancels the pole of the preamp, removing the long baseline recovery. Additional programmable shaping and buffering circuits allow us to optimize the gain and noise of the amplifier. Programming the chip is required prior to operation, which is carried out through a 4-wire serial port to set 16 registers which either control switches to set up signal paths in the chain or set the ten 12-bit DAC values to bias the circuits.

Fig. 3. *A generalized schematic of the new CSAv3.*
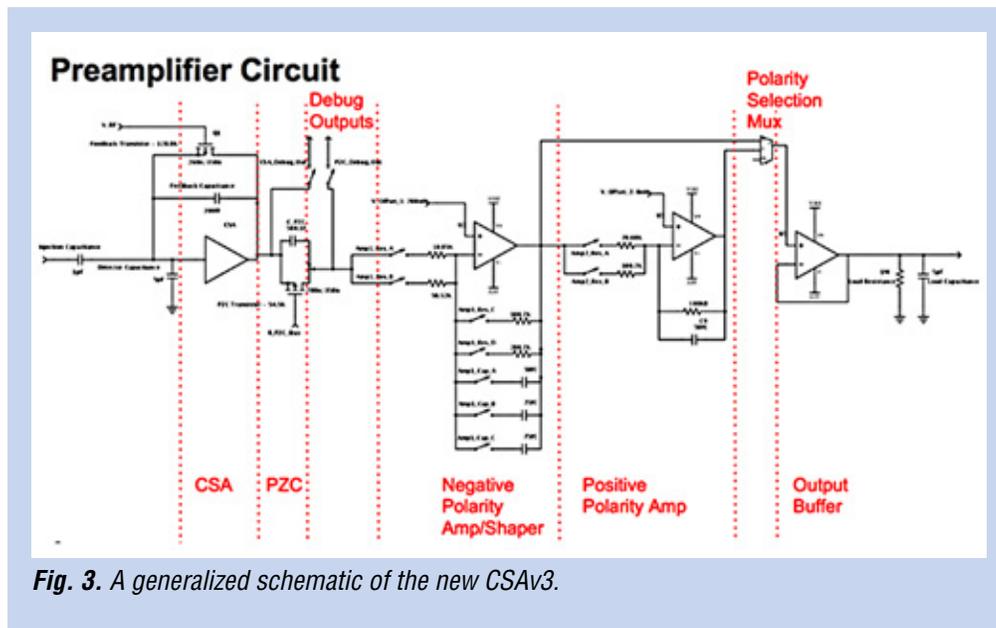
Initial performance tests with the amplifier show that it meets the specifications for gain, noise, rise-time, and fall-time [8]. In summary, the overall gain is approximately 9.5 mV/fC over a range of 0 to 60 fC input charge. Within this range, the gain linearity is within 7%, and the output pulse width is confined within 100 ns. The rms noise was estimated from a fit of noise measurements for different input load capacitances, and results in a noise equivalent of 586 e^- + 96 e^-/pF input load. The spread in gain between channels for the same bias settings was found to be minimal, but can be fine-tuned if required. An example of a measured waveform for a charge injection of 50 fC is shown in Fig. 4. Details of the design, simulation, and fabrication of CSAv3 can be found in [8].

Fig. 4. *Amplifier response to 50-fC input pulse with a 5-pF load. Note the 20-ns rise time and a return to baseline in 75 ns while retaining a noise value of ~1000 e^- rms.*
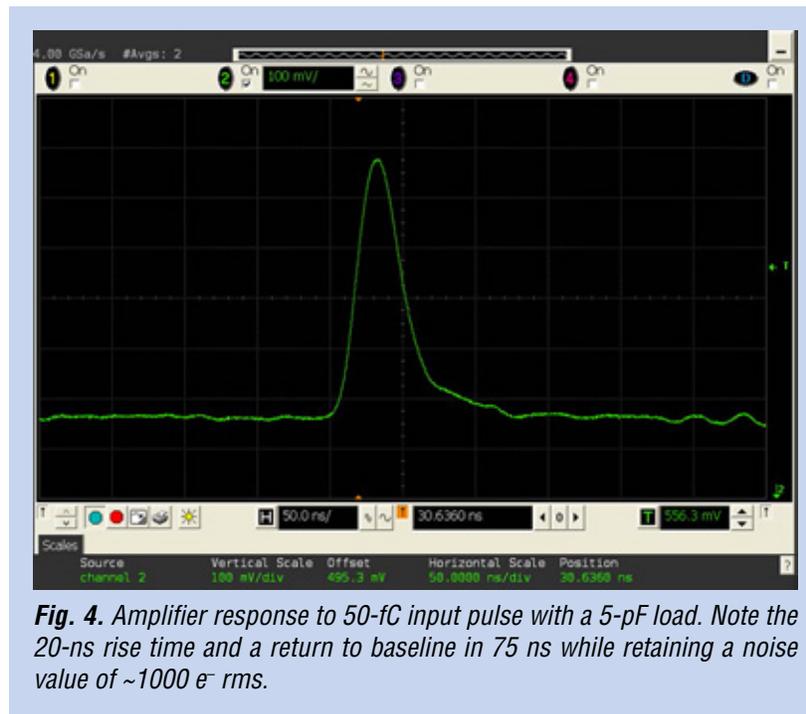
HalfGRAPH2

HalfGRAPH2 is a 16-channel, 1 giga-sample-per-second waveform digitizing chip with 12-bit resolution (Fig. 5). It is being designed in the Taiwan Semiconductor Manufacturing Company (TSMC) 0.25-μm CMOS technology, using Tanner EDA design and simulation tools. The circuit's heritage is the TeV Array Readout with GSa/s sampling and Event Trigger (TARGET) ASIC used for photomultiplier waveform sampling in the Cherenkov Telescope Array [9]. Each channel of this digitizer chip has a 2-stage analog storage mechanism. In the first stage, a short sampling array is subdivided into two sample windows, each with 32 switched-capacitor storage cells. In the second stage, in a ping-pong fashion, as one sample window is filling, the other is transferred into a larger storage array. This storage array has 8192 cells, organized as two banks of 64 rows of 64 samples each (also called a storage window) for every channel. This results in a continuous sample of 8.192 μs in length before being overwritten in a circular buffer.
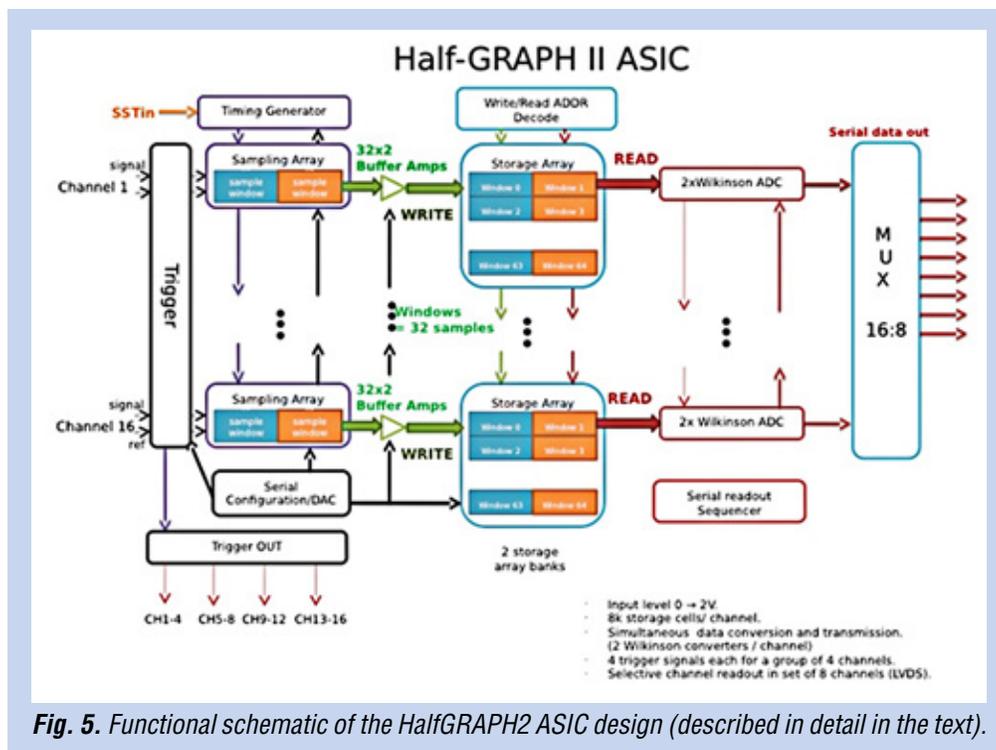
Fig. 5. *Functional schematic of the HalfGRAPH2 ASIC design (described in detail in the text).*

The input analog trigger circuit has four digital output lines that notify a control FPGA of a new event. A trigger pulse is set in place if the measured signal on a channel is higher than a preset threshold. Trigger lines are organized to cover channels 1-4, 5-8, 9-12, and 13-16. This allows finer localization of the strip where the event occurred. The trigger arrival into the FPGA marks the address in the storage array of the samples for that event.

In order to digitize the acquired signal, each channel uses two banks of 12-bit Wilkinson ADCs. An FPGA selects the storage window to be digitized. Thirty two analog samples in parallel on all 16 channels of the storage window are converted concurrently into digital values using comparators, a voltage ramp, and counting (12-bit counter) with a 500-MHz dual-phase clock until the comparator fires when the ramp exceeds the analog value on the cell. It takes 4.1 μs to complete the digitization. At this point, the 32 time samples of 12-bit data are sent out serially over Low Voltage Differential Signal (LVDS) lines with a 250-MHz clock to the FPGA in 1.5 μs (=12×32/250 MHz). This is done for a subset of eight channels in parallel, chosen by the FPGA based on trigger information, allowing the centroid calculation using the properly filtered amplitude derived from the waveform. When the data transfer begins, the next window is digitized by the second Wilkinson converter which takes over the next transmission, saving 1.5 μs.

As the FPGA has the address of the events in the storage array, it can prevent the overwriting of those cells. Therefore, the throughput of the system is limited by the 4.1-μs conversion time of the ADCs. The maximum throughput of one channel is 240 kHz, but there is no deadtime at rates below this frequency due to the multiple buffering. With five independent ASICs per axis, the event rate that can be supported is 1.2 MHz. The readout rate can be greatly increased by decreasing the bit resolution. For a 10-bit conversion, the event rate could reach 5 MHz. As the event data will be digitally filtered by the FPGA processing, 10 bits will most likely be more than enough to achieve a high signal-to-noise ratio.

The dies were received in 2015, and mounted in LQFP64 carriers (Fig. 6). Initial power tests for the HalfGRAPH2 shows it drawing 20 mW per channel at 2.5 V. An FPGA mezzanine card (FMC) was designed and fabricated to test two HalfGRAPH2 chips with two CSAv3 chips, for a total of 32 channels. The board form factor was designed to match the Xilinx ML605 evaluation board that would control the circuit. This allowed us to set all necessary digitizer and amplifier parameters remotely, and provided an on-board test-signal generator. The data output used a gigabit Ethernet connection to the downstream computer for analysis. The initial firmware was developed to capture events over the set threshold in the storage buffer, digitize them, and pass the raw values downstream (similar to a 32-channel sampling scope) so its raw performance could be assessed (rms noise, pedestal variation, readout rates, power draw, etc.). Within the storage window, each analog storage cell with its own comparator will have a DC pedestal value that must be subtracted from every measurement (Fig. 7). Figure 8 is an example of a digitized 50-fC pulse with the pedestal subtracted for each sample. Analyzing the pedestal-subtracted baseline indicates we are measuring ~7 ADU counts rms (1 ADU = 236 e$^-$) or 1650 e$^-$ rms, 50% higher than expected, though there might be a contribution from a residual fixed pattern in the pedestal subtraction. However, we have at our disposal a large number of samples across the typical pulse such that a low-pass filter within the FPGA can be used to increase the signal-to-noise ratio.
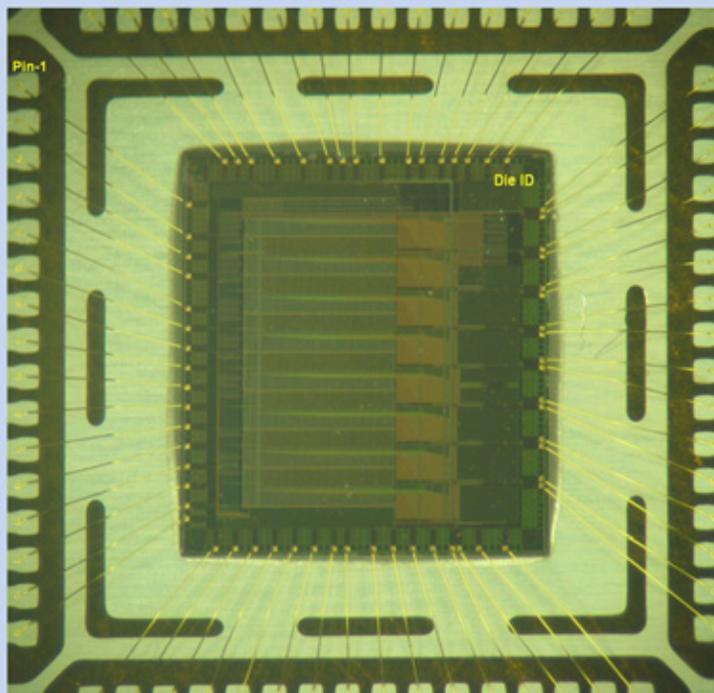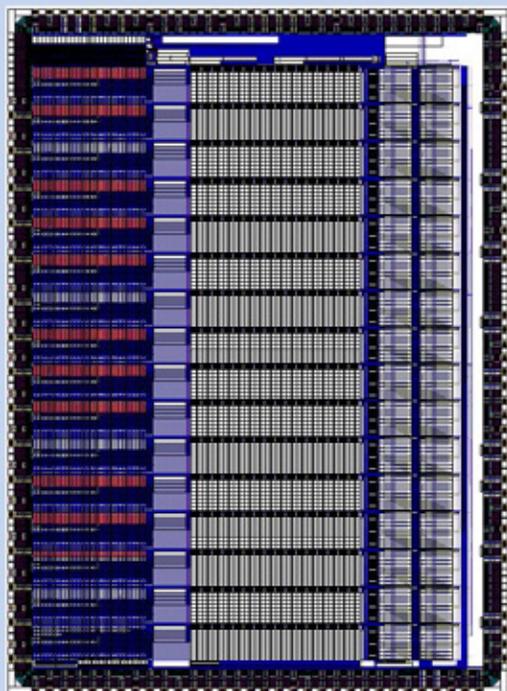
Fig. 6. *HalfGRAPH2 16-channel ASIC layout (left) and die mounted in carrier (right).*
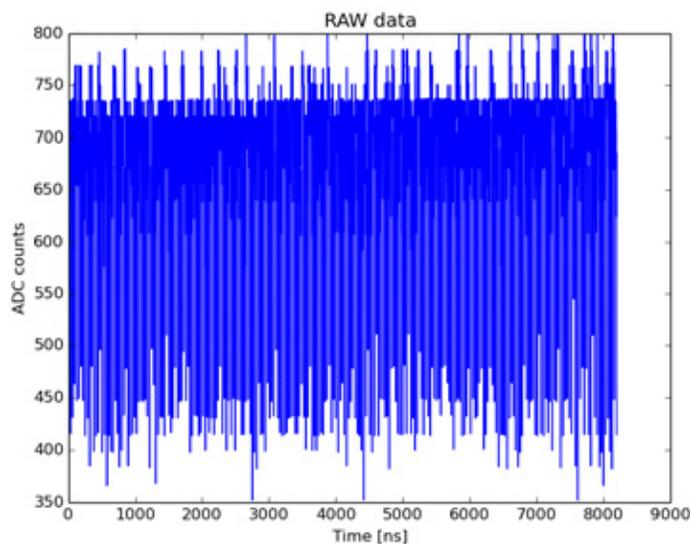
Fig. 7. *Single-channel halfGRAPH2 output of all 8192 samples of the baseline of the CSAv3 output (no pulse) showing the distributions of fixed DC pedestal per sample that must be stored and subtracted.*
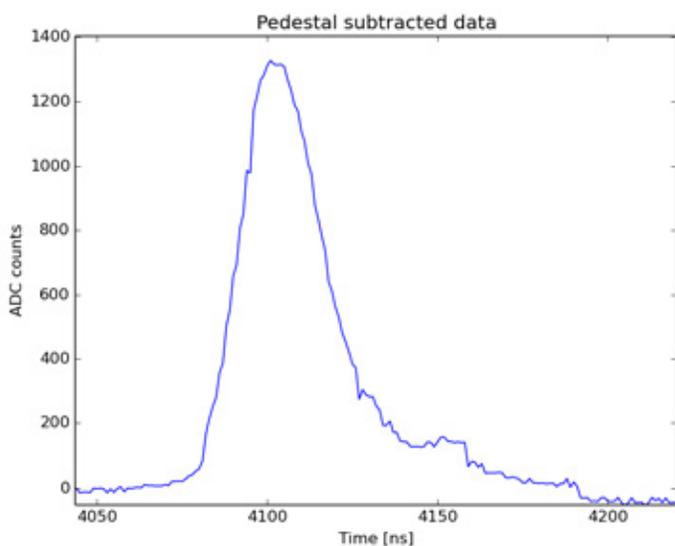
Fig. 8. *Single 50-fC pulse input to CSAv3 and digitized by the HalfGRAPH2.*

FPGA Controller

In parallel with the ASIC testing described above, but slightly delayed to take advantage of what we learned, we designed the electronics layout for the full 160 channels of the 50 mm × 50 mm anode readout (Fig. 9). The sensitive preamps must be mounted close to the anode to minimize capacitance loading of the input, and the HalfGRAPH2 digitizing ASICs must be close to the preamp outputs to minimize their output load. Given these constraints, as well as the desire to fit the electronics into a small enclosure mounted directly to the detector backplate (Fig. 10), we decided to construct two printed circuit boards: an amplifier board with 10 CSAv3 chips and a digitizer board with 10 HalfGRAPH2 chips and two FPGAs (ArtixAX200), one for each axis, X and Y. The digitizer board will interface with a downstream FPGA development board (e.g., SP601) via 11 LVDS pairs.
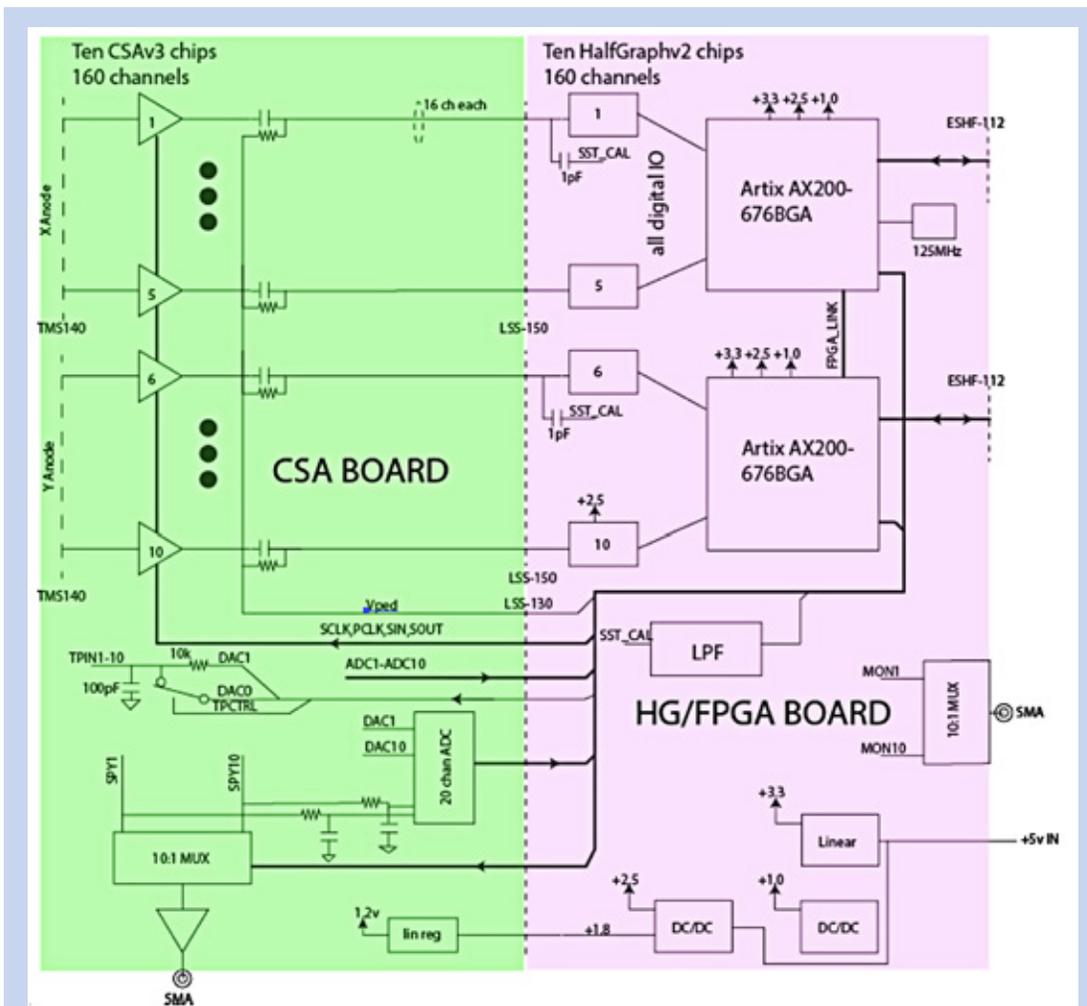
Fig. 9. *High-level schematic of 50-mm detector electronics. 160-channel amplifier board (left) and 160-channel digitizer board with two FPGAs to control ASICs and calculate event centroids (right).*
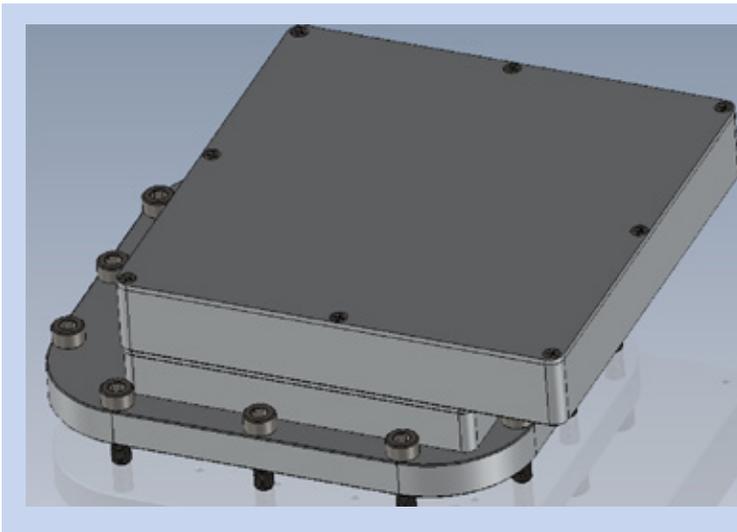
Fig. 10. *Rendering of two electronics boxes (amplifier and digitizer) mounted to 50-mm detector backplate .*

The 160 total anode channels (80 × 80) are input to a CSAv3 amplifier board using two Samtec TMS-140-01-S-D connectors, and the 160 amplified signals pass through an inter-board connector (Samtec LSS-150-02-F-DV-A) to the ten HalfGRAPH2 chips on the digitizer board. Additional connectors also exist for inter-board power, control, and command/data out.

The main data interface (using 11 LVDS lines running at 100 MHz double data rate, DDR, to the development board) communicates with both FPGAs, X and Y, and is controlled by the downstream host. Initially in Raw output mode, we transmit all 160-channel samples of 128 ns duration just for triggered events, achieving 8000 events/s using both X and Y interfaces. Eventually, when the internal FPGAs are tasked with calculating the centroids themselves, only one interface (X) will be needed, as the bandwidth of sending just X, Y, and pulse-height for each event is much smaller, so the rate can reach 16 Mevents/s.

As of May 31, 2016, the amplifier board has been fabricated (Fig. 11), programmed, and successfully tested as a pulse amplifier. The digitizer HalfGRAPH2 board has been designed (Fig. 12) and is under fabrication. The firmware is 90% completed and 30% simulated.
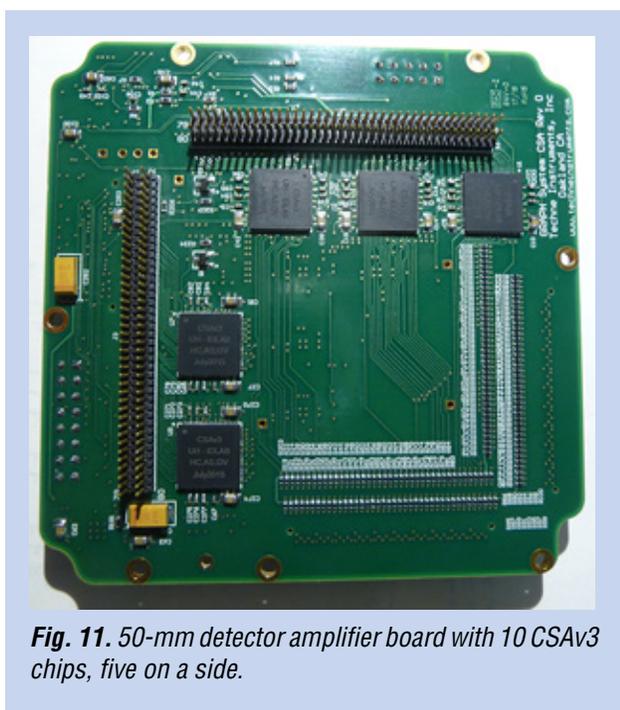
Fig. 11. *50-mm detector amplifier board with 10 CSAv3 chips, five on a side.*
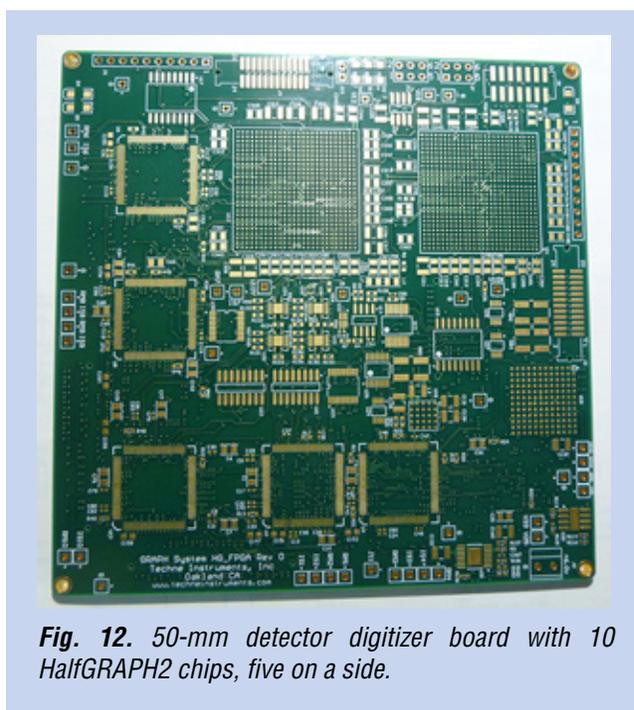
Fig. 12. *50-mm detector digitizer board with 10 HalfGRAPH2 chips, five on a side.*

50-mm XS Detector

There are two key aspects to our new flight-like 50 mm × 50 mm XS detector design. The first is a photolithographic and laser-cut XS anode design made with polyimide. Polyimide's dielectric constant is lower than that of alumina ceramic by a factor of three, resulting in lower individual strip capacitance and thus lower amplifier noise. The top strip pattern is first etched in the copper, after which a laser ablates the material between the strips. This top layer is then bonded to the bottom strip pattern etched on a much thicker polyimide substrate. The input side of the anode is shown in Fig. 13, installed in the 50-mm XS detector, with measured strip capacitances matching our design model. Outputs from the 80 × 80 strips go through a hermetic seal consisting of 2 × 80-pin connectors sealed with vacuum epoxy (Fig. 14). The other key aspect of our detector is using a Kovar and ceramic brazed body to mount the MCPs over the XS anode. This technique is used in vacuum image tube construction to make a strong, robust, and clean detector that can survive launch stress. Figure 13 shows the brazed body mounted over our XS anode onto a vacuum back-plate with three high voltage (HV) feedthroughs (MCPs removed to show the anode below).
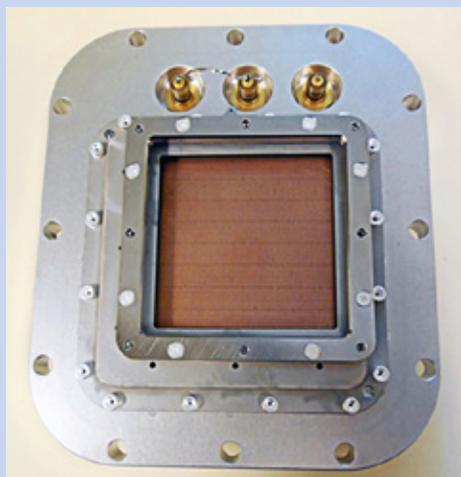
Fig. 13. *View of windowless 50-mm XS detector mounted on a vacuum flange with three HV feed-throughs showing the XS anode (MCPs removed).*
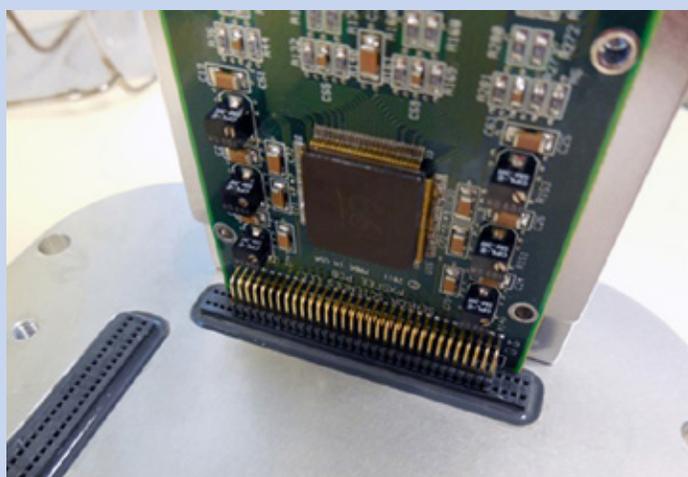
Fig. 14. *External side of detector showing 80-contact feed-throughs (×2) sealed with epoxy and a 64-channel preamp board plugged into one axis.*

Imaging Results with 50-mm Detector

Since the readout ASICs and boards are still being fabricated, we used our existing PXS_II electronics and 64-channel amplifier boards to read out the central 64 × 64 strips of this 80 × 80 XS anode. This corresponds to a central active area of 40 mm × 40 mm. The results below use a stack of two MCPs from Photonis USA with 10-µm pores on 12.5 µm centers 53.7 mm × 53.7 mm and 60:1 L/d ratio (600-µm-thick each). We measured the spatial resolution and linearity, and acquired flat fields to measure the UV response uniformity to 183-nm light from a Hg pen-ray lamp.

To measure the spatial resolution, we used a pinhole mask grid mounted directly on the input MCP. The pinholes are 10 µm in diameter and spaced 1 mm apart on a square grid (Fig. 15), an excellent method of sampling the Point Spread Function (PSF) across the field of view. To measure the spatial resolution, we had to bin the X, Y event data to 8192 × 8192 (5-µm pixels) to resolve the PSF. The inset of Fig. 15 shows the X dimension PSF (top strips) of a single pinhole. The average spatial resolutions in the X and Y dimensions were 17.5 µm FWHM and 22 µm FWHM, respectively.
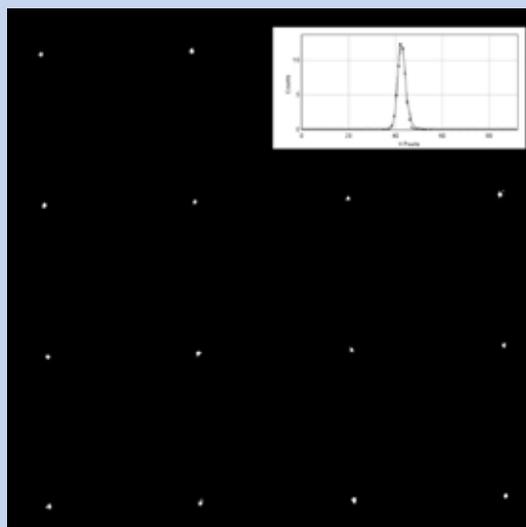
Fig. 15. *UV image of pinhole mask of 10-µm holes on 1-mm square grid. Inset shows the PSF of a single hole with resolution of ~4 pixels FWHM (20 µm).*

The detector linearity can also be measured with the pinhole mask data, as the pinholes are uniformly spaced at 1 mm. Figure 16 shows residuals (in μm) to a linear fit to pixel position of the pinhole vs. pinhole number. The ±15-μm deviation from zero is smaller than the detector spatial resolution measured above, and comparable to the hexagonal 12.5-μm pore spacing. This measurement attests to the accuracy of the photolithographic anode strip regularity.

Fig. 16. Residuals to linear fit of derived pinhole position across central 40 mm of the 50-mm XS detector.
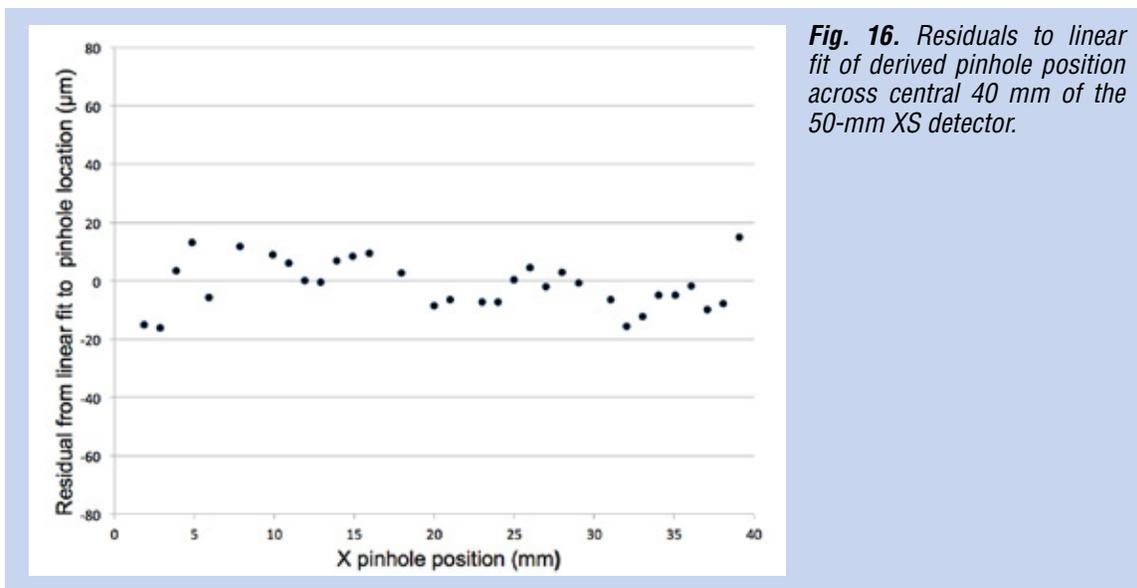
No detector has a perfectly flat response. For MCP detectors, a uniform input illumination can reveal MCP sensitivity variations plus nonlinearities in the X, Y determination of the charge cloud centroid by the anode. To measure response flatness, we collected more than 30 billion counts to achieve 460 counts per 5-μm pixel. Figure 17 is a small, 2.5 mm × 2.5 mm section of a UV flat field. There is a hint of fixed-pattern noise, and compressing the data in both dimensions reveals the presence of a differential nonlinearity at the strip spacing in the Y (bottom) dimension. The effect is at the 3% level peak-to-peak, and can be corrected with a lookup table. We used this flat field to divide another flat field taken the next day (140 counts per 5-μm pixel) and binned to 20-μm pixels. The second flat had only 34% of the counts of the first flat, but the resultant divided image, Fig. 18, shows no fixed pattern and is consistent with Poisson statistics expected from the two images. The image pixel values histogram (Fig. 18 inset) has a standard deviation of 2.3%.

Fig. 17. Small section of very deep (2500 cts/pxl) flat field showing a small but noticeable fixed pattern noise.

Fig. 18. Image from Fig. 17 divided by deeper flat field. Residual variation consistent with expected Poisson statistics (2% standard deviation, inset).
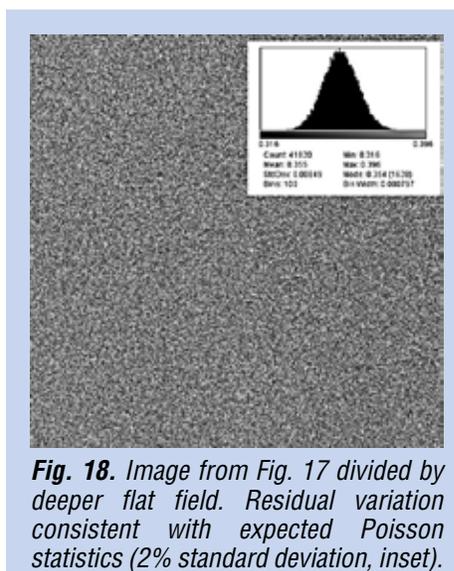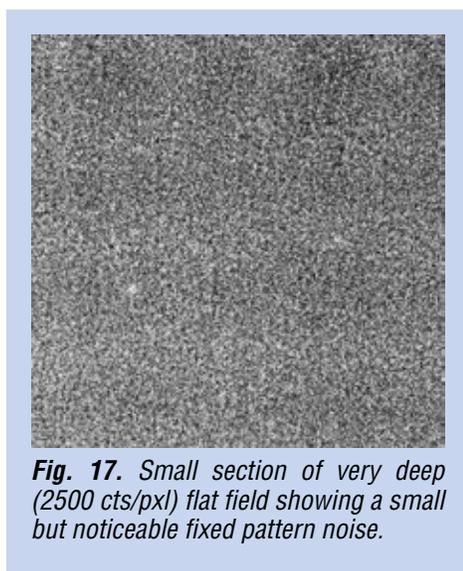
Environmental Testing of 50-mm Detector

One of the main goals of this SAT program was to advance the TRL of the 50-mm detector system. Since the new 50-mm detector on its backplate is a new design, we decided to go beyond testing its performance on the bench, and confirm its performance at temperature extremes, as well as its ability to survive the g-forces of standard rocket launches.

The detector and front-end electronics were mounted onto a vacuum housing inside a thermal chamber and cycled from –30°C to +45°C (Fig. 19). We measured detector performance from –15°C to +45°C, allowing the temperature to equilibrate for ~1 hour at each test level, before taking a deep UV flat field image. Because we had a smattering of small dead spots on the detector that acted as spatial fiducials, we were able to notice a shift of ~30 microns in the image over a 60°C temperature swing. Since this shift was in the MCP-bias direction, we believe it was due to electron-cloud kinematics caused by thermally induced MCP gain variation. It speaks to the XS detector's excellent spatial resolution that we can even measure this effect and in all other measures – resolution, background rate, and dynamic range – the detector worked flawlessly.
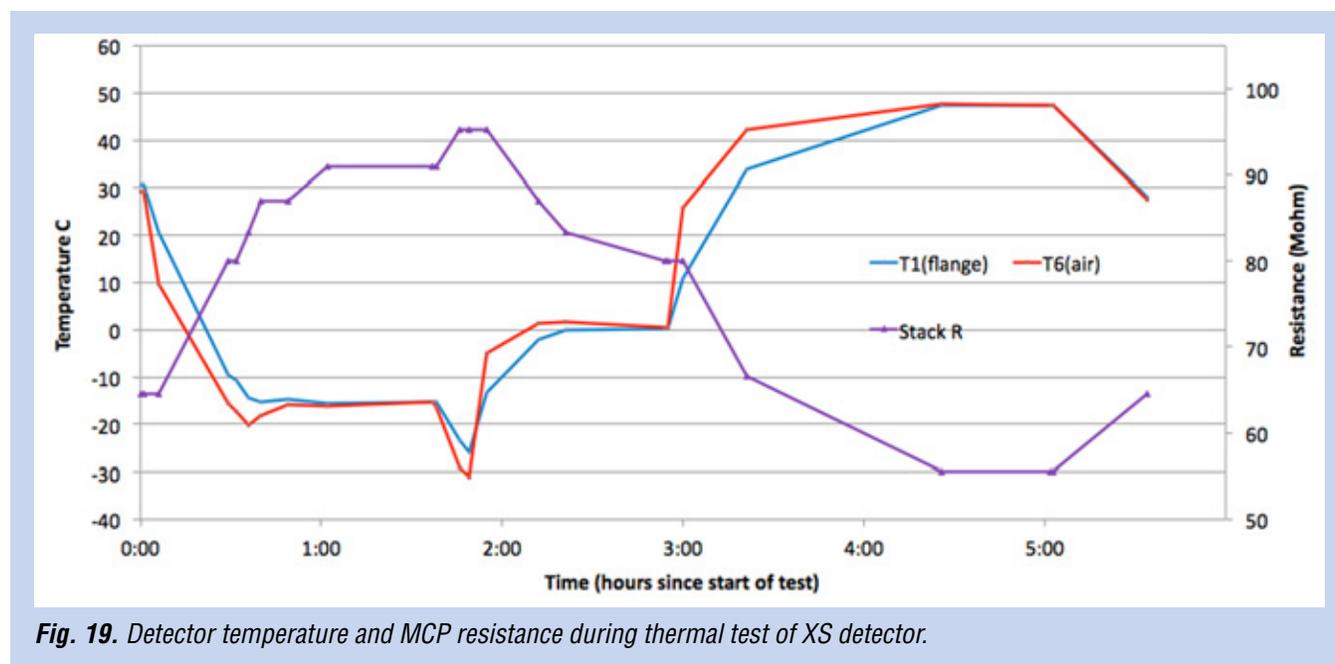
Fig. 19. *Detector temperature and MCP resistance during thermal test of XS detector.*

We also used the SSL vibration table to vibrate the detector (without the electronics) to 14.1 g (rms) as recommended in the GSFC General Environmental Verification Standard, GEVS (GSFC-STD-7000A). Figure 20 shows the detector backplate (air side) on the test fixture, and Table 1 shows the vibration spectrum levels applied to the detector. UV imaging performance was exactly the same before and after vibration, showing this new detector design is ready for flight vibrations.
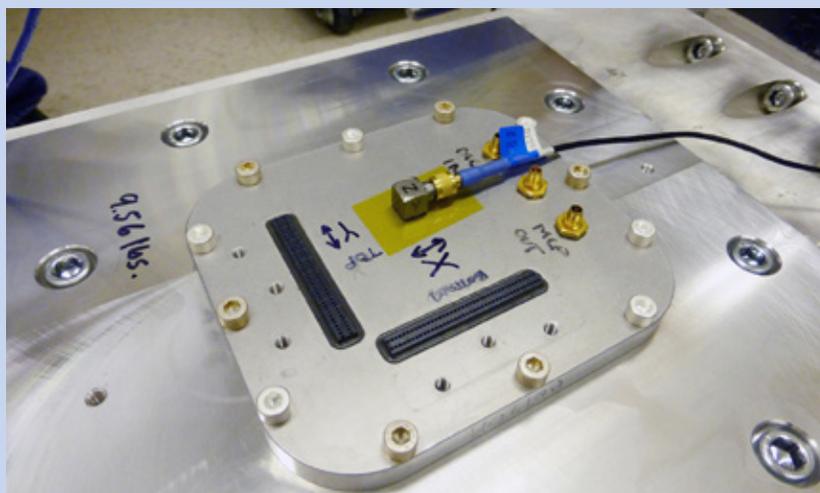
Fig. 20. *50-mm XS detector mounted on vibration table at SSL.*

Frequency (Hz)	g²/Hz	dB/Octave
20	0.026	5.97
50	0.16	0
800	0.16	-5.97
2000	0.026	–

Table 1. *Vibration frequency spectrum (14.1 g rms).*

The 100 mm × 100 mm XS Detector

Though we are not finished with the 50-mm detector development, the fact that both ASICs work gives us confidence that the electronics system will soon be completed. Last year we proposed to the NASA SAT program to continue the scaling of the XS technology to larger format size plus other improvements to increase its TRL. We plan to double the size (quadruple the area) of a XS detector to 100 mm × 100 mm active area, while demonstrating high TRL with vibration and thermal tests. Again, this larger size is not targeting a specific mission, but will demonstrate a large-format design that can be scaled easily to a similar format while reducing risk. Along with a new detector mechanical design, we plan to combine our working ASIC designs into a single ASIC (the "GRAPH" chip) using 130-nm CMOS technology, to reduce readout volume, mass, and complexity. As such, we are converting all of our sub-circuit libraries used in the 250-nm process HalfGRAPH2 to TSMC 130-nm process which we first plan to use for a HalfGRAPH3 and then combined with the CSAv3 into the GRAPH ASIC (The CSAv3 was already designed in the 130-nm process). We also plan to demonstrate the radiation hardness of the existing ASIC designs, and if insufficient, improve the radiation hardness of the new Graph ASIC.

The 100 mm × 100 mm Mechanical Design

The brazed-body design (Fig. 21) is scaled up by approximately a factor of two, having an output aperture below the MCPs of 103 mm while the active field of view is set by a 100 × 100 open mask of 25-μm thickness between the top and bottom MCPs. It is designed to hold square Photonis Inc. MCPs up to 110 mm in size. The XS anode design (Fig. 22) is also scaled to 160 strips per axis, but with a slight increase in strip pitch from the 635 μm of the 50-mm anode to 645 μm for the 100-mm anode. This results in a 103 mm × 103 mm anode with enough strips at the edges to sample the 100-mm field of view fully. The anode outputs will now be distributed on all four corners of the anode so the mechanical cutouts through the vacuum backplate can be more symmetric for increased strength. It also facilitates the electronics board layout where the GRAPH chips can be spread out on the printed circuit board. The vacuum backplate will be made of stainless steel and be weight-relieved (Fig. 23).
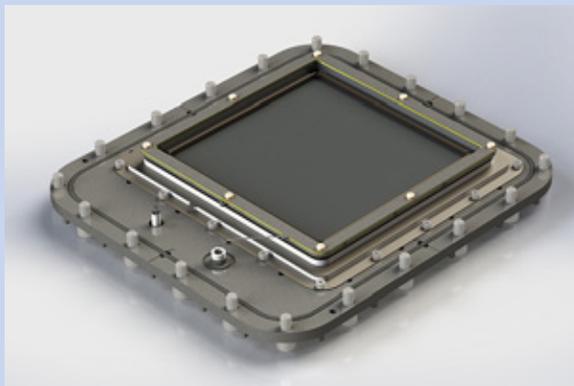
Fig. 21. *Rendering of 100-mm brazed body on hermetic backplate (vacuum-side view with two HV feedthroughs). Brazed body holds MCPs directly over XS anode (not seen).*
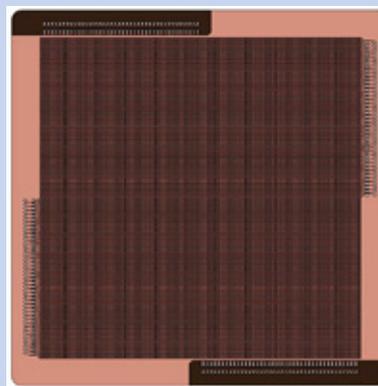
Fig. 22. *Schematic of 100-mm XS anode. Note the four distributed output connectors along the edges of the anode.*

Fig. 23. *100 mm detector stainless steel backplate (air side) showing the 4 × 80 channel anode connectors equally spaced around the anode perimeter.*

Path Forward

Once we finish the fabrication and bench testing of the new 160-channel amplifier and digitizer boards, we will couple them to the 50-mm detector and confirm the imaging performance meets or exceeds the performance demonstrated with the laboratory PXS2 electronics. We can then do a thermal and vibration test of the ASIC electronics as we did for the 50-mm detector. This effectively finishes the 50-mm development as we move to the 100-mm detector effort: new ASICs, radiation testing, new larger-format detector, and 320-channel electronics, all tested in flight-like environments. We have made a quick start with the mechanical design of the new detector and will soon follow with new electronic layouts, all taking advantage of the information gleaned from the 50-mm detector testing.

References

[1] J. Vallerga, R. Raffanti, M. Cooney, H. Cumming, G. Varner, and A. Seljak, "*Cross strip anode readouts for large format, photon counting microchannel plate detectors: developing flight qualified prototypes of the detector and electronics*," Proc. SPIE, **9144**, 91443J (2014)

[2] K. Hoadley, K. France, N. Nell, R. Kane, T.B. Schultz, M. Beasley, J.C. Green, J.R. Kulow, E. Kersgaard, and B.T. Fleming, "*The assembly, calibration, and preliminary results from the Colorado high resolution Echelle stellar spectrograph (CHESS)*," Proc. SPIE, **9144** (2014)

[3] P. Scowen et al., "*The Star Formation Observatory (SFO) mission to study cosmic origins*," Proc. SPIE, **7010**, 115 (2008)

[4] K. Sembach, M. Beasley, M. Blouke, D. Ebbets, J. Green, F. Greer, E. Jenkins, C. Joseph, R. Kimball, J. MacKenty, S. McCandliss, S. Nikzad, W. Oegerle, R. Philbrick, M. Postman, P. Scowen, O. Siegmund, H.P. Stahl, M. Ulmer, J. Vallerga, P. Warren, B. Woodgate, and R. Woodruff, "*Technology Investments to Meet the Needs of Astronomy at Ultraviolet Wavelengths in the 21st Century*," Astro2010: The Astronomy and Astrophysics Decadal Survey, Technology Development Papers, no. 54 (2009)

[5] J. Vallerga, R. Raffanti, A. Tremsin, O. Siegmund, J. McPhate, and G. Varner, "*Large-format high-spatial-resolution cross-strip readout MCP detectors for UV astronomy*," SPIE **7732** (2010)

[6] X. Michalet, R.A. Colyer, J. Antelman, O.H.W. Siegmund, A. Tremsin, J.V. Vallerga, and S. Weiss, "*Single-quantum-dot imaging with a photon-counting camera*," Current Pharmaceutical Biotechnology **10** (5), 543-558 (2009)

[7] F.B. Berendse, R.G. Cruddace, M.P. Kowalski, D.J. Yentis, W.R. Hunter, G.G. Fritz, O. Siegmund, K. Heidemann, R. Lenke, A. Seifert, and T.W. Barbee Jr., "*The joint astrophysical plasmadynamic experiment extreme ultraviolet spectrometer: resolving power*," SPIE Conference Series, **6266**, 31 (2006)

[8] H.S. Cummings, A. Seljak, G. Varner, J. Vallerga, R. Raffanti, and V. Virta, "*CSAv3, a fast, low-power and low-noise charge sensitive amplifier ASIC chip for a UV-imaging detector*," JINST, submitted (2016)

[9] K. Bechtol, S. Funk, A. Okumura, L.L. Ruckman, A. Simons, H. Tajima, J. Vandenbroucke, and G.S. Varner, "*TARGET: A multi-channel digitizer chip for very-high-energy gamma-ray telescopes*," Astroparticle Physics, **36**, 156-165 (2012)

For additional information, contact John Vallerga: jvv@ssl.berkeley.edu

Raising the Technology Readiness Level of 4.7-THz Local Oscillators

Prepared by: Qing Hu (MIT)

Summary

The 63-µm (4.744 THz) [OI] fine-structure line is an important spectral line for astrophysics observations. Despite the great potential, however, astrophysical observation of the [OI] line has rarely been performed because the 4.744-THz frequency is beyond the reach of most implemented local oscillators (LOs) in sensitive heterodyne receivers involving cryogenic mixers. In this three-year NASA Strategic Astrophysics Technology (SAT) project, we plan to raise the Technology Readiness Level (TRL) of THz quantum-cascade lasers (QCLs) for LO applications to 5 or beyond, bridging the "mid-TRL gap" between a promising enabling technology and a mission-ready component. The project started in March 2016 and is planned to conclude in February 2019.

The objective will be achieved by developing antenna-coupled 3rd-order distributed feedback (DFB) lasing structures, and in parallel, designing and growing high-performance quantum-cascade gain media with peak frequency around 4.7 THz. By end of the project, we will develop single-mode DFB lasers with frequency within 10 GHz of the target 4.744-THz line, continuous wave (cw) output power of ~5 mW, wall-plug power efficiency (WPE) of ~0.5% at an operating temperature of ~40 K, and beam patterns narrower than 10×10 degrees^2.

The project will be carried out in the PI's laboratory at MIT, with the molecular beam epitaxy (MBE) wafers provided by Dr. John Reno of Sandia National Laboratories through a user agreement.

Background

The 63-µm (4.744 THz) [OI] fine-structure line is the dominant cooling line of warm, dense, neutral atomic gas. Because of its great intensity in high UV photodissociation regions (PDRs) and shocks, this line is superior for probing regions of massive star formation and the centers of galaxies. It is a unique probe of PDRs, shock waves from stellar winds/jets, supernova explosions, and cloud-cloud collisions. These radiative and mechanical interactions shape the interstellar medium of galaxies and drives galactic evolution. The size scale of the interactions can excite [OI] emission over many parsecs. Moreover, the emission regions are often complex, with multiple energetic sources processing the environment. Spectrally resolved observations of the [OI] line with a heterodyne receiver array will allow users to disentangle this convoluted interaction and permit the study of the energy balance, physical conditions, morphology, and dynamics of these extended regions. In this way, such a receiver array will provide new and unique insights into the interrelationship of stars and gas in a wide range of galactic and extragalactic environments.

This project mainly addresses NASA's Strategic Subgoal 3D, "*Discover the origin, structure, evolution, and destiny of the universe, and search for Earth-like planets.*" It also addresses NASA's Strategic Subgoal 3A, "*Study planet Earth from space to advance scientific understanding and meet societal needs*"; and NASA's Strategic Subgoal 3C, "*Advance scientific knowledge of the origin and history of the solar system, the potential for life elsewhere, and the hazards and resources present as humans explore space.*" The development will significantly reduce the risk of several proposed suborbital projects such as the Gal/Xgal U/LDB Spectroscopic/Stratospheric THz Observatory (GUSTO), a long-duration balloon payload. The systems this project will develop include a 7-element heterodyne receiver array for the 4.744-THz [OI] line.

DFB structures are required to generate robust single-mode lasing output. Currently, 1st-order, 2nd-order, and 3rd-order DFB lasers have been demonstrated (the grating period of an nth-order DFB grating is n times the half-wavelength in the gain medium). Among these, the 3rd-order DFB structures show the greatest promise for LO applications, because of their compact size and good beam patterns. Despite the promise of 3rd-order DFB lasers, the phase mismatch limits total length to less than 1 millimeter so the beam is still quite divergent. In addition, the low extraction efficiency yields a low WPE of 0.1%. In this SAT project, we plan to further develop this promising technology by developing the following.

- Perfectly phase-matched 3rd-order DFB lasers, to generate even narrower beam patterns and higher output power levels;
- Novel antenna-coupled 3rd-order DFB structure to increase WPE; and
- Better-performance gain medium, peaked at 4.74 THz.

Objectives and Milestones

The project objectives are to develop single-mode DFB lasers with frequency within 10 GHz of the target 4.744-THz line, cw output power level greater than 5 mW, WPE ≥0.5% at an operating temperature of ~40 K, and beam patterns narrower than 10×10 degrees^2. The annual milestones are listed in Table 1.

Year	Milestones
Year 1 (3/2016 – 2/2017)	• Complete the design of perfectly phase-matched 3rd-order DFB lasers aimed for ~4.7 THz • Develop a high-yield dry-etching process using inductive-coupled plasma (ICP) to achieve clean and smooth sidewalls with high aspect ratios • Grow ~3 MBE wafers based on improved QCL designs • Fabricate devices using a combination of dry and wet etching
Year 2 (3/2017 – 2/2018)	• Continue to improve the fabrication process for higher quality and higher yield • Grow ~3 MBE wafers based on improved designs • Develop perfectly phase-matched (n_{eff} = 3.00±0.02) 3rd-order DFB with a modest value of $\alpha_m \approx 2$ cm^{-1} to ensure a robust single-mode operation and $\eta_{WPE} \approx 0.1\%$ • Design phase-matched 3rd-order DFB structures integrated with half-wave antennae
Year 3 (3/2018 – 2/2019)	• Grow ~3 MBE wafers based on improved designs • Develop phase-matched 3rd-order DFB coupled with integrated antennae with a more aggressive value of $\alpha_m \approx 10$ cm^{-1}, achieving $\eta_{WPE} \approx 0.5\%$ with ≥5 mW power at ~40 K. The phase matching should be good enough for a long device for the high output power and with beam divergence ≤10×10 degrees^2

Table 1. *Milestones of this SAT project.*

Progress and Accomplishments

Prior to the beginning date of the current SAT project, we successfully developed a single-mode 3rd-order DFB laser that lases within 3 GHz of the target 4.744-THz [OI] line [1]. Although the power level is lower than desired due to imperfect phase matching and the lack of integrated antennas (which as discussed above will be pursued in the SAT project), it is adequate to pump a single-element hot-electron bolometer (HEB) mixer. One device has been integrated with the Stratospheric Terahertz Observatory (STO-2) long-duration balloon (LDB) experiment. Unfortunately, weather conditions delayed the STO-2 launch to next year.

This SAT project started on 3/1/2016 and funding arrived at MIT a month later, so little progress can be reported at this early date. We have started the design process for perfectly phase-matched 3rd-order DFB lasers aimed for ~4.7 THz. To speed up the design process, we purchased a new, more powerful workstation with ~300 GB RAM. The three-fold increase in memory compared to our existing machines, along with more powerful CPUs will enable us to simulate more complicated, irregular 3D structures and explore a larger parameter space more quickly.

The design of novel, antenna-coupled, perfectly phase-matched 3rd-order DFB structures requires clever analysis and accurate numerical validation, which is what we have been pursuing. Fabrication of the designed structures will require a sophisticated combination of dry and wet etching, which will be pursued in the second half of Year 1 (9/1/16 – 2/28/17). The design and growth of high-performance THz gain media is also a highly challenging process, which will also be pursued in the second half of Year 1, with the aid of sophisticated numerical packages, including Schrödinger and Poisson solvers. The growth process will be carried out by Dr. John Reno of Sandia National Laboratories. Sandia has all the required equipment, and Dr. Reno has a long track record in the growth of record-setting THz gain media.

Path Forward

At this early stage, we expect our work will closely follow the annual milestones listed above.

Reference

[1] J.L. Kloosterman, D.J. Hayton, Y. Ren, W. Kao, J.N. Hovenier, J.R. Gao, T.M. Klapwijk, Q. Hu, C.K. Walker, and J.L. Reno, "*Hot electron bolometer heterodyne receiver with a 4.7-THz quantum cascade laser as a local oscillator*," Appl. Phys. Lett. **102**, 011123 (2013)

For additional information, contact Qing Hu: qhu@mit.edu

A Far-Infrared Heterodyne Array Receiver for CII and OI Mapping

Prepared by: Imran Mehdi (PI; JPL, Caltech) and Paul Goldsmith (JPL, Caltech)

Summary

This task was proposed under the 2012 Strategic Astrophysics Technology (SAT) call and was funded in January 2014 for a period of three years. Heterodyne spectroscopic instruments are the only technical possibility for obtaining velocity-resolved spectra in the far-infrared (Far-IR). Building on the Heterodyne Instrument for the Far-Infrared (HIFI) hardware developed by JPL, the focus of this task is to demonstrate a working 16-pixel heterodyne array receiver system. Most components for this system have been demonstrated, but a full 16-pixel system needs to be tested to bring this technology to Technology Readiness Level (TRL) 5. This receiver system enables science beyond HIFI for the next generation of heterodyne instruments on platforms including long-duration and ultra-long-duration balloons, and aircraft observatories such as the Stratospheric Observatory for Infrared Astronomy (SOFIA). GaAs Schottky-diode-based high-power multipliers pumped by W-band power amplifier (PA) modules, superconducting hot-electron-bolometer (HEB) -based mixers, low-power cryogenic intermediate frequency (IF) amplifiers, and a digital back-end will be integrated and demonstrated in a modularized 16-pixel receiver with TRL 5. The approach will result in a modular architecture for Far-IR array receivers for upcoming suborbital and space-based Cosmic Origins (COR) observing opportunities.

This work is carried out by a team of JPL scientists and technologists, including Imran Mehdi, Paul Goldsmith, Jon Kawamura, Jose Siles, Robert Lin, Choonsup Lee, Bruce Bumble, Adrian Tang, Rod Kim, and Jenna Kloosterman.

Background

The details of the evolution of molecular clouds and the formation of the next generation of stars out of the dust and gas in these dense regions remain mysterious. It is abundantly clear from a large number of Herschel photometric observations with the Photodetector Array Camera and Spectrometer (PACS) and the Spectral and Photometric Imaging Receiver (SPIRE) that the dust is filamentary in nature and that the filaments contain a large number of dense cores [1-4]. Many of these are self-gravitating and likely to form stars, but evidence of star formation is far from universal. What cannot be determined from the photometry is the velocity structure of these filaments, or their relationship to the various phases of the Interstellar Medium (ISM). Photometry cannot trace the processes that lead to the origin of the filaments and the likelihood that stars will form in the cores that form within them [5-8]. Velocity information is required to assess the role of turbulence and gravity in determining the kinematics of the ISM and its evolution into new stars. Not surprisingly, the best tracers of velocity are the strongest available lines – CII and OI, which are complementary in that they trace different regimes of extinction. The molecular tracer CH can be used as a surrogate for H_2, and thus trace the total gas column density. CH has a ground state that interacts strongly with magnetic fields through the Zeeman effect, making it a potential tracer of magnetic fields.

High-spectral-resolution observations will facilitate determination of velocity along the line of sight, allowing the relative motions and states of the ISM to be mapped and correlated with the observed dust structures and evolution of starless and pre-stellar cores. Simultaneous observation of combinations of lines correlated with previous photometric maps allows direct observation of the interactions between ISM phases and the connection of the gas with the dust. High resolution is required to understand the turbulence and dynamics of this interaction, as well as to de-convolve the contributions along the line of sight. Understanding how star formation proceeds in galaxies other than the Milky Way, with

different metallicities and at different times in the evolution of the universe, is currently one of the hottest topics in astronomy. However, understanding these sources will require advanced spectroscopy and better understanding of "prototypical" nearby sources in our own and nearby galaxies. The 1.9-THz fine-structure line of CII gas is a tracer of the different phases of the ISM. The ISM contains ionized gas, atomic gas, molecular gas, and dense molecular gas that is directly associated with star formation (Fig. 1). The [CII] line is the main cooling line in the ISM that is heated by newly formed stars and is therefore a tracer of star formation. A multi-pixel heterodyne receiver is ideally suited for measuring the velocity-resolved spectra of [CII] as well as other tracer gases in the ISM.

Fig. 1. *The [CII] 1.9-THz fine-structure line is a tracer of the different phases of the ISM. The chemistry and physical conditions of the ISM can be constrained by observing the velocity-resolved spectra of CII and other tracer gases present in the ISM (PDR, photo-dissociation region).*
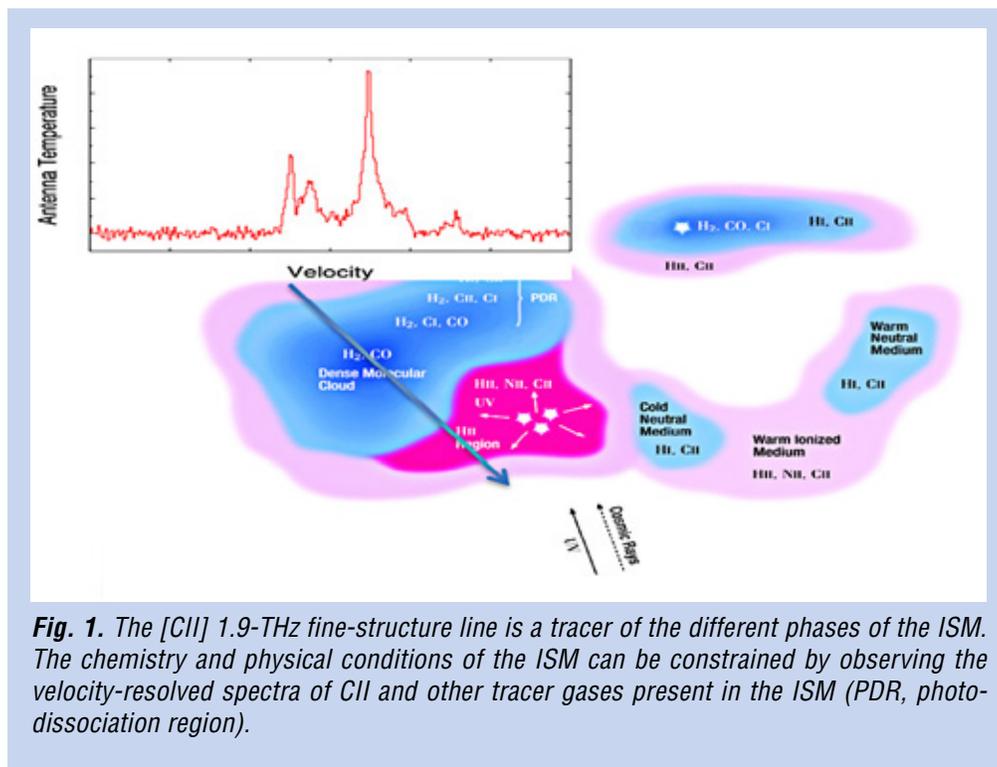
Heterodyne array receivers in the Far-IR range will be required to answer questions raised in the 2010 Decadal Survey, New Worlds, New Horizons in Astronomy and Astrophysics (NWNH) [9]. HIFI provided the first glimpse into the universe in this frequency range but had only a single pixel and the mission has now been decommissioned (after using up the cryogen). Technology being developed under this task will allow one to map large areas of the sky instantaneously and provide contextual information that is difficult to patch with single-pixel systems. At the conclusion of this work, we intend to demonstrate a 16-pixel array receiver covering 1.9-2.07 THz at TRL 5.

Objectives and Milestones

The main objective of this task is to advance heterodyne array receiver technology from TRL 4 to 5. This will be accomplished by building and characterizing a 16-pixel 1.9-THz array receiver that can enable mapping of the C+ line on platforms such as long-duration balloons and aircraft observatories. The technology is also compatible with flight instruments and can be used for future submillimeter-wave instruments for astrophysics. The proposed scheme of the 16-pixel array receiver is shown in Fig. 2 with only a single 1×4 module shown for clarity. The signal from the telescope is combined with the local oscillator (LO) signal via a diplexer, and then fed into the mixer element via a machined feed-horn. This approach provides the flexibility of quasi-optical coupling and redundancy since each mixer is pumped by a dedicated LO chain. The mixer and IF amp are cooled to cryogenic temperature (4 K) to provide higher sensitivity.
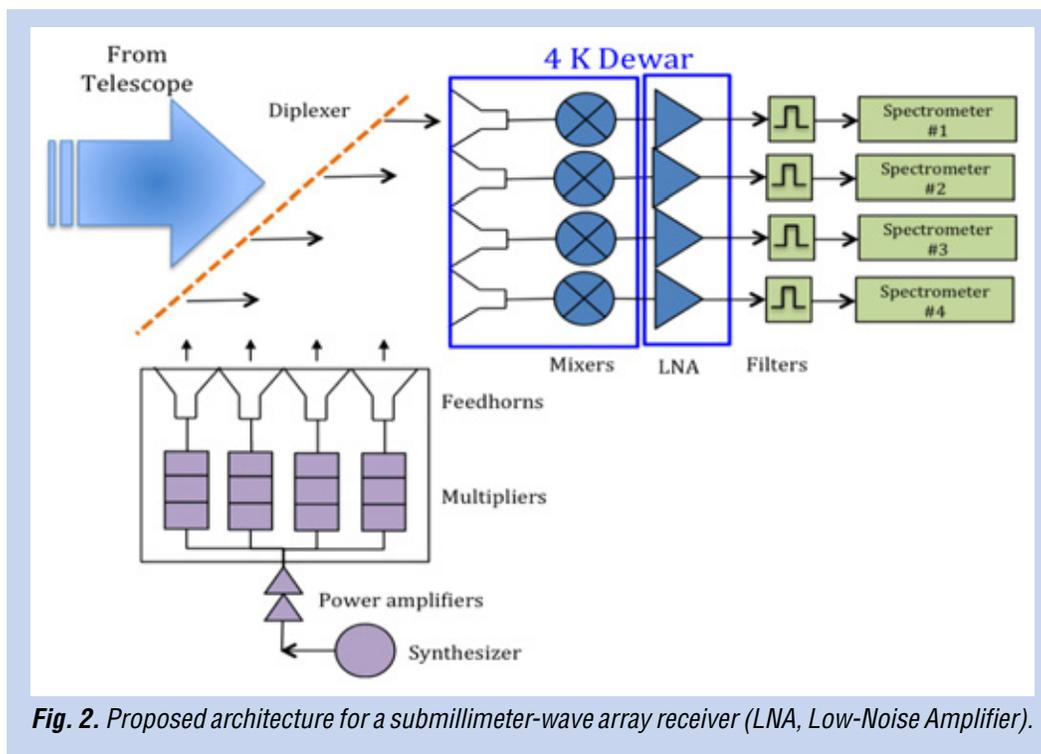
Fig. 2. *Proposed architecture for a submillimeter-wave array receiver (LNA, Low-Noise Amplifier).*

The receiver system can be divided into three subsystems, namely:

1. LO subsystem.
2. Mixer and IF amplifier subsystem.
3. Back-end subsystem.

All three subsystems have been demonstrated in single-pixel systems. This task will bring all three subsystems together to define the 'relevant environment' as a functional 16-pixel array receiver. A number of technical problems have to be addressed for building up the array receiver. The architecture of the system, especially the LO subsystem, is critical as all of the LO signals need to be phase-locked. By demonstrating the operation of this 16-pixel receiver system, we will validate it has achieved TRL 5. Further TRL advancement would then require the determination of the relevant environment (balloon, aircraft, space-borne, etc.) and environmental tests such as thermal and Radio-Frequency (RF) cycling, etc., consistent with the selected platform.

Table 1 lists the major milestones associated with the full three-year development effort. Funding for this task was made available in January 2014 and significant progress has been accomplished, as detailed in the next few sections.

Milestone	Completed by	Status
System design		
System architecture design	March 2014	Completed
Interface design	June 2014	Completed
Production of 3-D drawing	August 2014	Completed
Development of high-sensitivity HEB array		
Design of mixer devices and waveguide housing	July 2014	Completed
Fabrication of HEB devices	September 2014	Completed
Fabrication of waveguide housing	October 2014	Completed
Assembly of 4-pixel mixer array	December 2014	Completed
Fabrication of optimized HEB mixers	April 2016	Completed
Fabrication of 16-pixel block	June 2016	In progress
Assembly and testing of 16-pixel mixers	August 2016	
Development of LO subsystem		
Design of first-stage tripler	March 2014	Completed
Design of second-stage tripler	May 2014	Completed
Procurement of power amps	October 2014	Completed
Fabrication of multiplier chips	December 2014	Completed
Fabrication of multiplier blocks	March 2015	Completed
Assembly of 4-pixel prototype	July 2015	Completed
Design of 16-pixel module	December 2015	Completed
Fabrication of 16-pixel block	February 2016	Completed
Integration of 16-pixel LO subsystem	April 2016	Completed
Characterization of 16-pixel LO subsystem	May 2016	In progress
Back-end electronics		
Design of CMOS-based back-end spectrometer	June 2015	Completed
Prototype assembly with 4-pixel readout	July 2015	Completed
Spectrometer integration with mixer array	August 2015	Completed
Detailed characterization of CMOS back-end	December 2015	Completed
System integration and validation		
Assembly of 4-pixel receiver	September 2015	Completed
Test and validation of 4-pixel receiver	November 2015	Completed
Assembly of 16-pixel receiver	September 2016	
Test and validation of 16-pixel receiver	December 2016	

Table 1. *Most milestones related to this task have been achieved.*

Progress and Accomplishments

LO subsystem

With the successful demonstration of a 4-pixel LO subsystem that delivered sufficient power last year, the focus this year has been to develop a compact scheme that can be modularized to 16 pixels. This required using a combination of three triplers and the LO block (diagram in Fig. 3). Note that this particular system is based on stacking multiple metallic plates to achieve multi-pixel functionality. The scheme utilizes a 4-way power splitter (not shown in the block diagram as it goes into the page) that feeds the four W-band amplifiers that each drive 4 pixels at 1.9 THz.
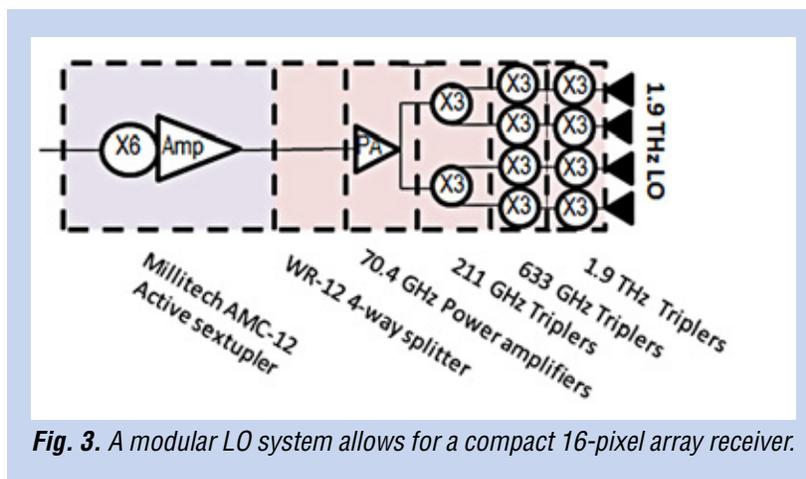
Fig. 3. *A modular LO system allows for a compact 16-pixel array receiver.*

A major issue with the packaging of the compact array is routing the device bias line. A novel solution has been proposed. In this approach the DC bias line is made on a thin piece of GaAs suspended across the waveguide channel (Fig. 4). Three-dimentional simulations suggest that this solution should work without degrading multiplier performance.
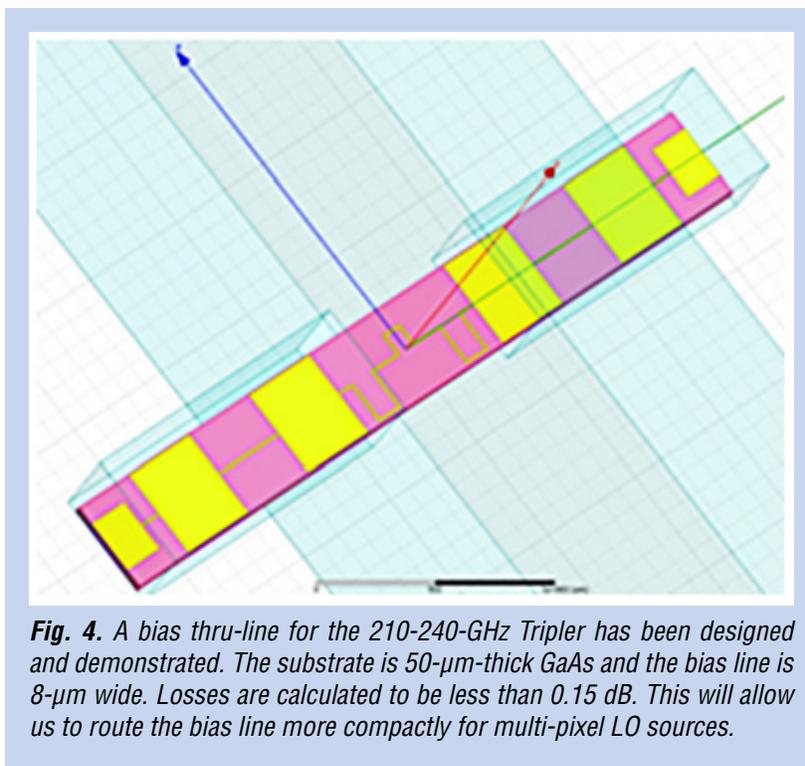
Fig. 4. *A bias thru-line for the 210-240-GHz Tripler has been designed and demonstrated. The substrate is 50-µm-thick GaAs and the bias line is 8-µm wide. Losses are calculated to be less than 0.15 dB. This will allow us to route the bias line more compactly for multi-pixel LO sources.*

LO circuits that can handle large amounts of input power are needed to make multi-pixel receivers. To this end, we designed a high-power first-stage multiplier chip that combines four chips into one structure. This resulted in world-record output-power levels at ~200 GHz. This will be used as the first-stage tripler for the 16-pixel source. The fabricated chip, along with a packaging schematic, and the measured results are shown in Fig. 5. Figures 6 and 7 show the fabricated chip and the measured response from the last two triplers respectively.
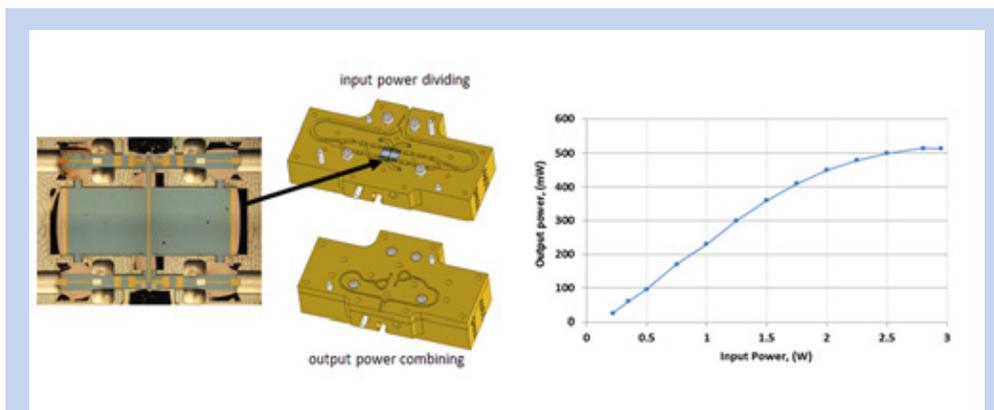
Fig. 5. *Performance of the 4-way-power-combined first-stage tripler. Due to the increased input power levels available at 70-75 GHz, this single chip can produce over 500 mW at 211 GHz, a new world record.*
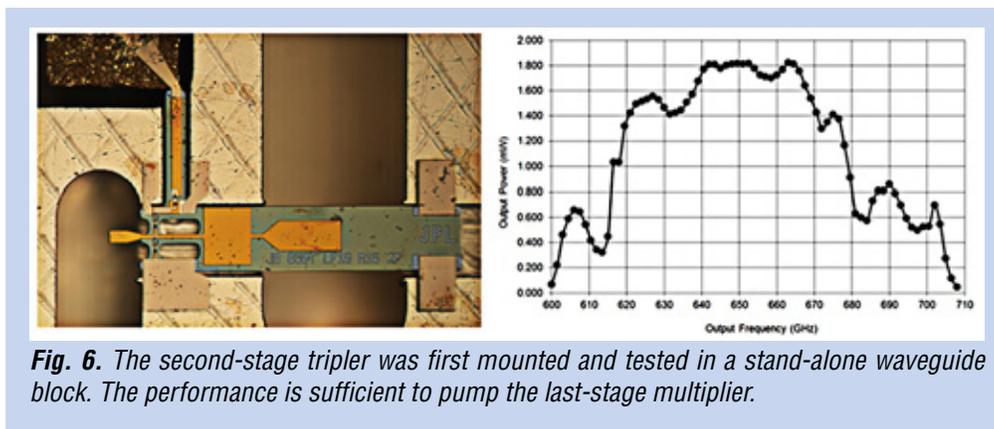
Fig. 6. *The second-stage tripler was first mounted and tested in a stand-alone waveguide block. The performance is sufficient to pump the last-stage multiplier.*
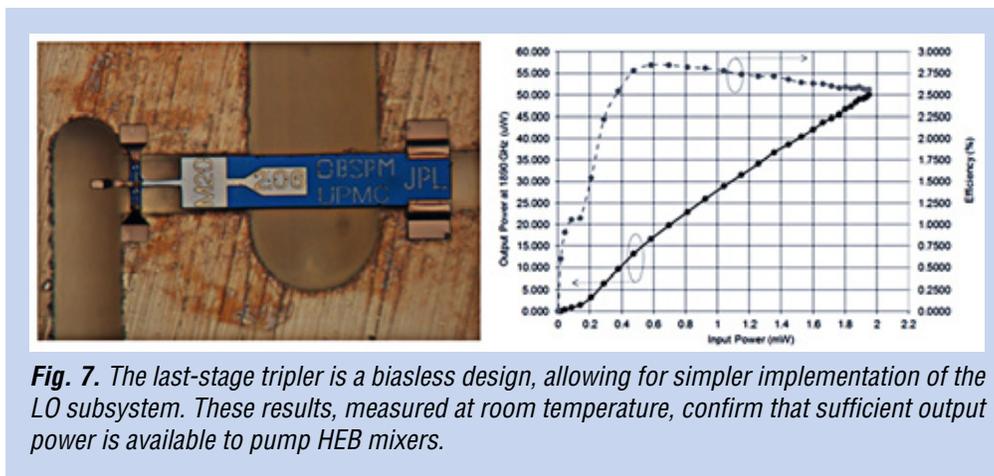
Fig. 7. *The last-stage tripler is a biasless design, allowing for simpler implementation of the LO subsystem. These results, measured at room temperature, confirm that sufficient output power is available to pump HEB mixers.*

A first-ever 16-pixel LO system is currently being built. A novel layer-by-layer approach has been conceived that allows us to make a compact 16-pixel LO source, based on the 2×3×3 configuration. The waveguide blocks are currently being fabricated. The last stage of the source is the most complicated. However, we are glad to report that it has been successfully fabricated and the completed blocks are shown in Fig. 8. The left panel shows the interface where the second-stage multiplier will feed the last-stage tripler. The right panel shows the five layers of copper that have been machined to house the last-stage tripler, with the 16 diagonal horns clearly visible. In the next reporting period these blocks will be populated with multiplier devices and then tested.

Waveguide interface for last stage tripler

16 horns for output beams

Fig. 8. *Machined 16-pixel block that will house the last-stage 1.9-THz multiplier.* Left: *Input side of the waveguide block, which will interface with the second-stage tripler.* Right: *Output side of the block with the 16 diagonal horns clearly visible.*
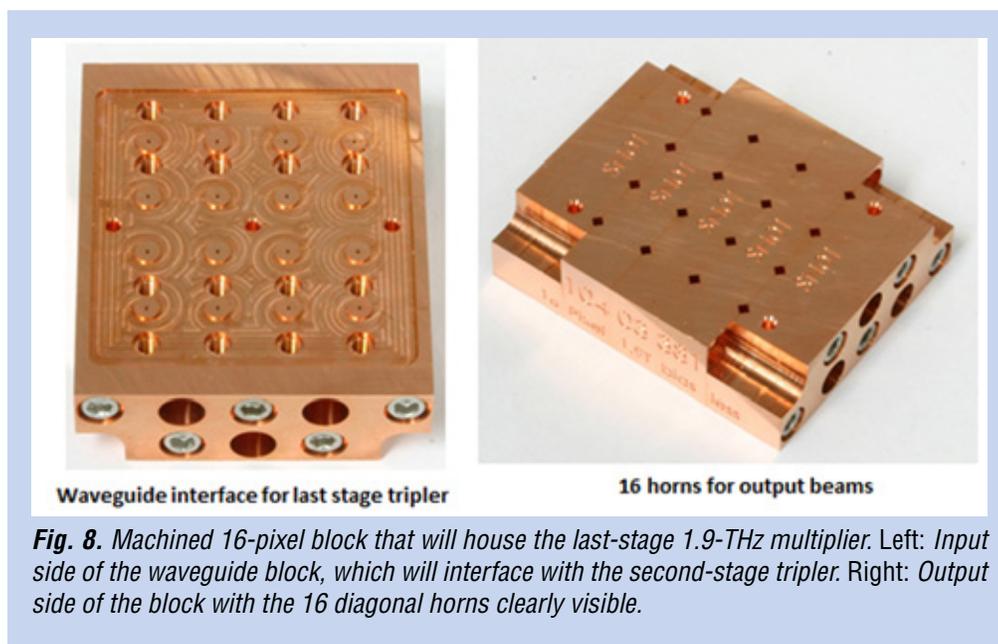
Hot Electron Bolometer mixer devices

HEB mixers provide one of the most sensitive detectors in this frequency range. This task enabled the fabrication of a number of HEB devices in JPL's Micro-Devices Laboratory. The chips are based on NbN junctions that have been shown to work very well in the THz range. The HEB mixers for this task were packaged in specially fabricated waveguide housings. We believe that by using waveguide-based structures we can provide a more controlled matching environment for the device, thus reducing out-of-band noise. Moreover, the waveguide approach allows us to implement more sophisticated circuit topologies such as balanced mixers, and provides a relatively straight-forward path toward building arrays. The 4-pixel block is shown in Fig. 9. A 5-mm pixel-to-pixel spacing was selected as a compromise between making a dense array and allowing acceptable assembly tolerances. The 4-pixel waveguide block is about 10 mm × 30 mm. A 16-pixel block is currently being machined and will be ready for characterization in late 2016.
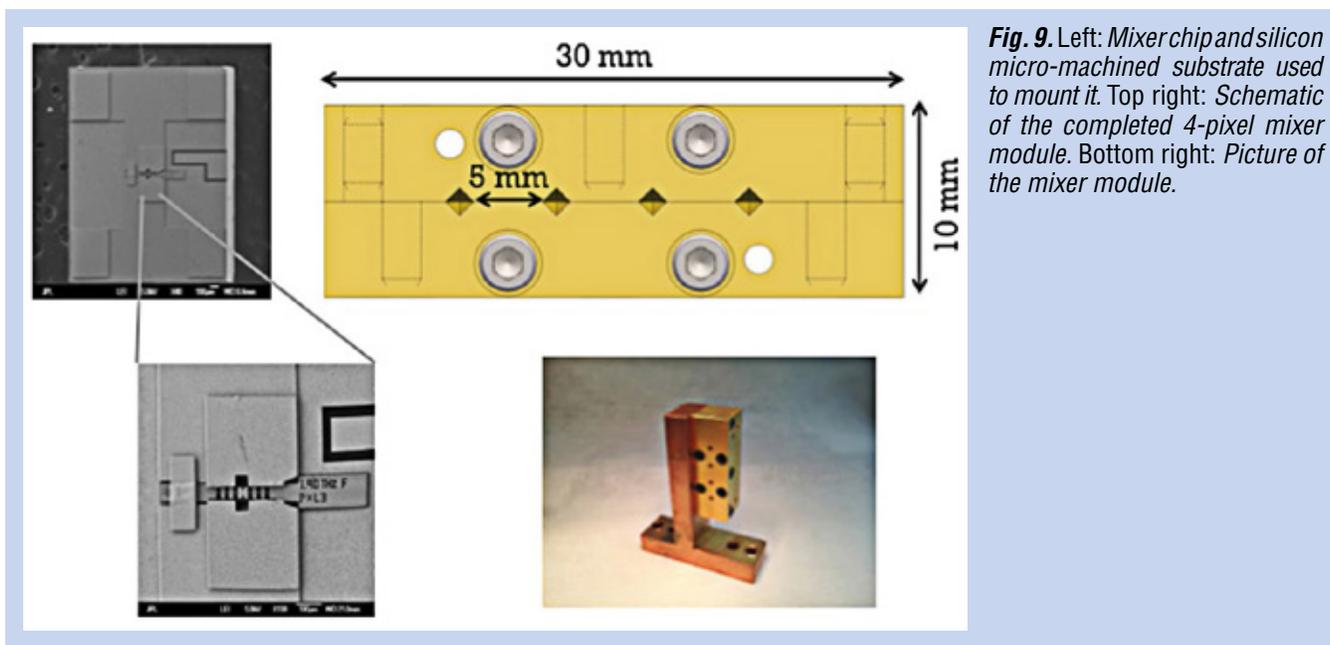
Fig. 9. Left: *Mixer chip and silicon micro-machined substrate used to mount it.* Top right: *Schematic of the completed 4-pixel mixer module.* Bottom right: *Picture of the mixer module.*

Receiver Back-End (CMOS 4-Channel System-on-Chip Spectrometer Processor)

The system-on-chip (SoC) -based spectrometer processor module for the 16-pixel sub-millimeter spectrometer is driven by four custom CMOS chips (four pixels per module), developed in fiscal year (FY) 2015 (Fig. 10). The focus this year was to package this board into a more robust package (Fig. 11) that can be used for the receiver test. A Rhapsody Pi microcontroller was used to interface with the CMOS board, and software was developed to enable reading the spectra from the CMOS back-end.
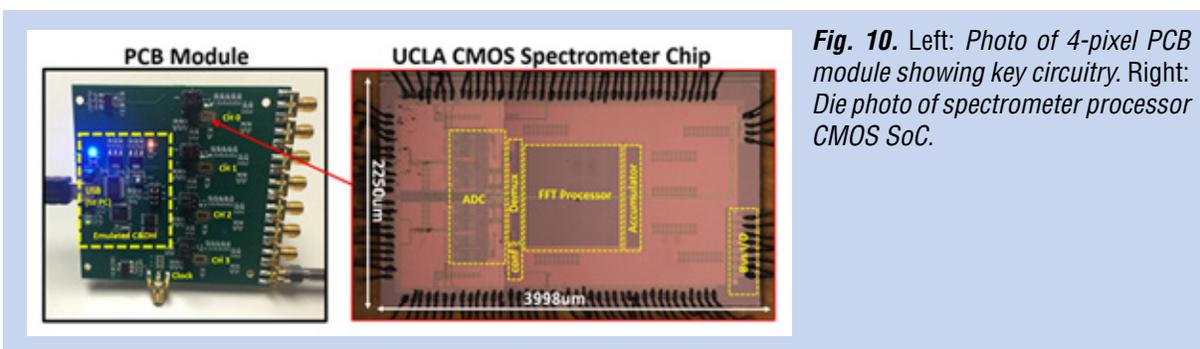
Fig. 10. Left: *Photo of 4-pixel PCB module showing key circuitry.* Right: *Die photo of spectrometer processor CMOS SoC.*
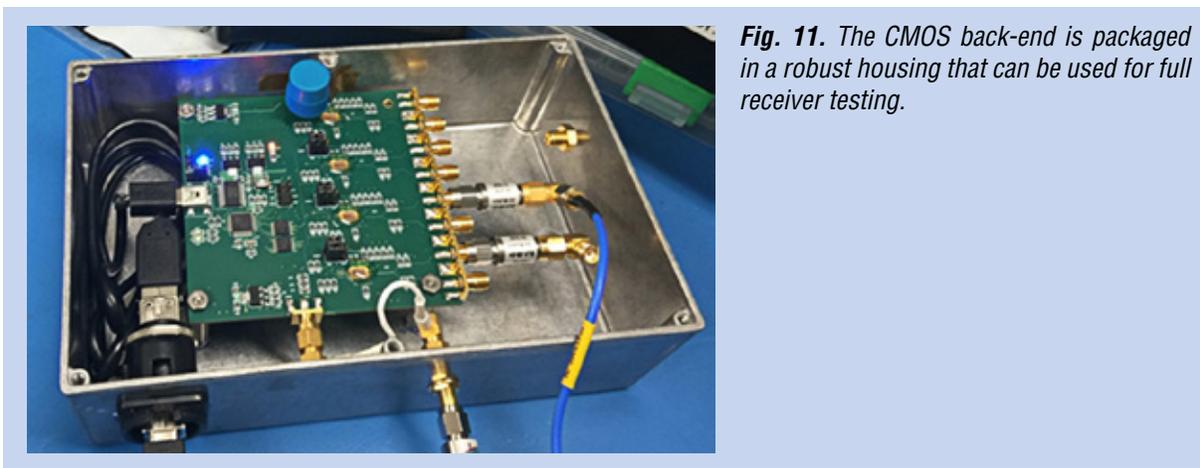
Fig. 11. *The CMOS back-end is packaged in a robust housing that can be used for full receiver testing.*

Multi-Pixel Receiver Integration and Testing

With the major subsystems of the receiver completed, the receiver integration and characterization work has begun, using an existing cryogenic setup. While minor adjustments for bias and Field of View (FOV) have already been made, the current configuration of the cryostat allows testing of two pixels at a time. The schematic of the receiver testing setup is shown in Fig. 12.
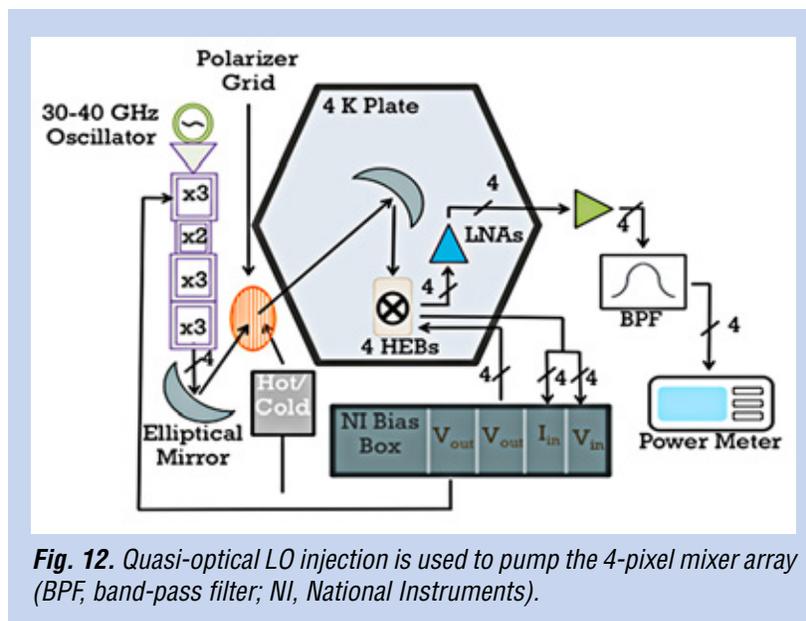
Fig. 12. *Quasi-optical LO injection is used to pump the 4-pixel mixer array (BPF, band-pass filter; NI, National Instruments).*

The 4-pixel LO chain, described above, was characterized for output power at room temperature, with the measured results shown in Fig. 13. While three of the four pixels produce more power, all four provided sufficient power to pump the HEB mixers. The best pixel puts out more than 30 microwatts at 1900 GHz.
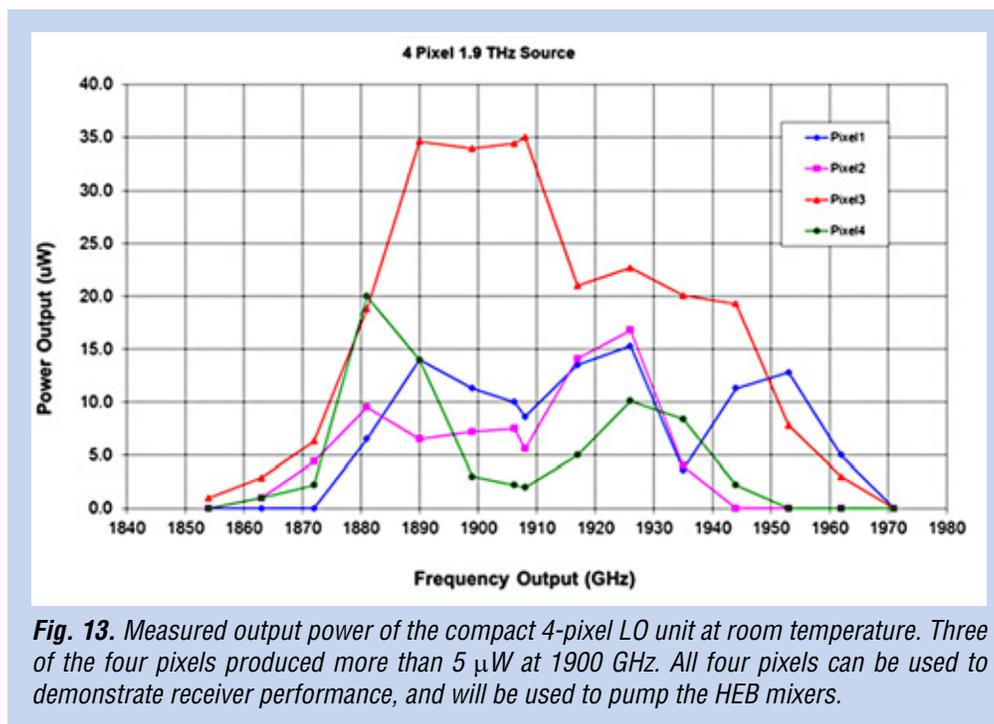
Fig. 13. *Measured output power of the compact 4-pixel LO unit at room temperature. Three of the four pixels produced more than 5 μW at 1900 GHz. All four pixels can be used to demonstrate receiver performance, and will be used to pump the HEB mixers.*

The LO signals are focused using an elliptical mirror into the cryostat which holds the mixer block. The LO chain and the mirror can be manipulated to achieve proper alignment. The measured current-voltage (IV) of the four pixels is shown in Fig. 14 along with the measured noise temperature. Double side-band (DSB) noise temperature of 900 to 1800 K was measured. The lower number compares well with state-of-the-art sensitivities that have been measured at these frequencies. The higher number is most likely due to a non-optimum mixer chip and can be corrected by using the appropriate chip.
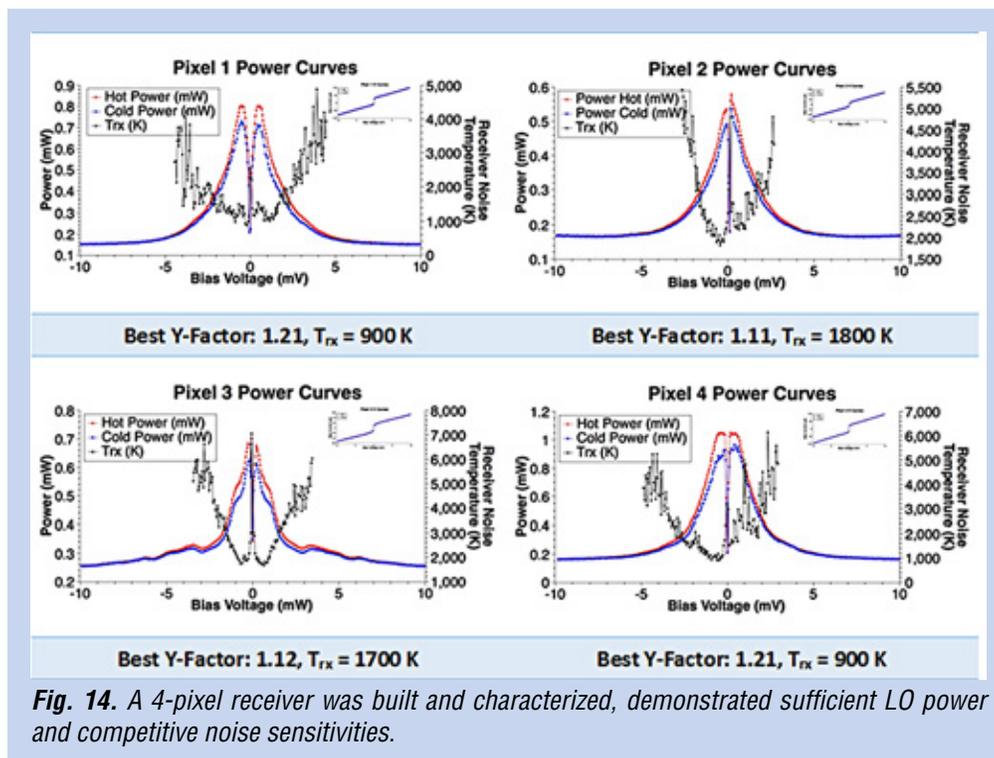
Fig. 14. *A 4-pixel receiver was built and characterized, demonstrated sufficient LO power and competitive noise sensitivities.*

Path Forward

Sixteen-pixel hardware for the LO was fabricated and is currently being assembled for testing. The 16-pixel mixer hardware should be completed shortly. Once all the hardware is available, the main focus of the task will be to characterize a fully operational sub-millimeter-wave array receiver.

Acknowledgement

References

[1] S. Molinari et al., "*Clouds filaments, and protostars: The Herschel Hi-GAL Milky Way*," Astron. & Astrophys., **518**, L100 (2010)

[2] Ph. Andre et al., "*From filamentary clouds to prestellar cores to the stellar IMF: Initial highlights from the Herschel Gould Belt Survey*," Astron. & Astrophys., **518**, L102 (2010)

[3] A. Menshchikov et al., "*Filamentary structures and compact objects in the Aquila and Polaris clouds observed by Herschel*," Astron. & Astrophys., **518**, L103 (2010)

[4] V. Konyves et al., "*The Aquila prestellar core population revealed by Herschel*," Astron. & Astrophys., **518**, L106 (2010)

[5] P. Padoan, M. Juvela, A.A. Goodman, and A. Nordlund, "*The turbulent shock origin of proto-stellar cores*," Astrophys. J., **553**, 227 (2001)

[6] T. Nagai, S.-I. Inutsuka, and S.M. Miyama, "*An origin of filamentary structure in molecular clouds*," Astrophys. J., **506**, 306 (1998)

[7] P. Ocvirk, C. Pichon, and R. Teyssier, "*Bimodal gas accretion in the Horison-MareNostrum galaxy formation simulation*," Mon. Not. R. Astron. Soc., **390**, 1326 (2008)

[8] F. Nakamura and Z.-Y. Li, "*Magnetically regulated star formation in three dimensions: the case of the Taurus molecular cloud complex*," Astrophys. J., **687**, 354 (2008)

[9] "*New Worlds, New Horizons in Astronomy and Astrophysics*," Decadal Survey report from the Committee for a Decadal Survey of Astronomy and Astrophysics, National Research Council, ISBN 0-309-15800-1, available at http://www.nap.edu/catalog/12951.html (2010)

For additional information, contact Imran Mehdi: Imran.mehdi@jpl.nasa.gov

Kinetic Inductance Detector Arrays for Far-IR Astrophysics

Prepared by: Jonas Zmuidzinas (PI; Caltech); Goutam Chattopadhyay, Peter Day, C. Darren Dowell, and Rick Leduc, (JPL); Pradeep Bhupathi, Matt Hollister, and Attila Kovacs (Caltech); and Chris McKenney (NIST)

Summary

This project was initiated in 2013 as a two-year project and has now been extended into a fourth year (2016) at no additional cost. The project focuses on the development of sensitive detector arrays for far-infrared (Far-IR; λ = 50-500 μm) astrophysics. The detectors must be exquisitely sensitive, capable of measuring power as low as 10^{-16} to 10^{-19} W in a one-second measurement, known as the noise-equivalent power (NEP). Not surprisingly, the detectors operate at very low temperatures, typically in the range 0.1 - 0.3 K. The evolution of Far-IR detector technology has been very rapid. In the early 1990s, Far-IR instruments typically contained only a few hand-built detectors. The Spectral and Photometric Imaging Receiver (SPIRE) instrument for the Herschel Space Observatory (HSO), developed in the early 2000s, had several hundred detectors. The largest ground-based instruments, Submillimetre Common-User Bolometer Array-2 (SCUBA-2) on the James Clerk Maxwell Telescope (JCMT), and the Atacama Pathfinder EXperiment (APEX) Microwave Kinetic Inductance Detector (A-MKID) camera, now contain 10,000 and 20,000 pixels, respectively. However, Far-IR arrays remain very expensive, difficult to produce and operate, and a significant impediment for future development of the field.

The goal of our project is to develop and demonstrate Far-IR detector arrays using kinetic inductance detectors (KIDs) [1]. The ultimate aim is to provide inexpensive, high-performance, large-format arrays suitable for use on a wide range of platforms including airborne, balloon-borne, and space-borne telescopes. Specific project goals include laboratory demonstrations of arrays targeting the sensitivity and optical power levels appropriate for several of these platforms, along with an end-to-end, full-system demonstration using a ground-based telescope. Ground-based demonstrations of imaging detectors operating at 350 and 850 μm were performed in a succession of observing runs at the Caltech Submillimeter Observatory (CSO) starting in 2013; the most recent was in May 2015, shortly before the CSO was permanently shut down. The CSO KIDs are made from titanium nitride (TiN), an excellent choice given the relatively high photon background for ground-based and airborne imagers. Aluminum KIDs are likely a better choice for low-background space applications; within the last year, further work on aluminum devices led to process improvements for higher yield, followed by testing with a cryogenic blackbody source. Finally, as part of the system design of KID instruments, a chirped-readout approach achieved "first light" testing at CSO in May 2015, where it was compared with the more traditional fixed-tone readout.

Background

The universe shines very brightly at Far-IR wavelengths. In fact, about half the photon energy ever produced by stars and galaxies over the history of the universe falls in the Far-IR band. This remarkable fact was originally predicted by Frank Low and Wallace Tucker in 1968, based on a handful of early Far-IR observations of galaxies. It was first demonstrated observationally in 1996 by Jean-Loup Puget and collaborators, working with data collected by the NASA Cosmic Background Explorer (COBE) satellite. To put it differently, there is just as much light in the Far-IR as there is in the visible/Near-Infrared (Near-IR) band. This simple fact alone makes it imperative to study the universe in the Far-IR. Fortunately, the technology to image and survey the universe in this band is now becoming available.

Fundamentally, the high luminosity of the universe in the Far-IR is intimately tied to the process of star formation. Star formation occurs deep inside thick clouds of interstellar dust and gas. The dust provides a shield against radiation that would otherwise heat and ionize the gas, and allows the gas to form molecules, cool to temperatures below 10 K, and become quite dense. Gravitational collapse of these dense cores then leads to star formation, but the radiation produced by a newly formed star cannot escape its dusty cocoon. Instead, the stellar radiation is absorbed by the surrounding dust and gas, heating this material to temperatures around 50 - 100 K and causing it to glow brightly in the Far-IR. The Far-IR radiation readily escapes these thick clouds, providing a view of sites of recent star formation, sites that are often entirely invisible in the optical/Near-IR. Such Far-IR studies can be performed locally by imaging sites of star formation in the Milky Way. In addition, the Infrared Astronomical Satellite (IRAS) survey showed that many galaxies are bright in the Far-IR. Indeed, galaxy-galaxy collisions are believed to be a key factor in the evolution of galaxies, and such collisions often trigger giant bursts of star formation that provide a large boost to the Far-IR luminosity. The HSO provides a recent example of the importance of Far-IR observations for studying star formation both near and far, in our galaxy and across cosmic time. Indeed, many of the brightest Far-IR galaxies found by Herschel are undetectable by the Hubble Space Telescope (HST) and the largest ground-based optical telescopes.

The Decadal Survey reports provide a long history of strong support for Far-IR astrophysics, starting with the 1982 Field Report recommendation for the construction of a 10-20-m space-borne Far-IR telescope, known as the Large Deployable Reflector (LDR). As with many Decadal recommendations, this project was never built, due to budget issues, but the recommendation did stimulate NASA technology investments and continued support from Decadal panels that ultimately led to NASA's participation in HSO, launched by the European Space Agency (ESA) in 2009. NASA is again considering its future in this field: a "Far-Infrared Surveyor" mission was described in the 2013 report chartered by the Astrophysics Division, titled "Enduring Quests, Daring Visions: NASA Astrophysics in the Next Three Decades." Following a June 2015 NASA workshop held in Pasadena CA, which again highlighted the abundant scientific opportunities in the Far-IR, NASA is now performing a study for a flagship-class Far-IR mission in preparation for the 2020 Decadal Survey.

Far-IR detector arrays have evolved rapidly over the past two decades. In the early 1990s, Far-IR detectors were built laboriously, individually, by hand. By circa 2000, several instruments were fielded using lithographically fabricated arrays with a few hundred detectors in which the detectors were read out with individual amplifiers and wiring. The development of superconducting detectors, coupled with the invention of multiplexed readout schemes, propelled the field to its present level of arrays with up to ~1000 pixels. A good example is the ground-based SCUBA-2 instrument, which contains eight array tiles, each with 1280 detectors, for a total of ~10^4 pixels. However, the transition-edge sensor (TES)/Superconducting Quantum Interference Device (SQUID) technology used for SCUBA-2, while flexible and adaptable to broad range of requirements, is expensive and difficult to produce. Indeed, detectors now often constitute the largest single budget item for new Far-IR instruments, and impose a bottleneck on future advances. The goal of our project is to show that the simpler, lower-cost KID technology [1, 2] can meet the needs of a similarly broad range of applications, ranging from ground-based to space instruments. KID technology was proposed by our group in 1999 and, with support from NASA, has shown very rapid development over the past decade. However, instrument groups have often been hesitant to adopt the technology due to its lower level of maturity. Our project addresses this issue head-on using full-system, end-to-end demonstrations on a ground-based telescope, as well as laboratory testing to explore a range of sensitivity levels.

Objectives and Milestones

The primary goals of our project are to perform laboratory demonstrations of KID arrays suitable for airborne, balloon, and space platforms; and to perform an end-to-end, full-system demonstration of an instrument on a ground-based telescope. The key performance specifications are shown in Table 1.

Platform	Optical Power	NEP_{phot} (W / Hz$^{1/2}$)	NEP_{goal} (W / Hz$^{1/2}$)	TRL goal
Space (90 μm)	0.12 fW	7.3×10^{-19}	5×10^{-19}	$3 \rightarrow 4$
Balloon (350 μm)	18 pW	1.5×10^{-16}	7×10^{-17}	$3 \rightarrow 4$
SOFIA (90 μm)	26 pW	3.4×10^{-16}	1.7×10^{-16}	$3 \rightarrow 4$
Ground (350 μm)	100 pW	6.5×10^{-16}	3.3×10^{-16}	$3 \rightarrow 6$

Table 1. *Performance specifications for Far-IR continuum detectors relevant to this project.*

Our approximate schedule (check marks indicate achieved milestones) for these tasks is as follows.

- Space – laboratory demonstration:
  - ✓ April 2014 – Design, fabrication, and test effort leading to successful operation of a suitable device in darkness;
  - ✓ Second half of 2014 – Process improvements; and
  - ✓ First half of 2015 – Testing of device with small, known optical load.
- Ground – on-sky demonstration with CSO telescope:
  - ✓ April 2013 – End-to-end system 350-μm demonstration, but with some limitations (single polarization, sensitivity somewhat worse than background limit); and
  - ✓ August 2014 and May 2015 – Additional demonstrations (dual polarization, better sensitivity, on-sky test of chirped readout, 850-μm detection).
- Balloon – laboratory demonstration:
  - ✓ Previous iterations of tested devices designed primarily for ground-based work have satisfied this performance requirement.
- Stratospheric Observatory for Infrared Astronomy (SOFIA) – laboratory demonstration:
  - ▪ First half of 2015 – Test of efficiency and sensitivity for λ = 90 μm operation (not achieved).

Over the course of the project, our effort focused on the highest and lowest background situations.

Progress and Accomplishments

Titanium nitride KIDs targeting NEP ≈ 10^{-16} W/Hz$^{1/2}$

The first on-sky testing of JPL-produced Far-IR (λ = 350 μm) KIDs was performed in April 2013, four months after the start of our project. These detectors were made from TiN, which has convenient properties for the Far-IR [3]. Overall, this end-to-end system demonstration at CSO was very successful, and images of astrophysical sources were obtained with quality equivalent to those produced by facility Far-IR imagers. However, the detector design had not been optimized prior to the observing run, resulting in a sensitivity penalty of roughly 10× relative to the photon-background limit achieved by the CSO's 350-μm facility camera, the Submillimeter High-Angular Resolution Camera (SHARC) II.

In the following year (May 2013 – July 2014), work on higher-background (NEP ≈ 10^{-16} W/Hz$^{1/2}$) detectors focused on design and implementation of dual-polarization response (Fig. 1), introduction of a micro-lens array to the detector package for radiation concentration, and tuning of the Ti vs. N ratio and hence critical superconducting temperature to achieve best sensitivity. Further improvements were made to the method of coupling the KIDs to the readout line, and to the fabrication process. Three methods for silicon micro-lens array fabrication were pursued in the last 12 months – laser machining by commercial source (Veldlaser), gradient-index lenses designed and micro-machined by our own team, and anisotropic etching using a mask of hemispherical photo-resist bumps. A Parylene film applied by a commercial vendor is used for anti-reflection coating. The laser-machined and gradient-index lenses have been tested optically with the KID arrays and shown to work well in concentrating the radiation and improving responsivity.
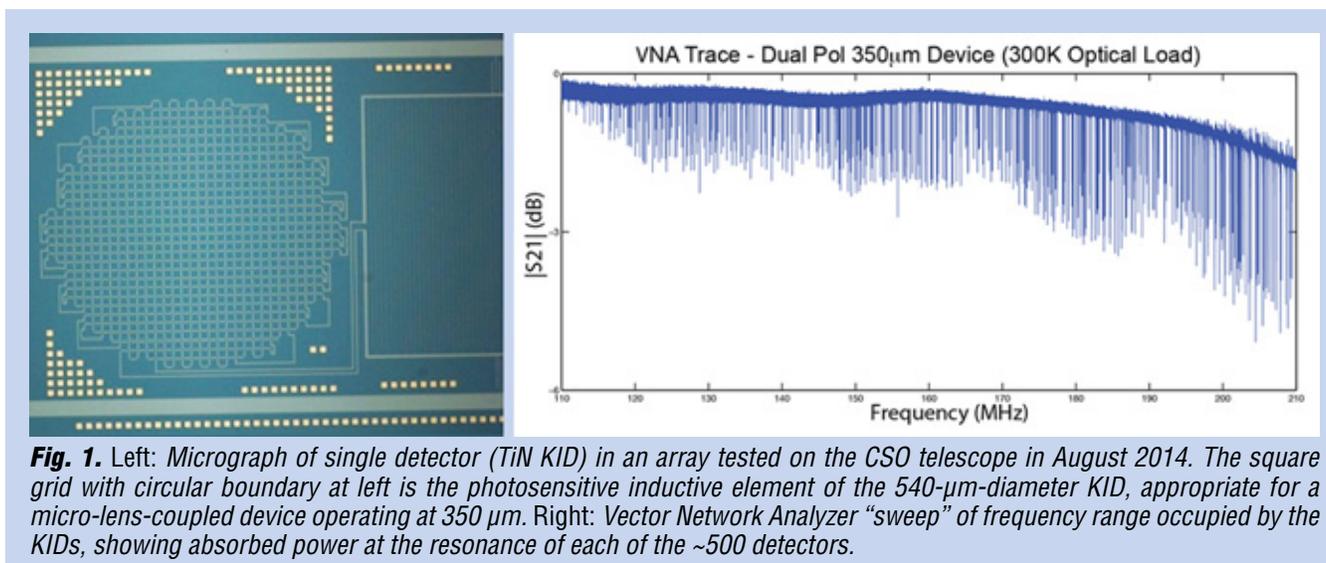
Fig. 1. Left: *Micrograph of single detector (TiN KID) in an array tested on the CSO telescope in August 2014. The square grid with circular boundary at left is the photosensitive inductive element of the 540-µm-diameter KID, appropriate for a micro-lens-coupled device operating at 350 µm.* Right: *Vector Network Analyzer "sweep" of frequency range occupied by the KIDs, showing absorbed power at the resonance of each of the ~500 detectors.*

As a result of detector design improvements, the TiN detectors are background-limited at 350 µm for 100 to 300 K loads in the lab. An array of 488 such detectors with the Veldlaser micro-lenses was brought to CSO for testing and system demonstration in August 2014. The instrument showed a substantial (~3×) sensitivity improvement relative to the April 2013 run, but did not yet match the performance achieved with SHARC II.

A subsequent (September 2014 – April 2015) intensive testing campaign in the laboratory indicated an inadequate baffling of stray light, a problem that had also been encountered during the development of SHARC II. The optical filtering was modified to more closely match the scheme adopted for SHARC II, and laboratory testing of this revised scheme indicated a substantial sensitivity improvement, about what was needed to close the remaining gap relative to SHARC II. The instrument was brought to the CSO for a third time in May 2015 for testing. Although the instrument was installed and operated successfully, the weather was not favorable, and the 350-µm atmospheric opacity was too high during the run to allow useful observing. It was thus impossible to adequately evaluate the sensitivity of the instrument. Unfortunately, the closure of the CSO prevented us from making any further progress in this direction.

Since reaching a background-limited full-system sensitivity at 350 µm for the CSO ground-based instrument was considered our project's top priority, and given the challenges faced in reaching that goal, we focused our efforts on that task rather than attempting additional demonstrations of detectors suitable for balloon instruments at 350 µm or SOFIA instruments at 90 µm. However, TiN-based MKID detector arrays [4] will be used on the NASA-funded BLAST-TNG Far-IR balloon payload, with flights scheduled for 2017. An alumnus of our SAT project, Chris McKenney, now works at NIST Boulder and is a key contributor to this effort.

Aluminum KIDs targeting NEP ≈ 10^{-18} W/Hz$^{1/2}$

While TiN KIDs cover a broad wavelength range for detectors operating with > pW background power, aluminum KIDs are more appropriate for ~ fW backgrounds. In general, the volume of a KID optimized for NEP scales with background power [5]. At the small volume needed for space backgrounds, the much lower resistance of aluminum makes it easier to satisfy the condition for efficient radiation absorption for a device with convenient surface area.

Our work on Al KIDs for the Far-IR began in the first year of this project. We fabricated KID arrays (Fig. 2) using aluminum absorbers with an absorber line-width of 150 nm on a 15-µm pitch and a volume of 38 µm³. The 20-nm-thick aluminum has a per square resistance of 1 ohm, resulting in an effective absorber resistance of 100 ohms, appropriate for matching to radiation through silicon.

Fig. 2. Left: *Micrograph showing a section of the small-volume Al absorber. Lines as narrow as 150 nm were fabricated using the deep UV stepper lithography system at JPL's Micro-devices Laboratory. Narrower lines were fabricated using e-beam lithography.* Right: *A section of an array of aluminum KIDs with 150-nm line-width. The pixel design is similar to the TiN design shown in Fig. 1; the major difference is a much smaller area-filling factor for the Al absorber, due to the much lower resistivity of aluminum vs. TiN (IDC, interdigitated capacitor).*

We have two lithographic tools we can use to achieve these 150-nm wide lines, the Canon FPA3000-EX6 5× deep ultraviolet projection lithography stepper, and the JEOL JBX-9300 FS electron-beam lithography system. The e-beam tool can easily achieve these dimensions, but the patterns are serially written and the process is slow and costly. The stepper exposes in a parallel fashion one field at a time and is faster, but is limited in resolution and depth of focus, requiring significant lithographic optimization to achieve these dimensions. We have produced KIDs using both approaches.

Array sensitivity (Fig. 3) was estimated using thermal calibration. In this method, the array base temperature is swept, and the frequency response to the thermally generated quasi-particle population is measured to derive the response to input optical power. In order to convert from optical power to quasi-particle density changes, the recombination time needs to be known. However, this is not straightforward to infer from response time measurements when the resonance frequency is in the ~300 MHz range, because the resonator response time is normally slower than the quasi-particle recombination time. To estimate detector sensitivity, we have assumed a recombination time of 1 ms, which has been previously measured for aluminum. The derived sensitivity of ~2×10^{-19} W/Hz$^{1/2}$ (Fig. 3) is very encouraging.

Fig. 3. Left: *Calibration of detector sensitivity using thermal measurements. The resonance frequency is measured vs. bath temperature (inset). The response of the detector to absorbed power is inferred from the measured frequency shift vs. thermal quasi-particle density.* Right: *Measured frequency noise spectrum expressed in NEP units using the thermal response data and assuming a quasi-particle lifetime of 1 ms.*

In our experience, high-yield fabrication of aluminum detector arrays is considerably more difficult than for TiN; this is likely because aluminum is softer and more chemically reactive. To improve yield and durability, we have investigated arrays made of aluminum with a thin (~10 nm) protective TiN layer deposited on top. The bilayer is patterned in a single step. The electrical properties of the bilayer are dominated by the aluminum due to its higher conductivity and lower kinetic inductance. Arrays made with bilayer have shown a very high (95%) yield. A typical transmission spectrum is shown in Fig. 4.

Fig. 4. *Transmission of an Al/TiN bilayer array with 150-nm absorber line-width.*
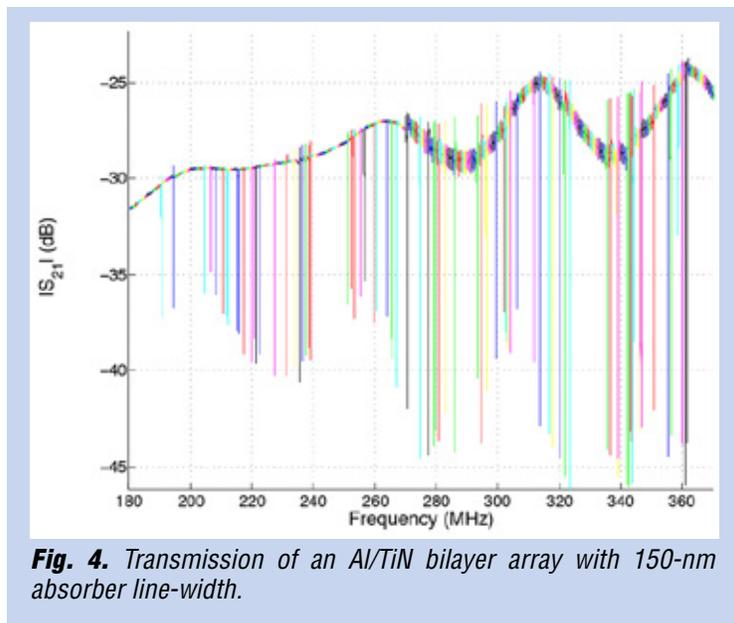
The bilayer arrays were tested optically using a blackbody source internal to the cryostat. The detector response and noise were measured to derive an optical NEP. The noise spectra, expressed in NEP units, are shown in Fig. 5 (left) for various blackbody temperatures. The increase in noise with blackbody temperature and the shape of the curves suggest that the detectors are photon-noise-limited over the range of powers corresponding to the higher of the blackbody temperatures studied ($T_{load} \geq 16$ K). Figure 5 (right) compares the measured and expected noise as a function of optical power. The measurement and photon-noise prediction agree for optical power greater than about 1 pW.

Fig. 5. Left: *Noise spectra of an Al/TiN bilayer detector for various blackbody temperatures. The noise is expressed in NEP units by dividing by the measured responsivity.* Right: *Measured vs. expected noise as a function of optical power.*
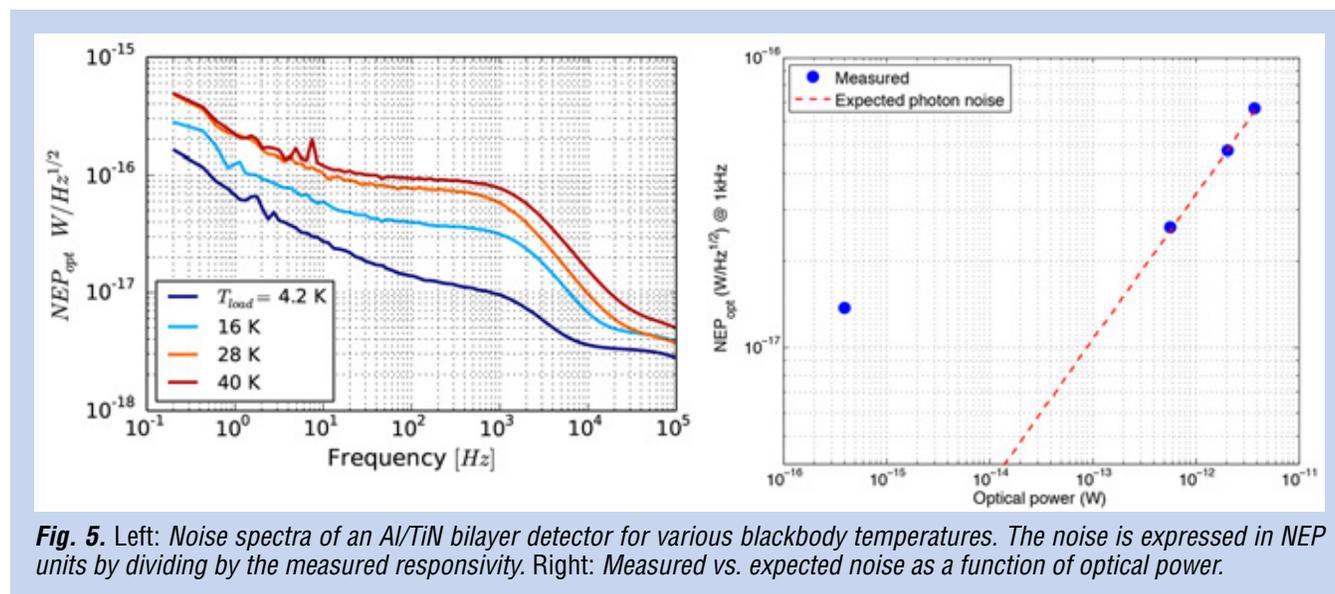
The NEP of about 10^{-17} W/Hz$^{1/2}$ measured with the blackbody at 4.2 K falls short of the expectation for these detectors and of the sensitivity calculated by assuming a 1 ms quasi-particle lifetime. We believe the sensitivity is degraded because the detector responsivity is limited by a much shorter lifetime, which may be due to several effects. First, the T_c of the bilayer was measured to be 1.9 K, which is considerably higher than for pure aluminum. Measurements of a range of superconducting materials have found that the maximum lifetime varies with T_c approximately as T_c^{-3}. Second, we believe that an excess quasi-particle population may be present due to the leakage of pair-breaking radiation into the detector housing, which decreases the lifetime due to self-recombination. Third, it is possible that the presence of the TiN over-layer causes a reduction in the quasi-particle lifetime compared to that of clean aluminum.

Recently, all-aluminum detectors have been successfully fabricated and tested at JPL. These devices have shown considerably higher responsivity than the TiN-overlayer devices, indicating that NEP below 10^{-18} W/Hz$^{1/2}$ could soon be within reach.

Chirped readout for KIDs

In a traditional KID readout, each of the resonances is excited with a fixed tone, and the time-variable amplitude and/or phase shift of the tone due to changes in incident radiation is recorded. This works well in many instruments, and is the primary readout technique for our CSO demonstration camera. However, the fixed-tone readout loses sensitivity when the resonances shift in frequency by half a line-width or more. A chirped readout addresses this issue; the entire frequency band containing the resonances is excited using a broadband, short-duration chirped pulse, which allows resonant frequencies to be excited and read out even if they move significantly in frequency. In detail, the radio-frequency chirped pulse is applied to the input line. Then, during a "listening" period, the output signal consisting of a superposition of the ring-down signals from all the resonators is digitized and Fourier-transformed, and the resonators that are ringing due to the chirp excitation are identified and stored. This chirping and identification can be done at kHz rates.

We have been developing a chirped readout using a PC-based system containing a commercial Analog-to-Digital and Digital-to-Analog Converters (ADC/DAC) board and a Graphics Processing Unit (GPU) board. This system achieved "first light" at CSO (albeit in poor weather) with the KID demonstration camera in May 2015 (Fig. 6). During these tests, we successfully read out all detectors in the 350-μm KID array in the 125-250 MHz range, at up to 3.6 kHz readout rate. The system showed low 1/f noise (Fig. 6), and the performance compared favorably with the fixed-tone readout. For the majority of detectors, the sensitivity was essentially the same for both readouts; for each of the remaining detectors, the loss of sensitivity is understood as insufficient readout power (resulting in amplifier-dominated noise) or excessive readout power (resulting in a distorted and less-responsive resonance). These observations led us to develop a new signal processing scheme that does not suffer distortion or loss of performance at high power, and which will therefore provide considerable margin in the power level of the chirp pulse, making it possible to read out the entire array with full sensitivity. Given the advantages and recent demonstration of the chirped readout, it will be an important part of our KID-based systems going forward.
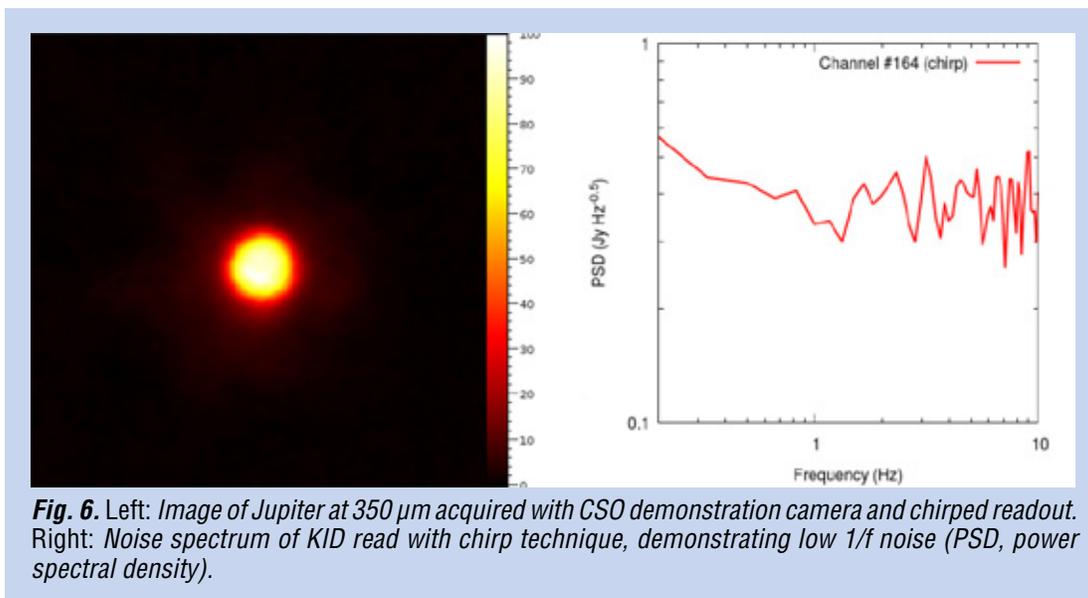
Fig. 6. Left: *Image of Jupiter at 350 µm acquired with CSO demonstration camera and chirped readout.* Right: *Noise spectrum of KID read with chirp technique, demonstrating low 1/f noise (PSD, power spectral density).*

Path Forward

Our two-year project, now in its fourth year, is very nearly completed. Although we have accomplished a significant fraction of our original goals, there is considerable work left for the future. Instrument testing at the CSO has given us high confidence that KID arrays are very strong contenders for use in future Far-IR space astrophysics missions. Although the closing of the CSO prevents us from continuing our instrument tests at 350 µm, we will seek other opportunities for ground-based testing.

From our perspective, the major outstanding issue is a demonstration that a low NEP in the 10^{-19} W/Hz$^{1/2}$ range can be achieved in an array that combines low readout frequency (100-200 MHz), high yield, and high optical efficiency. Recent work at JPL confirms that an aluminum-based array remains a good option. We have also identified a promising new direction, phonon recycling, that combines the fabrication and optical efficiency advantages of TiN detectors with the sensitivity advantage of high-quality, clean aluminum films; this concept was selected for a 2016 NASA Astrophysics Research and Analysis (APRA) award.

References

[1] P.K. Day, H.G. LeDuc, B.A. Mazin, A. Vayonakis, and J. Zmuidzinas, "*A broadband superconducting detector suitable for use in large arrays*," Nature **425**, no. 6960, 817-821 (2003)

[2] S.P. Doyle, P. Mauskopf, J. Naylon, A. Porch, and C. Duncombe, "*Lumped element kinetic inductance detectors*," Journal of Low Temperature Physics **151**, no. 1-2, 530-536 (2008)

[3] H.G. Leduc, B. Bumble, P.K. Day, B.H. Eom, J. Gao, S. Golwala, B.A. Mazin, et al., "*Titanium nitride films for ultrasensitive microresonator detectors*," Applied Physics Letters **97**, no. 10, 102509-102509 (2010)

[4] J. Hubmayr, J. Beall, D. Becker, H.M. Cho, M. Devlin, B. Dober, C. Groppi, G.C. Hilton, K.D. Irwin, D. Li, P. Mauskopf, D.P. Pappas, J. Van Lanen, M.R. Vissers, Y. Wang, L. F. Wei, and J. Gao, "*Photon-noise limited sensitivity in titanium nitride kinetic inductance detectors*," Appl. Phys. Lett. **106**, no. 7, 073505 (2015)

[5] J. Zmuidzinas, "*Superconducting microresonators: Physics and applications,*" Annu. Rev. Condens. Matter Phys. **3**, no. 1, 169-214 (2012)

For additional information, contact Jonas Zmuidzinas: jonas@caltech.edu

Predictive Thermal Control Technology for Potential HabEx Mission

By H. Philip Stahl (MSFC)

Imaging and characterizing Earth-like planets requires the ability to block 10^{10} of the host star's light with a 10^{-11} stability. For an internal coronagraph, this requires correcting wavefront errors and keeping that correction stable to a few picometers rms for the duration of the science observation. Providing this capability requires a thermally stable telescope.

Predictive Thermal Control Technology (PTCT) is a multiyear effort to develop, demonstrate, mature towards TRL 6, and assess the utility of model-based Predictive-Thermal-Control (PTC) technology to enable a thermally stable telescope. PTCT demonstrates technology maturation by model validation and characterization testing of traceable components in a relevant environment. PTCT's efforts are conducted in consultation with the Cosmic Origins Office and NASA Program Analysis Groups.

To mature Thermally Stable Telescope technology, PTCT has defined three objectives:

1. Validating models that predict thermal optical performance of real mirrors and structure based on their structural designs and constituent material properties, i.e., coefficient of thermal expansion (CTE) distribution, thermal conductivity, thermal mass, etc.
2. Deriving thermal system stability specifications from wavefront stability requirement.
3. Demonstrating utility of a Predictive Control thermal system for achieving thermal stability.

To achieve these objectives, PTCT defined a detailed technical plan with five quantifiable milestones:

1. Develop a high-fidelity flight-traceable model of the AMTD-2 1.5-meter ULE® mirror, including 3D CTE distribution and reflective optical coating, that predicts its optical performance response to steady-state and dynamic thermal gradients under bang/bang and proportional thermal control.
2. Derive specifications for thermal control system as a function of wavefront stability.
3. Design and build a predictive Thermal Control System for a 1.5-meter ULE® mirror using new and existing commercial-off-the-shelf components that sense temperature changes at the ~1-mK level, and actively controls the mirror's thermal environment at the ~20-mK level.
4. Validate the model by testing a flight-traceable 1.5-m class ULE® mirror in a relevant thermal-vacuum environment in the MSFC X-ray and Cryogenic Facility (XRCF) test facility.
5. Use the validated model to perform trade studies to determine how thermo-optical performance can be optimized as a function of mirror design, material selection, mass, etc.

PTCT advances the state-of-the-art by developing a predictive control method that uses a thermal 'model in the loop' to control the thermal system. Our goal is to demonstrate a 'system' technology solution that enables a thermally stable telescope for exoplanet science that keeps the telescope at a constant temperature independent of where it looks on the sky.

High-Efficiency Continuous Cooling for Cryogenic Instruments and sub-Kelvin Detectors

By James Tuttle (GSFC)

Although large diffraction-limited telescopes are approaching a size limited by available launch vehicles, there is still an enormous "discovery space" open to astrophysics through the use of advanced low-temperature instruments and deep sub-Kelvin detectors. These devices offer the potential for orders-of-magnitude improvement in sensitivity and spectral resolution. In the past, cryogenic instruments have been large, expensive, and power-hungry, consisting of complex cooling chains with multiple coolers using different technologies. High cost and complexity have been the major impediment to the selection of missions using these advanced capabilities.

We propose to develop a compact cooling system that will span more than a factor of 200 in temperature, lifting heat continuously at temperatures below 50 mK and rejecting it at over 10 K, simplifying the overall cryogenic system. The device, based on Adiabatic Demagnetization Refrigerators (ADRs), will have high thermodynamic efficiency. The prototype system will exceed the requirements of all currently conceived cryogenic detector arrays, including those for flagship missions such as the Far-IR Surveyor, Inflation Probe, X-ray Surveyor, and possibly HabEx and LUVOIR. In particular, it will have more than five times the cooling power at 50 mK than previous sub-Kelvin coolers, greatly relaxing the requirements on heat generation in large detector arrays, and simplifying the thermal design of the focal-plane assemblies.

ADRs by themselves have no moving parts and produce no measurable vibration. However, upper-stage mechanical coolers have been linear piston devices that export significant vibration. Ameliorating the problems due to upper-stage cooler vibrations has contributed to increased costs on recent astrophysics missions such as JWST and Astro-H. By raising the heat-reject temperature to 10 K, the proposed sub-Kelvin cooler becomes compatible with recently demonstrated extremely low-vibration mechanical coolers, eliminating this problem for future missions. Furthermore, a complete cooling chain with extremely low vibration will enable the use of advanced sub-Kelvin detectors on missions with tight pointing requirements.

Multi-stage ADRs offer great flexibility. In addition to continuous cooling at the lowest temperatures, the prototype will have a stage that provides enough power at 4 K to cool a modest-sized telescope. This stage could be scaled up to cool a large (multi-meter) telescope. Continuous stages could be added at other temperatures to provide cooling to, for example, Superconducting Quantum Interference Device (SQUID) arrays for Transition Edge Sensors (TESs) or High Electron Mobility Transistors (HEMTs) for Microwave Kinetic Inductance Detectors (MKIDs).

Now is the time to pursue this effort. Our team recently completed the end-to-end design, build, and on-orbit qualification of the ASTRO-H ADR. Launched successfully in February 2016, the ADR now provides a stable 50-mK on-orbit detector-array temperature. In September 2015, our team demonstrated a laboratory ADR that provided cooling at 4 K and rejected heat to 10 K. We are presently building continuous ADRs with heat rejection at 4.5 K that have much higher cooling power per unit mass than the traditional, ASTRO-H-style "single-shot" ADRs. In short, the team is now ready to make this technology mission-selectable by 2020. At the conclusion of this work, NASA will have a TRL-6 magnetic cooling system ready for missions in the coming decades.

Appendix D
Acronyms

A

AAS . . . . American Astronomical Society
ADC. . . . . Analog-to-Digital Converter
ADM . . . . Absolute-distance Meter
ADU . . . . Analog-to-Digital Unit
AES . . . . Auger Photoelectron Spectroscopy
AFM. . . . . Atomic Force Microscopy
AFRC . . . . Armstrong Flight Research Center
AGN. . . . . Active Galactic Nuclei
AIP . . . . Astrophysics Implementation Plan
ALD . . . . Atomic Layer Deposition
ALMA. . . . . Atacama Large Millimeter/submillimeter Array
A-MKID . . . . Atacama Pathfinder EXperiment (APEX) Microwave Kinetic Inductance Detector
AMM . . . . Arnold Mirror Modeler
AMTD . . . . Advanced Mirror Technology Development
AO. . . . . Applied Optics
AOS . . . . Active Opto-thermal Stability
APD. . . . . Avalanche Photo Diode
APEX . . . . Atacama Pathfinder Experiment
APL . . . . Applied Physics Laboratory, Johns Hopkins
APRA . . . . Astrophysics Research and Analysis
AR . . . . Anti-Reflection
Ar . . . . Argon
ARC . . . . Ames Research Center
ARPA-E . . . . Advanced Research Projects Agency-Energy
ASIC . . . . Application-Specific Integrated Circuit
ASU . . . . Arizona State University
ATLAST . . . . Advanced Technology Large-Aperture Space Telescope
AURA. . . . . Association of Universities for Research in Astronomy

B

BPF . . . . Band-Pass Filter

C

CCD. . . . . Charge-Coupled Device
CHESS . . . . Colorado High Resolution Echelle Stellar Spectrograph
CME. . . . . Coronal-Mass Ejection
CMOS . . . . Complementary Metal-Oxide Semiconductor
COBE. . . . . Cosmic Background Explorer
COPAG . . . . Cosmic Origins Program Analysis Group
COR. . . . . Cosmic Origins
COS . . . . Cosmic-Origins Spectrograph
COTS . . . . Commercial off the Shelf
CSA . . . . Charge-Sensitive Amplifier
CSO . . . . Caltech Submillimeter Observatory
CTE . . . . Coefficient of Thermal Expansion

cw . . . . continuous wave
CWI . . . . Cosmic Web Imager

D

D . . . . Diameter
DAC . . . . Digital-to-Analog Converter
DC . . . . Direct Current
DDR . . . . Double Data Rate
DFB . . . . Distributed Feedback
DLR . . . . Forschungszentrum der Bundesrepublik Deutschland für Luft- und Raumfahrt
(German   Aerospace Research Center)
DMD . . . . Digital Micro-mirror Device
DSB . . . . Double-Side Band

E

EC . . . . Executive Committee
ECR . . . . Electron Cyclotron Resonance
eLISA . . . . evolved LISA
EMCCD . . . . Electron-Multiplying Charge-Coupled Device
EoR . . . . Epoch of Reionization
ESA . . . . European Space Agency
ExEP . . . . Exoplanet Exploration Program
ExoPAG . . . . Exoplanet Program Analysis Group

F

Far-IR . . . . Far-Infrared
Far-UV . . . . Far-Ultraviolet
FIR . . . . far-IR
FIREBall . . . . Faint Intergalactic medium Redshifted Emission Balloon
FIRS . . . . FIR Surveyor
FMC . . . . FPGA Mezzanine Card
FOV . . . . Field of View
FPGA . . . . Field Programmable Gate Array
FS . . . . Fused Silica
FUSE . . . . Far-Ultraviolet Spectroscopic Explorer
FUV . . . . Far Ultraviolet
FWHM . . . . Full-Width at Half-Maximum
FY . . . . Fiscal Year

G

GALEX . . . . Galaxy Evolution Explorer
GEVS . . . . General Environmental Verification Standard
GMOX . . . . Gemini Multi-Object eXtra-wide-band Spectrograph
GOLD . . . . Global-scale Observations of the Limb and Disk
GPU . . . . Graphics Processing Unit
GRAPH . . . . Gigasample Recorder of Analog waveforms from a PHotodetector
GSFC . . . . Goddard Space Flight Center
GUSSTO . . . . Galactic/Xtragalactic ULDB Spectroscopic Stratospheric Terahertz Observatory
GWs . . . . Gravitational Waves

H

HabEx . . . . Habitable Exoplanet
HAWC . . . . High-resolution Airborne Wide-bandwidth Camera
HDST . . . . High Definition Space Telescope

HEB. . . . . Hot Electron Bolometer
HEM . . . . Heat Exchanger Method
HF. . . . . Hydrogen Fluoride
HIFI. . . . . Heterodyne Instrument for the Far Infrared
HIRMES . . . . High-Resolution Mid-infrarEd Spectrometer
HQ . . . . Headquarters
HSO. . . . . Herschel Space Observatory
HST . . . . Hubble Space Telescope
HV. . . . . High Voltage

I

IBM . . . . International Business Machines Corp.
ICON . . . . Ionospheric Connection Explorer
ICP . . . . Inductive-Coupled Plasma
IDC . . . . Interdigitated Capacitor
IEEE. . . . . Institute of Electrical and Electronics Engineers
IF. . . . . Intermediate Frequency
IFU . . . . Integral Field Unit
IGM . . . . Intergalactic Medium
iPlas. . . . . Innovative Plasma Chemical Vapor Deposition
IR . . . . Infrared
IRAS . . . . Infrared Astronomical Satellite
ISM . . . . Interstellar Medium
IV . . . . Current-Voltage

J

JATIS . . . . Journal of Astronomical Telescopes, Instruments, and Systems
JAXA . . . . Japanese Aerospace eXploration Agency
JCMT . . . . James Clerk Maxwell Telescope
JPL. . . . . Jet Propulsion Laboratory
JVST. . . . . Journal of Vacuum Science and Technology
JWST . . . . James Webb Space Telescope

K

KID . . . . Kinetic Inductance Detector (or Device)
Kr . . . . Krypton

L

LBNL . . . . Lawrence Berkeley National Lab
LDB . . . . Long-duration Balloon
LDR . . . . Large Deployable Reflector
LET . . . . Linear Energy Transfer
LIDAR . . . . Light Detection and Ranging
LIGO . . . . Laser Interferometer Gravitational-Wave Observatory
LISA. . . . . Laser Interferometer Space Antenna
LISM . . . . Local Interstellar Medium
LLLCCD . . . . Low-Light-Level Charge-Coupled Device
LN . . . . Liquid Nitrogen
LNA . . . . Low-Noise Amplifier
LO . . . . Local Oscillator
LUVOIR . . . . Large UV/Optical/IR
LVDS . . . . Low-Voltage Differential Signaling

M

MAOS . . . . Massive Active Opto-Thermal Stability
MBE. . . . . Molecular Beam Epitaxy
MCP. . . . . Micro-Channel Plate
MEMS . . . . Micro-Electro-Mechanical-System
MFC. . . . . Mass-Flow Controller
MIDEX. . . . . Medium-Class Explorer
MIT . . . . Massachusetts Institute of Technology
MKID. . . . . Microwave Kinetic Inductance Detector
MOS . . . . Multi-Object Slit Spectrograph
MSFC. . . . . Marshall Space Flight Center
MTF. . . . . Modulation Transfer Function
MTSSP . . . . Measurement Techniques in Solar and Space Physics

N

NASA. . . . . National Aeronautics and Space Administration
Near-IR . . . . Near-Infrared
NEP . . . . Noise-Equivalent Power
NI . . . . National Instruments
NIR . . . . Near-Infrared
NIS . . . . Normal-Insulator-Superconductor
NIST . . . . National Institute of Standards and Technology
NPR. . . . . NASA Procedural Requirements
NRC. . . . . National Research Council
NUV. . . . . Near-Ultraviolet
NWNH . . . . New Worlds, New Horizons in Astronomy and Astrophysics (2010 Decadal Survey)

O

OTA. . . . . Optical Telescope Assembly

P

PACS . . . . Photodetector Array Camera and Spectrometer
PATR . . . . Program Annual Technology Report
PCB . . . . Printed Circuit Board
PCOS . . . . Physics of the Cosmos
PDR. . . . . Photo-Dissociation Region
PDR. . . . . Preliminary Design Review
PEALD . . . . Plasma-Enhanced Atomic Layer Deposition
PI . . . . Principle Investigator
PM. . . . . Primary-Mirror
PMA. . . . . Primary Mirror Assembly
PMOS . . . . P-type Metal-Oxide-Semiconductor
PSD . . . . Power Spectral Density
PSF . . . . Point Spread Function
PTE . . . . Pressure-Tight Enclosure
PVD. . . . . Physical Vapor Deposition
PXS . . . . Parallel Cross Strip
PZ . . . . Pole-Zero
PZC . . . . Pole-Zero-Cancellation

Q

QCL. . . . . Quantum-Cascade Laser
QE. . . . . Quantum Efficiency
QSO. . . . . Quasi-Stellar Object

R

RAL . . . . Rutherford Appleton Laboratory
R&D. . . . . Research and Development
RF . . . . Radio Frequency
RFI . . . . Request for Information
RIT . . . . Rochester Institute of Technology
rms . . . . root mean square
ROSES . . . . Research Opportunities in Space and Earth Science

S

SAT . . . . Strategic Astrophysics Technology
SB . . . . Solar-Blind
SCUBA-2 . . . . Submillimetre Common-User Bolometer Array-2
SEE . . . . Single Event Effect
SEU . . . . Single Event Upset
SFO . . . . Star Formation Observatory
SHARC II . . . . Submillimeter High-Angular Resolution Camera II
SIG . . . . Science Interest Group
SIOSS. . . . . Science Instruments, Observatory, and Sensor Systems
SL . . . . Superlattice
SLAR . . . . SL-doped, AR-coated
SLS . . . . Space Launch System
SM. . . . . Secondary-Mirror
SMD. . . . . Science Mission Directorate
SMEX. . . . . Small Explorer
SMFL . . . . Semiconductor and Microsystems Fabrication Laboratory
SN . . . . Signal-to-Noise
SoC . . . . System-on-Chip
SOFIA . . . . Stratospheric Observatory for Infrared Astronomy
SPICA . . . . Space Infrared Telescope for Cosmology and Astrophysics
SPIE. . . . . Society of Photo-optical Instrumentation Engineers
SPIRE. . . . . Spectral and Photometric Imaging Receiver
SPUD. . . . . Solid-state Photon-counting Ultraviolet Detector
SQUID . . . . Superconducting Quantum Interference Device
SR&T . . . . Supporting Research and Technology
SSL . . . . Space Sciences Laboratory
STDTs . . . . Space and Technology Definition Teams
STM. . . . . Science Traceability Matrix
STO . . . . Stratospheric Terahertz Observatory
STScI . . . . Space Telescope Science Institute

T

TARGET. . . . . TeV Array Readout with GSa/s sampling and Event Trigger
TCOR. . . . . Technology development for Cosmic Origins
TES . . . . Transition Edge Sensor
TI . . . . Texas Instruments
TiN . . . . Titanium Nitride
TMA. . . . . Trimethylaluminum
TMB. . . . . Technology Management Board
TRL . . . . Technology Readiness Level
TSMC. . . . . Taiwan Semiconductor Manufacturing Company

U

UC . . . . University of California
UHV . . . . Ultra-High Vacuum
ULE . . . . Ultra-Low Expansion
UPS . . . . Ultraviolet Photoelectron Spectroscopy
US . . . . United States
USA . . . . United States of America
USB . . . . Universal Serial Bus
UV . . . . Ultraviolet
UVIS . . . . Ultraviolet/Visible
UVOIR . . . . UV/Optical/IR

V

Vis . . . . Visible light
VUV . . . . Visible and UV

W

WaSP . . . . Wafer-Scale Imager for Prime
WFE . . . . Wavefront Error
WFIRST . . . . Wide-Field Infrared Survey Telescope
WPE . . . . Wall-plug Power Efficiency

X

Xe . . . . Xenon
XGA . . . . eXtended Graphics Array
XPS . . . . X-ray Photoelectron Spectroscopy
XRCF . . . . X-Ray and Cryogenic Facility
XRS . . . . X-Ray Surveyor
XS . . . . Cross-Strip